Comprehensive study on the effects of various stressors on soft corals and zooxanthellae

DISSERTATION

zur Erlangung des Doktorgrades der Naturwissenschaften
(Dr. rer. nat.)

der

Naturwissenschaftlichen Fakultät II
Chemie, Physik und Mathematik

der Martin-Luther-Universität
Halle-Wittenberg

vorgelegt von

Frau Ayu Christien Rahaweman

This dissertation has been written under the supervision of Prof. Dr. Ludger A. Wessjohann, and the mentorship of Dr. Andrea Porzel and Dr. Pauline Stark at the Department of Bioorganic Chemistry of the Leibniz Institute of Plant Biochemistry (L-IPB) in cooperation with the Martin Luther University of Halle-Wittenberg and Leibniz Centre for Marine Tropical Research (ZMT), Bremen.

1st Reviewer: Prof. Dr. Ludger Wessjohann

2nd Reviewer: Prof. Dr. Mohamed A. Farag

Date of public defense: 11.10.2023

Now to HIM who is able to do immeasurably more than all we ask or imagine, according to his power that is at work within us (Ephesians 3:20)

Table of Contents

Contents

Acknowledgements

I wish to thank all the people who directly or indirectly contributed to the realization of this work.

Especially, I am sincerely indebted to Prof. Dr. Ludger Wessjohann, who despite his numerous commitments accepted to supervise my PhD thesis and hosted me at the Leibniz Institute of Plant Biochemistry (IPB) as a DAAD doctoral fellow. His significant contribution during the design of my PhD project made me knowledgeable about the current trends of modern natural products chemistry, including metabolomics. His advices, encouragements, suggestions, and support were valuable for a successful scientific career and beyond. Dr. Andrea Porzel as my mentor, my advisor and research project leader, sincerely deserves my highest thankfulness for her guidance, great support, fruitful discussions, and truthful encouragement. I also wish to express my profound gratitude to Dr. Katrin Franke, Dr. Pauline Stark, and Dr. Norbert Arnold for the mentorship, guidance, encouragement, and personal concern about the success of my thesis and future plans. This work would not have been possible without the scientific and technical support from many people of the IPB: my mentor Dr. Andrea Porzel, who taught me how to handle the NMR machine, measured my samples, and provide critical discussions for structure determinations and NMR metabolomics. This is extended to Dr. Andrej Frolov and Annegret Laub, our experts of MS. Gudrun Hahn, Martina Brode and Martina Lerbs for their help in NMR measurements, antibacterial assay, growing the bacteria, and cytotoxic assays, respectively. Mrs. Ines Stein is acknowledged for her help with administrative and residence permit matters, and I also thank Dr. Frank Broda for the help with IT and help to solve many problems related to IT and software. I thank my colleagues Ismail bin Ware, Yen Lam, Mthandazo Dube, and Jonas Kappen, as well as all the other members of NWC for the good atmosphere, friendship, help, and discussions. I would like to acknowledge our collaborators in the pharmacy department at MLU, Prof. Timo Niedermeyer who also served as my second mentor, as well as Diana Barera, who helped me with MS-Imaging measurements and very informative and deep discussions. Thanks are extended to Dr. Achim Meyer and Dr. Sonia Bejarano for our great collaboration in ZMT, who provided me living corals in ZMT, help with the genetic identification of soft corals and zooxanthellae, as well as provide the things I needed in the lab at Bremen. I thank Prof. Bettina Hause and Hagen Stellmach for their help in histology profiling of my corals samples. I also wish to acknowledge all my former lecturers at the IPB University (Indonesia), especially my former M.Sc. supervisors Dr. Kustiariyah Tarman, who encouraged and motivated me to study in Germany, as well as for her teaching and mentorship. I am grateful to the DAAD committee members, referees and staff. In addition, I also wish to thank the people without whom I could not have been what I am. Special acknowledgements go to my late mother Mrs. Josina Rahawarin for her steadfast and unconditional love and prayers. Special thanks also for my sisters and brother for love,

prayers, support, pattience, and encouragement. Whenever I doubted, they are always there to say with a trustful heart: “You can do it in Jesus’s name.” Especial thanks go to my husband Ron Hablasch and family for their support, love and patience, also for being my family in Germany. I am profoundly thankful to all my fellow Christians for their great spiritual support and life changing teaching in heart, so that I may know the mystery of God’s love and mercy, namely, Christ, in whom are hidden all the treasures of life, success, peace of heart, wisdom, and knowledge, etc. Finally, financial support from the DAAD for the Biodivesity and Health programm is highly appreciated. I am grateful to the IPB for supporting the lab costs and travel to conferences.

List of Abbreviations

AMPA	Aminomethylphosphonic acid
AP	Atmospheric pressure
ATCC	American type culture collection
ATP	Adenosine triphosphate
BLAST	Basic local alignment search tool
BR	Bootstrap support
CAB	Coral-associated bacteria
CID	Collisioin induced dissociation
CMC	Cytochrome c oxidase subunit 1
CV	Cell viability
d	Doublet in NMR
dd	Doublet of doublet in NMR
DHB	2,5-dihydroxybenzoic acid
DMP	Dimethyl phthalate
DMSO	Dimethylsulfoxide
DNA	Deoxyribonucleic acid
DSS	Dark spot syndrome
EDTA	Ethylenediaminetetraacetic acid titrated
EPSPS	5-Enolpyruvyl-shikimate-3-phosphate synthase
ESI	Electrospray ionization
FA	Fatty acid
GBH	Glyphosate-based herbicide
HESI	Heated electrospray ionization
HMDS	Hexamethyldisiloxane
HMBC	Heteronuclear multiple bond correlation
HQ	High-quality
HRMS	High-resolution mass spectrometry
HSQC	Heteronuclear single quantum correlation
IC50	Half-maximal inhibitory concentration
J	Coupling constant (in NMR)
LC-MS	Liquid chromatography-mass spectrometry
LDPE	Low-density polyethylene
LHCII	Light-harvesting complex II
LSM	Laser scanning microscopy
m/z	Mass-to-charge-ratio
m	Multiplet in NMR
MALDI	Matrix assisted laser desorption/ionization
MS	Mass spectrometry
NME	Normalized collision energy
NMR	Nuclear magnetic resonance
OD	Optical density
OP	Organophosphorous
PAE	Phthalic acid esters
PAM	Pulse amplitude modulation
PC	Principle component
PCA	Principle component analysis
PET	Polyethylene terephthalate
ppm	Parts per million
PQ	Plastoquinone
PSII	Photosystem II
PUFA	polyunsaturated fatty acid
QC	Quality control
R_f	Retention factor
RLU	Relative luminescence unites
ROS	reactive oxygen species
s	Singlet in NMR
SDR	Shut down reaction
S/N	Signal-to-noise ratio
sp.	Species
t	Triplet in NMR
TBP	Tetrabromopyrrole
TIC	Total ion chromatogram
TLC	Thin layer chromatography
t_R	Retention time
UHPLC	Ultra high performance liquid chromatography
UV	Ultraviolet
UWS	Ulcerative white spots
WBD	White band disease
WGA	Wheat germ agglutinin
WS	White syndrome
YBD	Yellow band disease

Summary

Coral reefs are a complex ecosystem that serve a vital role as a main habitat for over 25% of marine organisms. Soft corals, a part of coral reefs biomass, have a remarkable potential as producer of a wide range of compounds with distinct chemical structures. However, these invertebrates are extremely vulnerable to changes in their environment. In response, they produce secondary metabolites which act as chemical defense against predators and environmental changes. Beside of that, morphological changes (e.g. color, tentacle behavior), as well as in their symbionts are markers of coral stress in the first place. In this thesis, the first comprehensive investigation regarding the effects of various elicitors on corals morphology and their secondary metabolites was conducted.

Three soft coral species, namely *Sarcophyton glaucum* Quoy, *Lobophytum crassum* Marenzeller, and *Xenia umbellata* Lamarck were studied. In order to investigate the metabolite composition in these soft corals, TLC, LC-ESI-HRMS, and ^{1}H-NMR analyses were performed. As a result, extracts of investigated soft corals contain a wide range of natural products, including diterpenes, cembranoids, alkaloids, and steroids. Multivariate data analysis (e.g. PCA) of the LC-ESI-HRMS and ^{1}H-NMR data revealed a difference in metabolite compositions for *X. umbellata* compared to the two other soft corals. The species-specific metabolites of each soft coral were responsible for this segregation, particularly species-specific terpenoids (e.g. diterpenes and sesquiterpenes) and cembranoids. Further on, MALDI-MS imaging was used to investigate the spatial distribution of metabolites within coral bodies. In total 7 known compounds from soft corals and 4 known compounds from zooxanthellae were detected.

Furthermore, the effect of elicitors was investigated. For five days, *S. glaucum*, *L. crassum*, and *X. umbellata* were exposed to a variety of stressors, including glyphosate, simazine, oxybenzone, octinoxate, $CuSO_4$, DMP, microplastic, and *V. campbellii*. Under optimized analytical conditions, 38 metabolites were tentatively identify via ^{1}H-NMR and 85 metabolites via LC-ESI-HRMS, including diterpenes, sesquiterpenes, steroids, alkaloids, fatty acids, and lipids. Chronic exposure to DMP and $CuSO_4$ caused significant stress to soft corals. The exposure to these two elicitors affected their metabolite composition, as impaired in the segregation of these extract groups in PCA score plots. Fatty acids are the primary components responsible for this segregation. These metabolites were detected in high abundance after elicitation (based on ^{1}H-NMR data). Interestingly, glyphosate had no effect on soft corals and zooxanthellae. Despite, the concentration of glyphosate used in this study were very high in comparison to those detected in marine environment.

Therefore, further experiments were performed to determine the concentration limit of glyphosate, at ecologically irrelevant very high concentrations, as it was assumed to the investigated coral species. Six different concentration of glyphosate were tested on three investigated soft corals. At the highest concentrations (1 g/L, 100 mg/L, and 50 mg/L), this

herbicide was extremely toxic to soft corals, as indicated by tentacle behaviour and polyp color. Similarly to the morphology result, these glyphosate concentrations affected the metabolite composition of the corals. These extracts were clearly distinct from other extracts in PCA score plot. In addition the extracts of *L. crassum* and *X. umbellata* treated with 50 mg/L were also separated from other extracts. In general, fatty acids were tentatively assigned as the metabolites responsible for group segregation in ^{1}H-NMR-PCA and LC-MS-PCA. Additionally, some diterpenes were detected as metabolites responsible for the separation of *L. crassum* extracts. The presence of diterpene in soft coral species could be associated with their bioactivity.

The bioactivity (antibacterial and cytotoxicity) of soft corals methanolic crude extracts were evaluated against two bacteria, *A. fischeri* and *B. subtilis*, as well as against HT29-colon cancer and PC3-prostate cancer cell lines. *S. glaucum* and *L. crassum* extracts tested at a concentration of 500 µg/mL inhibited *A. fischeri* completely (100%). Interestingly, six extracts of *L. crassum* treated with glyphosate and $CuSO_4$ demonstrated extremely high activity against the Gram negative bacterium *A. fischeri*, with average IC50 values of 7.60 µg/mL and 11.76 µg/mL, respectively. In comparison to *A. fischeri*, all extracts of the corresponding soft corals exhibited only weak to moderate antibacterial activity against the Gram positive bacterium *B. subtilis*. Furthermore, a low concentration of soft coral extracts (0.05 µg/mL) had no effect on the viability of both cancer cell lines, while a higher concentration (50 µg/mL) induced a strong inhibition, with a percentage of cell viability less than 3%, indicating an anticancer potential. From this study arise numerous questions that remain unanswered. Nevertheless, this research contributes to major understanding of the complex relationship between soft corals and their endosymbiont (zooxanthellae), focusing on their secondary metabolites and morphology behavior in response to environmental stressors.

Zusammenfassung

Korallenriffe sind ein komplexes Ökosystem, das als Hauptlebensraum für über 25 % der Meeresorganismen eine wichtige Rolle spielt. Weichkorallen, die einen Teil der Biomasse von Korallenriffen ausmachen, haben ein bemerkenswertes Potenzial als Produzenten einer breiten Palette von Verbindungen mit unterschiedlichen chemischen Strukturen. Diese wirbellosen Tiere reagieren jedoch äußerst empfindlich auf Veränderungen in ihrer Umwelt. Als Reaktion darauf produzieren sie Sekundärmetaboliten, die als chemische Abwehrstoffe gegen Fressfeinde und Umweltstressoren dienen. Darüber hinaus sind morphologische Veränderungen (z. B. Farbe, Tentakelverhalten) und Veränderungen ihrer Symbionten die ersten Anzeichen für Korallenstress. In dieser Arbeit haben wir die erste umfassende Studie über die Auswirkungen verschiedener Auslöser auf die Morphologie der Korallen und ihre sekundären Stoffwechselprodukte durchgeführt.

Drei Weichkorallenarten, nämlich *Sarcophyton glaucum* Quoy, *Lobophytum crassum* Marenzeller, and *Xenia umbellata* Lamarck, wurden untersucht. Um die Zusammensetzung der Metaboliten in diesen Weichkorallen zu untersuchen, wurden TLC-, LC-ESI-HRMS- und ^{1}H-NMR-Analysen durchgeführt. Die Extrakte der untersuchten Weichkorallen enthalten eine breite Palette von Naturstoffen, darunter Diterpene, Cembranoide, Alkaloide und Steroide. Die multivariate Datenanalyse (z. B. PCA) von LC-ESI-HRMS- und ^{1}H-NMR-Daten ergab einen Unterschied in der Zusammensetzung der Metaboliten von *X. umbellata* im Vergleich zu den zwei anderen Weichkorallenarten. Die artspezifischen Metaboliten jeder Weichkoralle waren für diesen Unterschied verantwortlich, insbesondere artspezifische Terpenoide (z. B. Diterpene und Sesquiterpene) und Cembranoide. Die räumliche Verteilung der Metaboliten innerhalb der Korallenkörper wurde mit MALDI-MS untersucht. Mit diese Methode wurden insgesamt 7 bekannte Verbindungen aus Weichkorallen und 4 bekannte Verbindungen aus Zooxanthellen nachgewiesen.

Darüber hinaus wurde die Wirkung von Auslösern untersucht. Fünf Tage lang wurden *S. glaucum*, *L. crassum* und *X. umbellata* einer Reihe von Stressoren ausgesetzt, darunter Glyphosat, Simazin, Oxybenzone, Octinoxat, $CuSO_4$, DMP, Mikroplastik und *V. campbellii*. Unter optimierten Bedingungen wurden 38 Metaboliten durch ^{1}H-NMR und 85 Metaboliten durch LC-ESI-HRMS vorläufig identifiziert, darunter Diterpene, Sesquiterpene, Steroide, Alkaloide, Fettsäuren und Lipide. Die chronische Exposition gegenüber DMP und $CuSO_4$ verursacht bei Weichkorallen erheblichen Stress. Die Exposition gegenüber diesen beiden Auslösern wirkte sich auf die Zusammensetzung der Metaboliten aus, was sich in der Aufteilung dieser Extraktgruppen in den PCA-Score-Plots widerspiegelt. Fettsäuren sind die Hauptkomponenten, die für diese Aufteilung verantwortlich sind. Diese Metaboliten wurden nach der Behandlung mit Stressoren in großen Mengen nachgewiesen (basierend auf ^{1}H-NMR-Daten). Darüber hinaus wurde in dieser Studie ein interessantes Phänomen beobachtet, nämlich dass Glyphosat keine Auswirkungen auf Weichkorallen und Zooxanthellen hatte.

Zudem war die in dieser Studie verwendete Glyphosatkonzentration im Vergleich zu den in der Meeresumwelt vorkommenden Konzentrationen sehr hoch.

Daher wurden weitere Experimente durchgeführt, um die Konzentrationsgrenze von Glyphosat zu bestimmen, die für die untersuchten Korallen toxisch ist. Sechs verschiedene, Ökologisch irrelevant hohe Konzentrationen von Glyphosat wurden an den drei untersuchten Weichkorallen getestet da die Algensymbionten dann ansprechen sollten. Bei den höchsten Konzentrationen (1 g/L, 100 mg/L und 50 mg/L) war dieses Herbizid extrem giftig für Weichkorallen, wie aus dem Verhalten der Tentakel und der Polypenfarbe hervorgeht. Ähnlich wie die Morphologie beeinflussten die höchsten Konzentrationen von Glyphosat (1 g/L und 100 mg/L) die Zusammensetzung der Metaboliten in den Korallen. Diese Extrakte unterschieden sich im PCA-Score-Plot signifikant von den anderen Extrakten. Darüber hinaus unterschieden sich die mit 50 mg/L behandelten Extrakte von *L. crassum* und *X. umbellata* ebenfalls von den anderen Extrakten. Fettsäuren wurden als die Metaboliten annotiert, die für die Gruppentrennung in der ^{1}H-NMR-PCA und LC-MS-PCA verantwortlich sind. Außerdem tragen Diterpene zur Trennung der *L. crassum*-Extrakte bei. Das Vorhandensein von Diterpenen in Weichkorallenarten könnte mit ihrer Bioaktivität zusammenhängen.

Die Bioaktivität (antibakteriell und zytotoxisch) von methanolischen Rohextrakten aus Weichkorallen wurde an zwei Bakterien, *A. fischeri* und *B. subtilis*, sowie an HT29-Darmkrebs- und PC3-Prostatakrebszelllinien untersucht. Extrakte aus *S. glaucum* und *L. crassum*, die in einer höheren Konzentration (500 µg/mL) getestet wurden, hemmten Gram-negatives *A. fischeri* vollständig (100%). Interessanterweise zeigten sechs Extrakte von *L. crassum*, die mit Glyphosat oder $CuSO_4$ behandelt wurden, eine extrem hohe Aktivität gegen *A. fischeri* mit durchschnittlichen IC_{50}-Werten von 7,60 µg/mL bzw. 11,76 µg/mL. Alle Extrakte der entsprechenden Weichkorallen wiesen nur eine schwache bis mäßige antibakterielle Aktivität gegen Gram-positives *B. subtilis* auf. Darüber hinaus hatte eine niedrige Konzentration von Weichkorallenextrakten (0,05 µg/mL) keine Auswirkung auf die Lebensfähigkeit der beiden Zelllinien, während eine höhere Konzentration (50 µg/mL) eine starke hemmende Wirkung mit einem Prozentsatz der Zelllebensfähigkeit von weniger als 3 % zeigte. Diese Studie wirft noch viele unbeantwortete Fragen auf. Dennoch trägt diese Forschung zum Verständnis der komplexen Beziehung zwischen Weichkorallen und ihren Endosymbionten (Zooxanthellen) bei, wobei der Schwerpunkt auf ihren Sekundärmetaboliten und ihrem morphologischen Verhalten als Reaktion auf Umweltstressoren liegt.

I. Introduction and research objectives

1.1. Introduction

The oceans cover approximately 71% of the earth's surface and are known for their high biodiversity of marine organisms [1]. These organisms have been the subject of natural product research for decades. Corals are a primary focus, as these invertebrates are well-known for their potential to produce marine natural products [1, 2]. Soft corals (Cnidaria: Anthozoa: Octocorallia), in particular, are one of the most abundant coral representatives in the benthic zone of the sea, and are responsible for the biomass of coral reefs [3]. They present an important structural component of coral reef communities almost equal with the scleractinian (hard) coral. Octocorallia belong to the ± 3.200 species of the order Alcyonacea, which is comprised of the families Xeniidae, Nephtheidae, and Alcyoniidae [4]. This coral group produces a high diversity of secondary metabolites. Almost 95% of novel secondary metabolites from cnidarians were discovered from soft corals [1, 5].

As Alcyonacea, *Sarcophyton glaucum* Quoy, *Lobophytum crassum* Marenzeller, and *Xenia umbellata* Lamarck, have evolved an extraordinary capacity for producing a diverse range of compounds. The genera of these soft corals are known as producer of a large number of secondary metabolites, particularly cembranoids, terpenoids, steroids, ceramides, cerebrosides, fatty acids, and lipids [6-22]. Over 100 diterpenes and 20 biscembranoids were isolated from *Sarcophyton* species [23]. In addition, *Lobophytum* was reported to be a rich source of cembranoids, with over 250 different metabolites isolated from this genus [24]. The soft coral genus *Xenia* produces a large number of new terpenoids, with more than 200 terpenes have been identified [25]. In nature, these compounds act as chemical defense against fish predators and/or competing to other reef organisms, as well as pathogens (bacteria and parasites) [26-29]. Thus, these organisms represent potential resources of numerous novel chemicals for use in drug discovery assays.

However, due to the climate change and several environmental stressors, the coral ecosystem, particularly soft corals, is deteriorating. This situation is primarily a result of environmental stressors, such as increased temperature, increased carbon dioxide levels, which result in ocean acidification, sea level rise, and increased freshwater runoff, as well as human activity [30-32]. Human activity has been implicated in the decline of coral reefs both directly and indirectly; for example, chemical pollutants (e.g. nutrients, metals, and organic chemicals from agriculture, tourism, or industry) have been shown to have a detrimental effect on corals [30, 33-36]. Chemical pullutants are associated with human consumption and chemical waste generated during agricultural/industrial and persons daily activity, for instance sunscreen products [37-39], pesticides [40, 41], metal traces [42, 43], and plastics [44-46].

Moreover, these stressors have a detrimental effect by promoting soft coral diseases, increasing coral mortality over the last decades. Additionally, these stressors may have an effect on soft coral secondary metabolites, which can either increase or decrease as a response to the stress. However, studies examining the effect of environmental stress on soft coral metabolites have received significantly less attention due to a variety of factors, including analytical difficulties, low molecular masses, and ionic properties [47-49]. Nevertheless, the ability to address the aforementioned questions has been significantly enhanced by –omics techniques, which have transformed biological research into a data-rich discipline [50].

Metabolomics is currently the most advanced –omics tool, defined as the study of low-molecular-weight compounds from organisms (e.g. cells, tissues, or biological fluids) under treatment/physiological conditions [51]. In some cases, metabolomics has been shown to be more sensitive to biochemical activity than transcriptomics and proteomics [52, 53]. Apart from its sensitivity, this technique has a broad range of potential applications in the fields of ecology, toxicology, and agriculture [52, 54, 55]. Therefore, it is ideal for monitoring an organism's response to a stress condition or environmental interference [53, 56, 57]. These characteristics of metabolomics strongly suggest that this technique has the potential to advance our understanding of coral response to stressors, as well as the application of metabolomics to the study of the coral reef's ecological, and soft coral in particular [56-59].

In the recent years, metabolomics techniques have been applied to the coral metabolome in order to gain insight into the complexity of metabolites found in soft coral [56, 58, 60]. Furthermore, metabolomics in soft coral has been proved to investigate the soft corals responses to elicitors (chemical stressors) [58]. Apart from chemical stressors, this method was also used to investigate environmental stressors (global climate change), such as thermal and CO_2 level stress on *Sarcophyton ehrenbergi* and *S. glaucum* [60]. However, no single analytical technology or protocol exists for analyzing an organism’s entire metabolome and obtaining a complete metabolic profile [61]. Nevertheles, this aim can be accomplished by combining several hyphenated and high-throughput techniques, such as liquid chromatography (LC), gas chromatography (GC), coupled with mass spectrometry or nuclear magnetic resonance (NMR) spectroscopy [56, 57, 62]. Moreover, multivariate data analysis, specifically principal component analysis (PCA) and hierarchical cluster analysis (HCA) are the optimal methods for analyzing large data sets generated by analytical techniques. The purpose of this analysis is to reduce the dimensionality of the dataset in order to gain a better understanding of the dataset trends generated by tested samples, and to assess the significant variations observed at the metabolome level [63]. As a response to these perspectives, we conducted research on soft corals to gain a better understanding of how corals respond to a variety of stressors in the marine environment. To the best of our knowledge, this is the first study to document the elicitors’ effects on *S. glaucum*, *L. crassum*, and *X. umbellata* in detail.

1.2. Research objectives

The general objective of this thesis was to investigate the effects of elicitors (chemical, biological and physical stressors) on the soft corals *Sarcophyton glaucum*, *Lobophytum crassum*, and *Xenia umbellata*; morphologically and chemically. The applied stressors comprised herbicides (glyphosate and simazine), sun-blocker components (oxybenzone and octinoxate), copper sulfate, micro-plastic and plasticizer (dimethyl phthalate), as well as a coral pathogen (*Vibrio campbellii*).

In particular, this investigation covered many aspects which are described in several chapters. The aim of these studies was:

- Chapter IV: Characterization and comparison of the metabolite composition in *S. glaucum*, *L. crassum*, and *X. umbellata*, by using hyphenated techniques (TLC, LC-ESI-HRMS, and ^{1}H-NMR), as well as their spatial distribution in the corals body using MALDI-MSI.
- Chapter V: Comprehensive investigation of elicitor effects (morphologically and chemically) on *S. glaucum*, *L. crassum*, and *X. umbellata*, including application of multivariate data analysis in order to determine secondary metabolites variation of soft corals as response to elicitors.
- Chapter VI: Bioactivity (antibacterial and cytotoxicity) screening of soft coral extracts for the evaluation of their potential for new bioactive natural products
- Chapter VII: Investigation of glyphosate effects on the morphology and metabolite composition of *S. glaucum*, *L. crassum*, and *X. umbellata*, as well as the determination of the bioactivity of extracts from soft corals after glyphosate exposure.

II. General description of soft corals *Sarcophyton glaucum*, *Lobophytum crassum*, and *Xenia umbellata*

2.1. Coral reefs

Coral reefs are the most complex, biodiverse, and productive ecosystems [32, 64], covering approximately 280.000 – 600.000 km^2 of marine area in tropical and subtropical oceans (Figure 1) [35, 65]. As diverse ecosystems, coral reefs are known as "rainforests" of the sea because they contain nearly one-quarter of all marine organisms, including fishes, algae, crustaceans, and mollusks [31]. In addition, the main organisms in coral reefs are corals (hard corals and soft corals), which are known as reef-builders. Hard corals are invertebrates (phylum Cnidaria, class Anthozoa, and order Scleractinia) that are distinguished by their ability to produce calcium carbonate using energy supplied by zooxanthellae (symbiotic dinoflagellate) living in their tissues.

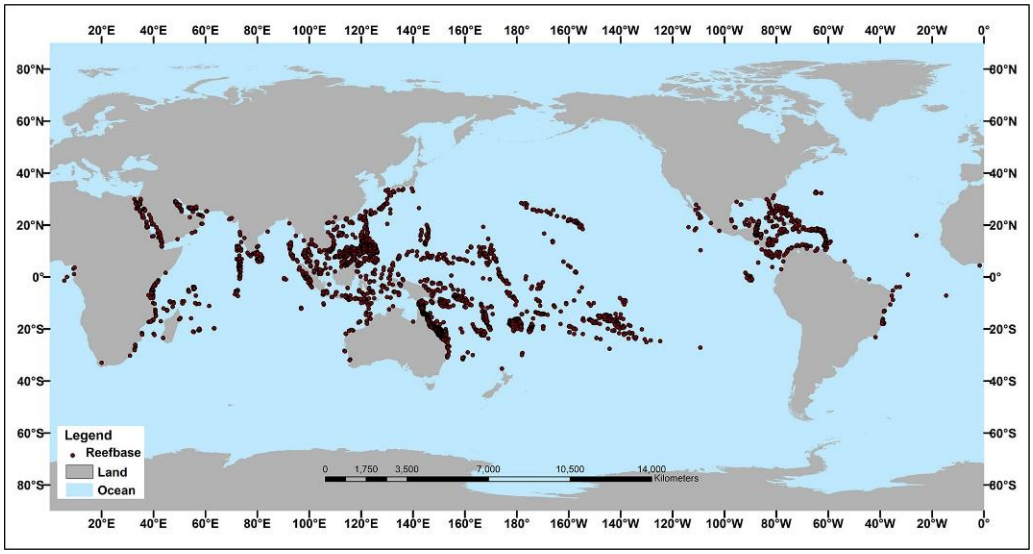

Figure 1 The distribution of reef building corals within tropical and subtropical waters; (NOAA, 2021)

With nearly 800 known species, hard corals (scleractinians) are the largest order of anthozoans [66, 67]. Soft corals, in addition to hard corals, are components of coral reefs which highly contributed to coral reef biomass [3]. Soft coral (Order alcyonacea; subclass octocorallia) is a dominant group in the sea's benthic zone, which contains over 3000 species. It is an important structural component of coral reef communities, nearly as important as scleractinian coral. This group of coral is comprised of the families Xeniidae, Nephtheidae, and Alcyoniidae [4].

The biodiversity of coral species is very high. However, numerous studies in recent decades have revealed that coral reefs are extremely vulnerable to changes in environmental conditions [30, 33, 68]. This situation is primarily caused by environmental stressors such as elevated temperature and carbon dioxide levels which leads to ocean acidification, rising sea levels, and freshwater runoff, as well as by human activity [31, 33]. As a result of environmental stress, approximately 30% of coral species died in the early 1980s, and nearly

90% of coral reefs may be destroyed in the next few decades if conservation measures are not implemented [33, 69-71]. Corals have many benefits to humans, including the role as a producer of some potential bioactive compounds [1, 72-74]. However, there are many negative consequences connected to coral loss induced by human activity. Therefore, the efforts on coral conservations in global is extremely necessary.

2.2. Biology of soft corals

Soft corals (Alcyonacea) are distinguished from hard corals by their absent ability to produce calcium carbonate skeletons. Instead of producing calcium carbonate biomass, soft corals produce a small amount of calcareous material called sclerites. Sclerites provide support for the soft body of coral as well as a grainy texture that protects it from predators [75]. For energy source, soft corals thrive in nutrient-rich waters with the help of their endosymbiont dinoflagellates (zooxanthella) as a major energy source. In the taxonomy position, this organisms belong to invertebrates, phylum Cnidaria. The taxonomy of soft coral according to GBIF.org (Global Biodiversity Information Facility) is described below:

Kingdom : Animalia
Phylum : Cnidaria
Class : Anthozoa
Subclass : Octocorallia
Order : Alcyonacea
Family : Alcyoniidae (Lamouroux, 1812)

As octocoralia, the polyps of soft corals which always have eight tentacles can be distinguished from hard corals, with polyps possessing multiples of six tentacles. Most octocorals have only one type of polyp (monomorphic) namely autozooid which is responsible for food capture and reproduction. Differently, some species are dimorphic, due to the appearances of a second type of polyp namely siphonozooid, which is smaller and has no rudimentary tentacles. The primary function of this organ is to irrigate colonies with seawater, as well as to transport the dissolved and small suspended food particles into the colonies [75]. The structure of octocoral polyps (autozooid and siphonozooid) are described in Figure 2.

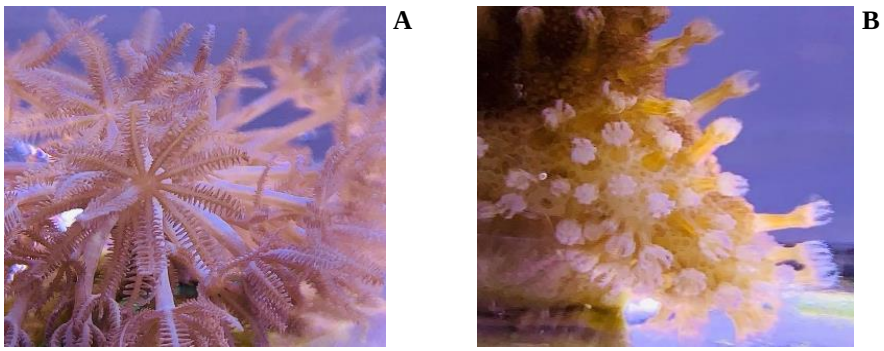

Figure 2 Structure of octocoral polyps. A: autozooids of *Xenia umbellata*, B: siphonozooids of *Lobophytum crassum* as dark dots around the bases of the larger and fully developed autozooids

Fabricius and Alderslade (2001) described that the autozooid of soft coral has a cylindrical or tubular structure with a mouth and tentacles at one end. The autozooid's upper body is composed of eight tentacles with finger-like extensions along each side called pinnules. Pinnate tentacles are mobile and contractile covered with sensory cells and stinging capsules, and filled with symbiotic algae (Figure 3). In addition, soft corals are characterized by their sclerites, which are used to classify soft corals into genera or species. Sclerites occur in varying concentrations in soft corals, and some octocorals are sclerite-free. This calcareous particles are produced by specialized cells which formed polycrystalline aggregates of calcite, a type of calcium carbonate. The shapes, sizes and color of sclerites vary among species of soft corals. Therefore, they are the most important feature used in the identification of octocorals [75].

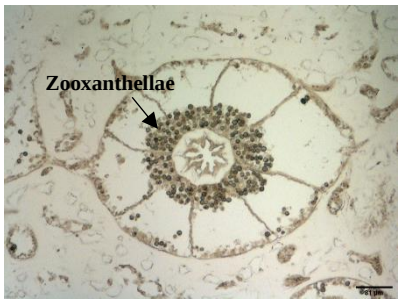

Figure 3 Cross-section through an autozooid polyp under light microscopy

Octocorals reproduce in three ways: through broadcasting eggs and sperm, internal reproduction, and larval brooding [76]. Some soft corals e.g. *Heteroxenia* and *Xenia* are hermaphroditic, thus, each mature colony contains both male and female reproductive structures [77]. On the other hand, asexual reproduction (propagation) is widespread and predominate in soft corals, including runner formation, colony fragmentation, fission, and budding [75]. Typically, propagation techniques are used on soft corals with a large body mass, such as *Sarcophyton* sp., *Lobophytum* sp., and *Sinularia* sp. In order to survive, soft corals require nutrition from the water column. They use autozooids to extract organic matter from the water, including phytoplankton cells, ciliates, bacterioplankton, and other microzooplankton [78, 79]. The majority of soft coral nutrition is provided by their symbiotic algae (zooxanthellae), which are found within the soft corals' tissue, particularly their gastrodermal cells. The coral protects the algae and provide compounds required for their photosynthesis, e.g. carbon dioxide ($CO_{2(aq)}$), ammonium (NH_4^+), and phosphates, which are metabolic "waste products" of the coral. In exchange, the algae provide some organic products, such as glucose, glycerol, and amino acids, which are used by corals to synthesize proteins, lipids, and carbohydrates, as well as calcium carbonate ($CaCO_3$) [80, 81].

2.3. Description of *Sarcophyton glaucum, Lobophyton crassum,* and *Xenia umbellata*

2.3.1. Morphology

Soft corals (Cnidaria: Anthozoa: Octocorallia) are one of the dominant invertebrate groups in the benthic area of the sea. This group of coral contributes an important structural component of coral reefs, which contributes to coral reef biomass [3]. The majority of soft corals are classified into three families: Xeniidae, Nephtheidae, and Alcyoniidae.

a. *Sarcophyton glaucum*

Sarcophyton glaucum (Quoy & Gaimard, 1833 in WoRMS, 2010) (family Alcyoniidae) is a large benthic coral commonly referred to as leather coral. The colonies have a smooth structure and a mushroom-shaped polypary. The mushroom-shape and sclerites within the coenenchymal tissue are used to identify this species [82]. Sclerites of this soft coral species are up to 2.0 mm large and spindle shaped [83]. *S. glaucum* is typically brown in color due to the presence of their symbiont (zooxanthellae) within their tissue. However, under stress, the color turns grey or greenish due to the loss of zooxanthellae [84]. As a polyp organism, *S. glaucum* live as colony and depends on the polyps for elemental functions [85]. Figure 4 illustrates the morphology of *S. glaucum.*

Figure 4 Morphology of *Sarcophyton glaucum*; A: propagated colony at ZMT, B: colony in the field (*www.meerwasser-lexikon.de*)

b. *Lobophytum crassum*

Belonging to the same family as *Sarcophyton* sp. (Alcyoniidae), *Lobophytum crassum* (Marenzeller, 1886 in WoRMS, 2010) is also an important members of shallow reef communities in the Indo-West Pacific. According to Marenzeller (1886), the *Lobophytum* genus contains approximately 43 species. *L. crassum* has smaller interior sclerites (< 0.5 mm and oval) than *Sarcophyton* species. The colony has feeding polyps (autozooids) and water pumping polyps (siphonozooids) (shown at Figure 2). Autozooid polyps possess short fat body columns (*ca*.1 cm) with eight branched tentacles with white color, and the siphonozooids are located on the body membrane as small holes on the surface [75]. In the wild and under normal conditions, the color of the *L. crassum* is light brown. However, when subjected to stress, the color of this species changed to grey and yellowish shades in between. The surface of *L. crassum* is harder than that of *S. glaucum* due to clubs with indistinct heads

ca. 0.10-0.20 mm in length and the spindles in the interior of the lobules, as well as long sclerites growing near the surface [86]. The morphology of *L. crassum* is shown in Figure 5.

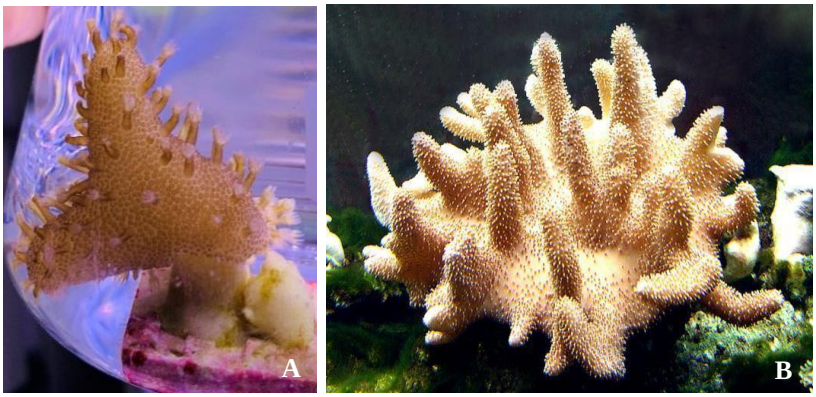

Figure 5 Morphology of *Lobophytum crassum*; A: propagated colony at ZMT, B: colony in the field (*www.meerwasser-lexikon.de*)

c. *Xenia umbellata*

Xenia umbelatta (Lamarck, 1816 1886 *in* WoRMS, 2010) (family Xeniidae) is a type of pumping coral, found in abundance on coral reefs in the Red Sea and the Indo-Pacific. Different to *S. glaucum* and *L. crassum*, this soft coral is a member of the Xeniidae family. The autozooid and siphonozooid polyp tentacles of *Xenia* species are well-known for their rhythmic pulsation [87]. *X. umbellata* is defined by its polyps, characterized by the number of rows of pinnules (lateral projections) along the tentacles, and the number of pinnules per row. Their morphology is illustrated in Figure 6. The colonies of *X. umbellata* are small and soft with cylindrical stalk, undivided or branched, and terminating in one or more domed polyp-bearing regions. Xeniid sclerites are relatively simple (size up to 0.025 mm diameter), with low structural diversity compared to the sclerites of other octocoral families [88]. As with other zooxanthellae symbiotic organisms, *X. umbellata* derives the majority of energy from the photosynthesis products of their symbiont (zooxanthellae).

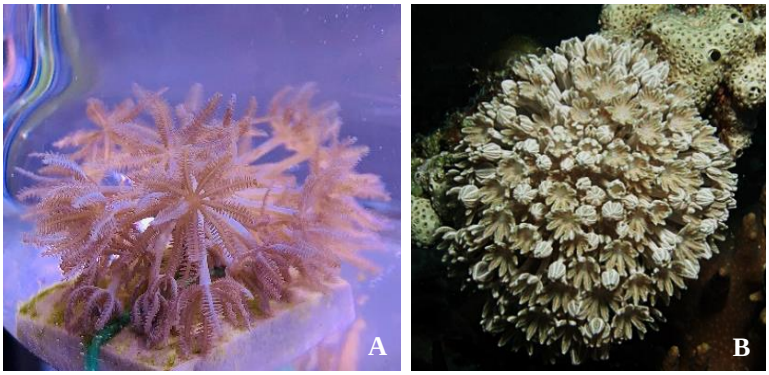

Figure 6 Morphology of *Xenia umbellata*; A: propagated colony at ZMT, B: colony in the field (*www.meerwasser-lexikon.de*)

2.3.2. Genetic identification

The three soft corals were described on the basis of their morphology, in addition a DNA-based species identification was carried out by our cooperation partner from ZMT

Bremen. DNA extraction was successful for all three species and resulted in six sequences listed Table 1. All three analyses (mutS, COI, and 28S) supported the identification of three well-defined soft coral species that matched the overall morphology: *Sarcophyton glaucum* and *Lobophytum crassum* (both Alcyoniidae), and *Xenia umbellata* (Xenidae). These results are summarized in Table 1.

Table 1 Molecular species identification of soft corals in this study

Sample of this study	Gene	% HQ	Species (No of specimen)	Alignment length [bp]	Overall mean distance
Sarcophyton glaucum	mutS	89.4	*Sarcophyton glaucum* (6)	708	0
Lobophyton crassum	mutS	89.0	*Lobophyton crassum* (3)	708	0
			Lobophytum borbonicum (1)	708	0
	COI	69.5	*Lobophyton crassum* (4)	815	0
	28S	26.1	*Lobophyton crassum* (11)	69	0
			Lobophytum depressum (1)	69	0
Xenia umbellata	mutS	84.7	*Xenia umbellata* (11)	714	0
			Xenia hicksoni (2)	714	0
	COI	39.7	*Xenia umbellata* (9)	375	0
			Xenia hicksoni (2)	375	0
	28S	40.0	*Xenia umbellata* (8)	515	0
			Xenia hicksoni (2)	515	0

The mutS sequences were assembled and supplemented with 204 Genbank sequences obtained via BLAST and word searches (preferably museum voucher), aligned using mafft, and manually trimmed. The final alignment, which included 711 positions and 207 sequences, was used to derive phylogenetic relationships (Figure 11 and 12). The best fitting substitution model was the Tamura 3 parameter model with Gamma distribution as inferred with MegaX [89]. The resulting mutS gene tree was calculated in Raxml and demonstrated 100 percent bootstrap support (BR) for *S. glaucum* and *L. crassum* at the genus level, and 98 percent for *X. umbellata* (Figure 7 and subtrees in Figure 8). The collapsed triangle in subtree 3 summarized identical *Xenia* sequences which are listed in Table 2.

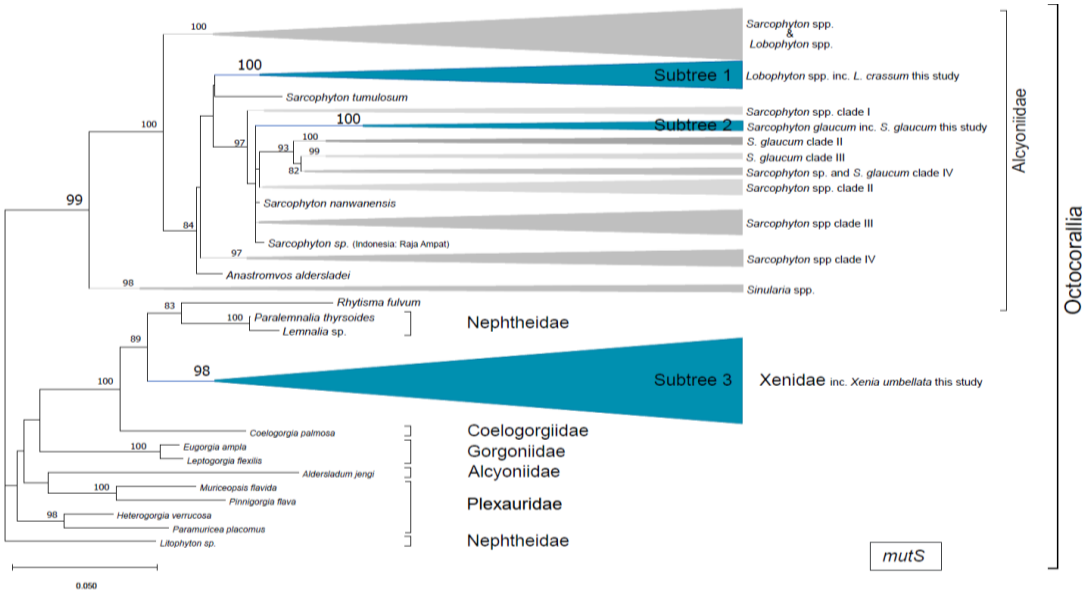

Figure 7 mutS gene tree tracing the phylogenetic relationships among the Octocoralia (*S.glaucum*, *L. crassum*, and *X. umbellata*) in this study. For better visibility parts of the tree containing the target sequences from this study were collapsed but fully expanded in Figure 8.

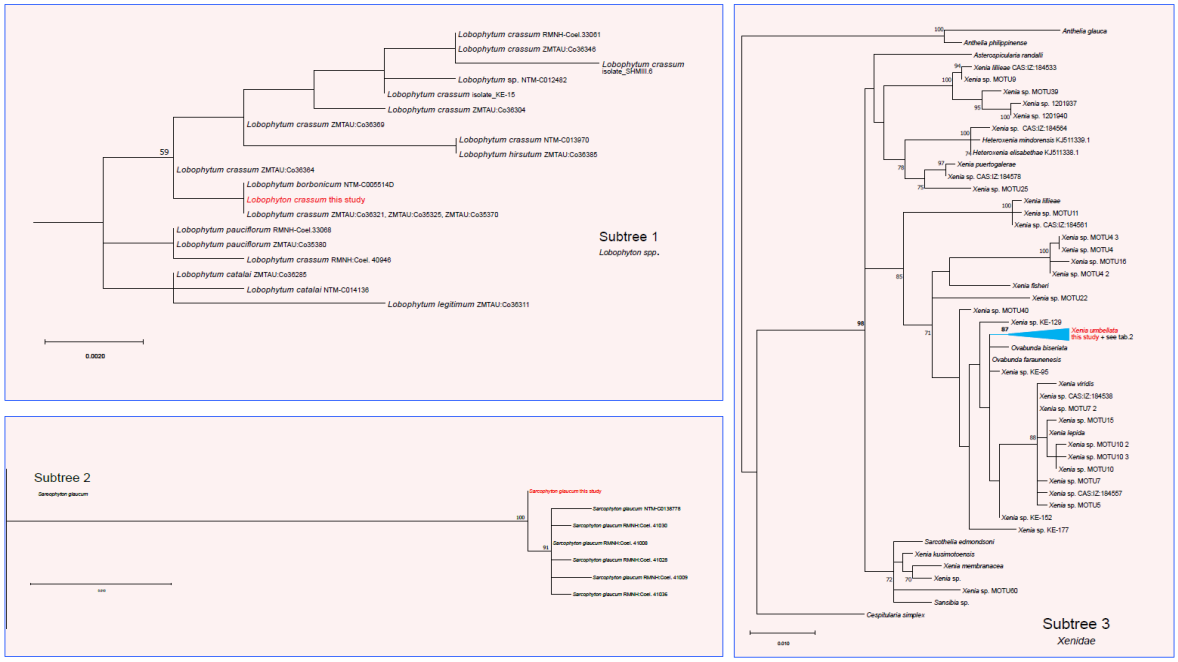

Figure 8 Phylogenetic sub-tree of each species *Lobophytum* spp (1), *S. glaucum* (2), and Xenidae (3)

The *Sarcophyton* specimen did not match with an identical entry in Genbank, but eight out of nine different positions in the mutS sequence from this study were related to unresolved purine or pyrimidine bases (Y/R for TC or GA) thus might be PCR or sequencing artefacts. Nevertheless, the BR is 100% for the *S. glaucum* cluster (subtree 2 in Figure 12). The *Lobophyton* specimen was identical to *L. crasssum* and *L. borbonicum* for mutS, to *L. crassum* for COI (Accesion No.: KF955107.1, MH516352.1, MH516359.1, MH516551.1; all museum vouchers) and *L. crassum* (MG583546.1, MG583545.1, MG583544.1, MG583543.1, MG583542.1, MG583541.1, MG583540.1, MG583539.1, MG583537.1, MG583534.1, KF915408.1) and *L. depressum* (MG583538.1) for 28S.

Table 2 Sequences with 100% identity to *Xenia* sp. from this study. The sequence length of the specimen from this study used to compare the identity is given in brackets.

Species with identical sequences	Museum voucher	Accession No. mutS (714bp)	Accession No. COI (376bp)	Accession No. 28S (155bp)
Xenia umbellata	ZMTAU:36792	KT590460.1	KT590441.1	MK400153.1
Xenia umbellata	ZMTAU:36791	-	KT590440.1	KY442370.1
Xenia umbellata	ZMTAU:37034	KT590459.1	-	-
Xenia umbellata	ZMTAU:36790	KT590458.1	KT590439.1	KY442369.1
Xenia umbellata	ZMTAU:36788	KT590457.1	KT590438.1	KY442367.1
Xenia umbellata	ZMTAU:36883	KT590456.1	-	-
Xenia umbellata	ZMTAU:36877	KT590455.1	-	-
Xenia umbellata	ZMTAU:36780	KT590454.1	KT590437.1	KY442359.1
Xenia umbellata	ZMTAU:36784	KT590453.1	KT590436.1	-
Xenia umbellata	ZMTAU:36783	KT590452.1	KT590435.1	KY442362.1
Xenia umbellata	USNM:1202016	KC864921.1	KC864990.1	KY442391.1
Xenia umbellata	USNM:1202005	KC864912.1	KC864981.1	KM201437.1
Xenia hicksoni	ZMTAU:Co34073	MK396705.1	MK396749.1	MK400170.1
Xenia hicksoni	ZMTAU:Co34072	GQ342529.1	GQ342463.1	JX203759.1

In addition, the symbionts (zooxanthellae) that live inside the soft corals' endodermal cells were identified genetically. *Symbiodinium* cells were collected from the incubation water column, and then the pbsA gene was amplified and sequenced. The sequence identity was confirmed using BLAST searches. As a result, the zooxanthellae of *S. glaucum* and *L. crassum* were 100% identical (*Symbiodinium* sp. DJT-2013h), and were distinct to a clade of zooxanthellae found in *X. umbellata* (*Symbiodinium glynnii* DJT-2013h) (Table 3). The clade of the symbiont will probably affect the symbiont's nutrition supply to the host, as well as the metabolite composition in the host, and the sensitivity to stressor compounds.

Table 3 BLAST results of *Symbiodinium* psbA sequences in the nucleotide database (GenBank)

Host species	Length [bp]	HQ [%]	Best Blast hit	e-value
Sarcophyton glaucum	100	75.0	*Symbiodinium* sp. DJT-2013h isolate Bar05_80 (psbA)	1e-08
Lobophytum crassum	92	30.4	*Symbiodinium* sp. DJT-2013h isolate Bar05_80 (psbA)	6e-06
Xenia umbellata	896	87.7	*Symbiodinium glynnii* (psbA)	1e-73

The difference of the e-value is related to the differences in sequence length.

2.4. Environmental conditions and their influence to soft corals

Soft corals are extremely sensitive to environmental stress. There are numerous environmental stressors that affect soft corals, including: a) physical stressors, i.e. high temperature, mechanical disturbance, microplastics, b) chemical stressors, namely acidification, level of CO_2, heavy metals pollution, sunscreen components, plasticizer, and pesticide exposure, c) biological stressors such as infection of pathogens (microorganisms) and predatory fish [39, 90-95]. Above all, human activity has been identified as a cause of coral reef decline, both directly and indirectly. [2, 34, 36, 96, 97].

a. Physical stressor

Climate change, including an increase in seawater temperature and acidification of the ocean, is a significant risk factor for physical stress on corals especially soft corals [93, 98]. The high temperature (thermal stress) of sea water cause photo-oxidative stress on corals, and further leads to loss of zooxanthellae from their body [95, 98, 99]. Beside of high temperature of sea surface the mechanical disturbance and the microplastics induction also contributed to the stress of soft corals [100]. Increases in ocean acidification can limit the capacity of corals to produce calcium carbonate, and further caused declines in reef accretion as well as reduced coral growth [101-104]. Furthermore, the stressors mentioned above can lead to the large-scale coral bleaching, paling in color of coral colonies [105]. Over the last several decades, a combination of high temperatures and ocean acidification has reduced coral cover by up to 5% per year in some regions and resulted in coral cover loss of approximately 50–80% [106, 107].

b. Chemical stressor

Chemical stressors are associated with human consumption and chemical waste generated during agricultural/industrial as well as household activity. One of the products

consumed by human worldwide is personal care items, including sunscreens (UV filters). In general, sunscreen metabolites are detected at concentrations higher than 1 ppm in seawater [37]. These substances have similar side effects as other xenobiotics, including causing bleaching, damaging DNA, and eventually killing corals [37-39]. Danovaro et al. demonstrated that sunscreens, even at low concentrations cause rapid and complete coral bleaching as a result of their ability to initiate the lytic viral cycle in zooxanthellae with latent infections [92].

Approximately 25% of coral reefs worldwide are threatened by agricultural pollutants [108]. Pesticides are the most common agricultural pollutants that affect coral, particularly in Queensland and Great Barrier Reef (GBR) waterways [91], as well as in intertidal/subtidal sediments, including mangroves, seagrass, and waters surrounding coral reefs [109-111]. The contamination of pesticides in the marine ecosystem has the potential to destroy organisms in this ecosystem. Several pesticides have been reported as toxic component to coral reef biota, namely organophosphorous (OP) insecticides e.g. chlorpyrifos; herbicides e.g. glyphosate (Roundup®); triazine herbicides e.g. atrazine, simazine, ametryn and irgarol; and urea herbicides e.g. diuron and tebuthiuron [40, 41].

c. Biological stressor

Besides their endosymbiont dinoflagellate (zooxanthellae), there are numbers of other microorganisms which interact with the corals, i.e. bacteria, archaea, viruses, and other eukaryotic microorganisms [112, 113]. Some are found as mutualistic microorganisms, but some are known as pathogens to the corals. Coral pathogens such as *Vibrio shilonii*, *V. coralliilyticus*, *V. campbellii*, and *Serratia marcescens* have been identified as causal agents of coral bleaching [114]. Several diseases on corals have been reported, mostly caused by *Vibrio* spp., i.e. dark spot syndrome, shut down reaction caused by *Vibrio harveyi* and *V. alginolyticus*, as well as ulcerative white spots, black band disease type II, yellow band disease, white syndrome disease, white band disease, which further cause the decline of coral populations [115-119].

2.5. Metabolomics study on soft corals

Metabolomics is a rapidly growing field of omics technology. This technique is defined as the comprehensive measurement, identification, and quantification of all low-molecular-weight metabolites (<1 kDa) in a biological specimen using a high-throughput approach. Metabolomics can be classified into two approaches: targeted and untargeted. Targeted metabolomics quantifies known metabolites that belong to a particular pathway or class of molecules. This method entails absolute quantification via an internal standard in order to identify known compounds associated with specific pathways based on the study's hypotheses [120, 121]. In contrast, untargeted metabolomics is used to identify and quantify as many metabolites as possible [120]. This approach can be used to rapidly assess a large number of metabolites at the same time and to provide a more complete picture of an

organism's status [122, 123]. Additionally, one of the significant advantages of the untargeted approach is the possibility of discovering novel compounds. In untargeted metabolomics, multivariate data analysis is used to generate hypotheses based on sample difference and classification [124].

In general, metabolomics analysis entails three stages: preparatory work, analytical work, and data processing and interpretation [125] (Figure 9). The first step is to design an experiment to address a specific biological question. This includes the selection of appropriate material, the number of replicates, the sample sizes, and the collection as well as storage conditions for natural product resources. Further, the sample preparation is necessary in metabolomics experiments, including grinding, extraction, and centrifugation for analysis. Different types of analytical techniques can be used to collect data, which have been developed recently, including NMR and chromatographic separation of metabolites via LC-MS and GC-MS. NMR metabolite profiling provides a complete and quantitative metabolite signature for a complex extract, whereas the LC-MS method improves sensitivity by separating individual chemical components into distinct peaks. This method increased the possibility of identifying novel metabolites with low abundance [56, 126, 127].

Metabolomics techniques have been used in recent years to investigate the coral metabolome in order to provide insight into the complexity of metabolites in soft coral. [56, 60, 128]. Farag et al. (2016) used a comparative MS and NMR approach to compare secondary metabolite profiling from corals, revealing differences in metabolite composition between species [56]. For the first time, this approach was used to investigate the metabolism of *Sarcophyton* sp. in relation to their genetic diversity and growth habitat. As a result of this study, it was determined that a comparative metabolomics approach utilizing UPLC-MS and NMR can be a highly effective tool for capturing the (secondary) metabolome status and complexity of soft corals, as well as for monitoring corals and the factors (genetic and environmental) that contribute to their metabolite differences.

Furthermore, metabolomics in soft coral has been proved to investigate the responses of soft corals against elicitors (chemical stressors). Farag et al. (2017) conducted research to determine the effect of biotic and abiotic stressors on the natural product pathways of soft coral and associated algae (zooxanthellae) [58]. Apart from chemical stressors, Farag et al. (2018) examined environmental stressors (global climate change), such as thermal and CO_2 level stress on the soft corals *S. ehrenbergi* and *S. glaucum* [60]. To analyze the data and test their hypotheses, they used multivariate data analysis, specifically principal component analysis (PCA) and hierarchical cluster analysis (HCA). The purpose of this analysis is to reduce the dimensionality of the dataset in order to gain a better understanding of the dataset trends generated by tested samples and to assess the significant variations observed at the metabolome level [63].

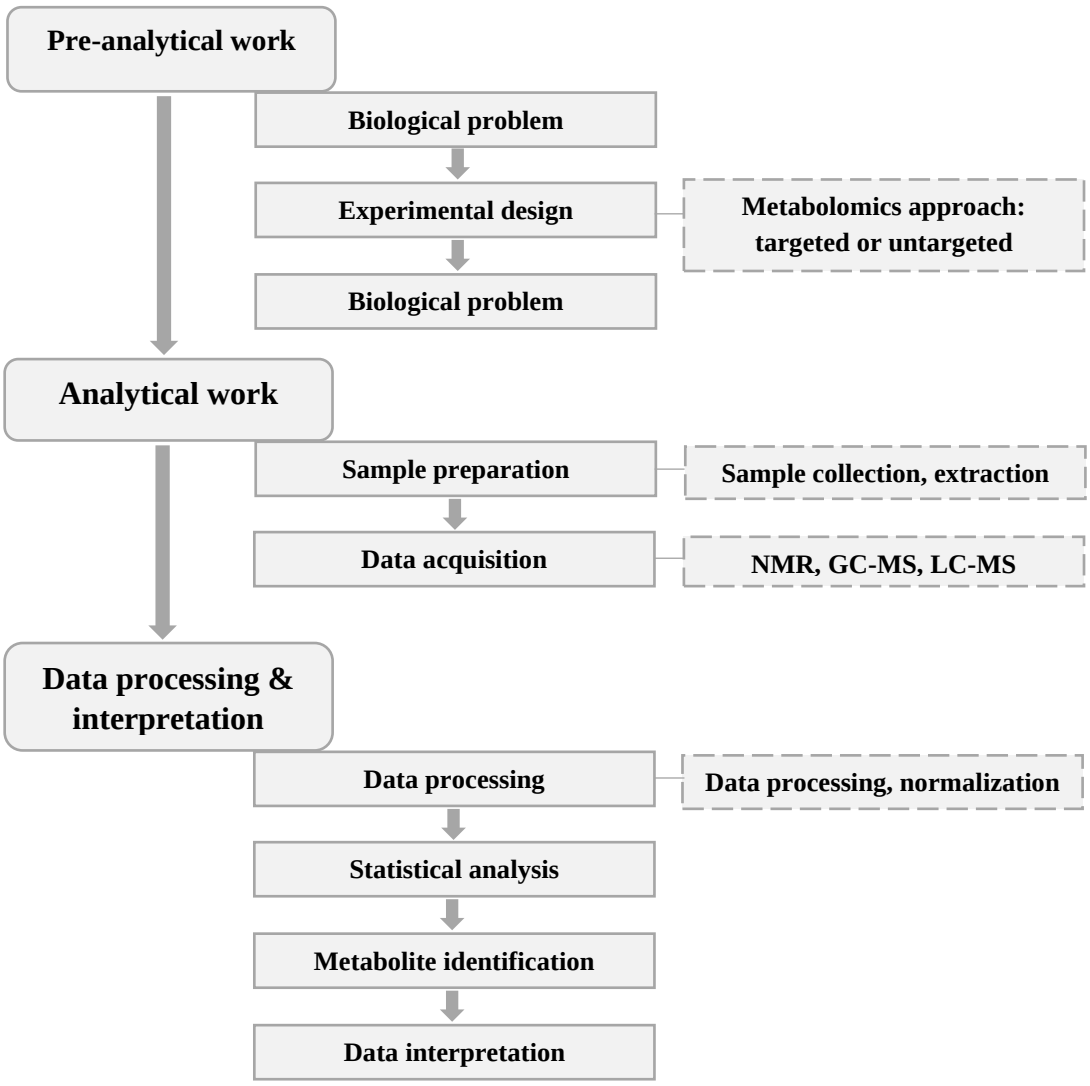

Figure 9 Metabolomics analysis workflow

Similar to the work of Farag, Wessjohann, and coworkers, Santacruz et al. (2019) compared the metabolite composition of 28 soft corals, belonging to 5 genera (*Plexaura*, *Antillogorgia*, *Eunicea*, *Plexaurella*, and *Pseudoplexaura*) from the Caribbean coast of Colombia using liquid chromatography-high resolution mass spectrometry [57]. There is an additional approach for data analysis in this study, in which data processing was performed using Galaxy 4.0 software. Furthermore, they conducted a statistical analysis of the data using the MetaboAnalyst platform.

III. Materials and method

3.1. Soft coral culture

Sarcophyton glaucum Quoy, *Lobophytum crassum* Marenzeller, and *Xenia umbellata* Lamarck are soft corals cultured prior to 2011 in the Leibniz Centre for Tropical Marine Ecology (ZMT) in Bremen, Germany. As these are long-lived aquarium strains, the origin of collection for all three species is unknown. Fragments (*ca*. 1.5-2 cm^2) of each cluster of *S. glaucum* and *L. crassum* were generated from a single colony of these soft coral species, and immediately attached onto the nubbin. The soft coral *Xenia umbellata* was purchased as a 3x3 cm per fragments from a mariculture coral trader (Coralaxy GmbH, Bentwisch, Germany).

All soft coral fragments were then kept in an initial 2500 L maintenance aquarium in the marine experimental facility (MAREE) at ZMT, with recirculation system at 26 ^oC with a 50 cm distance between coral nubbins and a blue/white combination light of two 39 W fluorescence light bulbs (Figure 10). To maintain the salinity of the water, the artificial sea water (detailed composition see Table 4) was changed daily, while other water parameters were monitored once per week and adjusted as needed. As part of the simulated tropical marine environment facility at the ZMT, this aquarium contained fish, invertebrates and algae, since soft corals are heterotrophic organisms.

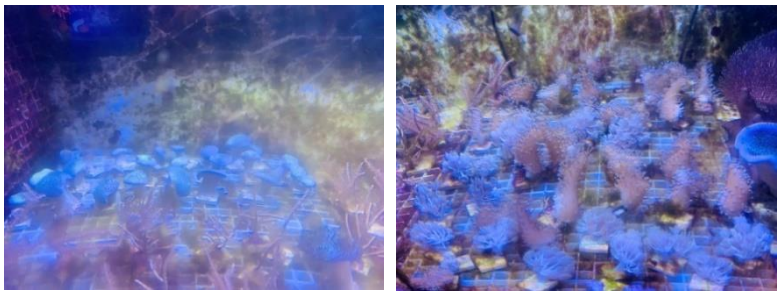

Figure 10 Fragments of soft corals in the maintenance aquarium

3.2. Chemicals and reagents (elicitors)

Methanol-D4 (99.80% D) and hexamethyldisiloxane (HMDS) were purchased from Deutero GmbH (Kastellaun, Germany). For calibration of chemical shifts, HMDS was added to a final concentration of 0.86 mM. Isopropanol and formic acid (LC-MS grade) were obtained from Baker (The Netherlands); Milli-Q water was used for LC analysis. All chemicals as elicitors: glyphosate, simazine, oxybenzone, and octinoxate were purchased from Sigma Aldrich (Germany), $CuSO_4$ was purchased from Carl Roth (Germany), plasticizer dimethyl phthalate (DMP) was purchased from Fluka (Italy), irregularly shaped polyethylene terephthalate (PET) micro-plastic was obtained from Goodfellow® GmbH Germany (PET powder ES306030), density: 1.3-1.4 g/cm^3. The culture media for *Vibrio campbellii* (marine broth CP73.1) was purchased from Carl Roth (Germany).

Table 4 Mean values (± SE) of selected physicochemical parameters of the seawater in the coral maintenance tank at MAREE, ZMT

Parameter	Mean (± SE)
Temperature [°C]	25.5 ± 0.4
Salinity [ppt]	34.7 ± 0.1
pH	7.97 ± 0.07
NO_3^- [mg/L]	1.19 ± 0.78
PO_4^{3-} [mg/L]	0.07 ± 0.03
Ca^+ [mg/L]	400.13 ± 18.25
Mg^+ [mg/L]	1289.46 ± 41.43
K^+ [mg/L]	336.02 ± 29.20
Sr^+ [mg/L]	2.63 ± 0.15

Note: KH [odh]= 5.92 ± 0.77; Ta [mmol/L]= 2114.41 ± 275.29

3.3. Genetic identification of soft corals species

The taxonomic identification was done using the barcoding region mutS for all three soft coral species. For DNA extraction, 5 mg of tissue were cut from the upper part of the coral using a scalpel, the capitulum (head) in case of the two leather corals and polyp with branch tissue for the *Xenia* specimen. DNA extraction was done using the Quick-DNA Universal Kit (Zymo Research, USA). Approximately 5-10 mg tissues were digested in 500 µL Genomic Lysis Buffer at 55 °C for 2h. After lysis, the cell debris was removed by centrifugation at 12000 xG. All subsequent steps followed the manufacturer's recommendations by using 13000 xG until the final step with 50 µL elution buffer at 16000 xG. DNA integrity was visually checked on an agarose gel.

The volume of 2 µL of 1:5 dilutions of the extracted DNA were used in 50 µL PCR reactions with the Msh1 primer ND42599F 5' GCCATTATGGTTAACTATTAC 3' [129] and mut3458R 5' TSGAGCAAAAGCCACTCC 3' [130]. The PCR conditions were one initial denaturation for 2.0 min at 94 °C; followed by 35 cycles of 1.5 min at 94 °C, 1.5 min at 58 °C, and 1.0 min at 72 °C, and the final extension step was for 5.0 min at 72 °C. PCR products were visually checked on an agarose gel, SAP digested and sequenced at StarSeq (Mainz). For taxonomic identification, sequences were primer and quality trimmed using the default parameter in Geneious Prime 2020.1.2 [131] and denovo assembled. The assembled consensus sequences were used to collect similar sequences from Genbank via BLASTn in the Nucleotide collection plus additional taxonomic searches for Msh1 in this nucleotide database (NCBI). The harvested sequences were aligned using Mafft [132] and trimmed by eye at both ends. The taxonomic assignment was done by calculating a Neighbor Joining phylogenetic tree in Mega X [89] using the default parameters except using 1000 bootstrap replicates.

3.4. Genotyping of zooxanthellae

Sequences of the non-coding region of the plastid psbA minicircle ($psbA^{ncr}$) were used to compare symbiont genotypes from the three soft coral species. DNA extractions from the genetic identification of soft coral species were used as described above with the primer 7.4-Forw, 5′ - GCA TGA AAG AAA TGC ACA CAA CTT CCC - 3′, and 7.8-Rev, 5′ - GGT

TCT CTT ATT CCA TCA ATA TCT ACT [133] and the following PCR conditions: 94 °C for 2 min; then 40 cycles of 94 °C 10 s, 55 °C for 30 s and 72 °C for 2 min; followed by a final extension at 72 °C for 10 min. PCR products were visually checked on an agarose gel, SAP digested, sequenced and processed in Geneious Prime 2020 as described for the genetic identification of soft corals species. The resulting *Symbiodinium* psbA sequences were matched with sequences in the nucleotide database (GenBank) using BLAST.

3.5. Elicitation

3.5.1. Elicitors preparation

In this experiment, the elicitors were classified into three categories: chemical, physical, and biological elicitors. Chemical elicitors included a widely used herbicide (glyphosate), a fungicide (simazine), two sun-blockers (oxybenzone and octinoxate), a plasticizer (dimethyl phthalate), and a heavy metal component ($CuSO_4$). Micro-plastic was used as the physical elicitor, while *Vibrio campbellii* was used as the biological elicitor. Separate stock solutions of glyphosate, simazine, oxybenzone, octinoxate, and plasticizer were prepared in deionized water at a concentration of 100 mg/L, whereas $CuSO_4$ was prepared at a concentration of 1 mg/L and further diluted with water to final concentrations according to Table 5. In addition, two separate concentrations of glyphosate were prepared (100 mg/L and 1000 mg/L). For the biological elicitor, this study used a concentration of 1 x 10^7 bacteria *Vibrio campbellii* (ATCC 25920). The detailed concentrations of the elicitors are shown in Table 5.

Table 5 Concentrations of the elicitors

Elicitor	Concentration	Concentration (µM)
Glyphosate	5 mg/L	30
Glyphosate	10 mg/L*	60
Glyphosate	25 mg/L	148
Glyphosate	50 mg/L	295.7
Glyphosate	100 mg/L	591.4
Glyphosate	1000 mg/L	5914
Simazine	10 mg/L*	49.6
Oxybenzone	10 mg/L*	43.8
Octinoxate	10 mg/L*	34.4
$CuSO_4$	100 µg/L*	0.627
Plasticizer (DMP)	100 µg/L*	0.515
Microplastic	±1500 particles/100 mL*	

Note: * = selected concentration for elicitation process (Chapter V)

Vibrio campbellii (ATCC 25920/DSM 19270) in this experiment is part of the bacteria collection in the ZMT. Since the bacterium *Vibrio campbellii* belongs to the safety level 1 group, the treatments were performed in the microbiology laboratory (biosafety level 2) at ZMT. Before start the experiment, the bacteria were grown in the marine broth media CP73.1 (Carl Roth, Germany) for 24 h at 30 °C, with 35 rpm. A concentration of 1 x 10^7 bacteria cells was applied as a selected concentration for the treatment. This concentration was determined using optical density (OD) of bacteria. The result of OD was then calculated to the number of cell, which is OD_{600} of 1.0 = 8 x 10^8 cells/mL.

3.5.2. Elicitation process: Stress treatments of soft corals

Individual soft coral fragments were transferred from the maintenance tank to a separate 250 mL Erlenmeyer (i.e. experimental jars). Each Erlenmeyer flask was filled with 200 mL of sea water containing elicitors according to Table 5 and the coral was placed in this Erlenmeyer. The elicitation process was carried out in the incubator cabinets Panasonic® cooled incubator MIR-254-PE, and the experimental jars were randomly placed in the incubator cabinet equipped with temperature control unit to ensure a constant temperature (16 ^{o}C). The lamp was placed in the cabinet with 50 cm distance from jars. The blue/white combination light was provided by an Aquaillumination® lamp (Hydra FiftyTwo HD) and controlled through the free myAI® App for smart phones and tablets. The adjusted composition of the light produced optimal fluorescence (15% of blue light and 45% of white light) with the intensity 120-130 lx. Sea water in the jars was gentle aerated by pumping compressed air through a glass pipette (Pasteur pipette). The design and the real cabinet are shown in the Figure 11.

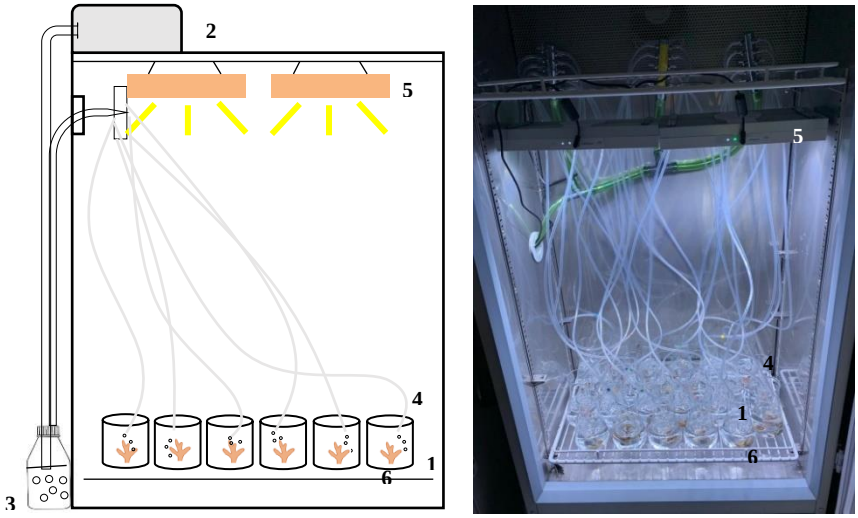

(a) (b)

Figure 11 Schematic overall set up with with physical and chemical elicitors; 1: experimental tank, 2: pumping compressed air, 3: water for moisture the air bulb, 5: Aqua-illumination lamp, 6: soft coral fragment; (b) Photo of the overall setup at the ZMT

All of the experiments were conducted in three biological replicates for each soft coral species over a five-day period with daily water exchange. Three soft coral fragments were exposed to control conditions to account for any possible effects of the experimental environment. To alleviate soft coral stress in their new environment (incubator), one day acclimatization of soft coral fragments was performed. The purpose of acclimatization was to adapte the soft corals to the new environment after movement and change condition. The soft coral's responses to elicitors was observed and documented daily in order to record the polyp structure and their behaviour during elicitation. The investigated soft corals species were divided into three batches for the experiment. *S. glaucum* was the first batch, followed by *L. crassum* in the second batch, and *X. umbellata* in the third batch.

Herein, all experiments with *V. campbelii* were conducted in the laboratory of safety level 2 at ZMT, Bremen, for safety reasons. The condition was established similarly to the cabinet culture for other treatments. Experimental jars were filled with 200 mL of sea water containing *V. campbelli* bacteria at a concentration of 1 x 10^7 cells. As a substitute for the cabinet, an aquarium equipped with a water bath was used to maintain the culture's temperature. The experimental jars were randomly placed in a 28 °C water bath aquarium under a blue/white combination light with the same properties as described previously. The Aquaillumination® lamp was installed in the cabinet 35 cm away from the jars. A gentle aeration of the sea water in the jars was accomplished by pumping compressed air through a glass pipette (Pasteur pipette). The treatment facility's design is depicted in Figure 12.

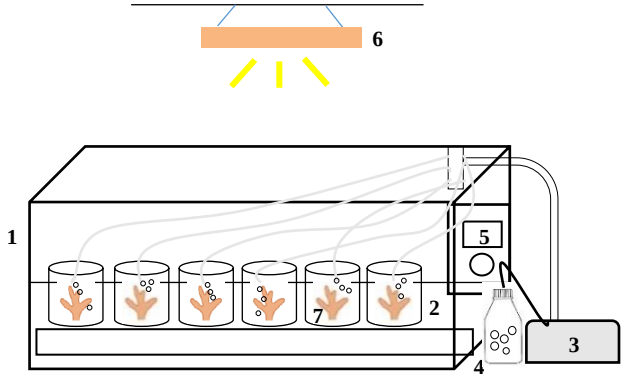

Figure 12 Schematic overall set up treatment with *Vibrio campbellii*, 1: aquarium, 2: experimental tank, 3: pumping compressed air, 4: water for moisture the air bulb, 5: temperature controller for aquarium, 6: Aqua-illumination lamp, 7: soft coral fragment

3.6. Determination of soft coral responses during stress treatments

3.6.1. Morphological response

The coral responses were observed every day and recorded with the camera. Morphology of soft corals includes color, retraction of tentacles of *S. glaucum* and *L. crassum*, as well as the tentacles pumping rate of *X. umbellata*. These features were recorded to ascertain the elicitor's effect on soft corals. Furthermore, the dead individuals of *S. glaucum* and *L. crassum* were identified based on their morphology (e.g. color and retraction of tentacles). The tentacles of *X. umbellata* were included as the indicator to determine the stress of soft coral in this species, which shown in the rhythm of the pumping rate per minute. Five randomly chosen tentacles from each individual soft coral were used to determine their pumping rate, and further quantified using a hand counter.

3.6.2. Zooxanthellae quantification

The density of zooxanthellae populations was determined using a quadruplicate hemocytometer. The water from the soft coral culture (before and after treatment) in the jars was collected separately in falcon tubes (50 mL) and centrifuged (4000 xG; 5 minutes) to separate the zooxanthellae (pellet) from the water (supernatant). The pellet was then resolved with sea water (5 mL) for further centrifugation. The supernatant was removed from the pellet, and 1 mL of sea water was added. The pellet and seawater were then homogenized

with a vortex mixer until no visible clumps remained. The zooxanthellae cells were counted using a hemocytometer under a light microscope. Three equal-sized squares of the big square were used to count the number of zooxanthellae in each treatment experiment. The total of zooxanthellae cells per mL was calculated according to following formula.

$$\text{zooxanthellae cell} = \frac{\Sigma \text{ cell observe}}{\Sigma \text{ observe square}} \text{ x } \Sigma \text{ square per chamber x } 10^4$$

3.6.3. Pulse amplitude modulation (PAM) fluorometry measurements

The photochemical efficiency of photosystem II (PSII) is used to determine the chlorophyll content of green plants. This method can be also used to determine the PSII photochemical efficiency of symbiotic microalgae (zooxanthellae) within soft coral tissue. The PSII yield was determined on all nubbins of soft coral fragments using a pulse amplitude modulated (PAM-2500) portable chlorophyll fluorimeter (Walz, Germany). The main optical fiber of the PAM instrument was put on the top (umbrella) of the investigated soft corals (*S. glaucum* and *L. crassum*) with the distance of *ca*. 3-5 mm, since the zooxanthellae are mainly concentrated in this part. For *X. umbellata*, the optical fiber of PAM was placed *ca*. 1 cm above the colony to prevent damage, due to the easy breaking of their tentacles. All measurements were performed in dark condition. The soft corals in each jar were placed in the dark box for 20 minutes before the PSII measurement. The yield of PSII (*Y* (PSII)) is defined according to following formula.

$$\text{Y (PSII)} = \frac{(\text{Fm}' - \text{F})}{\text{Fm}'}$$

Y (PSII) : Yield of photosystem II
Fm′ : Maximum fluorescence yield in the given light state of chlorophyll
F : Steady state fluorescence yield

3.6.4. Histology profiling of soft corals tissue after stress treatments

The soft corals were cut with a clean scalpel and immediately placed in the histological fixative Carnoy's solution (ethanol/chloroform/acetic acid, 6/3/1 [v/v/v]) for 2 h at 4 °C, followed by placement in 70% ethanol [134] until further analysis. Each fragment of coral tissue and skeleton was decalcified in 10% neutral EDTA (ethylenediaminetetraacetic acid titrated to pH 7.00 with NaOH) by changing the solution every 24 hours until only tissue remained. Afterwards, samples were stored in 70% ethanol at 4 °C until further processing. Following that, the tissue was successively embedded in a solution of 10-30 percent ethanol at room temperature for 40 minutes, 50% for 3 hours, 70% overnight, and finally 100% for 20 minutes, eosin for approx. 20 minutes, 50-100 percent rotihinsol for 1 hour at room temperature, and 50-100% paraplast for 1 hour at 60 °C.

The embedded samples of the soft corals tissue were sectioned at 10 µm thickness using a rotary microtome Microm Microtome (HM325). The tissue sections were stretched at 42 °C and backed to Poly-L-Lysin coated slides overnight. Slides were deparaffinized, while exchanged in several solutions, e.g. roticlear 1 and roticlear 2 (each 10 min), roticlear/iso-

propanol (1/1 [v/v]), propanol, propanol:ethanol (1:1), 96% ethanol, 70% ethanol, 50% ethanol, and 30% ethanol each for 5 min, respectively. Tissue slides were rinsed in PBS for 10 min (two times), and were stained with wheat germ agglutinin (WGA) in PBS for 20 min, followed by overnight enclosure in rotimount DAPI (4′,6-diamidino-2-phenylindole). Coral tissue were then visualized using a Laser Scanning Microscopy (LSM) 880 (Zeiss, Germany) with the Plan-Apochromat 10x0.45 M27 lens 10x0.3 lens with the detection range appropriate for the detection of dyes, driven by Zen software (version 4.6). Zooxanthellae chlorophyll auto fluorescence was induced when the tissue sections were excited with laser diode 405/30 excitation and HeNe 633. Mucocyte cell fluorescence was generated by exciting the WGA-conjugated Alexa Fluor 647 through a λ 633 nm and 405 nm for chlorophyll. The images obtained under these two channels were artificially colored green (zooxanthellae) and red (mucus-WGA).

3.7. Chemical investigation (metabolite profiling) of soft coral metabolites

3.7.1. Sample preparation and metabolite extractions

After five days elicitation, each of the soft coral was then cut with a clean scalpel and transferred to liquid nitrogen. The frozen soft coral tissues were ground with a pestle in a mortar using liquid nitrogen and kept at -20 °C until further analysis. The frozen powder of soft coral materials were lyophilized until dryness, and then weighted. In total, 81 soft corals samples from three different species were harvested. All samples were then transferred to Eppendorf tubes containing 3 stainless steel balls (5 mm) and ground for 30 seconds with a mill grinder at the frequency of 30.0 l/s. The grinding was performed twice with a break of 1 min in between to avoid warming of the samples. For each species, a quality control (QC) sample was prepared, which is contained of equal parts of all individual samples.

Freeze dried soft coral samples (50 mg each) were extracted with 1.0 mL of CD_3OD containing hexamethyl-disiloxane (HMDS) at a concentration of 0.86 mmol/L as internal standard using an ultrasonic bath for 15 min. Extracts were then vortexed vigorously for 20 s and centrifuged at 14000 xG for 5 min to remove debris. After centrifugation, the supernatant was transferred into a 5 mm NMR tube for ^{1}H-NMR measurement. For LC-ESI-HRMS, 8 mg of freeze dried soft coral samples were extracted with 1.0 mL methanol containing 8 µg/mL umbelliferon as internal standard using an ultrasonic bath for 15 min. Extracts were then centrifuged at 14000 xG for 5 min to remove debris. 100 µL of supernatant was aliquoted and diluted to a concentration of 2 mg/mL for the MS measurement.

3.7.2. Thin layer chromatography (TLC) analysis

For each sample, 15 µL extract (20 mg/mL in methanol) was applied on TLC Silica Gel plates (60 F254, 20 × 10 cm, Merck). The analysis was performed with the mobile phase *n*-hexane/ethyl acetate (3:2 v/v). After elution, the TLC spots were visualized under fluorescence light at λ 366 nm and 254 nm (Camac photovisualizer), as well as with vanillin sulfuric acid reagent followed by heating.

3.7.3. Analysis of metabolites via NMR

The ^{1}H NMR spectra of soft corals extracts were recorded with an Agilent (Varian) VNMRS 600 NMR spectrometer operating at a frequency of 599.83 MHz at 25 °C. ^{1}H-NMR spectra were measured with: pulse angle = 90°, relaxation delay = 27.2737 s, acquisition time = 2.7 s, pulse repetition rate (r1) = 30 s, pulse width (pw) = 7μs (90°), number of scans = 160, number of measured point (np) = 64K data points, and zero filling 128K. The standard CHEMPACK 8.1 pulse sequences (gHMBCAD and gHSQCAD) implemented in Varian VNMRJ 4.2A spectrometer software was used to record the HMBC and HSQC spectra of the QC samples. Chemical shifts were referenced to internal HMDS (δ ^{1}H: 0.062 ppm; δ ^{13}C: 1.96 ppm).

3.7.4. NMR data processing and PCA analysis

^{1}H NMR spectra were automatically Fourier transformed using the standard VNMRJ window function and zero filling. The spectra were referenced to internal HMDS at 0.062 ppm (δ ^{1}H). Further, MestReNova version 11.0.2-18153 (Mestrelab Research S.L., Spain) was used to pre-process spectra, such as removal of regions without signals (i.e. the noise and internal standard region), as well as phasing and baseline correction (Bernstein polynomial fit). A binning size of 0.02 ppm was used, with additional cut out the solvent and HMDS signal, and then binned data table (.csv) was generated. The solvent regions at 4.50-5.10 ppm (water), 3.11-3.40 ppm (CD_3OD), and 6.40-6.60 ppm; 7.00-7.80 ppm (elicitors) were removed before the generation of the bin table, and the total sum normalization was applied. The bin table was further analysed with R program (version 3.6.3.) and the PCAmethods (1.78.0) package was utilized.

3.7.5. Analysis of metabolites via LC-ESI-HRMS

The positive ion high resolution ESI mass spectra were obtained by use of an Orbitrap Elite mass spectrometer (Thermo Fisher Scientific, Bremen, Germany) system equipped with a HESI electrospray ion source (spray voltage 3.5 kV; source heater temperature: 300 °C; capillary temperature 325 °C; FTMS resolution 30.000). Nitrogen was used as sheath and auxiliary gas. The MS system was coupled with an ultra-high performance liquid chromatography (UHPLC) system (Dionex UltiMate 3000, Thermofisher Scientific), equipped with a RP C18 column (2.7 µm; 150 x 2.1 mm; Nucleoshell; Macherey-Nagel; column temperature: 45 °C). The CID mass spectra (buffer gas: helium) were recorded in data dependent acquisition mode (dda) using normalized collision energies (NCE) of 35%.

For UHPLC separation a gradient system was used starting from H_2O:CH_3CN 90:10 raised to 5:95 (each of them containing 0.1% formic acid, isocratic for 1 min) within 12 min and then hold on 5:95 for further 2 min; flow rate 400 µL/min; injection volume 5 µL; autosampler temperature 8 °C. The instrument was externally calibrated by the Pierce® LTQ Velos ESI positive ion calibration solution (product number 88323, Thermo Fisher Scientific, Rockford, IL, 61105 USA). The QC sample was injected every sixth sample, and three

biological replicates were extracted and analyzed in parallel under the same conditions. The data were evaluated with the Xcalibur software 2.2 SP1 (Thermo Fisher Scientific).

3.7.6. LC-ESI-HRMS data processing for multivariate data analysis

The raw spectra of samples and QCs were converted to .mzML format using ProteoWizard (3.0.11110) to get centroided data. The data were then processed in R (version 3.6.3) using XCMS (version 3.8.2). Peak picking was carried out based on the CentWave algorithm with the following parameters: findChromPeaks (ppm=15, peakwidth=c(7,25), sntresh=10, noise=10000, prefilter=c(3,100000)). The peaks were grouped within the biological replicates with groupChromPeaks (minFraction = 0.6, bw = 2). After peak grouping retention time correction was performed using LOESS correction, and then peak grouping was repeated. Missing values were filled with fillPeaks function. Afterwards data was logarithmized and batch correction based on study samples with least-squares regression was applied; available in the R package BatchCorrMetabolomics (0.1.14). Principal component analysis was performed with PCAmethods (1.78.0) package.

3.7.7. MS-Imaging AP-MALDI-MSI

The soft coral tissues from *L. crassum* and *S. glaucum* were collected after being treated with the elicitors in November 2020. The collected tissues were then embedded in the 2% CMC. Embedded samples were stored in the freezer -80 °C until the sectioning. Tissues of soft corals were sectioned in the transverse direction with thickness 50 µm at -20 °C with a cryostat (Leica CM 1850) and placed on the SuperFrost Plus slides. After drying in a vacuum desiccator (*ca*.10 min), the samples were imaged using a manual epi-fluorescence microscope (Zeiss Axio Observer), applying the tile tool which allows to form a single image by joining several individual images together, and an Axiocam 712 color digital camera for further comparison with the MS-imaging results.

For the MS-imaging, the tissue section was coated with 20 mg/mL DHB matrix (2,5-dihydroxybenzoic acid, 98% purity, Sigma-Aldrich) in acetonitrile/water (1:1 v/v) using a pneumatic sprayer (SunCollect, SunChrome). As spraying gas, nitrogen was used, total amount of 13.67 µg/mm^2 DHB in 19 layers were applied on the tissue slide. The first three layers were sprayed with a reduced flowrate.

The samples were then measured by AP-MALDI-MSI on a Fourier transform orbital trapping mass spectrometer (Q Exactive Plus, Thermo Fisher Scientific) equipped with an AP-MALDI(ng) UHR source (MassTech; laser spot size <10 µm). Imaging experiments were conducted in positive ion mode for 100–1000 *m/z* with 140.000 resolution, one microscan, 5E6 AGC target, 500 ms maximum injection time, 4.5 kV spray voltage, 450 °C capillary temperature, and 60% for the S-lens RF value. Pixel size 50 µm, mode CSR (Constant Speed Rastering), scanning velocity 5.75 mm/min, pulse rate 6000 Hz, and laser energy was 31 %. The centroid raw data were then converted from the Thermo *.raw files to

*.imzML using the MassTech imzML Converter (ng) 1.0.1 (merge strategy “Average”). The converted file was loaded into MS-Reader (MSi Reader 1.01) for further analysis.

3.8. Bioactivity assay of the soft corals extracts

3.8.1. Antibacterial assay against Gram positive *Bacillus subtilis*

The antibacterial activity against *Bacillus subtilis* was determined by turbidimetric assay followed the method described by dos Santos et al. [135]. The tested concentration of extracts for antibacterial assay against *B. subtilis* was 500 µg/mL and 50 µg/mL. Chloramphenicol (100 µM) was used as a positive control to induce complete inhibition of bacterial growth. The test was conducted in clear 96 well plates with flat bottom floor (Greiner Bio-one), with a final total volume of 200 µL of TY medium containing 1% DMSO. Color controls without bacteria were treated in the same way to eliminate the influence of colored compounds for each test sample. The plate with lid was incubated under shaking (50 rpm) at 30 °C for 20 h and the absorption was measured at λ= 612 nm using the TecanGeniosPro microplate reader.

3.8.2. Antibacterial assay against Gram negative *Aliivibrio fischeri*

Antibacterial assays against *Aliivirio fischeri* were performed against the bacterial test strain DSM507. The assay was performed on black flat bottom 96 well plates (Brand cellGradeTMpremium, STERILE R) with a final volume of 200 µL of BOSS medium containing 1% DMSO per well (100 µL of diluted bacterial solution and 100 µL of test solution). The tested concentration of extracts for this assay was 500 µg/mL and 50 µg/mL. The plates were incubated in the dark for 24 hours without a lid and without shaking at a temperature of 23 °C and a humidity of 100 percent. The bioluminescence (measured in relative luminescence units, RLU) is proportional to cell density and was calculated after 24 hours using the TecanGeniosPro microplate reader. The results (mean standard deviation value, n=6) are given as relative values to the negative control (bacterial growth, 1% DMSO without test compound) (percent inhibition).

3.8.3. Cytotoxicity assay

Cytotoxicity was determined using two human cancer cell lines, i.e. PC-3 (prostate cancer) and HT-29 (colon adenocarcinoma) the method described by Porzel et al. [136]. The concentrations of extracts were 50 µg/mL and 0.05 µg/mL. MTT and CV assays were used to assess cell viability after 48 hours of incubation. Using an automated microplate reader, the absorbance was measured at 540 nm with a reference wavelength of 670 nm. Digitonin was used as a positive control.

IV. Chemical characterization of the soft corals *Sarcophyton glaucum*, *Lobophytum crassum*, and *Xenia umbellata*

Abstract

Coral reefs are a complex ecosystem that plays a role as a "home" for over 25% of all marine organisms. Soft corals, in particular, have a remarkable ability to synthesize a wide range of compounds with distinct chemical structures (i.e. terpenoids, steroids, alkaloids, cembranoids, and fatty acids). Three soft coral species, namely *Sarcophyton glaucum*, *Lobophytum crassum*, and *Xenia umbellata*, have been investigated in this study. In order to investigate the secondary metabolites in these three soft corals, TLC, LC-ESI-HRMS, and ^{1}H-NMR analyses were performed. In total, 45 and 41 metabolites were tentatively annotated from extracts of all three soft corals by using LC-ESI-HRMS and ^{1}H-NMR, respectively. The extracts of these soft corals contain a wide range of natural products, including diterpenes, cembranoids, alkaloids, and steroids. Multivariate data analysis (e.g. PCA) of the LC-ESI-HRMS and ^{1}H-NMR data revealed a difference in metabolite compositions between *X. umbellata* and the two other soft corals, *S. glaucum* and *L. crassum*. The species-specific metabolites of each soft coral were responsible for this segregation, particularly species-specific terpenoids (e.g. diterpenes and sesquiterpenes) and cembranoids. Moreover, MALDI-MS imaging was used to investigate the spatial distribution of selected metabolites within their bodies. In total, seven known compounds from soft corals and four known compounds from zooxanthellae were detected in the samples. The spatial distribution of each metabolite was discernible, which corresponded to the location of zooxanthellae within the coral body. This method may be beneficial as a guide for isolating specific compounds within the soft coral body.

4.1. Introduction

Over the last 60 years, the metabolites of soft corals have been investigated. Soft corals have evolved an extraordinary capacity for producing a diverse range of compounds with novel chemical structures and a broad range of biological activities. *Sarcophyton*, *Lobophytum*, and *Xenia* are known as producer of a large number of secondary metabolites, particularly cembranoids and terpenoids. The review of Liang and Guo (2013) describes the isolation of 165 diterpenes and 29 biscembranoids from *Sarcophyton* species between 1995 and July 2011 [23]. In addition, the genus *Lobophytum* was reported to be a rich source of cembranoids, with over 250 different metabolites isolated from this genus [24]. The soft coral genus *Xenia* has produced a large number of new terpenoids. To date, more than 200 terpenes have been identified, including sesquiterpenes, diterpenes, and steroids [25]. In nature, these compounds act as chemical defense against fish predators, competing other reef organisms, as well as pathogens (bacteria and parasites) [26-29]. Due to the fact that these three soft coral

species belong to distinct families and species, their metabolite compositions may be different. Furthermore, the distribution of metabolites within the coral body varies, which could be a result of their biosynthesis, function, or the location of their endosymbiont within their body. Therefore, the main aim of this chapter was to investigate the chemical characteristic (secondary metabolites) in these soft corals, as well as their spatial distribution in the coral body.

4.2. Experimental

The three species of soft corals in this study (*S. glaucum*, *L. crassum*, and *X. umbellata*) were investigated in 2019-2021. The soft corals were collected and genetically identified (see Chapter II) at ZMT Bremen. The lyophilized materials were ground using a ball mill to homogenize the powder material. The powder of soft coral samples were then extracted with different solvents (methanol, 80% aqueous methanol, ethyl acetate, *n*-hexane, and chloroform) in order to select the most suitable solvent to extract maximal number of different metabolites. Methanol was selected as optimal solvent after comparison of the different extracts by TLC, LC-ESI-HRMS, and ^{1}H-NMR analysis. TLC analysis was performed on soft coral extracts as the initial test in order to gain an information of metabolite diversity in crude extracts. Furthermore, to conduct a more detailed analysis, metabolite profiling was performed using LC-ESI-HRMS to obtain species-specific fingerprints. Additionally, the crude extracts were analyzed by ^{1}H-NMR in parallel to determine the presence of some non-ionizable metabolites. Moreover, the spatial distribution of secondary metabolites within the coral bodies was performed by using MALDI-MS Imaging. For detailed procedures see Chapter III.

4.3. Result and discussion

4.3.1. Thin-layer chromatography (TLC)

Thin-layer chromatography (TLC) is a rapid and effective method for determining the presence of non-volatile components in natural source extracts. This approach was used as the initial method for determining the metabolite diversity present in extracts of various soft coral species in this study. To separate the complex mixture in the extracts, the combination of some eluents is necessary. TLC analysis of methanolic extracts from three investigated soft corals was performed using a combination of *n*-hexane and ethyl acetate (3:2 v/v) as the eluent. The TLC plate was visualized using light at λ 366 and 254 nm, as well as the vanillin-sulfuric acid reagent for visualization of the specific compound groups. The TLC screening of soft corals methanolic extracts is shown in Figure 13.

The TLC profiles of each species were compared, and significant differences were observed particularly in the *X. umbellata* extract. The TLC result in Figure 13 indicates that *X. umbellata* extract contains more bands corresponding to metabolites than the other two soft coral extracts. Unfortunately, the majority of compounds found in *S. glaucum* and *L.*

crassum are UV inactive which made it difficult to observe the diversity of metabolites present in these samples. The single visible blue fluorescence (R_f 0.45) at 366 nm corresponds to the internal standard umbelliferon (u, Figure 13). In general, all extracts contain a high concentration of strong red fluorescent compounds that were detected at 366 nm. The strong red fluorescence bands (I, Figure 13) with R_f value of 0.5 to 0.9 are chlorophylls and their degradation products. Chlorophyll contained in the extracts is derived from the symbiont of soft corals (zooxanthellae).

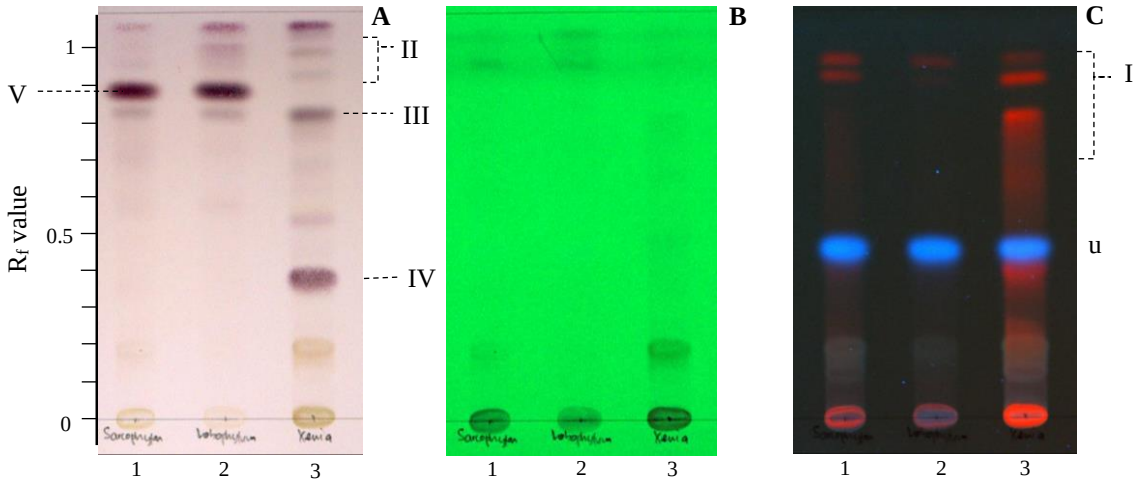

Figure 13 Thin-layer chromatography (TLC) of crude methanolic extracts of *Sarcophyton glaucum* (1), *Lobophytum crassum* (2), and *Xenia umbellata* (3) (c = 20 mg/mL, mobile phase *n*-hexane/ethyl acetate (3:2 v/v)), visualized by vanillin-sulfuric acid (A), under UV-light (254 nm (B), 366 nm (C)); I=chlorophylls, II=sarcophine, III= gorgosterol, IV= xeniolide O, V= sarcophytoxide, u= umbelliferon (reference compound)

Moreover, a vanillin-sulfuric reagent with additional heating was used to detect the compounds in soft coral extracts. Numerous bands were detected, including several known diterpenes such as sarcophine and sarcophinone (II) at R_f values of 0.8-0.97. These compounds were visualized by their pink coloration, which fades to brown over time, as is typical of diterpene moieties [137]. In addition, gorgosterol (III), a marine sterol containing three-membered ring was detected after spraying with vanillin reagent followed by heating at R_f value 0.7. This was verified by comparison with a reference. The large blue-purple spot at R_f 0.89 (V) in *S. glaucum* and *L. crassum* extracts, as well as the smaller blue-purple spot at R_f 0.4 (IV) for *X. umbellata* extracts correspond to terpenoid compounds. It was confirmed by the purple-blue color after reagent spraying and heating. These two metabolites are the major compounds in each soft coral species which were identified based on the LC-MS as xeniolide O (IV) and sarcophytoxide (V). Beside of the common bands, the extracts contain number of unknown species-specific compounds.

4.3.2. LC-ESI-HRMS analysis

To investigate more about the secondary metabolites in the *S. glaucum*, *L. crassum* and *X. umbellata*, LC-ESI-HRMS was performed. The combination of liquid chromatography and

tandem mass spectrometry enhanced the in-depth investigation of crude extracts of natural resources, including their chemical composition. The corresponding extract of each sample was separated on a Nucleoshell column using a gradient system of solvents, and further detection by a high-resolution Orbitrap mass spectrometer which allowed detection of *m/z* values. To determine the optimal extract concentration for measurement, a linear dynamic range analysis was performed. Eight milligrams of the material were extracted and diluted in a variety of concentrations (see Appendix 2).

As a result, two milligrams of extracts demonstrated the best detection of analytes with an intensity range of 10^3-10^7. In order to monitor the performance of the UHPLC (retention time shifts and external calibration), an internal standard (umbelliferon 8 µg/mL) was added to the extraction solvents. Additionally, to ensure the reproducibility of sample preparation and instrument performance, a pooled sample, designated QC, was prepared and measured for each eight samples. To annotate the metabolites in the extract, an MS/MS experiment was performed on each compound to determine its fragmentation pattern. The metabolites from three soft coral extracts separated using reversed-phase UHPLC and their total ion chromatograms are shown in Figure 14. The metabolites detected in the chromatogram were tentatively annotated by their accurate mass and MS/MS fragmentation pattern, and confirmed using literature data and databases.

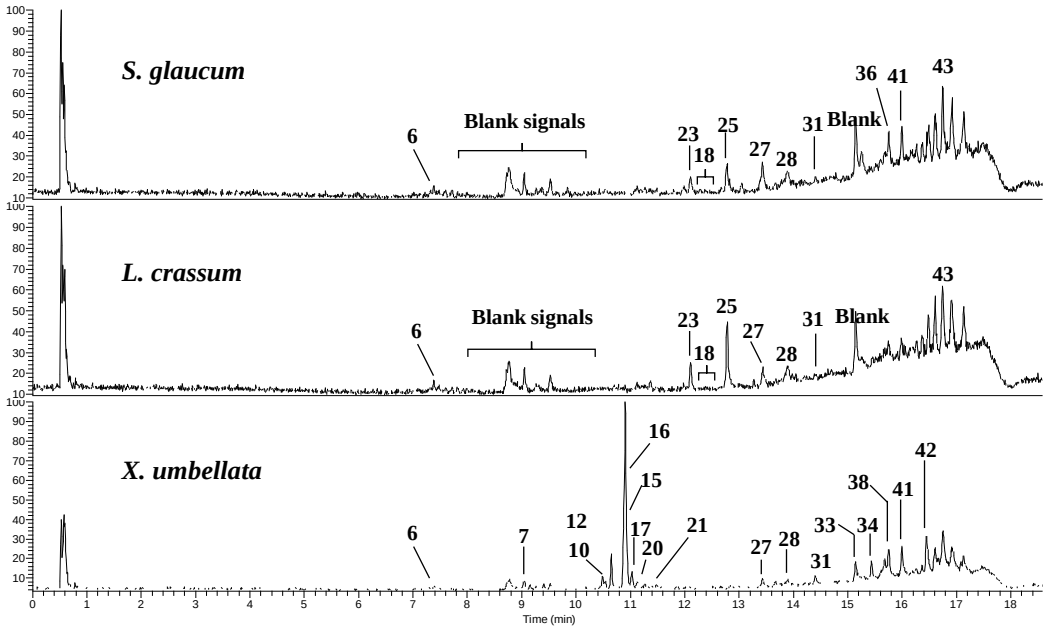

Figure 14 Total Ion Chromatogram (TIC, *m/z* 100-1500) in positive ion mode of *Sarcophyton glaucum*, *Lobophytum crassum*, and *Xenia umbellata*; numbers = peak numbers listed in Table 6

According to this result, polar compounds, specifically organic acids were detected at the start of the elution process (0-2 minutes). Moreover, diterpenes and some diterpene alkaloids were detected in the retention time range of 7-12 minutes, while the non-polar component, namely lipids and steroids, as well as long chain lipids were detected in the retention time range of 13-17 minutes. Similar with the TLC profiling, the LC-ESI-HRMS

chromatogram of three correspondent soft corals displays the difference between *X. umbellata* and the two other species. *X. umbellata* has more peaks than *S. glaucum* and *L. crassum*. This indicates that the metabolites in this species were both well-ionized in the positive ion mode and well-separated in the column.

Table 6 Tentative annotation of metabolites detected by HR-LC-MS in soft corals extracts

Comp.	$[M+H]^+$ *m/z*	t_R (min)	Molecular formula	Δ (ppm)	MS^2 product ions, *m/z* (elemental composition, rel. intensity [%])	Identification (metabolite class)	Species
P.1	116.1070	0.57	$C_6H_{14}NO$	-1.039	116.0899 ($C_6H_{14}NO$, 35), 72.0808 ($C_4H_{10}N$, **100**)	Methylpiperidine-oxide	X
P.2	138.0549	0.59	$C_7H_8NO_2$	-0.616	120.0470 (C_7H_6NO, **100**)	Anthranilic acid	S, L
P.3	146.1173	0.58	$C_7H_{16}NO_2$	-1.884	87.0439 ($C_4H_7O_2$, **100**), 60.0806 ($C_3H_{10}N$, 36)	4-Aminobutyric acid betaine †	X
P.4	162.1124	0.60	$C_7H_{16}NO_3$	-0.616	130.0863 ($C_6H_{12}NO_2$, 31), 116.1069 ($C_6H_{14}NO$, 65), 102.0912 ($C_5H_{12}NO$, **100**), 86.0967 ($C_5H_{12}N$, 7), 60.0808 ($C_3H_{10}N$, 9)	Dihydroxy-2-(hydroxymethyl)-6-methylpiperidinium	S, L
P.5	210.1123	0.64	$C_{11}H_{16}NO_3$	-0.904	178.0863 ($C_{10}H_{12}NO_2$, 2), 150.0913 ($C_9H_{12}NO$, **100**), 121.0885 ($C_8H_{11}N$, 12)	2-Methyl-3-hydroxy-6-(methyl-4-butanoate)pyridine	X
P.6	202.0855	7.35	$C_{12}H_{12}NO_2$	-3.539	174.0539 ($C_{10}H_8NO_2$, 38), 132.0321 (C_8H_6NO, 61), 124.0868 ($C_7H_{10}NO$, **100**)	1-(6-Hydroxy-7-methylisoquinolin-1-yl)ethanone	S, L, X
P.7	452.2634	9.03	$C_{24}H_{38}NO_7$	-1.899	434.2529 ($C_{24}H_{36}NO_6$, 5), 417.2268 ($C_{24}H_{33}O_6$, **100**), 357.2058 ($C_{22}H_{29}O_4$, 21), 297.1847 ($C_{20}H_{25}O_2$, 4), 251.1792 ($C_{19}H_{23}$, 3), 195.1168 ($C_{15}H_{15}$, 3)	Diterpene alkaloid	X
P.8	230.2475	9.26	$C_{13}H_{28}NO_2$	-1.308	212.2370 ($C_{13}H_{26}NO$, **100**), 186.1858 ($C_{11}H_{24}NO$, 3), 147.1708 ($C_{11}H_{15}$, 1),	Amino alcohol	X
P.9	299.1822	9.53	$C_{16}H_{27}O_5$	-2.201	299.1818 ($C_{16}H_{27}O_5$, **100**), 281.1801 ($C_{16}H_{25}O_4$, 33), 200.1071 ($C_{10}H_{16}O_4$, 7)	Sesquiterpene	S, L
P.10	417.2370	10.48	$C_{24}H_{33}O_6$	-0.228	399.2173 ($C_{24}H_{31}O_5$, 5), 357.2055 ($C_{22}H_{29}O_4$, **100**), 297.1846 ($C_{20}H_{25}O_2$, 93), 279.1741 ($C_{20}H_{23}O$, 34), 251.1971 ($C_{19}H_{23}$, 16), 209.1322 ($C_{16}H_{17}$, 11)	Brianthein W	X
P.11	287.2371	10.56	$C_{20}H_{31}O$	1.284	269.2263 ($C_{20}H_{29}$, **100**), 229.1955 ($C_{17}H_{25}$, 23), 215.1794 ($C_{16}H_{23}$, 5), 137.1328 ($C_{10}H_{17}$, 2)	Sarcophytonin A *	S
P.12	471.2346	10.65	$C_{27}H_{35}O_7$	0.73	441.2217 ($C_{26}H_{33}O_6$, 3), 411.2134 ($C_{25}H_{31}O_5$, **100**), 381.2028 ($C_{24}H_{29}O_4$, 5), 339.1562 ($C_{21}H_{23}O_4$, 6), 195.1158 ($C_{15}H_{15}$, 2)	Diterpenoid	X
P.13	329.1750	10.80	$C_{20}H_{25}O_4$	0.651	311.1640 ($C_{20}H_{23}O_3$, **100**), 293.1532 ($C_{20}H_{21}O_2$, 53), 265.1587 ($C_{19}H_{21}O$, 22), 209.1327 ($C_{16}H_{17}$, 11), 195.1155 ($C_{15}H_{15}$, 5)	Diterpene	S
P.14	345.2062	10.81	$C_{21}H_{29}O_4$	-1.112	287.2010 ($C_{19}H_{27}O_2$, **100**), 273.1844 ($C_{18}H_{25}O_2$, 9), 203.1790 ($C_{15}H_{23}$, 5), 177.1733 ($C_{13}H_{21}$, 1)	Crassumolide C *	S, L
P.15	313.1798	10.85	$C_{20}H_{25}O_3$	0.28	295.1690 ($C_{20}H_{23}O_2$, **100**), 277.1583 (C20H21O, 9), 243.1377 ($C_{16}H_{19}O_2$, 24), 209.1324 ($C_{16}H_{17}$, 21), 169.1012 ($C_{13}H_{13}$, 13)	Rubifolide	X
P.16	513.2084	10.90	$C_{26}H_{34}O_9Na$ $[M+Na]^+$	-2.209	453.1873 ($C_{24}H_{30}O_7Na$, **100**), 371.1844 ($C_{22}H_{27}O_5$, 42), 311.1638 ($C_{20}H_{23}O_3$, 3), 293.1533 ($C_{20}H_{23}O_2$, 1), 265.1584 ($C_{19}H_{21}O$, 1), 195.1168 ($C_{15}H_{15}$, 2)	Xeniolide O †	X
P.17	355.1902	11.02	$C_{22}H_{27}O_4$	-0.664	337.1790 ($C_{22}H_{25}O_3$, 26), 295.1685 ($C_{20}H_{23}O_2$, **100**), 277.1581 ($C_{20}H_{21}O$, 42), 249.1632 ($C_{19}H_{21}$, 26), 195.1158 ($C_{15}H_{15}$, 1)	Diterpenoid	X
P.18	502.2922	11.12	$C_{25}H_{45}NO_7P$	-5.883	484.2817 ($C_{25}H_{43}NO_6P$, 6), 361.2734 ($C_{18}H_{36}NO_4P$, **100**), 330.2778 ($C_{17}H_{33}NO_3P$, 1), 269.2263 ($C_{20}H_{29}$, 2), 203.1797 ($C_{15}H_{23}$, 1)	1-*O*-Arachidonoyl-sn-glycero-3-phosphoethanolamine*	X
P.19	399.2142	11.39	$C_{24}H_{31}O_5$	-5.988	381.2025 ($C_{24}H_{29}O_4$, 57), 339.1921 ($C_{22}H_{27}O_3$, **100**), 321.1812 ($C_{22}H_{25}O_2$, 5), 283.1657 ($C_{19}H_{23}O_2$, 5), 241.1587 ($C_{17}H_{21}O$, 3)	Diterpenoid	L
P.20	490.3731	11.47	$C_{26}H_{52}NO_7$	-2.976	472.3637 ($C_{26}H_{50}NO_6$, **100**), 413.2905 ($C_{23}H_{40}O_6$, 34), 313.2721 ($C_{19}H_{37}O_3$, 19), 283.2621 ($C_{18}H_{35}O_2$), 252.1434 ($C_{18}H_{20}O$, 22), 199.0971 ($C_{14}H_{15}O$, 2)	Betaine lipid	X
P.21	434.2528	11.57	$C_{24}H_{36}NO_6$	-2.013	416.2266 ($C_{24}H_{34}NO_5$, 18), 357.2057 ($C_{21}H_{24}O_5$, **100**), 251.1789 ($C_{19}H_{23}$, 4), 209.1325 ($C_{16}H_{17}$, 2)	Betaine lipid	X
P.22	508.2539	11.90	$C_{28}H_{62}NO_6$	-0.449	490.4300 ($C_{28}H_{60}NO_5$, **100**), 431.3675 ($C_{25}H_{50}O_5$, 27), 329.3047 ($C_{20}H_{41}O_3$, 14), 295.2113 ($C_{18}H_{31}O_3$, 35), 239.1489 ($C_{14}H_{23}O_3$, 4), 189.1486 ($C_{13}H_{17}O$, 7)	Betaine lipid	X
P.23	482.3591	12.11	$C_{31}H_{48}NO_3$	3.967	464.3502 ($C_{31}H_{46}NO_2$, 68), 423.2768 ($C_{27}H_{37}NO_3$), 405.2764 ($C_{27}H_{35}NO_2$, 43),	Steroidal alkaloid	S, L

					184.0733 ($C_{12}H_{10}NO$, **100**)		
P.24	428.3724	12.28	$C_{25}H_{50}NO_4$	-2.511	369.2996 ($C_{21}H_{39}NO_4$, **100**), 283.2632 ($C_{18}H_{35}O_2$, 5), 267.2681 ($C_{18}H_{35}O$, 15),	Sphingolipid	S, L, X
P.25	303.2316	12.76	$C_{20}H_{31}O_2$	0.238	285.2214 ($C_{20}H_{29}O$, **100**), 267.2104 ($C_{20}H_{27}$, 16), 227.1792 ($C_{17}H_{23}$, 21), 163.1116 ($C_{12}H_{19}$, 16)	Sarcophytoxide †	S, L
P.26	418.2747	13.04	$C_{28}H_{36}NO_2$	0.232	354.2762 ($C_{23}H_{32}NO_2$, **100**), 218.1515 ($C_{14}H_{20}NO$, 1)	Cespitulactam B	S
P.27	466.2787	13.43	$C_{25}H_{40}NO_7$	-2.657	407.2263 ($C_{22}H_{30}O_7$, **100**), 357.1703 ($C_{21}H_{25}O_5$, 17), 297.1495 ($C_{19}H_{21}O_3$, 2), 209.1315 ($C_{16}H_{17}$, 1)	Betaine lipid	S, L, X
P.28	510.3908	13.53	$C_{33}H_{52}NO_3$	-2.021	492.3795 ($C_{33}H_{50}NO_2$, 85), 451.3171 ($C_{29}H_{41}NO_3$, 8), 433.3029 ($C_{29}H_{39}NO_2$, 42), 184.0732 ($C_{12}H_{10}NO$, **100**),	Steroidal alkaloid	S, L, X
P.29	557.2356	13.63	$C_{30}H_{37}O_{10}$	-4.619	539.2311 ($C_{30}H_{35}O_9$, 26), 497.2142 ($C_{28}H_{33}O_8$, **100**), 437.1932 ($C_{26}H_{29}O_6$, 20), 415.2113 ($C_{24}H_{31}O_6$, 23), 355.1901 ($C_{22}H_{27}O_4$), 295.1689 ($C_{20}H_{23}O_2$, 1)	Steroid	X
P.30	462.3603	14.14	$C_{28}H_{48}NO_4$	4.250	444.3500 ($C_{28}H_{46}NO_3$, 4), 338.3411 ($C_{22}H_{42}O_2$, **100**), 312.3259 ($C_{20}H_{40}O_2$, 1)	Nitrogenous fatty acid	S, L
P.31	562.3729	14.33	$C_{32}H_{52}NO_7$	-1.670	562.3759 ($C_{32}H_{52}NO_7$, **100**), 544.3631 ($C_{32}H_{50}NO_6$, 48), 485.3612 ($C_{29}H_{40}O_6$, 21), 252.1439 ($C_{14}H_{20}O_4$, 33), 178.1074 ($C_{11}H_{14}O_2$, 79)	Betaine lipid	X
P.32	282.2791	14.79	$C_{18}H_{36}NO$	-0.182	265.2520 ($C_{18}H_{33}O$, **100**), 247.2415 ($C_{18}H_{31}$, 73), 149.1322 ($C_{11}H_{17}$, 7)	Nitrogenous fatty acid	S, L
P.33	425.2918	15.14	$C_{24}H_{41}O_6$	3.49	425.2919 ($C_{24}H_{41}O_6$, **100**), 407.2899 ($C_{24}H_{39}O_5$, 10), 281.1726 ($C_{16}H_{25}O_4$, 1), 127.1161 (C_9H_{19})	Fatty acid	X
P.34	533.2538	15.43	$C_{32}H_{37}O_7$	0.694	515.2436 ($C_{32}H_{35}O_6$, **100**), 505.2601 ($C_{31}H_{37}O_6$, 3), 489.2661 ($C_{31}H_{37}O_5$, 3), 170.1437 ($C_{13}H_{14}$)	Xenia diterpenoid	X
P.35	581.3981	15.59	$C_{40}H_{53}O_3$	-2.361	563.3884 ($C_{40}H_{51}O_2$, **100**), 411.3619 ($C_{29}H_{47}O$, 4), 251.1799 ($C_{19}H_{23}$, 9)	Diatoxanthin *	S, L
P.36	650.5358	15.88	$C_{39}H_{72}NO_6$	0.545	649.4432 ($C_{39}H_{71}NO_6$, 70), 633.4551 ($C_{38}H_{66}NO_6$, 22), 594.3516 ($C_{36}H_{52}NO_6$, 19), 283.2630 ($C_{18}H_{35}O_2$, **100**)	N-containing lipid *	S, L
P.37	565.2803	15.97	$C_{33}H_{41}O_8$	1.212	547.2697 ($C_{33}H_{39}O_7$, **100**), 533.2537 ($C_{32}H_{37}O_7$, 7), 505.2594 ($C_{31}H_{37}O_6$, 8), 477.2696 ($C_{30}H_{37}O_5$, 9), 309.2463 ($C1_9H_{33}O_3$, 5)	Xenia diterpenoid	X
P.38	748.5851	16.17	$C_{41}H_{83}NO_8P$	-0.715	749.5746 ($C_{41}H_{84}NO_8P$, **100**), 748.5714 ($C_{41}H_{83}NO_8P$, 16), 704.5813 ($C_{40}H_{83}NO_6P$, 3), 492.3314 ($C_{32}H_{44}O_4$, 8), 413.2900 ($C_{30}H_{37}O$, 5)	Glycerophospholipid	X
P.39	648.4650	16.24	$C_{41}H_{62}NO_5$	3.361	589.3913 ($C_{38}H_{52}O_5$, 18), 505.3345 ($C_{33}H_{45}O_4$, **100**), 451.2927 ($C_{29}H_{39}O_4$, 15), 299.2387 ($C_{21}H_{31}O$, 2)	Betain lipid	X
P.40	871.5711	16.33	$C_{55}H_{75}N_4O_5$	-3.041	593.2758 ($C_{35}H_{37}N_4O_5$, 32), 563.2650 ($C_{34}H_{35}N_4O_4$, 5), 519.2750 ($C_{33}H_{35}N_4O_2$, **100**)	Pheophytin A *	S, L
P.41	786.5141	16.44	$C_{45}H_{72}NO_{10}$	1.943	750.4766 ($C_{44}H_{64}NO_9$, 13), 607.4345 ($C_{39}H_{61}NO_4$, **100**), 515.3873 ($C_{32}H_{53}NO_4$, 6), 333.2419 ($C_{21}H_{33}O_3$, 38), 257.1897 ($C_{18}H_{25}O$, 4)	Cerebroside	S, X
P.42	563.2645	16.66	$C_{33}H_{39}O_8$	1.004	535.2694 ($C_{32}H_{39}O_7$, **100**), 503.2434 ($C_{31}H_{35}O_6$, 18), 477.2224 ($C_{29}H_{33}O_6$, 2), 414.2041 ($C_{24}H_{30}O_6$, 2), 281.1945 ($C_{20}H_{25}O$,1)	Xenia diterpenoid	X
P.43	796.6213	16.77	$C_{46}H_{86}NO_9$	-11.25	796.5223 ($C_{46}H_{86}NO_9$, **100**), 510.3920 ($C_{33}H_{52}NO_3$, 14), 349.2093 ($C_{24}H_{29}O_2$, 6)	Cerebroside	S, L, X
P.44	436.4158	16.91	$C_{28}H_{54}NO_2$	0.792	418.4023 ($C_{28}H_{52}NO$, 100), 363.3098 ($C_{27}H_{39}$, 12), 251.1849 ($C_{19}H_{23}$, 19), 145.1221 ($C_{11}H_{13}$, 2)	Sphingolipid	X
P.45	794.6049	17.57	$C_{46}H_{84}NO_9$	-12.22	793.5367 ($C_{46}H_{83}NO_9$, 4), 751.4654 ($C_{44}H_{65}NO_9$, 3), 613.3148 ($C_{34}H_{47}NO_9$, 1), 519.2921 ($C_{32}H_{41}NO_5$, **100**), 517.2764 ($C_{32}H_{39}NO_5$, 83), 387.2478 ($C_{24}H_{35}O_4$, 2)	N-containing lipid	X

Note: S = *S. glaucum*, L= *L. crassum*, X= *X. umbellata*
* = Selected for MS-imaging
† = Major metabolites detected in NMR

In total, 45 metabolites were tentatively annotated from the three investigated soft corals. The annotated metabolites were limited to the well ionizing metabolites. Unfortunately, the majority of metabolites are unknown compounds which could not be annotated. Nevertheless, metabolite classes could be identified based on the distinctive fragmentation pattern of each feature. Some known terpenoids *i.e.* two known diterpenes brianthein W (P.**10**), rubifolide (P.**15**), and the major diterpene xeniolide O (**16**) were detected in the extracts of *X. umbellata* extracts. Nitrogenous compounds were the

predominant metabolites in this coral species. These compounds, which consist of alkaloids, amino alcohols, and betaine lipids, were abundant in the extracts of this species. Surprisingly, little research has been conducted on the nitrogenous compounds in *X. umbellata*. Moreover, two detected known pigments namely pheophytin A (P.**40)** and diatoxanthin (P.**35**) were detected in the coral tissues by using LC-HRMS, as well as in MS-imaging.

Multivariate data analysis (PCA) was then used to determine the chemical variance in the extracts of three soft corals studied. The raw data were converted and further used to produce the feature table. This table was generated by XCMS and further used to analyze the variation of metabolites in the investigated soft coral extracts using R studio. However, due to the appearance of isotopes and adduct ions, each compound is usually represented by multiple features as a result of the MS technique. As shown in Figure 15, the metabolite variance in the extracts of *X. umbellata* and two other soft corals (*S. glaucum* and *L. crassum*) displays clear separation into two groups in the PC1 (16.5% variance). In addition, the extracts of *S. glaucum* and *L. crassum* are separated in PC2 (8% variance). The results were further validated by examining the PC1 loadings plot in the direction of the compounds responsible for the separation of *X. umbellata* extracts from other soft corals.

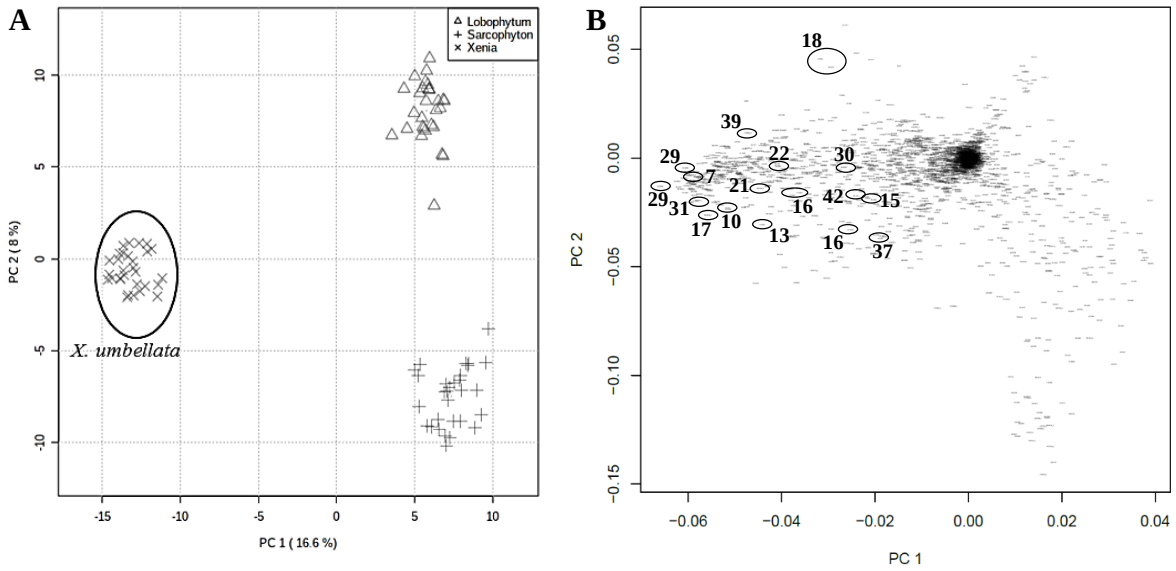

Note= Δ: *Lobophytum crassum*, +: *Sarcophyton glaucum*, ×: *Xenia umbellata*

Figure 15 Principle component analysis (PCA) of LC-ESI-HRMS data of soft corals extracts; A. scores plot, B. loadings plot with assigned peak numbers of Table 6

According to the loadings plot in the Figure 15, the main compounds responsible for the separation of *X. umbellata* were the specific-species compounds of this species. Most of these metabolites are in the group of diterpenes (P.**10**, P.**13**, P.**15**, P.**16**, P.**17**), two xenia diterpenoids (P.**37**, P.**42**), diterpene alkaloid (P.**7**), betaine lipids (P.**21**, P.**22**, P.**31**), nitrogenous lipids and fatty acids (P.**39**, P.**30**), phospholipids (P.**18**), and steroids (P.**29**). These metabolites were detected exclusively in *X. umbellata* extracts, which is probably due to the species differential production of secondary metabolites. In comparison to other soft

corals, the genus *Xenia* is known as a producer of numerous unique metabolites [138-143]. It is confirmed in this study that *X. umbellata* produces more metabolites in comparison to the two other investigated species. Unfortunatelly, the major bins causing the separation of *S. glaucum* and *L. crassum* in the PC2 are background signals, which could not be annotated. These signals in the chromatogram of *S. glaucum* and *L. crassum* are higher in comparison to in *X. umbellata*. This is one of the disadvantages of the LC-MS method, particularly with regard to the column used and the instrument condition. The summary of main compound classes found in the extracts of *S. glaucum*, *L. crassum*, and *X. umbellata* are shown in Figure 16.

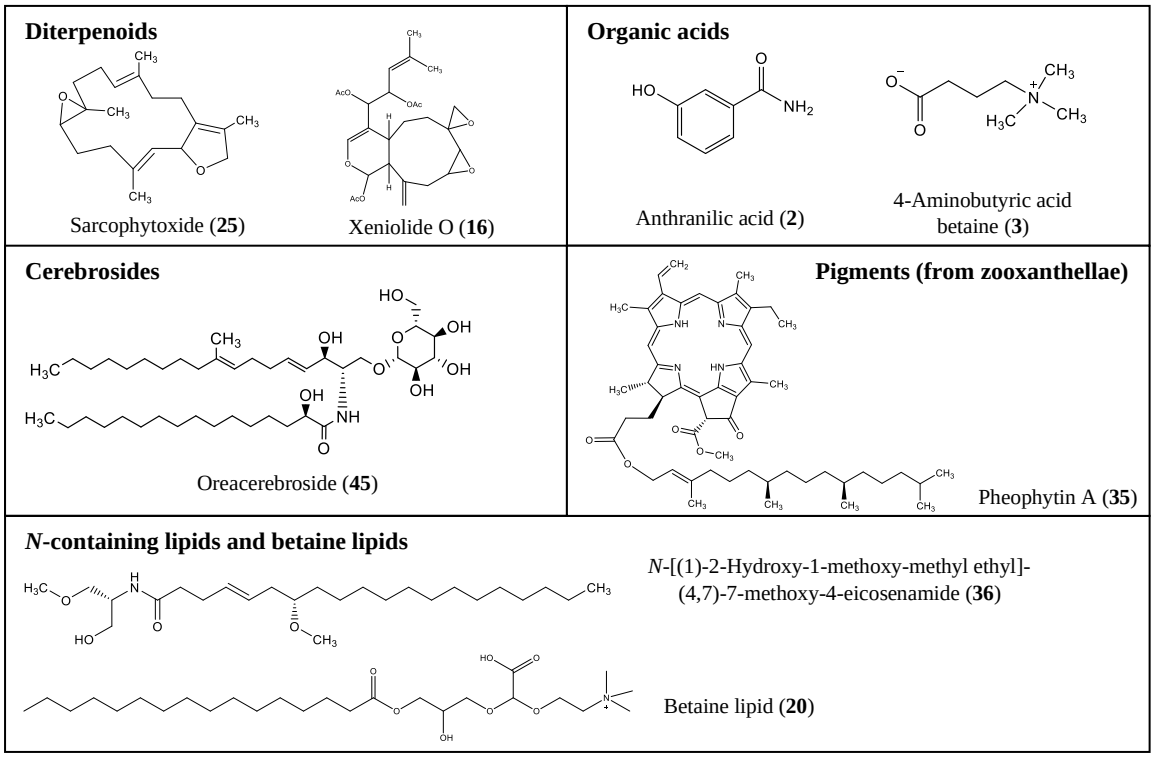

Figure 16 Metabolite classes detected (by LC-HRMS and TLC) in the extracts of *Sarcophyton glaucum, Lobophytum crassum*, and *Xenia umbellata*

4.3.3. ^{1}H-NMR profiling

In addition to UHPLC-MS measurements, which can only detect ionizable compounds, ^{1}H NMR spectroscopy was used to obtain a comprehensive and quantitative overview of the compounds present in the complex extracts. The ^{1}H-NMR spectra of the extracts of *S. glaucum, L. crassum*, as well as *X. umbellata* are shown in Figure 17. In general, the spectrum can be divided into several distinct parts based on the characteristic signals of typical compound classes, which are fatty acid (methylenes δ 0.90-0.93 ppm) area, sugar area (hydroxylated CH and CH_2 δ 3.4-4.6 ppm), and aromatic area (δ 5.5-8.5 ppm), as well as olefinic protons (mainly from fatty acids δ 5.3-5.36 ppm). By comparing the spectra of crude extracts to NMR spectra of known compounds (based on the literature), and evaluating 2D NMR analysis using HSQC, 18 compounds have been tentatively assigned (Figure 17 and Table 7). Furthermore, the major compound detected in the *S. glaucum* based on the LC-MS

(the highest peak) in comparison to ^{1}H NMR was tentatively annotated as sarcophytoxide (P.**25** in LC-MS and **3** in NMR) and its diastereomers in *L. crassum*. In *X. umbellata*, diterpene containing 9-membered ring diterpene xeniolide O (P.**16** and **17** in NMR) along with betaine derivates (P.**3**) were tentaivelly annotated as the major metabolites in this species.

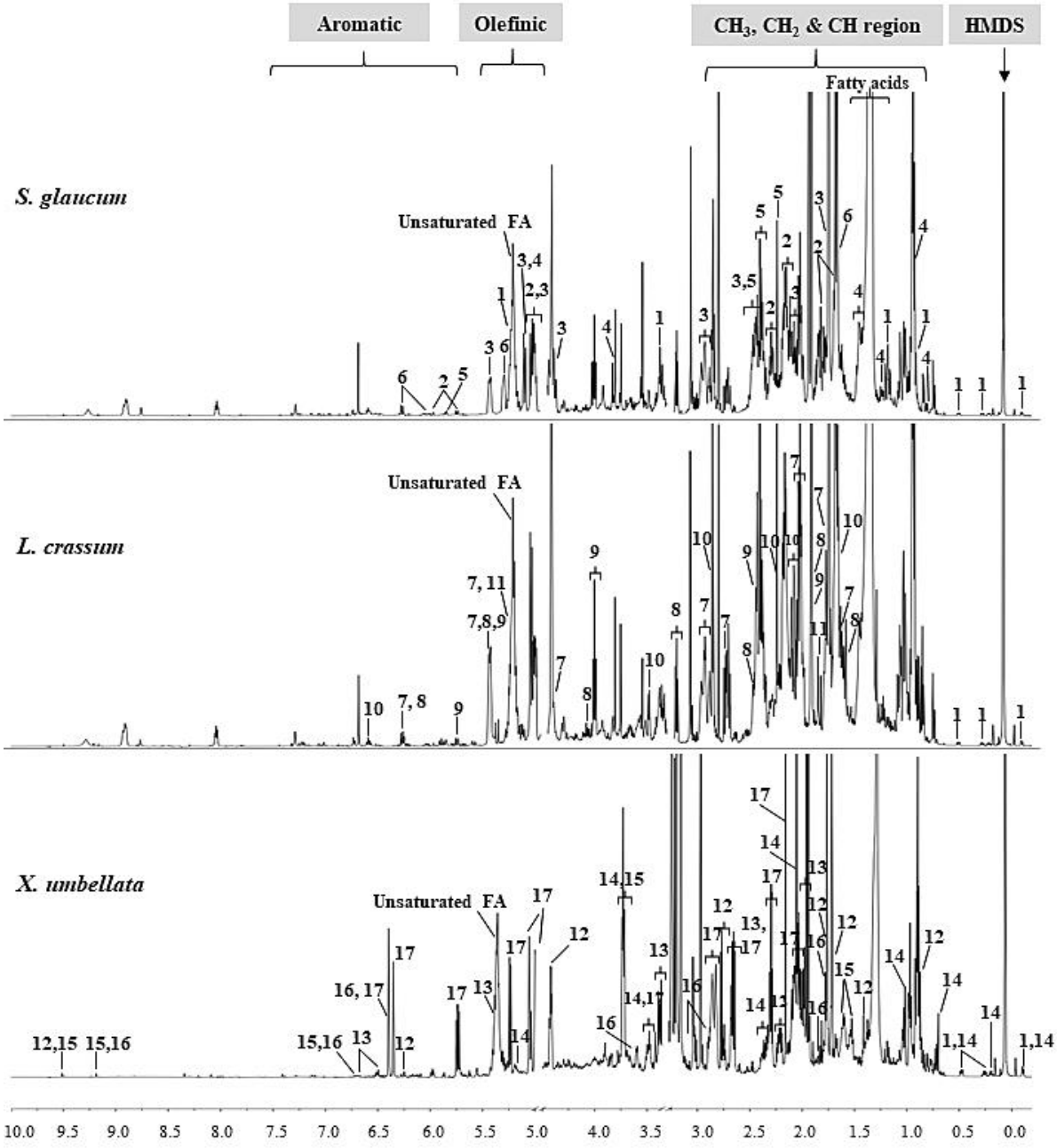

Figure 17 ^{1}H-NMR spectra of *Sarcophyton glaucum*, *Lobophytum crassum*, and *Xenia umbellata* extract; solvent = CD_3OD; numbers = number of tentative annotated compound listed in Table 7

Table 7 Tentative assignment of metabolites detected by ^{1}H-NMR (supported by 2D NMR data) in *Sarcophyton glaucum*, *Lobophytum crassum*, and *Xenia umbellata* extracts (solvent: CD_3OD)

Metabolite	Position	^{1}H, δ [ppm] multiplicity	^{13}C δ [ppm] HSQC	Species
Gorgosterol (**1**) 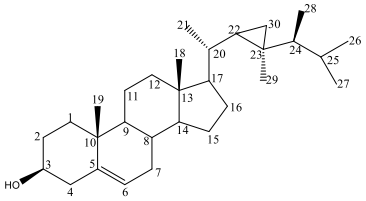	3	3.47 m	72.7	S, L, X
	6	5.37 m	129.3	
	21	1.03 s	21.7	
	22	0.26 m	30.8	
	26	0.98 s	22.7	
	27	0.87 s	20.9	
	29	0.90	14.5	
	30	0.48 dd -0.11 t	*n.d.*	
Sarcophine (**2**) 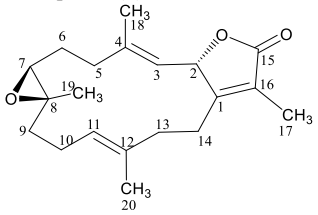	2	5.44	86.6	S
	3	5.35 dd	122.6	
	5	2.19 m	35.9	
	6	2.23 m	24.1	
	7	2.75	64.1	
	11	5.35	122.6	
	16	1.11 d	25.9	
	18	1.62 s	15.3	
	19	1.26 s	16.7	
	20	1.86 br s	18.1	
Sarcophytoxide (**3**) † 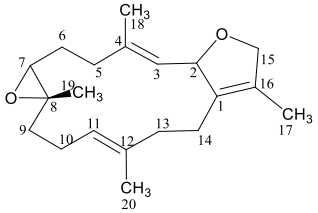	2	5.44	86.6	S
	3	5.25	126.3	
	5	2.19 m	35.9	
	6	2.23 m	26.1	
	7	2.75	64.1	
	16	4.46 m	79.1	
	18	1.62 s	15.3	
	19	1.26 s	16.7	
	20	1.86 br s	18.1	
Sarcophytolol (**4**) 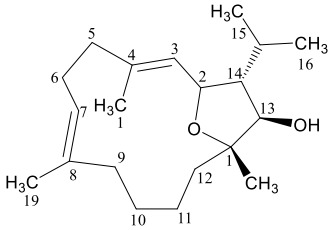	1	1.40 m	30.2	S
	2	4.50 dd	74.8	
	3	5.34[b] d	122.6	
	7	5.16 dd	124.8	
	11	1.78 m	28.7	
	14	3.89 d	70.4	
	15	1.18 m	30.0	
	17	0.77 d	20.2	
	19	1.60 s	16.2	
	20	0.90 s	14.5	
Glaucumolide A/B (**5**) 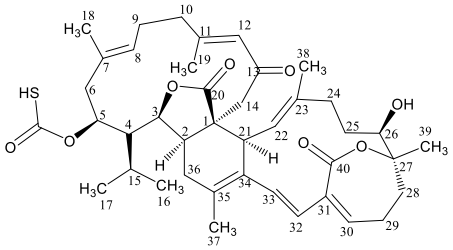	2	2.35 m	38.6	S
	6	2.22 m 2.14 m	43.0	
	8	5.24 dd	126.8	
	12	5.87 dd	122.4	
	15	2.23 m	24.1	
	17	1.11 d	26.1	
	19	2.15 s	30.7	
	22	5.16[c]	124.9	
	37	1.84 s	20.9	
Sarglaucol (**6**) 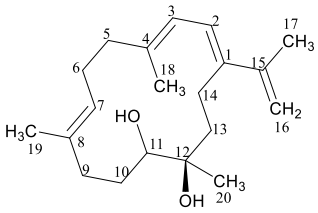	2	6.38 d	120.0	S
	3	6,14 d	117.6	
	5	2.23 m 2.00 m	24.2	
	7	5.18 t	127.4	
	9	2.19 m	35.9	
	16	5.16[c] s	124.9	
	17	1.94 s	24.4	
	18	1.62 s	15.8	
	19	1.60[c] s	16.2	
Locrassolide A (**7**)	1	2.83 m	40.2	L
	3	2.62 m	61.8	
	5	1.55 m 2.11 m	30.7	

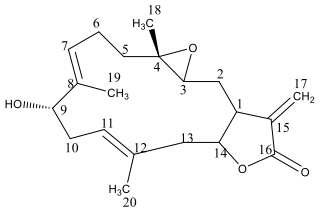	7	5.37	122.6	
	9	4.07	65.6	
	11	5.35 dd	122.7	
	14	4.46 ddd	79.1	
	17	6.38 d	120.1	
		5.57 d		
	18	1.32 s	17.7	
	19	1.66 s	10.1	
Crassumolide B (**8**) †	1	3.08 t	48.9	L
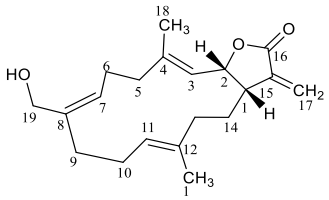	2	5.57 dd	85.3	
	3	5.06 d	125.9	
	5	2.32 m	35.1	
	7	4.96 br d	126.9	
	11	5.35 t	122.7	
	17	6.38 d	120.1	
		5.57 d		
	18	1.62 s	15.3	
	19	4.14 d	63.7	
	20	1.84	15.8	
Crassumolide C (**9**) †	2	5.57 dd	85.3	L
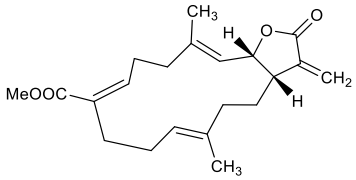	3	5.06 dd	125.9	
	5	2.32 m	35.1	
	7	4.96 br d	*n.d.*	
	11	5.35 t	122.7	
	17	6.38 d	120.1	
		5.57 d		
	18	1.62 s	15.3	
	20	1.84 s	15.8	
	OMe	3.62 s	59.5	
Lobocrassin A (**10**)	3	2.76 d	63.6	L
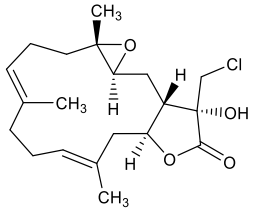	5	1.95 m	37.7	
		2.35 m		
	6	2.29 m	24.5	
	7	5.16 t	125.1	
	10	1.61 m	26.2	
	11	5.18 t	127.4	
	14	4.47	79.1	
	19	1.62 s	15.3	
	20	1.84 s	15.8	
Lobocrasol A (**11**)	3	5.37 d	129.3	L
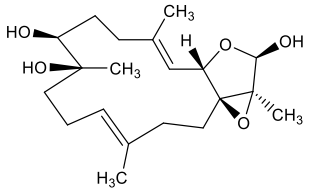	5	2.21 m	35.1	
	6	1.63 m	29.7	
		1.71 m		
	7	3.47 m	72.7	
	9	1.71 m	37.7	
	11	5.35 dd	122.7	
	16	3.36	*n.d.*	
	17	1.52 s	14.9	
	18	1.62 s	15.3	
	19	1.28[d] s	17.1	
	20	1.84 s	15.8	
Umbellactal (**12**)	3	9.19 s	*n.d.*	X
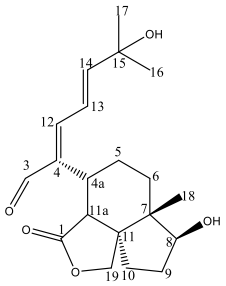	4a	2.74 t	33.8	
	6	1.79 m	29.1	
	8	4.43 t	63.6	
	9	2.08 m	29.1	
		1.77 s		
	10	1.72 s	35.0	
	11a	2.78 d	52.9	
	13	6.51 dd	124.6	
	14	6.25 d	159.5	
	17	1.41 s	33.3	
	18	0.89 s	17.8	
Xeniumbellal (**13**)	1	3.03 m	58.8	X
	3	9.19 s	*n.d.*	
	4a	3.50 dd	33.2	

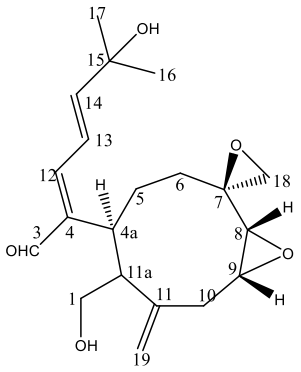	5	2.08 m 1.13 m	29.2	
	6	2.83 m 2.23 m	26.4	
	8	3.02 d	58.6	
	9	3.25 t	57.4	
	11a	3.25 t	52.2	
	13	6.51 dd	124.3	
	14	6.25 d	159.5	
	16	1.42 s	33.4	
	18	3.17 s	53.7	
Gorgst-3β-5α, 6β, 11α, 20(s)-pentol-3-monoacetate (**14**) 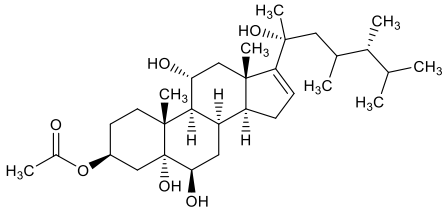	3	5.19 ddd	73.2	X
	4	2.22 m	26.4	
	6	3.49 br t	72.6	
	11	3.72 ddd	63.9	
	16	5.24 dd	121.2	
	18	0.69 s	12.4	
	21	1.03 s	21.6	
	22	0.26 td	52.4	
	26	0.98 d	22.7	
	29	0.48 dd	22.8	
	30	0.89 s	14.5	
	2` CH_3	2.04 s	21.0	
Xenibellol B (**15**) 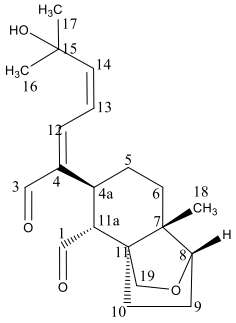	1	9.51 s	*n.d.*	X
	3	9.19 s	*n.d.*	
	4a	2.74 m	33.8	
	6	1.78 m	29.2	
	8	3.75 s	66.3	
	9	1.78 m 1.29*a* m	29.2	
	13	6.51 dd	123.3	
	14	6.25 dq	159.5	
	16	1.42[e] s	33.4	
	18	1.29[a] s	15.4	
	19	3.74 m	75.5	
Umbellacin A (**16**) 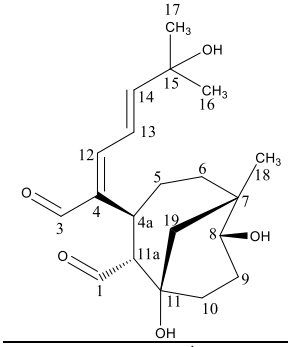	1	9.51 s	*n.d.*	X
	3	9.19 s	*n.d.*	
	4a	3.49 m	42.4	
	5	2.08 m 1.13 m	29.2	
	8	3.39	72.5	
	9	1.76 m 1.53 m	27.2	
	13	6.51 dd	124.3	
	14	6.25 d	159.5	
	16/17	1.42 s	33.4	
	18	1.03 s	21.6	
Xeniolide O (**17**) † 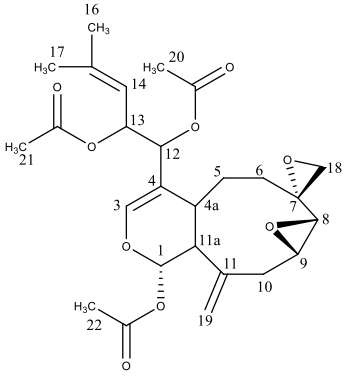	1	6.35 brs	92.5	X
	3	6.40 s	141.9	
	4a	2.88 m	30.5	
	6	2.00 m 2.22 m	26.3	
	8	3.33 d	57.7	
	9	3.03 m	58.7	
	11a	3.04 brs	39.4	
	12	5.24 d	77.0	
	13	5.74 dd	70.9	
	14	5.04 d	121.1	
	16	1.72 s	25.9	
	18	2.77 d	51.9	
	19	5.00 s 5.06 s	113.5	

	20	1.94 s	171.5	
	21	1.96 s	171.5	
	22	2.07 s	171.1	
Fatty acid (**18**)	$(CH_2$-$)n$	1.29	30.8	S, L, X
	CH_3 terminal	0.90	14.5	
Arachidonic acid (AHA), Eicosapentaenoic acid (EPA), Docosahexaenoid acid	CH-5/6-8/9-11/12-14/15-17/18	5.32-5.40 m		

Note: S= *S. glaucum*, L= *L. crassum*, X= *X. umbellata*
[†] Detected in the LC-MS
[a] Corresponds to overlapping NMR signals in fatty acids signal
[b] Corresponds to overlapping NMR signals in 3
[c] Corresponds to overlapping NMR signals in 4
[d] Corresponds to overlapping NMR signals in 10
[e] Corresponds to overlapping NMR signals in 12

Multivariate data analysis (i.e. PCA) was used to conduct additional analysis on the ^{1}H-NMR data. The PCA analysis of ^{1}H-NMR data from all soft corals shows a similar result to that based on LC-ESI-HRMS data. Both, MS and NMR based PCA revealed a clear separation of *X. umbellata* from the two other soft corals species (*S. glaucum* and *L. crassum*) with respect to PC1 (57.5% variance). In addition, *S. glaucum* were also separated from other species in PC2 (12.8% variance) (Figure 9). The results were further validated by examining the loadings plot in order to identify the bins responsible for the segregation of the *X. umbellata* extract.

The loading plot shows *X. umbellata* specific compounds, including umbellactal (**12**), gorgst-3*β*-5*α*,6*β*,11*α*,20(*s*)-pentol-3-monoacetate (**14**), umbellacin A (**16**), and an unknown compound (two singlets at δ ^{1}H 1.94 and 1.96 ppm) responsible for the segregation of *X. umbellata* from two other soft coral species. The unidentified compound most likely contains three -CH_3 (methyl groups) connected to nitrogen, which probably belong to betaine compounds. It can be correlated to the betaine constituents which are detected by using LC-MS (P.**3**). This hypothesis occurs as a result of the appearance of a singlet and its lack of connection to other carbon atoms. Moreover, the bins responsible for *S. glaucum* clustering belong to sarcophytoxide (**3**) and sarcophytolol (**4**), whereas the bins responsible for *L. crassum* clustering were locrassolide A (**7**), crassumolide B (**8**), and crassumolide C (**9**). Gorgosterol (**1**), a well-known soft coral steroid was detected in all three soft coral species. Additionally, fatty acids were found as an abundant component in soft coral extracts, as evidenced by the high intensity peak of this components. The high content of fatty acids is related to their symbiont which is known as a producer of fatty acids, further transferred to the soft corals as an energy source [144, 145].

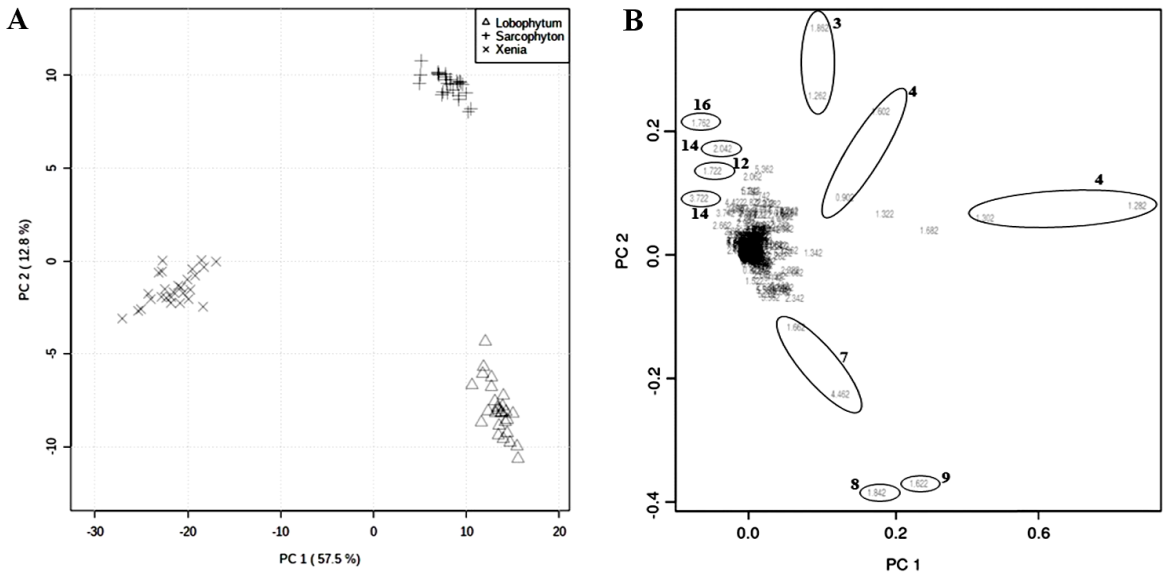

Note= Δ: *Lobophytum crassum*, +: *Sarcophyton glaucum*, ×: *Xenia umbellata*

Figure 18 Principle component analysis (PCA) of ^{1}H-NMR data from *Sarcophyton glaucum*, *Lobophytum crassum*, and *Xenia Umbellata* extracts; A. scores plot, B. loadings plot

4.3.4. Mass spectrometry imaging

In order to visualize the localization of metabolites in a biological sample, the combination of MS and imaging approaches can be utilized. This combination, namely mass spectrometry imaging (MSI), provides valuable information about the detailed localization of diverse metabolites, such as lipids, peptides, and proteins in a sample section [146-148]. A commonly used ionization method for MSI is the Matrix-assisted laser desorption/ionization (MALDI-MSI). This method is known as a soft ionization technique, and the fragmentations produced in-source are reproducible [149, 150]. It allows simultaneous visualization of hundreds of metabolites present in a biological sample without an extraction process.

To the best of our knowledge, no study has been conducted on the spatial distribution of metabolites in soft coral bodies so far. In fact, mass spectrometry imaging method could be used to determine the spatial distribution of soft corals metabolites, as well as of the endosymbiont algae (zooxanthellae) inside soft coral tissue. The spatial distribution of zooxanthellae is useful in order to determine their location within the corals body. Further, soft corals, as polyp organisms, defend themselves against predators and stress factors through the production of secondary metabolites. By using MSI, the distribution of these metabolites within the coral body can be determined. Therefore, in this study MALDI-MSI was used to investigate the spatial distribution of these secondary metabolites in both organisms (soft coral and zooxanthellae).

For the MALDI-MSI experiment, the soft corals were harvested and directly embedded in the carboxymethyl cellulose (CMC) material [151]. Afterwards the material has to be sectioned as thin as possible using a cryotome. However, the sectioning process was very challenging due to the sclerite distribution within the investigated tissue. Tissue sectioning

without damaging the structure was only possible with a tissue thickness of ≥ 50 µm, which then was selected as suitable tissue thickness to reduce tissue damage by the sclerite. This tissue thickness is actually relative high in comparison to other MALDI-MSI studies [151-153], which usually use between10 µm - 25 µm. As a compromise to the high thickness of the tissue, the double concentration of DHB matrix (2,5-dihydroxybenzoic acid) was applied on the tissue to facilitate a good ionization of metabolites. Despite the adapted method, a suitable sample section for *Sarcophyton glaucum* and *Lobophytum crassum* could be obtained. This was not possible with *Xenia umbellata* due to its non-compact body structure and high water content, which complicates the embedding process.

The performance of the developed method was validated with the detection of zooxanthellae-specific metabolites in *S. glaucum* tissue. The occurrence of zooxanthellae can be observed by the brownish color in the microscopic picture (Figure 19). According to this optical image (microscopic picture), the zooxanthellae are collocated mainly in the umbrella part of the soft coral. By detection of metabolites produced by zooxanthellae, the distribution and density of zooxanthellae inside of soft corals body can be observed. Therefore, two pigments, namely pheophytin A (P.**40**) (*m/z* $[M+H]^+$ 871.5711) and diatoxanthin (P.**46**) (*m/z* $[M+H]^+$ 581.3981), known to be produced only by zooxanthellae as photosynthetic organism were selected as the marker compound. The spatial distribution of two corresponding metabolites produced by zooxanthellae in the *S. glaucum* body are shown in Figure 19.

According to MALDI-MSI result, both pigments were collocated to areas of zooxanthellae (brown color in the optical image). It confirms the suitability of the adapted method, i.e. the tissue thickness, concentration of the matrix, as well as the chosen parameters for MALDI-MSI measurement. Interestingly, a slightly different pattern can be recognized for diatoxanthin which is located on the bottom of the siphonozooids (tentacles) of *S. glaucum*. According to the anatomy of soft coral, this location is associated with vesicles, namelly symbiosomes in the gastrodermal cells of the coral host that are directly connected to the siphonozooids as their “mouth” [154]. Some zooxanthellae are located in the syphonozooids in order to assist their host to acclimate the light for optimized photosynthetic performance and coral growth [155]. Zooxanthellae located in siphonozooids convert the xanthophyll diadinoxanthin to diatoxanthin [156, 157]. Therefore, high concentration of diatoxanthin are detected in this region. The zooxanthellae cells in this part migrate to the gastrodermal cells (symbiosomes) during movement of siphonozooids [158-160]. Therefore, a high concentration of diatoxanthin was also detected in the gastrodermal cells (symbiosomes) of the host (coral).

Optical image Pheophytin A (*m/z* $[M+H]^+$ 871.5711)

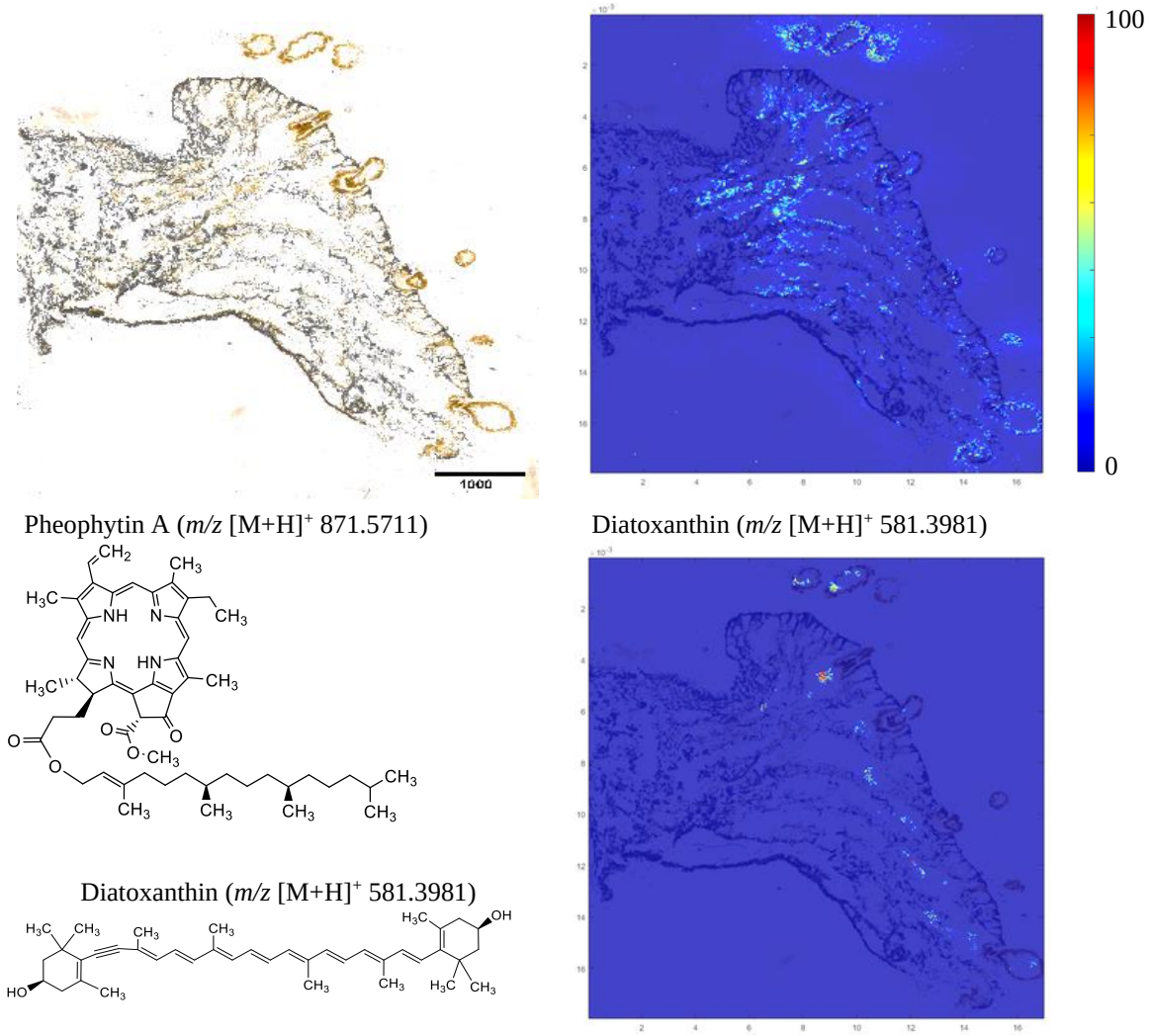

Figure 19 AP-MALDI-MSI of soft coral *Sarcophyton glaucum* with the spatial distribution of pheophytin A (*m/z* [M+H]+ 871.5711) and diatoxanthin (*m/z* [M+H]+ 581.3981); and full microscopic image

Furthermore, known and abundant metabolites isolated from *S. glaucum* and *L. crassum*, as well as from zooxanthellae were selected, and their presence in the sample was confirmed using MS-Reader software. In total, 7 known compounds from soft corals and 4 known compounds from zooxanthellae were detected in the samples. The purpose of this experiment was to distinguish the metabolites produced by soft corals and their symbiont. By using the marker compounds from each organism (soft coral and their symbiont), we could detect: 1) the location of zooxanthellae within the soft coral body, 2), the specific metabolites produced by each organism, and 3), the compounds which are produced as the result of symbiosis process of these organisms. In addition, the spatial distribution of each compound in soft corals body could be distinguished in this study. The details of selected compounds as well as spatial distribution of each compound in both investigated soft corals are shown in Appendix 4. In addition, four representative compounds namely sarcophytonin A (P.**11**), crassumolide C (P.**14**, **9**), phospholipid 1-*O*-arachidonoyl-sn-glycero-3-phosphoethanolamine (P.**19**), and the nitrogenous lipid (5,7,9)-2,3-dihydroxy-*N*-((2,3,4)-1,3,4-trihydroxytetradec-6-

en-2-yl)pentacosa-5,7,9-trienamide (P.**36**) isolated in both soft corals were chosen to observe the spatial distribution of these metabolites in the soft coral bodies using MS-imaging (Figure 20).

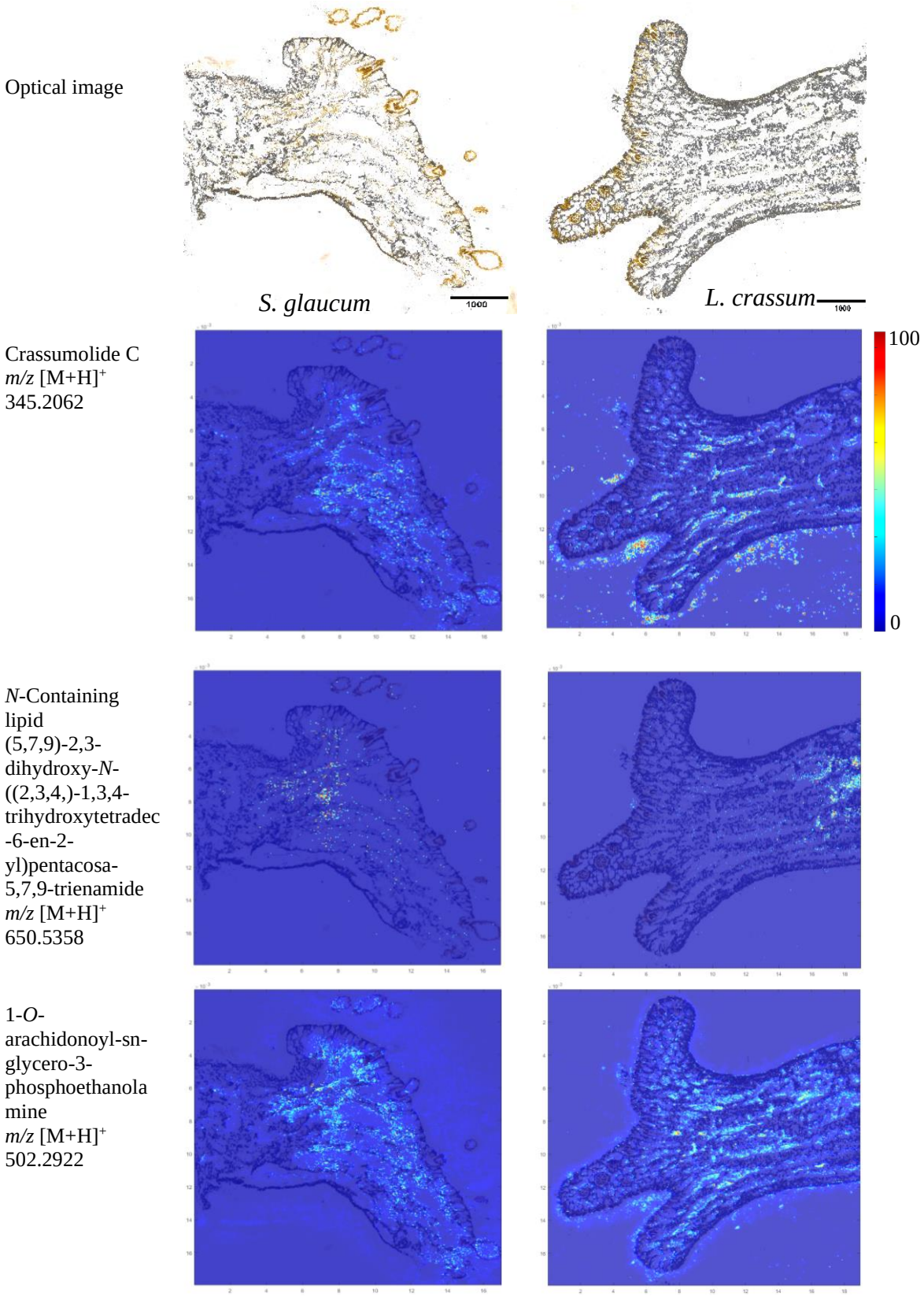

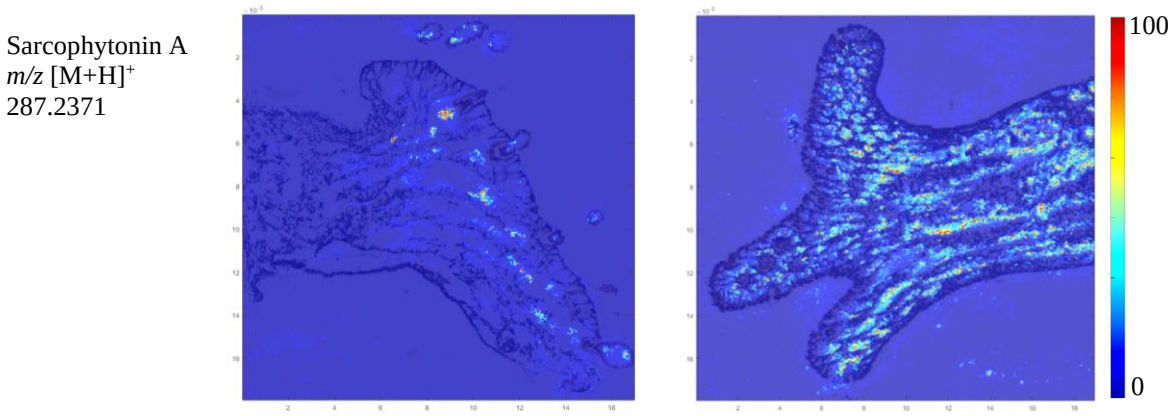

Figure 20 AP-MALDI-MSI of soft coral *Sarcophyton glaucum* and *Lobophytum crassum* with the spatial distribution of feature *m/z* $[M+H]^+$ 345.2062, 650.5358, 502.2922, 287.2371; and full microscopic image

According to the results in Figure 20, the distribution of each compound in the soft corals body was different, dependent of the compound classes. The cembranoid crassumolide C (**9**) (*m/z* $[M+H]^+$ 345.2422) was detected in the inner tissue of *S. glaucum* and *L. crassum* in an even distribution. However, some signals of this metabolite were detected around the targeted tissue (in the direction of sectioning), due to the migration (smearing) along the embedding material during the section. Nevertheles, it happened just for this section and did not appeared in other samples, which most likely due to the error during sectioning. Crassumolide C (**9**) was isolated for the first time from *L. crassum* as natural source [161]. Although this metabolite was initially isolated from *L. crassum*, it was also detected in *S. glaucum*. The uniform distribution of the cembranoid crassumolide C (**9**) in the soft coral body is related to the biological function of this compound group, which acts as chemical defense against predators [24, 162-164]. This compound exhibits a broad spectrum of anti-inflammatory and cytotoxic activity against a variety of cancer cell lines [161].

Beside of crassumolide C (**9**), the phospholipid 1-*O*-arachidonoyl-sn-glycero-3-phosphoethanolamine (*m/z* $[M+H]^+$ 502.2922; $C_{25}H_{44}O_7NP$) was also distributed in the whole bodies of *S. glaucum* and *L. crassum*, but it was also detected in low intensity at the outer membrane of both investigated species. This metabolite is an essential component of cell membranes; it consists of a hydrophilic head group and a hydrophobic tail, which confers amphiphilic properties on phospholipids [165]. The selective permeability of phospholipids benefits marine organisms by separating their organelles from the surrounding water, forming structural building blocks, and playing a critical role in cell biochemistry and physiology [145, 166]. Additionally, the presence of this phospholipid on the outer membrane (outer layer) of *S. glaucum* and *L. crassum* body confirmed that this phospholipid is also a constituent of the outer epidermis membrane of soft coral.

In contrast to crassumolide C (**9**) and phospholipid, the nitrogenous lipid (5,7,9)-2,3-dihydroxy-*N*-((2,3,4)-1,3,4-trihydroxytetradec-6-en-2-yl)pentacosa-5,7,9-trienamide (P.**36**) (*m/z* $[M+H]^+$ 650.5358) with the molecular formula $C_{39}H_{72}NO_6$ was localized around the

stem of investigated soft corals. In *S. glaucum* it occurs in the internal stem, and for *L. crassum* in the bottom end area of the stem. The distribution of nitrogenous fatty acids in this area of corals body may imply a role in the attachment mechanisms of this invertebrate to the solid surface, which aid in their integration with the substrate. The known process for this mechanism is due to corallite secretion. Each polyp of coral secretes a hard circular corallite (build of calcium carbonate), which help them to attach onto the surface of solid substrate [167].

Additionally, some studies revealed that there are some algae, so-called crustose coralline algae (CCA), that produce corallite to promote coral settlement on their substrate [168-170]. Moreover, coral-associated bacteria (CAB) e.g. *Pseudoalteromonas* contribute to the attachment of the corals by producing some secondary metabolites, e.g. cycloprodigiosin and tetrabromopyrrole (TBP) [171, 172]. Therefore, we conclude that this metabolite (*m/z* $[M+H]^+$ 650.5358) is probably produced by soft coral-associated microorganisms including algae. The interesting phenomenon was also observed in the spatial distribution of a cembrane diterpene, namely sarcophytonin A. This compound was detected in both soft corals in different areas. In *L. crassum*, this compound was detected in the whole body of this species. In the soft coral *S. glaucum*, sarcophytonin A collocated in the same area of diatoxanthin (pigment produced by zooxanthellae), which is in the gastrodermal cells of this soft coral. There are two possibilities: either this compound is produced as a result of the interaction between the two organisms (soft coral and zooxanthellae), or soft corals produce and store this metabolite in their gastrodermal cavity.

As described in some literature, Sarcophytonin A was isolated mostly from the genus *Sarcophyton* [137, 173-175]. However, the synthesis mechanism of this metabolite in the soft coral remains unknown. Nevertheless, there is evidence that the production of diterpenes and cembranoids in soft corals is related to the symbiont's biosynthesis activity [176-178]. Mydlarz et al. (2003) presented data that implicates the algal symbiont *Pseudopterogorgia elisabethae* as a biosynthetic source of their diterpenes based on ^{14}C labeling experiments [179]. Furthermore, Boehnlein et al (2005) used the radiolabeled GGDP (the ubiquitous diterpene precursor) to ensure the zooxanthellae as the responsible organism that produce diterpene in coral bodies. As a result, they conclude that diterpenes are produced within corals by some clades of algal symbiont, and not only localized in algae area [180]. Therefore, it is possible that sarcophytonin A is the symbiosis product of *S. glaucum* and their endosymbionts, which collocated in the gastrodermal cells.

4.4. Conclusion

This is the first study to examine inter- and intra-specific variation in secondary metabolites from three soft coral species, namely *Sarcophyton glaucum*, *Lobophytum crassum* and *Xenia umbellata*. The exact species of these corals were confirmed by using

mutS, COI, and 28S analysis. Moreover, by optimizing the sample preparation protocol and the measurement parameters within the analysis, a broad coverage of secondary metabolites was achieved. Overall, the untargeted metabolomics study based on ^{1}H-NMR, and LC-ESI-HRMS, combined with multivariate data analysis, enables the investigation of the chemodiversity of the investigated soft coral species. Due to the high detectability of secondary metabolites in positive ion mode compared to negative, LC-ESI-HRMS was only conducted in positive ion mode in this investigation. In negative ion mode, the most detected metabolites were fatty acids and lipids, which are irrelevant to our investigation.

A high degree of variability in the metabolites present in *X. umbellata* extracts in comparison to two other species. The TLC analysis indicates that the extract of *X. umbellata* contains more detectable metabolites than the extracts of the other two soft corals, which was also confirmed by LC-ESI-HRMS and ^{1}H-NMR. Multivariate data analyses of both LC-ESI-HRMS and ^{1}H-NMR data revealed that the compounds primarily responsible for the separation of *X. umbellata* were species-specific compounds, such as xeniolide O, gorgost-3-5, 6, 11, 20(s)-pentol-3-monoacetate, and umbellacin A, as well as unidentified nitrogenous lipids and fatty acids. This difference in metabolite profiles between *X. umbellata* and two other coral species may be explained by their phylogenetic position, as this former belongs to the Xenidae family, while *S. glaucum* and *L. crassum* belong to the Alcyoniidae. In addition, the major compound detected in *S. glaucum* (based on the LC-MS and ^{1}H NMR) was tentatively annotated as sarcophytoxide and its derivatives in *L. crassum*.

Furthermore, the spatial distribution of soft corals and zooxanthellae metabolites within the coral body was examined using MALDI-MS Imaging. The purpose of this study was to distinguish the marker metabolites produced by soft corals as well as their endosymbiont. This is the first study to employ MS-Imaging in order to investigate the distribution of soft corals and zooxanthellae metabolites in a systematic manner. In total, seven known compounds from soft corals and four known compounds from zooxanthellae were detected in the samples. This method may prove beneficial as a guide for isolating specific compounds within the soft coral body. Additionally, by observation of the spatial distribution of metabolites in soft corals' bodies, we can determine which metabolites are produced by soft corals or their symbiont, and which metabolites are a "symbiosis product" of these two organisms. It may contribute to a better understanding of the interaction between soft corals and zooxanthellae, particularly through their secondary metabolite biosynthesis. The presence of sclerites (particles of $CaCO_3$) in the coral tissue has been identified as a drawback of this method, which cause damage of sample, Moreover, the smearing of certain compounds (e.g. crassumolide C) during sectioning was observed, resulting in the migration of metabolite in the embedding medium. Therefore, the development of section method is necessary.

V. The effect of elicitors on *Sarcophyton glaucum*, *Lobophyton crassum*, and *Xenia umbellata*

Abstract

Soft corals are extremely vulnerable to changes in their environment. The responses to environmental change can be observed in their morphology (e.g. color, tentacle behavior), as well as in their symbiont (density of zooxanthellae and photosystem efficiency; PSII). The composition of secondary metabolites in soft corals is a further response, as such substances serve, e.g. as chemical defense in adverse conditions. Therefore, we studied all these responses in this study. The aim of this investigation was to determine the effects of various elicitors on the morphology and metabolite composition of soft corals and their endosymbiont, zooxanthellae. For five days, *S. glaucum*, *L. crassum*, and *X. umbellata* were exposed to a variety of stressors, including glyphosate, simazine, oxybenzone, octinoxate, $CuSO_4$, dimethyl phthalate, microplastic, and *Vibrio campbellii*. Chronic exposure to dimethyl phthalate and copper sulfate cause significant stress on the investigated soft corals. Under condition optimized for maximum separation, 38 metabolites were tentatively identified via ^{1}H-NMR and 85 metabolites via LC-ESI-HRMS, including diterpenes, sesquiterpenes, steroids, alkaloids, fatty acids, and lipids. Fatty acids are the primary components responsible for the separation of corals treated with dimethyl pthphthalate and $CuSO_4$ from the other extracts in the PCA score plot. These metabolites were detected in high abundance in these two extracts when compared to other extracts (based on ^{1}H-NMR data). In addition, nitrogenous lipids, cerebroside, steroid and steroidal alkaloid, were detected as additional metabolites in *L. crassum* extracts treated with $CuSO_4$. Coral stress was further determined by histological profiling of each soft coral tissue. This method was used to detect mucus production as a stress parameter. As a confirmation of the metabolite profiling results, dimethyl pthphthalate, $CuSO_4$, and *V. campbellii* act as elicitors, causing mucus production by corals as a chemical defense against elicitors and pathogen infection.

5.1. Introduction

Soft corals are extremely sensitive to environmental stress. There are numerous environmental stressors that affect soft coral, including high temperature, acidification, and level of CO_2, as well as chemical stressors which are produced by terrestrial activity (e.g. pesticides [91, 181, 182], heavy metals pollution [42, 43], sunscreen components [37, 92, 183], plasticizer and micro-plastics [44-46]. Some biological stressors such as infection by pathogens (microorganisms) and predatory fish are also catergorized as a stressors to this organism [39, 90-95]. All of these elicitors are potentially hazardous to soft corals, exacerbating coral bleaching and increasing the mortality of these invertebrates.

As a response to stress, coral morphology (e.g. color of the polyp, tentacle retraction, and the pulsation rate) are adapted in order to survive. Healthy *S. glaucum* is dark brown in color with a long elastic tentacle [83], whereas stress and possible bleaching of this coral are indicated by tentacle retraction and a change in the color of the soft coral umbrella [105, 184]. Similar to *S. glaucum*, the healthy *L. crassum* is brown-orange in color and contains extended autozooids and small siphonozooids in hole forms. The color of *L. crassum* becomes dark grey without any appearance of autozooids upon stress and bleaching. *X. umbellata* is unique in comparison to other two soft corals, especially their siphonozooids which are larger than in the other soft corals. This part of *X. umbellata* is used to determine the stress level by their pulsation rate. Beside the morphology of soft corals, including color and behavior of the tentacles and siphonozooids, the stress responses can be determined by the weight of individual corals, photosystem II efficiency, and number of zooxanthellae in the water.

The change of secondary metabolites in the soft corals may occur as response to stressors/elicitors, related to their function as a defense of corals under stressful conditions [185, 186]. Therefore, for more in-depth analysis of the soft corals' secondary metabolite profiles, and characterization of the chemical constituents, analytical techniques are required. The combination of 1D-^{1}H-nuclear magnetic resonance (NMR) and liquid chromatography coupled with mass spectrometry (LC-ESI-HRMS), as well as thin-layer chromatography (TLC) are the powerful tools to identify secondary metabolites, including soft coral constituents [56]. Furthermore, by using the multivariate data analysis (i.e. PCA), chemical variance in the soft corals can be observed, particularly of metabolite composition and levels in response to stressors.

5.2. Experimental

In order to determine the effect of elicitors on soft corals, a group of stressors was used to assess their effect on soft corals. Chemical elicitors in this study include a widely used herbicide (glyphosate), a fungicide (simazine), two sunblockers (oxybenzone and octinoxate), a plasticizer (dimethyl phthalate), and a heavy metal salt ($CuSO_4$). In addition, the physical elicitor was micro-plastic, while the biological elicitor was *Vibrio campbellii*. To observe the coral response, three soft coral species (*Sarcophyton glaucum*, *Lobophytum crassum*, and *Xenia umbellata*) were observed daily. The chemical structure of chemical elicitors used in this experiment are depicted in Figure 21.

The lyophilized material of 81 soft coral individuals from three species (*S. glaucum*, *L. crassum*, and *X. umbellata*) was extracted using different solvents. These solvents (methanol, 80% aqueous methanol, ethyl acetate, *n*-hexane, mixture of methanol and chloroform (1/1; v/v), and chloroform) were used to determine the most suitable solvent for maximal metabolite extraction from soft coral material. After comparing the extracts using TLC, LC-ESI-HRMS and ^{1}H-NMR, methanol was determined to be an optimal solvent due to the

abundance of features and peaks in the spectrum. To start the metabolite profiling study, TLC was used to obtain an overview of the soft coral metabolites present in the extracts. Afterwards, metabolites were determined using LC-ESI-HRMS and ^{1}H-NMR analysis for detailed analysis of metabolite profiles. The multivariate data analysis (i.e. PCA) was used to compare the obtained profiles and to identify the compounds that differed between treatments and species. The detected masses (compounds) were then manually annotated supported by databases and software tools, i.e. Reaxys, SciFinder, massbank.eu, and MetFamily. The experimental details are described in Chapter III.

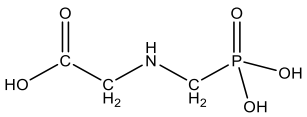

Glyphosate

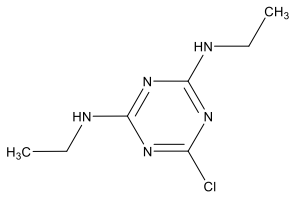

Simazine

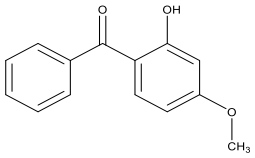

Oxybenzone

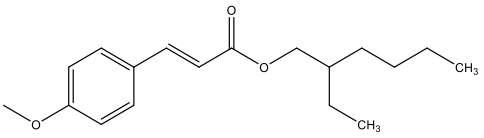

Octinoxate

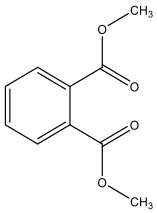

Dimethyl phthalate

Figure 21 Structures of chemical elicitors used in the experiment

5.3. Result and discussion

5.3.1. Morphological and physical effects on soft corals

a. Morphology

As a polyp organism, soft corals cannot move and change their habitat when confronted with unusual conditions. In order to survive, they must adapt to environmental changes. However, some of them are not able to adapt and become stressed, which eventually can lead to death. One of the stress responses of soft corals is tentacle retraction in order to reduce their consumption of toxic substances/elicitors in the water. Furthermore, under extreme conditions (e.g. high concentration of pollutant, temperature, and salinity), soft corals lose their algal symbiont and color, a condition known as coral bleaching, which results in physiological damage and coral mortality [187, 188]. The morphology of all soft corals after treatments are shown in Table 8, Figure 22 (*Sarcophyton glaucum*), Figure 23 (*Lobophytum crassum*) and Figure 24 (*Xenia umbellata*).

Table 8 Morphology of soft corals after stress treatment/elicitation

Soft coral sample / treatment		Morphology	
		Color of colony	Tentacle/siphonozooid
S. glaucum	Glyphosate	Brown-greenish	Expand
	Simazine	Brownish	Half retract
	Oxibenzone	Light brown	Half retract
	Octinoxate	Brown	Half retract
	$CuSO_4$	Light brown	Retract
	DMP	Brownish	Retract
	Micro-plastic	Brownish-grey	Expand
	Vibrio campbellii	Light brown	Half retract
	Control	Brown	Expand
L. crassum	Glyphosate	Brownish	Expand
	Simazine	Brownish	Expand
	Oxibenzone	Less light brown	Half retract
	Octinoxate	Brown	Half retract
	$CuSO_4$	Grey (thin membrane appear)	Retract
	DMP	Brown	Retract
	Micro-plastic	Brown	Half retract
	Vibrio campbellii	Brownish	Mostly retract
	Control	Brown	Expand
X. umbellata	Glyphosate	Light brown	Expand
	Simazine	Brownish	Half contract
	Oxibenzone	Brownish-grey	Mostly contract
	Octinoxate	Brownish-grey	Half contract
	$CuSO_4$	Grey	Contract
	DMP	Brownish	Mostly contract
	Micro-plastic	Light brownish	Half contract
	Vibrio campbellii	Brownish-grey	Contract
	Control	Brown	Expand

Note: retract → tentacle of *S. glaucum* and *L. crassum*; contract → tentacle/siphonozooids of *X. umbellata*

According to the results of this experiment, elicitors have a species-specific effect on the investigated soft corals. $CuSO_4$ and DMP, in general, are extremely toxic to all soft corals (*S. glaucum*, *L. crassum* and *X. umbellata*). In concentrations of 100 µg/L, these elicitors caused mortality of soft corals. *S. glaucum* was sensitive to all elicitors, except to glyphosate and micro-plastic. It is similar to *L. crassum*, which was also susceptible to these elicitors and to simazine. In comparison to the other species, *X. umbellata* exhibited a different response to elicitors. This soft coral was extremely sensitive to physical elicitors (micro-plastic) that caused tentacle damage. In addition, *V. campbelli* was shown to have a detrimental effect on this species. Interestingly, glyphosate even at 10 mg/L had no visible effect on all corals. Tentacles and siphonozooids were expanded, and the soft corals appeared healthy during elicitation (Figure 24).

As shown, $CuSO_4$ is very toxic to soft corals. This substance is a well-known trace element that is extremely toxic to marine invertebrates, including soft corals. $CuSO_4$ induces oxidative stress, DNA damage, and also has a detrimental effect on coral fertilization [189-191]. In contrast to $CuSO_4$, the effect of DMP on coral has not been thoroughly investigated. Nevertheless, this study is the first that documents the effect of DMP on soft coral. This substance has been detected in high concentrations in coral reefs as a byproduct of micro-plastic degradation and has been proposed as a potential hazard to coral ecosystem [46, 192,

193]. Additionally, we observed *V. campbelii*'s effect on these three soft corals. The infection with this bacterium appears to have a detrimental effect on corals, particularly on *X. umbellata*. In addition, this bacterium produces significant SOD activity, which leads to oxidative stress [194, 195].

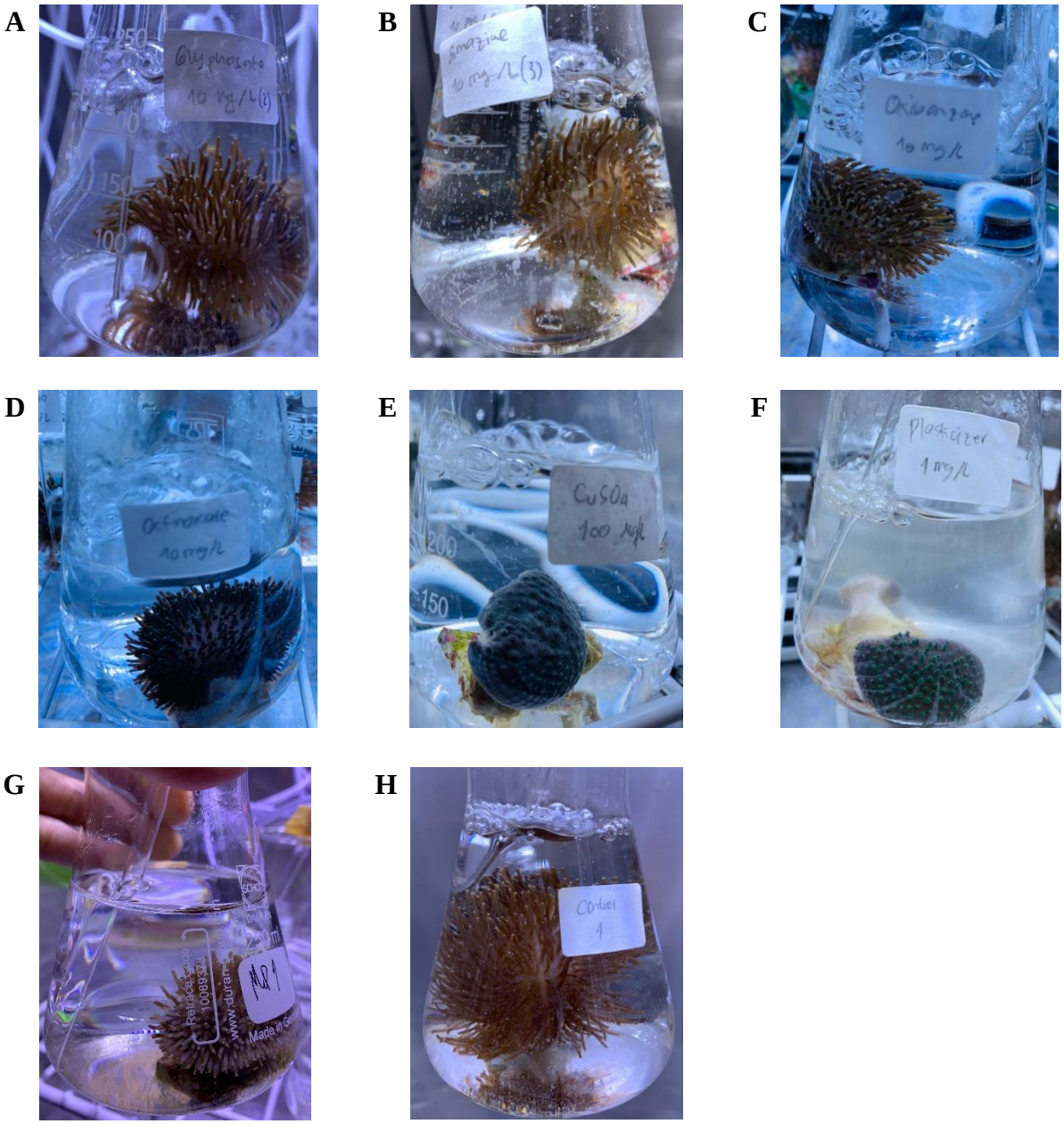

Figure 22 The morphology of *S. glaucum* after treatment with glyphosate (A), simazine (B), oxybenzone (C), octinoxate (D), $CuSO_4$ (E), plasticizer (F), micro-plastic (G), and without treatment (H)

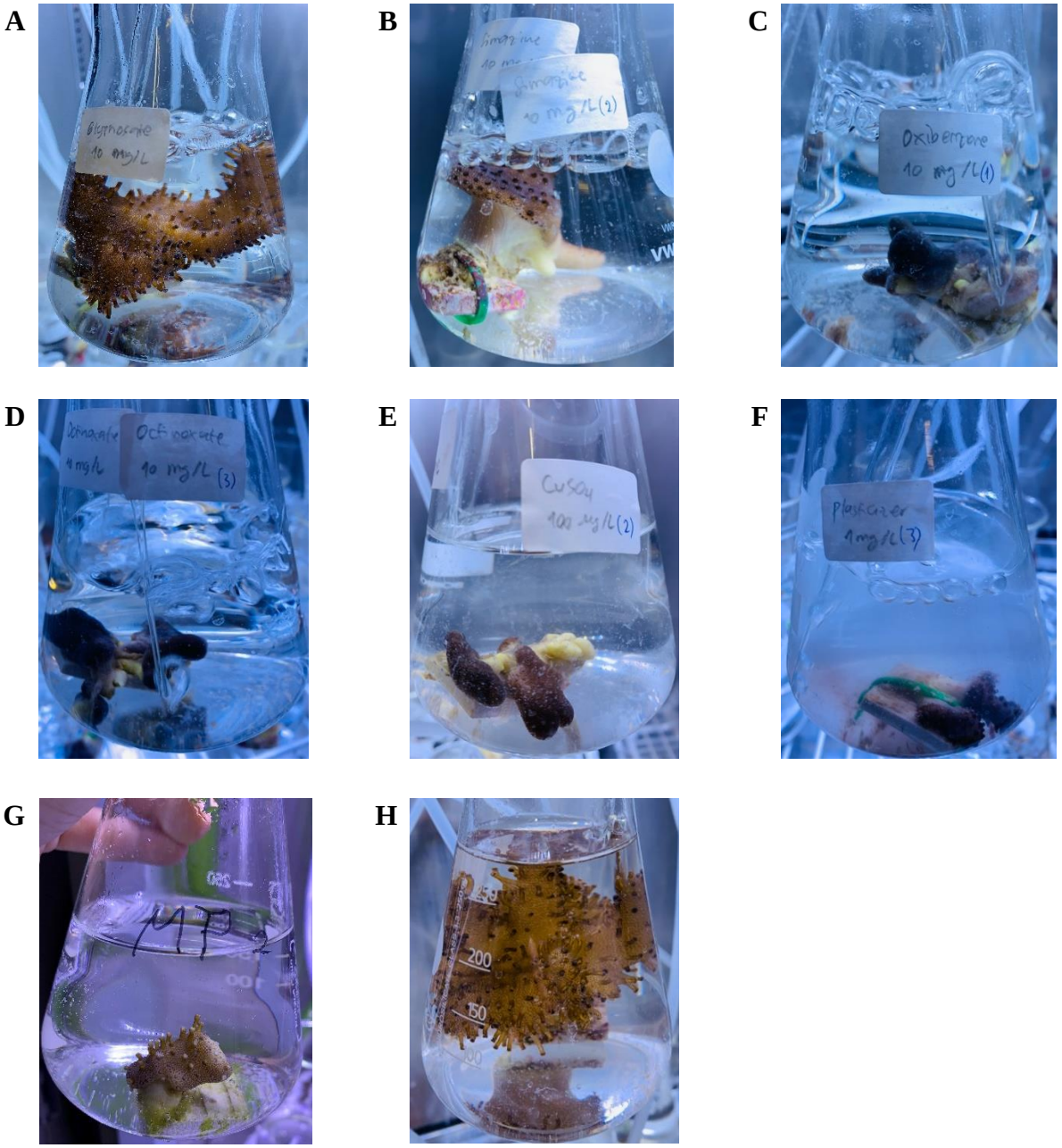

Figure 23 The morphology of *L. crassum* after treatment with glyphosate (A), simazine (B), oxybenzone (C), octinoxate (D), $CuSO_4$ (E), plasticizer (F), micro-plastic (G), and without treatment (H)

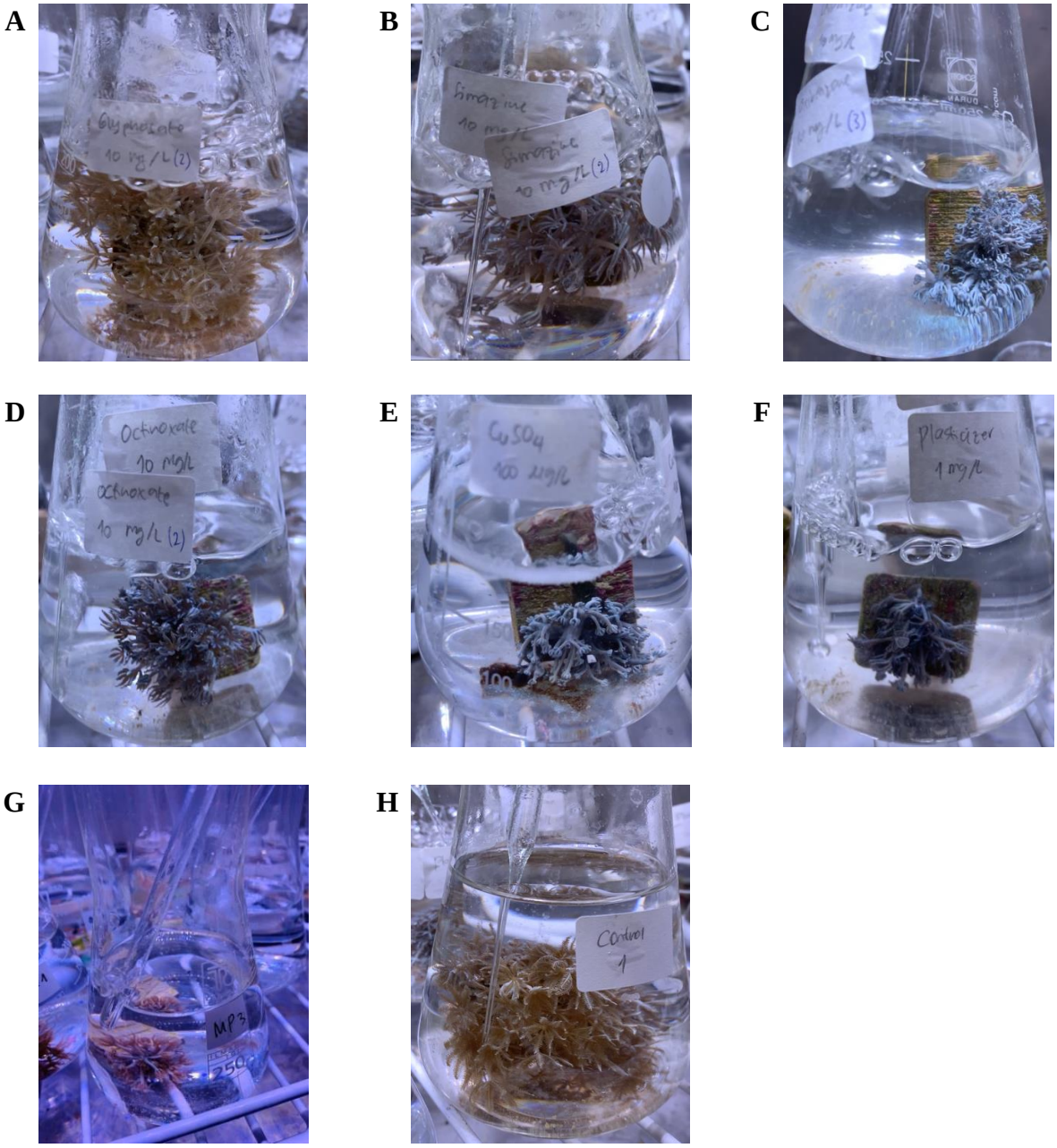

Figure 24 The morphology of *X.umbellata* after treatment with glyphosate (A), simazine (B), oxybenzone (C), octinoxate (D), $CuSO_4$ (E), plasticizer (F), micro-plastic (G), and without treatment (H)

It was surprising to discover that glyphosate had no effect on the morphology of these soft corals, despite the fact that a concentration of 10 mg/L (the concentration used in our experiment) is considered extremely high in comparison to the concentration of glyphosate detected in the ocean (ranging from 145 ng/L to 5.4 mg/L) [196-204]. Therefore, in order to investigate the effect of different glyphosate concentrations on soft corals in more detail, we conducted additional experiments and describe them separately in Chapter VII.

Apart from glyphosate, the effect of another pesticide (simazine) was detected. Simazine was toxic to *S. glaucum* and *X. umbellata*, affecting their morphology and pulsating rate. However, this herbicide had no effect on *L. crassum*. After treatment with simazine, *L.*

crassum remained healthy and exhibited similar morphology and behavior to the control. Direct effects of simazine on soft corals are unknown. Nevertheless, according to the mode of action of this herbicide, some researchers discovered that herbicides in the triazine family (i.e. simazine and atrazine) can inhibit electron transport during photosynthesis [205]. Therefore, it is possible that simazine has an effect on the soft coral's symbiont (zooxanthellae) rather than on the coral itself. Simazine destroys the photosynthesis system of zooxanthellae, and if used continuously, their photosynthesis process is disrupted, resulting in a reduction of nutrient supply to their host [206-209]. Due to a lack of nutrients, corals will become stressed and further expel the symbiont from their body. This expulsion of zooxanthellae from coral tissue can result in a susceptibility to bleaching [210].

The effect of the physical elicitor (micro-plastic) on *S. glaucum* and *L. crassum* during elicitation was not demonstrated physiologically. Micro-plactics, on the other hand, were capable of destroying the tentacle of *X.umbellata*. Micro-plastic particles were observed on the bodies of soft corals during the experiment, interfering with the movement of autozooids and siphonozooids. In the worst-case scenario, these particles can plug the pores of autozooids, obstructing gas and water circulation within the soft corals' bodies [44, 45].

Beside the morphology (body and tentacle behavior), the pumping rate of *X. umbellata* was also observed during the incubation (stress treatment). *X. umbellata* is a representative of the family Xeniidae which are known as pulsating corals. Instead of having the large body mass like *S. glaucum* and *L. crassum*, this species have unbranched stalks that are short, thick and smooth. The siphonozooids of Xenia which are used for pumping the water and organic/inorganic matters are bigger than in other soft corals, [211, 212]. According to previous research, certain inorganic ions and water temperature may influence the pulsation rates of xeniid soft corals [87, 213, 214]. Thus, the pulsation of Xenia's siphonozooids may be indicative for their stress. In order to observe *X. umbellata*'s stress response during elicitation, the pumping rate of siphonozooids was measured, and the results are shown in Figure 25.

After treatment with simazine, oxybenzone, $CuSO_4$, the plasticizer DMP, and *Vibrio campbellii*, the pulsation rate of *X. umbellata* was significantly reduced (P value <0.0001; Appendix 15) by nearly half compared to the control. On the other hand, glyphosate had no significant effect on pulsation of siphonozooids (P value= 0,7214; Appendix 15). As previously mentioned, $CuSO_4$ is very toxic for all investigated soft corals. This substance is one of the major compounds found in the aquatic ecosystem due to its use as an algaecide. This inorganic compound in the water can inhibit the movement of soft coral bodies, such as siphonozooids, thereby preventing re-filtration of the surrounding water [215, 216]. In addition, the effect of elicitors on the pulsation rate of *X. umbellata* tentacles was digitally documented as video ((DOI) 10.22000/566)*.

These videos are available via the following link:
https://www.radar-service.eu/radar/en/dataset/mwwipjWbqrEwLjex?token=DwzNJebKcUWGHjLkcCkZ

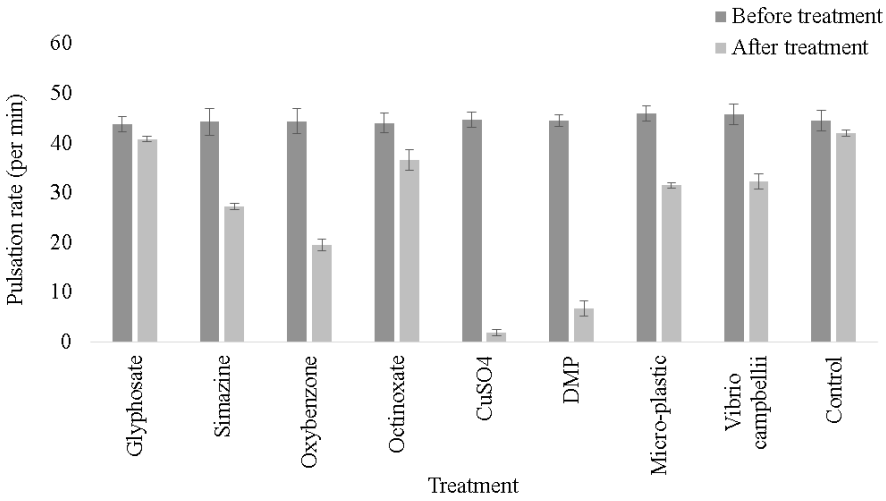

Figure 25 Pulsation rate of *Xenia umbellata*'s siphonozooids depending on treatment; statistical analysis (significance difference) by using Dunnett's multiple comparisons test is shown in Appendix 15

Regarding the effects of simazine and oxybenzone, the underlying mechanism of pulsation of *X. umbellata* remains unknown. However, there is a possibility that the effects of both components are related to the appearance and metabolism of zooxanthellae in their tissue. The elicitors can inhibit the energy required for zooxanthellae metabolism, for instance simazine was described to inhibite the photosystem of zooxanthellae by interfering with electron transfer [209]. Without electron transfer, sunlight energy cannot be converted to photosynthetic energy. Oxybenzone also has an effect on the photosynthesis activity of zooxanthellae by blocking the sunlight required for zooxanthellae energy excitation [217]. This elicitor interacted with the surface of soft corals on which zooxanthellae are distributed and inhibited the energy excitation of zooxanthellae. This condition resulted in soft corals experiencing oxidative stress, similar to the effect of *V. campbellii* on soft corals [195]. Although the micro-plastic had no effect on the pulsation rate of siphonozooids, these materials were attached to and broke the siphonozooids of *X. umbellata*. In this state, some siphonozooids became broken, impairing their ability to pulse properly.

b. Weight

S. glaucum, *L. crassum*, and *X. umbellata* were weighted before and after stress treatments. This procedure allowed us to correlate the amount of water lost and the zooxanthellae released. The weight of soft corals is shown in Figure 26. Generally, after treatment, the weight of soft corals decreased. The greatest weight loss up to 70% occurred in all soft corals treated with 100 µg/L of both $CuSO_4$ and DMP (P value <0.0001; Appendix 15). It is correlated with the behavior of soft corals, as the tentacles of *S. glaucum* and *L. crassum* were completely retracted after exposure to those two elicitors. This condition occurred as the response to toxic accumulation in the water. As result, soft corals will expel water from their bodies in order to flush out the toxins. On the other hand, retracting the tentacles aids the coral in consuming less toxin [87, 218, 219].

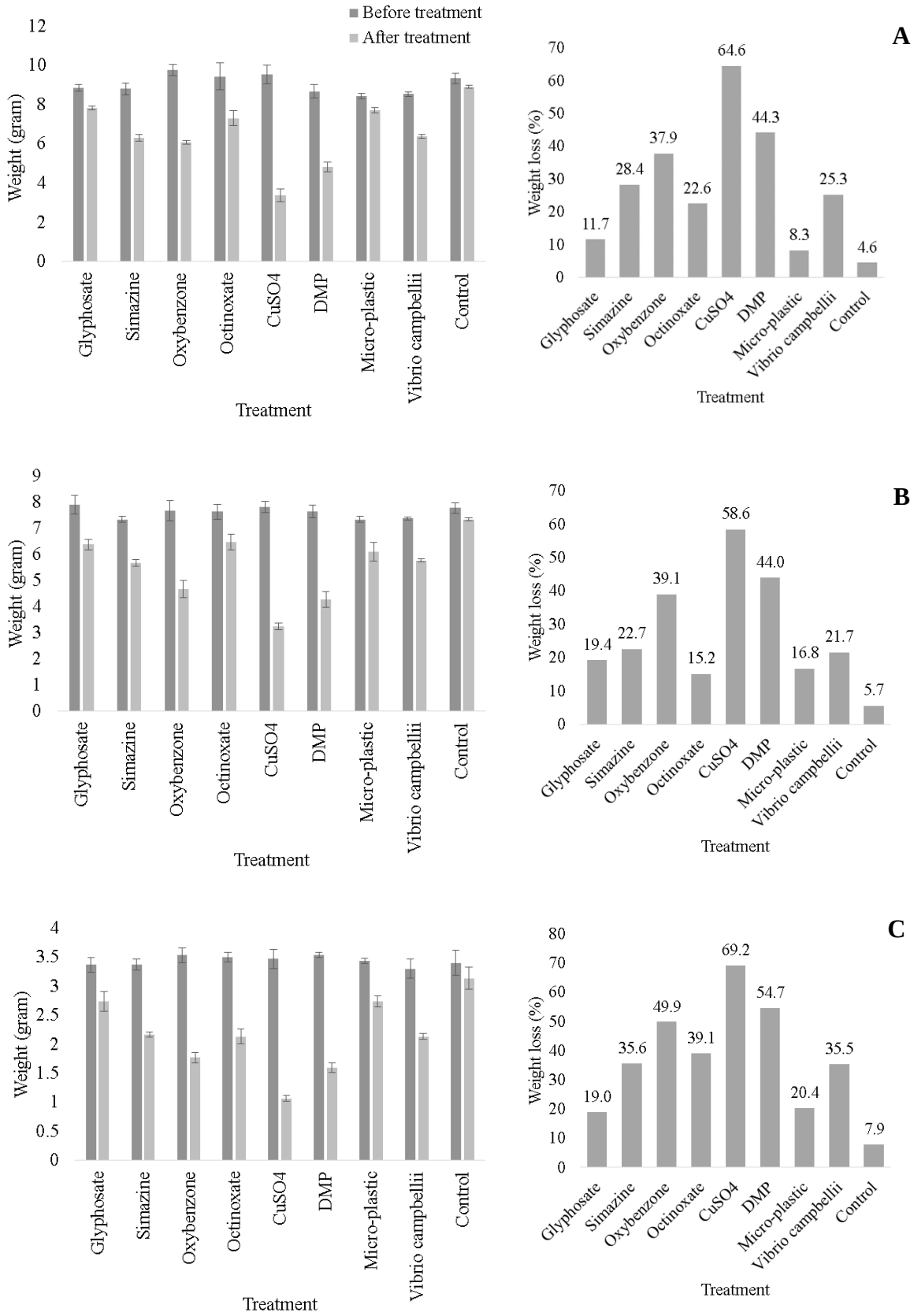

Figure 26 Weight of *Sarcophyton glaucum* (A), *Lobophytum crassum* (B) and *Xenia umbellata* (C); left= absolute number of soft corals weight (gram), right= relative percentage of weight loss (%) of coral after treatment; statistical analysis (significance difference) by using Dunnett's multiple comparisons test is shown in Appendix 15

Other elicitors, such as pesticides (glyphosate and simazine), sun-blocker components (oxybenzone and octinoxate), and *V. campbellii*, also caused weight loss in soft corals. All of these elicitors are referred as bleaching precursors [37, 39, 46, 92, 110, 192, 220-222]. Pesticides and oils (e.g. octinoxate) may cause zooxanthellae to be expelled from coral tissue [223, 224]. *V. campbellii*, a superoxide dismutase and catalase producer, has been shown to cause oxidative stress in zooxanthellae and soft coral [118]. This result can be correlated with the total number of zooxanthellae in the water column (Figure 28). On the other hand, glyphosate and micro-plastic have no significance effect on the weight of soft corals (P value= 0,0142; Appendix 15). However, each soft coral exhibits a unique toxicity response, which depends on the morphology and osmotic system of the species. The weight loss in control samples were observed in all investigated soft corals. This situation is expected since the adaptation process of the corals to the new environment, out of the maintenance aquarium, also causes some reaction (and minor stress).

c. Photosystem II efficiency

The efficiency of photosystem II (PSII) can be characterized by the quantification of the induction of chlorophyll fluorescence *in vivo*. These measurements served as a proxy for the physiological status of the autotrophic endosymbiotic zooxanthellae. The efficiency of PSII within soft coral endosymbiotic microalgae (zooxanthellae) is used to quantify photo-inactivation during coral bleaching [225]. The efficiency of photosystem II (PSII) has been measured in dark-adapted macrophytes in order to estimate its potential quantum yield. To conduct the measurement, each jar of soft corals was placed in a dark box for 20 minutes, and PSII as well as the chlorophyll photosystem yield was determined using a PAM 2500 portable fluorometer under dark conditions. In the dark, the photosytem apparatus of zooxanthellae is unfunctional. As a result, the photosystem will arrest at “state 1”, and cannot continue to “state 2” transition which causes several changes, also by phosphorylation of the Light-Harvesting Complex II (LHCII). A total of three measurements were taken from the body of each living soft coral to obtain a representative measurement for the soft coral fragment. To avoid damaging the soft corals, the optic fiber of the PAM instrument (5.5 mm diameter) was placed on top of the corals’ bodies at a distance of 2-5 mm during the measurements. The PSII values for all soft corals are depicted in Figure 27.

The PAM results for all samples indicated that the PSII of zooxanthellae in soft coral was significantly reduced after 4 days exposure to elicitors, especially to $CuSO_4$ and DMP (P value <0.0001; Appendix 15). It could be related to zooxanthellae mortality in soft coral tissue or zooxanthellae expulsion from their host. This was corroborated by visual observation of seawater medium. The color of water was brownish and the particles of zooxanthellae were visible on the bottom of incubation jar. Surprisingly, in contrast to soft corals treated with $CuSO_4$ and DMP, the PSII efficiency of zooxanthellae in *S. glaucum* treated with glyphosate was increased after treatment. It is probable that glyphosate at a

concentration of 10 mg/L acts as a fertilizer for the zooxanthellae due to the phosphorus content in this herbicide, or that this soft coral belongs to the group of glyphosate-resistant organisms.

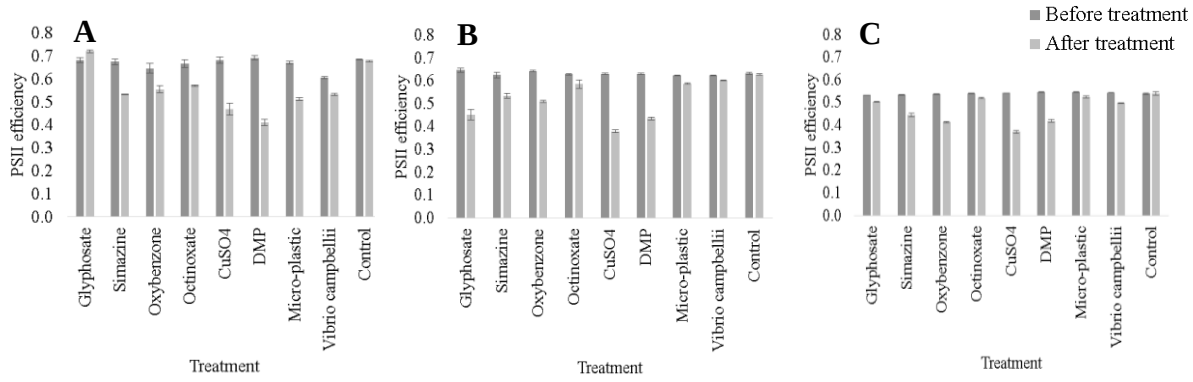

Figure 27 Photosystem II efficiency of *Sarcophyton glaucum* (A), *Lobophytum crassum* (B) and *Xenia umbellata* (C) before and after treatments; statistical analysis (significance difference) by using Dunnett's multiple comparisons test is shown in Appendix 15

Additionally, other treatments such as with simazine and oxybenzone were shown to have an effect on the PSII by reducing the zooxanthellae's PSII efficiency. The reasons for the decrease in zooxanthellae PSII efficiency are the degradation of the zooxanthellae protein and photosynthetic apparatus [225-227]. Simazine inhibited the PSII yield of zooxanthellae by destroying the photosynthesis apparatus of this organism [207]. As a result, zooxanthellae were unable to transfer energy to their host and produced highly reactive oxidative species (ROS) that are toxic to soft corals [207, 209, 228]. Oxybenzone, on the other hand, has a detrimental effect on zooxanthellae, and has been identified as a toxic component to corals. This organic UV filter is potentially harmful to corals and their larvae [37, 92, 183]. According to Downs et al. (2016), oxybenzone may act as an endocrine disruptor during skeletal development and may promote coral bleaching by inducing a viral lytic cycle in zooxanthellae [92]. Thus, by causing damage to the zooxanthellae, it affects photo-inhibitory damage and results in soft coral bleaching [223, 229].

d. Number of zooxanthellae associated

Soft coral bleaching is frequently quantified using indirect proxies for zooxanthellae densities [230]. Rather than assessing coral paleness or whitening, direct quantification of zooxanthellae cells provides the most unambiguous and determinative measure of soft coral and/or zooxanthellae during unfavorable conditions [231]. Further, the release of the endosymbiotic dinoflagelates from the soft coral body is a sign of stress, whether on the soft coral or on the zooxanthellae. Under normal conditions, zooxanthellae migrate or are expelled at a very low rate [232]. Corals normally release (expel) zooxanthellae from their bodies in order to maintain the right density of their symbiont as well as to maintain a constant amount of organic matter within their tissues [233, 234]. However, during adverse condition (e.g. high water temperature and salinity, as well as the contamination of toxic substance), this migration would be extremely rapid. Therefore, the stress of soft corals is

inversely proportional to the number of zooxanthellae released by them [235]. Using a hemocytometer, the density of zooxanthellae in water in this experiment was determined and expressed as the total number of zooxanthellae cells per milliliter. The zooxanthellae cell from the soft coral treated with *Vibrio campbellii* were not counted, due to sanitation reasons. The zooxanthellae densities in the water column is shown in Figure 28.

In general, density of zooxanthellae in the water colomn was increased after treatments (Figure 28 and Figure 29). However, the highest number of zooxanthellae cells in the water was observed in the water column of soft corals treated with $CuSO_4$ for *S. glaucum*, while the highest number in the water column of *L. crassum* and *X. umbellata* was observed after exposured to $CuSO_4$ and micro-plastic. $CuSO_4$ exposure is detrimental to soft corals and their symbiont. Copper is one of the essential trace element for biological function of algae. For instance, it forms part of the plastocyanin protein, which is involved in photosynthetic electron transport, and is also a cofactor of the enzymes Cu/Zn-superoxide dismutase, cytochrome c oxidase, and some other oxidative enzyme. However, in high concentrations, copper can be toxic to algae and also to a wide range of other marine organisms [236, 237]. In addition, copper sulfate may inactivate algae cells and cause cell lysis, depending on the concentration used [238]. Therefore, this substance may be toxic to both soft corals and zooxanthellae.

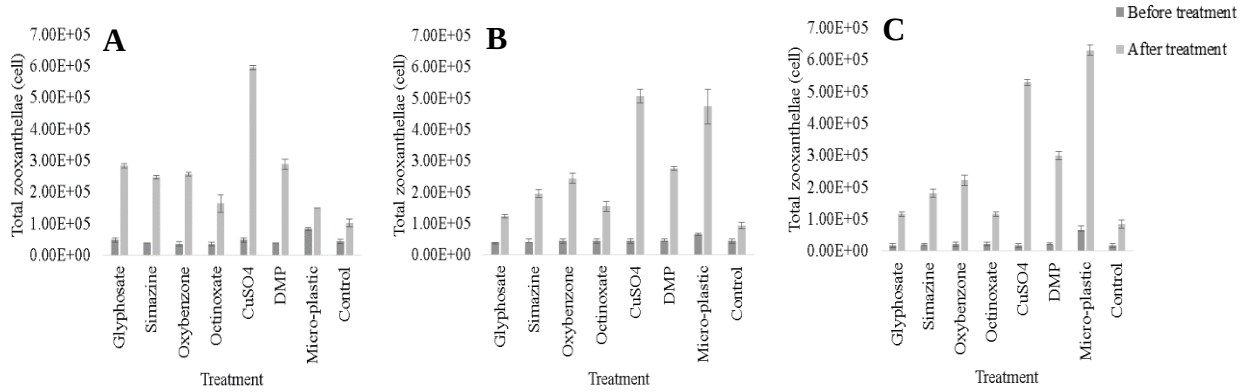

Figure 28 Density of zooxanthellae cell associated with *Sarcophyton glaucum* (A), *Lobophytum crassum* (B) and *Xenia umbellata* (C) before and after treatment; statistical analysis (significance difference) by using Dunnett's multiple comparisons test is shown in Appendix 15

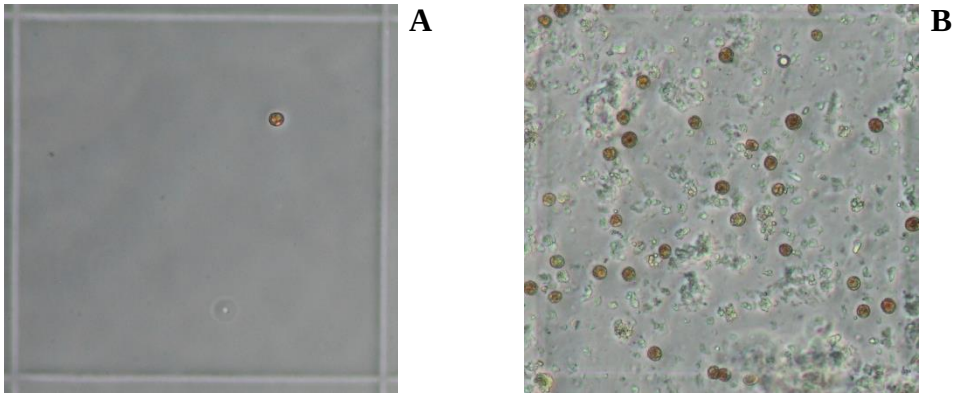

Figure 29 Zooxanthellae (*Symbiodinium* sp.) density of control sample (A) and treated with $CuSO_4$ (B) under microscope

A clear effect of micro-plastic on the expulsion of zooxanthellae from soft corals body was observed on *L. crassum* and *X. umbellata*, which was reflected by the high number of zooxanthellae in the water. Micro-plastic probably acts as precursor to zooxanthellae expulsion. Research by Reichert et al. (2018) found that micro-plastic has a negative effect on corals [239]. In another study, it was discovered that ingesting micro-plastic from commercial face wash (3-60 μm) can significantly impair zooxanthellae's ability to infect their host and further disrupt their relationship [240]. Moreover, micro-plastic exposure affects apoptosis and metabolism of zooxanthellae, as well as increases their oxidative stress [241]. In addition, another study found that the ingestion of Low Densiy Polyethylene (LDPE) micro-plastics (<100, 100-200, and 200-500 μm) led to release of zooxanthellae, and subsequent coral bleaching and necrosis [242].

5.3.2. Metabolite Profiling: The effect of chemical, biological, and physical stressors on soft coral metabolites (^{1}H NMR and LC-ESI-HRMS based metabolomics study)

a. Thin-layer chromatography

Thin-layer chromatography is a rapid and efficient technique for separating or identifying a mixture of non-volatile components in natural source extracts. This method is frequently used in order to rapidly identify the group of compounds. In this study, each extract was analyzed at a concentration of 20 mg/mL to determine the metabolite diversity present in soft coral species after treatment. The TLC screening of soft coral extracts in normal phase using *n*-hexane/ethyl acetate (3:2 v/v) as eluents is shown in Figure 30.

The combination of eluents allowed partial separation of compounds in the soft coral extracts. Non-polar compounds exhibit bands with a higher R_f value, whereas polar compounds retain a lower R_f value in the range 0-0.2. From this overview, it was clear that the extracts of soft corals with different treatments exhibit a similar pattern of metabolites, but differ in the intensity of each band. Moreover, variation in the composition of metabolites is observed between soft coral species as already described in Chapter IV. Unfortunately, the majority of the compounds isolated from those soft corals was UV inactive, which makes it difficult to detect using this method.

Under UV light λ 366 nm, the extracts exhibited a strong red fluorescence as a dominant band. The strong red fluorescent band (I) with R_f values in the range from 0.5 to 0.9 correspond to chlorophyll and its degradation products. The chlorophyll content of the soft corals extract is derived from zooxanthellae. This red fluorescent metabolites in extracts of *S. glaucum* treated with simazine and *V. campbelii* were observed at a low intensity under 366 nm UV light. Additionally, one red fluorescence signal at R_f 0.14 was observed at a high intensity in *S. glaucum* extracts treated with octinoxate and $CuSO_4$. In comparison to *S. glaucum*, the distinction between the *L. crassum* extracts was difficult to discern due to the low fluorescence intensities of extracts. In addition, the chlorophyll content in *L. crassum* is lower than in *S. glaucum*, as the algae harbor in this soft coral is not as abundant as in *S.*

glaucum, which is reflected in the brown color of each of these corals species. Furthermore, the difference in metabolite composition of extracts from *X. umbellata* treated with DMP was observed at λ 366 nm. Numerous bands were missing, for instance the red bands between R_f values 0.5-0.35. Moreover, extracts of *X. umbellata* treated with microplastic exhibit the most distinct profile under UV light at λ 254 nm, particularly by the appearance of a single band at R_f 0.74. Along with this band, two other bands in extracts of this soft coral treated with $CuSO_4$, *V. campbelii*, and DMP exhibit a strong signal extinction at λ 254 nm.

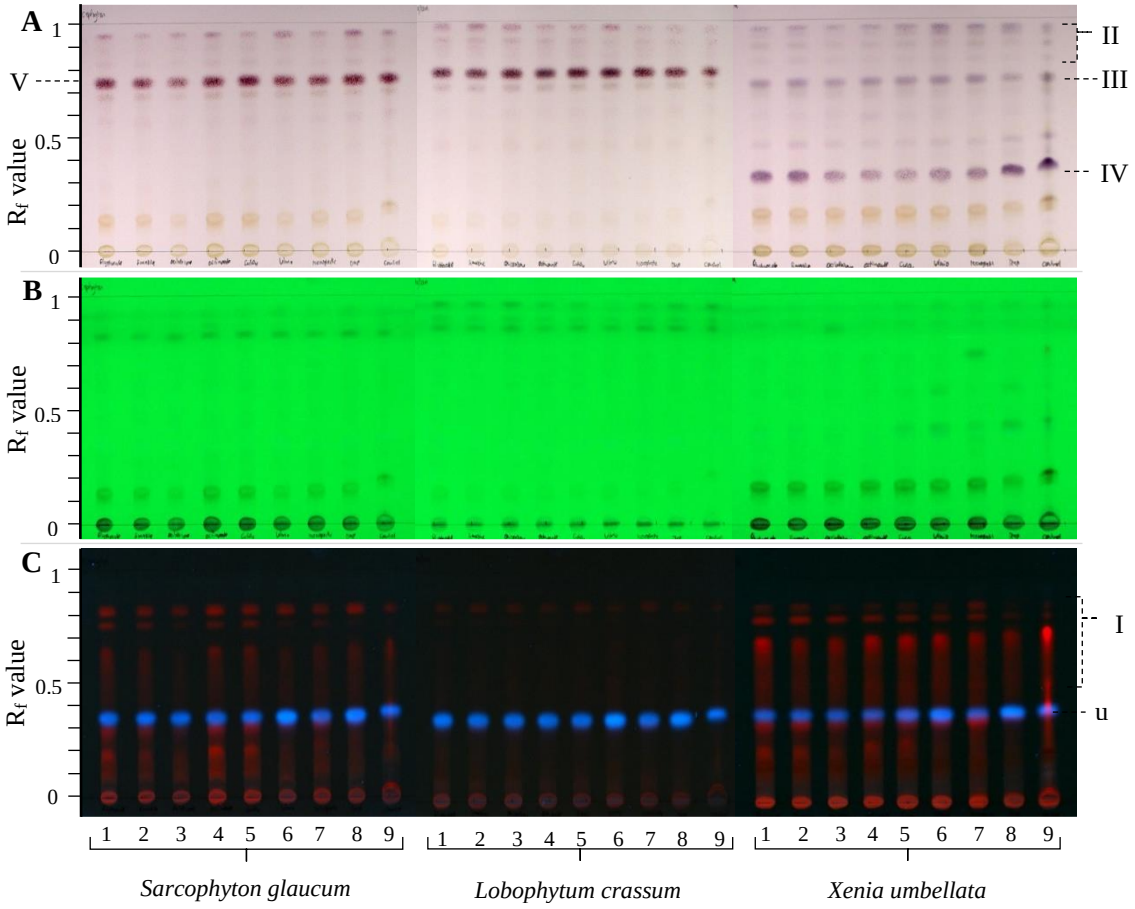

Note: 1= glyphosate, 2= simazine, 3= oxybenzone, 4= octinoxate, 5= $CuSO_4$, 6= *Vibrio campbellii*, 7= microplastic, 8= DMP, 9= control

Figure 30 Thin-layer chromatography (TLC) of crude methanolic extracts of soft corals treated with different elicitors (c = 20 mg/mL, mobile phase: n-hexane/ethyl acetate (3:2 v/v)), visualized by vanillin-sulfuric acid (A), under UV-light (254 nm (B), 366 nm (C)); I=chlorophylls, II=sarcophine, III= gorgosterol, IV= xeniolide O, V= sarcophytoxide, u= umbelliferon

The large blue-purple spot at R_f 0.89 (V) in *S. glaucum* and *L. crassum* extracts, as well as the smaller blue-purple spot at R_f 0.4 (IV) for *X. umbellata* extracts correspond to terpenoid compounds. It was confirmed by the purple-blue color after vanillin-sulfuric acid reagent spraying and heating. These two metabolites are the major compounds in each soft coral species, and were identified based on the LC-MS as xeniolide O (IV) and sarcophytoxide (V). Xeniolide O (IV), a 9-membered xenia diterpene was detected in high concentrations in *X. umbellata* extracts treated with DMP. This means that DMP exposure induces the production of diterpene in soft corals as a response to unfavorable conditions.

Apart from the ubiquitous bands, the extracts contain a variety of species-specific compounds. The extracts of *X. umbellata* were the most intense extracts under the UV light.

Based on this result, we conclude that TLC analyses of methanolic extracts of soft corals revealed the first insight about the complexity of these extracts. Also, TLC screening can provide information for a preliminary comparison of the various constituents within the investigated species. In additional, based on their chemical constituent, reaction with vanillin-sulfuric acid reagent gives hints on the compound classes, *i.e.* steroids, terpenoids, and diterpenes as well as chlorophyll from the soft coral's symbiont. However, without reference substances or additional characterization using multiple analytical methods, it is difficult to identify a specific compound. Therefore, additional characterization using analytical methods, such as ^{1}H-NMR and LC-ESI-HRMS-based profiling is required to compare metabolites under different treatment conditions per species.

b. ^{1}H-NMR profiling

^{1}H-NMR is a widely used analytical technique in metabolomics due to its high reproducibility. Recently, this method has been applied to crude extracts of soft corals in order to have insight into metabolites of these marine organism [56, 57]. NMR is particularly effective at detecting and characterizing compounds that LC-MS cannot detect easily, such as sugars, fatty acids, alcohols, polyols, and other low ionizing compounds. Moreover, this method proves excellent for detecting changes in the metabolite profiles of soft corals following stress treatments.

As shown in Figure 31, the ^{1}H-NMR profiles within species were quite similar, whereas the differences between species were large, particularly for *X. umbellata* extracts. In addition, ^{1}H-NMR spectra displays a diverse profile of extracts with different treatment for each species (highlighted in green color). This distinction is not only in the term of chemical composition, but also in the concentration of constituents. Some differences of ^{1}H-NMR spectra of the extracts were observed in the small signals between δ 8.00-9.50 ppm which probably is due to minor differences in pH or concentration of the NMR samples. In general, the extracts of all soft coral species treated with dimethyl phthalate and $CuSO_4$ exhibited marked differences in their profiles compared to other extracts. This distinction is also evident in multivariate data analysis.

According to the ^{1}H-NMR spectra, the content of fatty acids in soft coral extracts treated with dimethyl phthalate was relatively low in comparison to other extracts. Fatty acids were characterized by two signals at δ 1.27-1.33 ppm and δ 0.87-0.92 ppm corresponding to methylenes ($(CH_2)n$) and the CH_3 terminal group. In addition, the presence of unsaturated fatty acids were detected in ^{1}H-NMR spectra based on the proton multiplicity and chemical shift in the olefinic protons area (δ 5.32-5.40). However, due to the complexity of the extracts, the signals of fatty acids were overlapping. In comparison to fatty acids, sugar was not abundant in soft corals. Certain sugar moiety signals in the spectra of soft coral extracts

are associated with cerebrosides and ceramides. In this study, multivariate data analysis was used to determine the effect of stress treatment (elicitors) on each coral species and to compare it to the control (untreated).

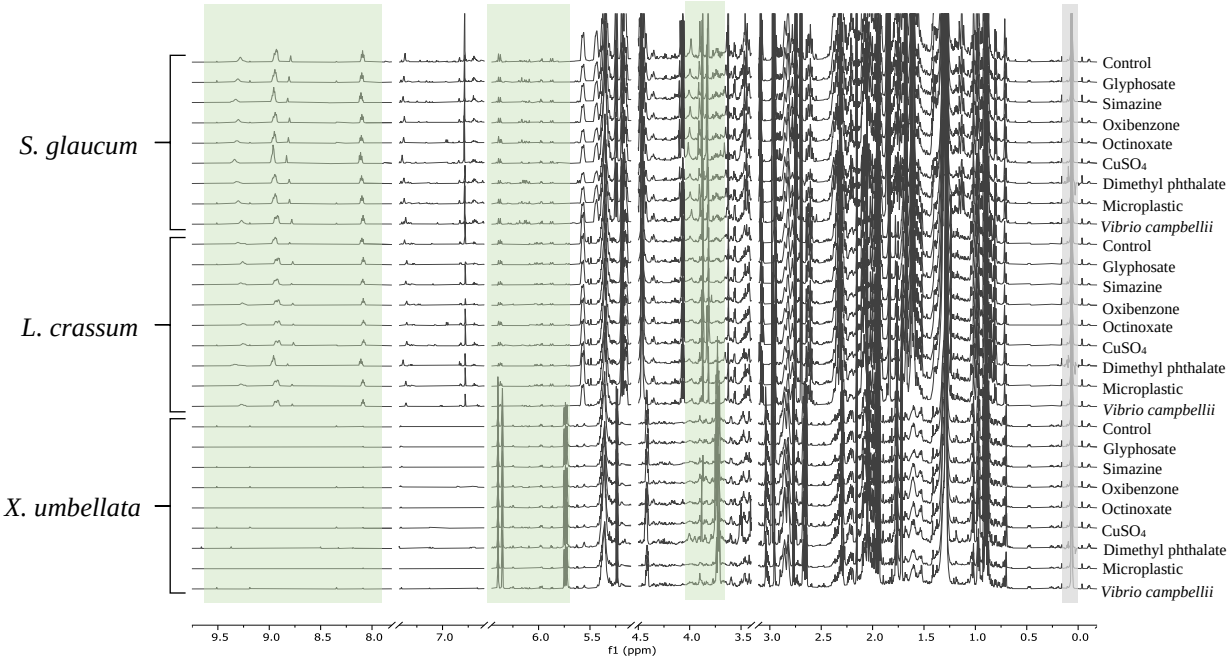

Figure 31 Stacked ^{1}H-NMR spectra (600 MHz, CD_3OD) of methanolic extracts of soft corals *Sarcophyton glaucum*, *Lobophytum crassum*, and *Xenia umbellata* treated with different elicitors. Solvent and elicitors signals are cut off (H_2O (4.50 – 5.10 ppm), CD_3OD (3.11-3.4 ppm), elicitors (6.4-6.6 ppm; 7.0-7.8 ppm)); spectra of elicitors are shown in Appendix 3

^{1}H-NMR based multivariate data analysis of *Sarcophyton glaucum* extracts

The ^{1}H-NMR data of *S. glaucum* were analyzed, and multivariate data analysis was used to determine the difference between *S. glaucum* extracts after treatment. The calculated PCAs are shown in Figure 32. In addition, 14 compounds were tentatively assigned based on 1D and 2D NMR spectra (HSQC), as well as comparison to literature (Figure 34, Appendix 5). The results shown in PCA scores plots (Figure 32. A) indicate that extracts of *S. glaucum* treated with DMP were distinct from other extracts in PC1 (variance 35.5%), whereas extracts of $CuSO_4$ treated sample were separated in PC2 (variance 20.1%). The bins causing the separation of each sample are shown in the corresponding loading plot (Figure 32.B), and were compared to the tentative metabolite assignments in Appendix 5. The separation of extracts of soft coral treated with DMP is due to the signal of fatty acids (**15**) (δ 1.28.132 ppm; 0.93 ppm). In addition, two unsaturated fatty acid signals at δ 5.34-5.36 ppm were responsible for this separation. In comparison to other extracts, fatty acids content in this sample was significantly higher (Figure 33.A). Regarding the clustering of $CuSO_4$ treated samples, the metabolite connected to the three bins responsible for separation in the area δ 3.88, 2.96, and 2.70 remain unknown.

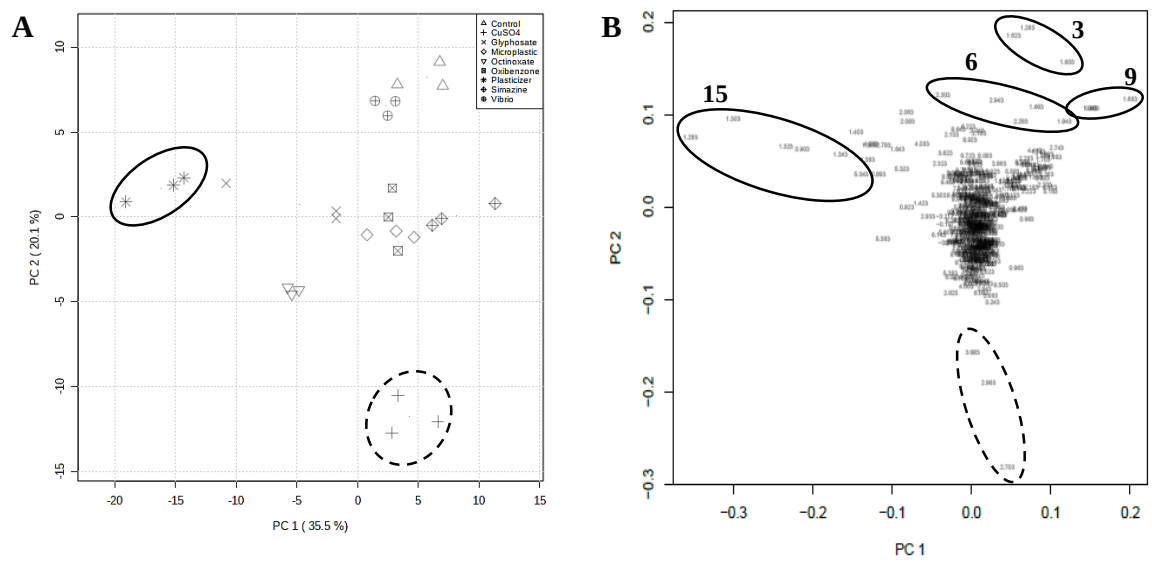

Note= Δ: Control, +: $CuSO_4$, ×: Glyphosate, ◇: Microplastic, ∇: Octinoxate, ⊠: Oxibenzone, ✱: Plasticizer, ◈: Simazine, ⊕: Vibrio

Figure 32 ^{1}H-NMR based PCA of *Sarcophyton glaucum* extracts; scores plot (a) and loadings plot (b)

The increase in fatty acid content of *S. glaucum* extract treated with DMP may be related to the amount of energy required by soft coral to survive under stress conditions. Fatty acids and lipids provide energy also to marine organisms such as corals [243, 244]. By increasing the amount of fatty acids in their bodies, soft corals can maintain their energy levels in this unfavorable environment. In addition, fatty acids and lipids in coral bodies play a role in the membrane permeability [245, 246]. Therefore, in order to maintain the membrane integrity in the stress condition, the synthesis of these metabolites is necessary. Fatty acids and lipids in the coral are also contributed by their endosymbionts, zooxanthellae [246, 247]. Moreover, a remarkable phenomenon was observed in soft coral extracts treated with *V. campbelli*, which clustered together with the control (untreated sample). These two groups of extracts were distinct from the others at PC2 (variance 20.1%) in the opposite direction of $CuSO_4$. This result confirmed that *V. campbelli* has no direct effect on *S. glaucum* metabolites. The compounds responsible for the separation of these two groups have been tentatively assigned as sarcophytoxide (**3**), sarglaucol (**6**), and ent-sarcophyolide E (**9**). In addition, these metabolites were detected as more abundant components in these two groups in comparison to other groups (Figure 33.b-d).

Sarcophtoxide, sarglaucol, and ent-sarcophyolide E are the major and specific metabolites found in the *S. glaucum* species. Sarglaucol ($C_{20}H_{32}O_2$) was isolated from *S. glaucum* and known as the precursor of tetraterpenoids [22], whereas sarcophytoxide ($C_{20}H_{30}O_2$) is a isoprenoid. These metabolites act as anti-predatory, which are produced by soft coral genus *Sarcophyton* [248]. The high concentration of this compounds in the control sample means that it was detected at a low concentration in the treated soft coral extract. The stress (elicitation) process altered the composition of these compounds in *S. glaucum* (i.e. the

terpenoids constituent). However, the mechanisms underlying this change are unknown and require additional analysis.

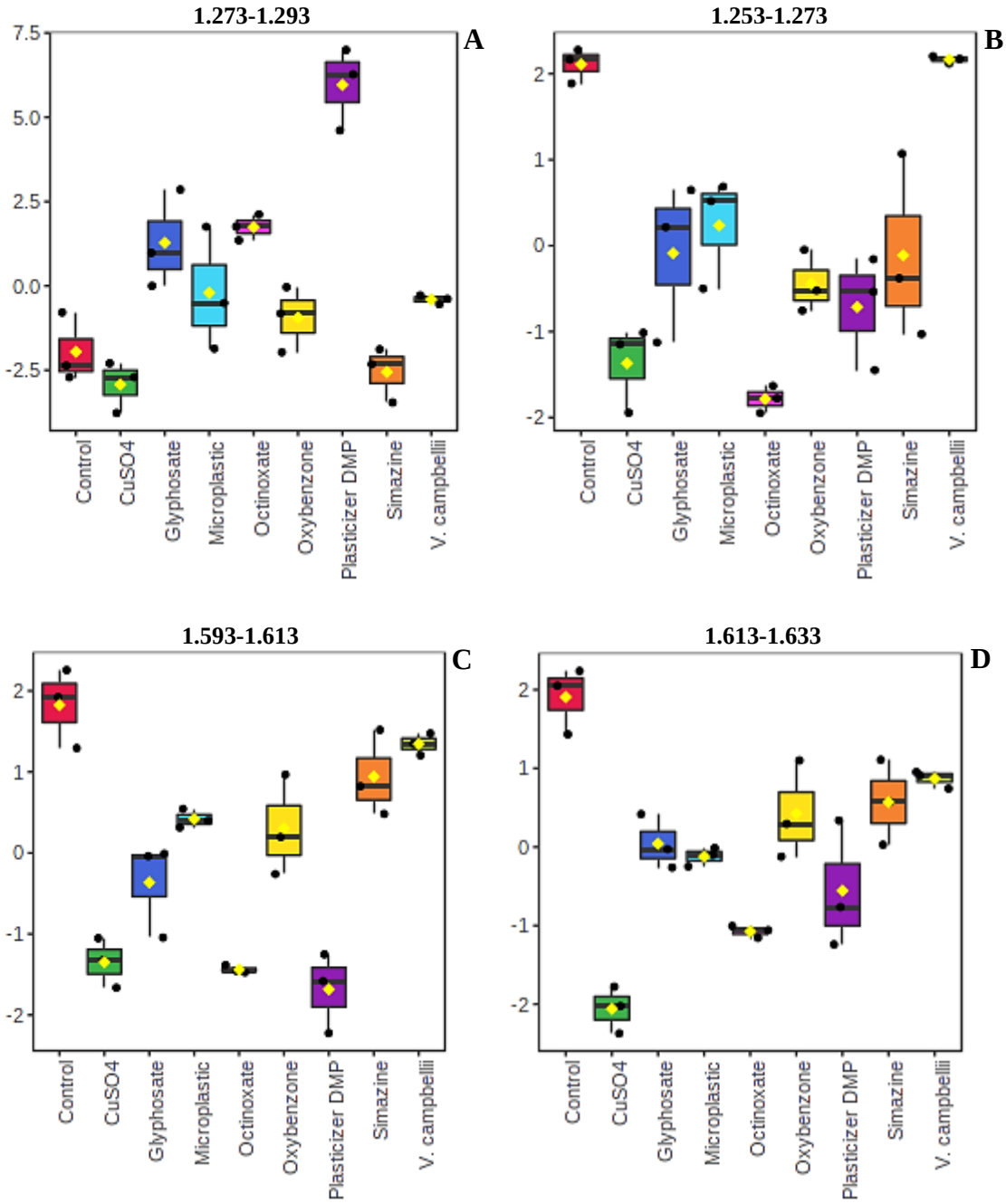

Figure 33 Boxplot showing the relative content of fatty acids (A), sarcophytoxide (B), sarglaucol (C), and ent-sarcophyolide E (D) based on selected bins of ^{1}H NMR spectra

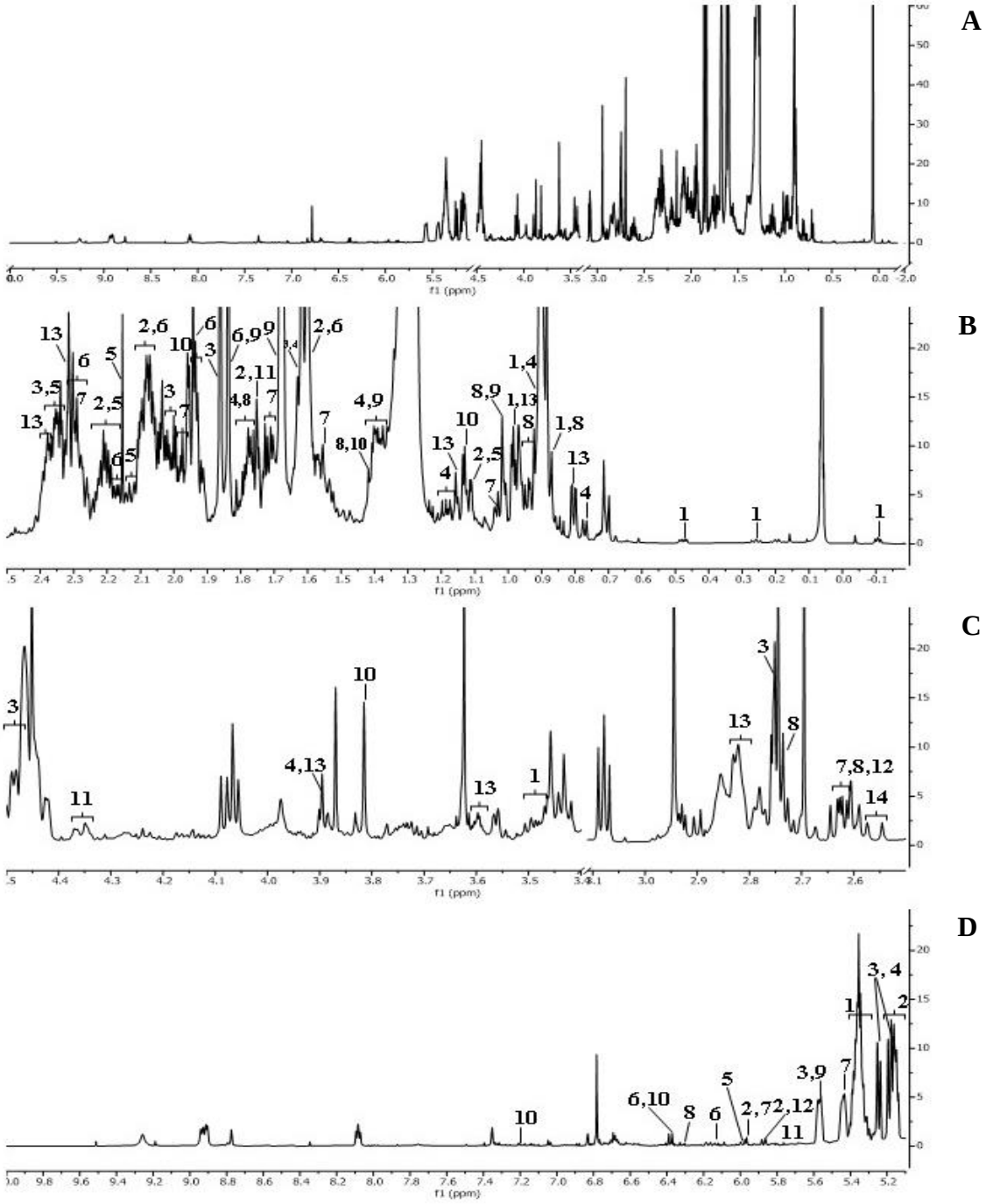

Figure 34 Full ^{1}H NMR spectrum (in CD_3OD) of *Sarcophytum glaucum* extract (A), expanded region from -0.2-2.5 ppm (B), 2.5-4.5 ppm (C), and 5.1-10 ppm (D), marked with the assigned peaks (Appendix 5); numbers= number of tentative annotated compound listed in Appendix 5

^{1}H-NMR based multivariate data analysis of *Lobophytum crassum* extracts

Similar to *S. glaucum* data, the ^{1}H-NMR data of *L. crassum* were analyzed in the same manner to determine the difference in their metabolite profiling after stress condition. The PCA result (score plot and loadings plot) are shown in Figure 35. Out of the extracts, 13 compounds with fatty acids were tentatively assigned (Figure 36 and Appendix 5).

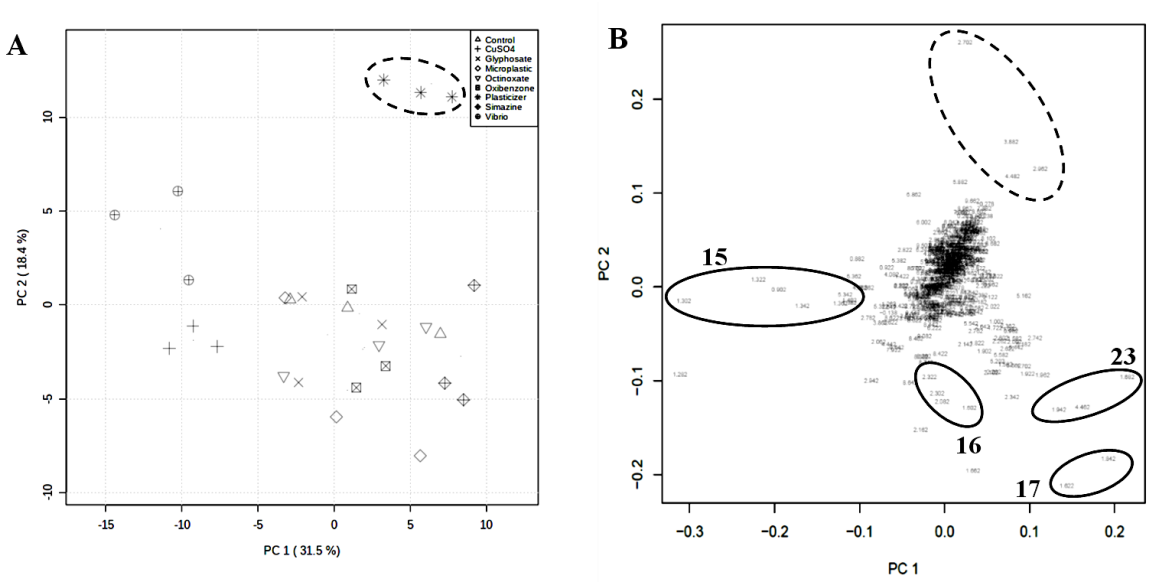

Note= Δ: Control, +: $CuSO_4$, ×: Glyphosate, ◇: Microplastic, ∇: Octinoxate, ⊠: Oxibenzone, ✳: Plasticizer, ◈: Simazine, ⊕: Vibrio

Figure 35 ^{1}H-NMR based PCA of *Lobophytum crassum* extracts; scores plot (a) and loadings plot (b)

PC2 (variance 18.4%) discriminate the extracts of *L. crassum* treated with DMP from other extracts. This separation is caused by four bins that correspond to four singlets at δ 2.70 ppm, 3.87 ppm, 2.95 ppm, which are the same signals that caused the separation in *S. glaucum*, and 4.47 ppm. These three signals most likely belong to metabolites which occur in both soft coral species. The compounds belong the signals in these bins, on the other hand, remain unknown. Different to *L. crassum* treated with DMP, the extracts of soft coral treated with *V. campbelli* and $CuSO_4$ were separated in PC 1 (31.5%). These two groups of extracts were clustering together in the same direction. Interestingly, *V. campbelli* shows a different effect on *L. crassum* compared to the effect on *S. glaucum*. In *L. crassum*, *V. campbelli* and $CuSO_4$ induced fatty acid production (Appendix 6). Fatty acids were identified as the component responsible for the separation of these two groups. As previously mentioned, fatty acids and lipids are an energy source for corals, and also contribute significantly to the carbon content of corals [243, 244]. Beside that, soft corals regulate their fatty acid and sterol compositions as a defense mechanism during environmental change. Moreover, unsaturated fatty acids have been shown to be cytotoxic to microorganisms (i.e. bacteria and fungi) [94]. Therefore, when exposed to stress, particularly during bacterial infection, the soft coral produces more fatty acids, likely as a defense mechanism.

Additionally, some metabolites were identified based on the bins responsible for the separation of soft coral extracts treated with simazine and oxybenzone. Locrassolide A (**16**), crassumolide B (**17**), and lobolide (**23**) were tentatively assigned as compounds underlying the separation of these two groups. The concentration of these three compounds were increased after the elicitation. This indicates that *L. crassum* synthesized these compounds as response to stress exposure. According to some studies, locrassolide A (**16**), crassumolide B

(**17**), and lobolide (**23**) are produced by *L. crassum* in order to protect itself from predators [249]. These metabolites possess a broad range of bioactivities, including antibacterial, cytotoxic, and anti-inflammatory properties [161, 250, 251].

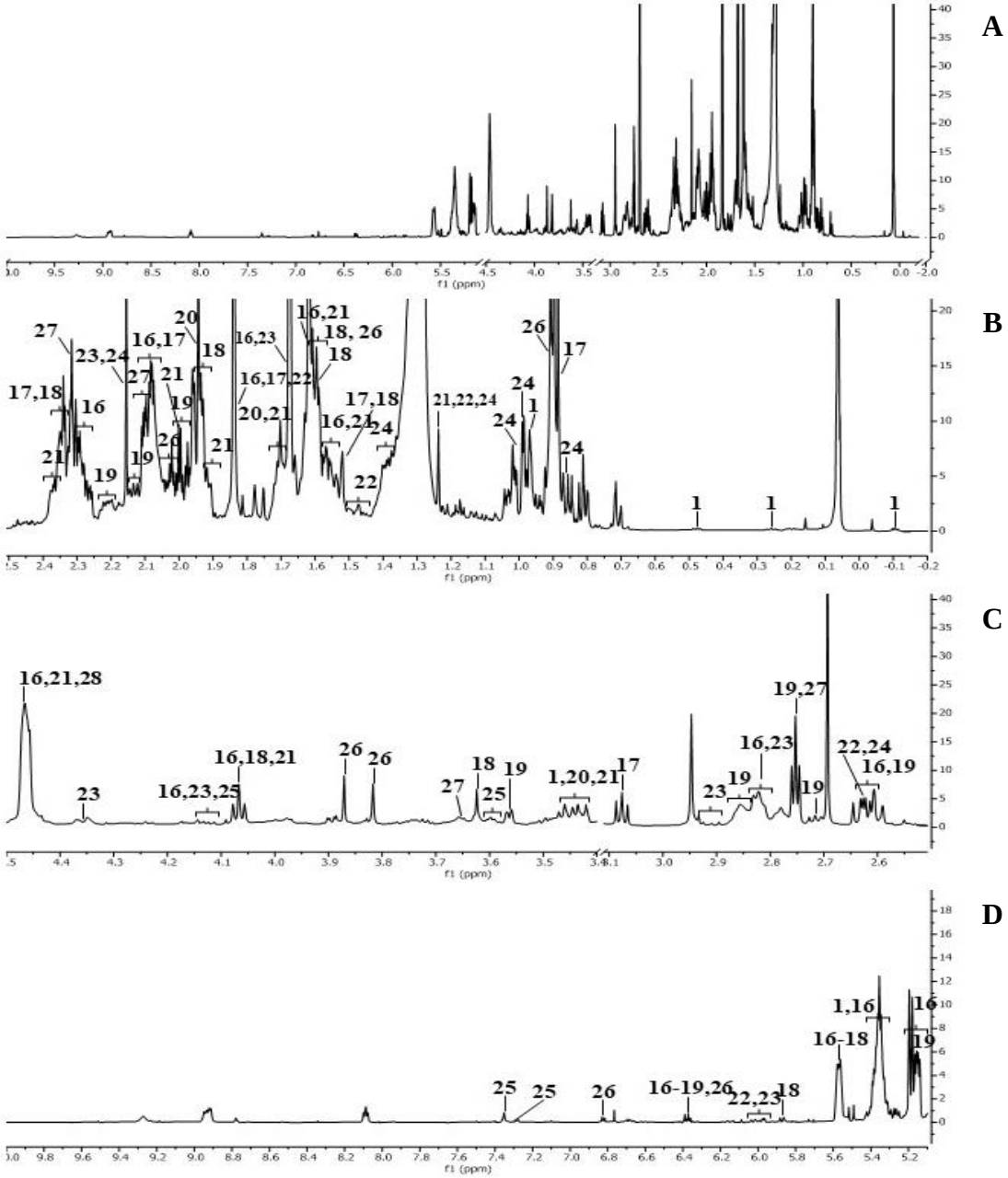

Figure 36 Full ^{1}H NMR spectrum (in CD_3OD) of *Lobophytum crassum* extract (A), expanded region from -0.2-2.5 ppm (B), 2.5-4.5 ppm (C), and 5.1-10 ppm (D), marked with the assigned peaks (Appendix 5); numbers= number of tentative annotated compound listed in Appendix 5

^{1}H-NMR based multivariate data analysis of *Xenia umbellata* extracts

Multivariate data analysis was used to determine the difference in metabolites on *X. umbellata* following stress treatments. In general, the metabolites in the extracts of *X. umbellata* differed from the two other soft coral species (described at Chapter IV). Nevertheless, it is necessary to investigate the metabolites of this soft coral after elicitation. Multivariate data analysis was used to address this question. The result of multivariate data

analysis (i.e. PCA) is shown at Figure 37. 12 metabolites have been tentatively identified from the extract of *X. umbellata*, which are shown at Figure 38 and Appendix 5.

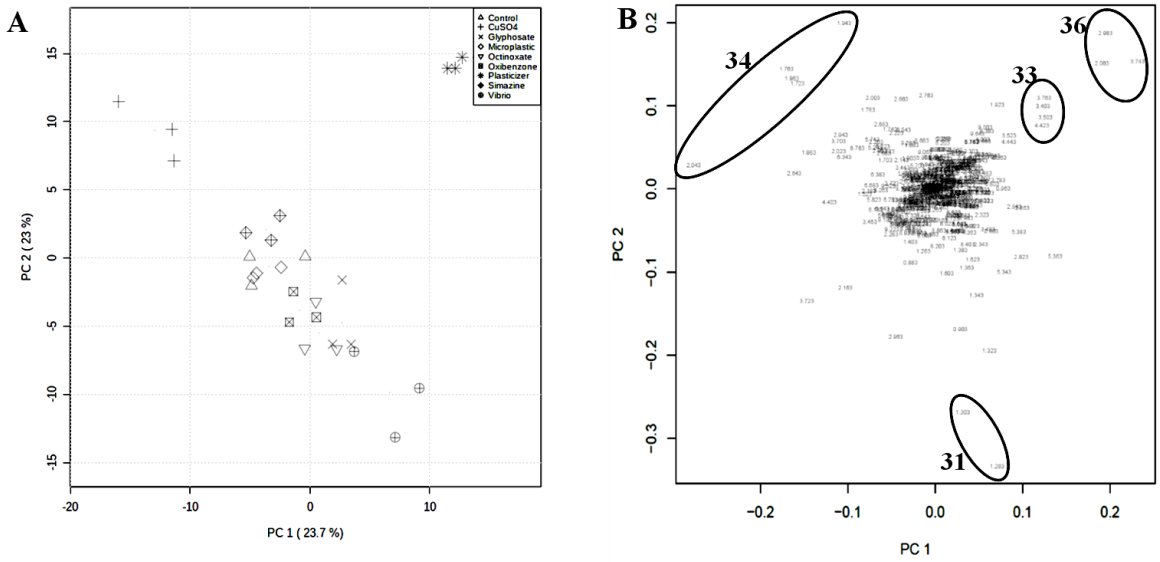

Note= Δ: Control, +: $CuSO_4$, ×: Glyphosate, ◇: Microplastic, ∇: Octinoxate, ⊠: Oxibenzone, ✱: Plasticizer, ◈: Simazine, ⊕: Vibrio

Figure 37 ^{1}H-NMR based PCA of *Xenia umbellata* extracts; scores plot (a) and loadings plot (b)

The PCA of the ^{1}H-NMR data of *X. umbellata* extracts show a clear separation of the extracts of DMP threated coral. This group was distinguished from the rest of the extracts in PC1 (variance 23.7%). In addition, together with extracts of soft corals treated with $CuSO_4$, this group was also separated from other extracts in PC2 (variance 23%). The bins responsible for the DMP group separation (Figure 37.B) have been tentatively assigned as xenibellal (**36**) and umbellacin C (**33**). The relative concentrations of xenibellal (**36**) and umbellacin C (**33**) were high in these extracts, but were extremely low in the other extracts (Appendix 7).

Interestingly, while extracts of *X. umbellata* treated with $CuSO_4$ coincide with DMP-treated samples in PC2, it was also clearly distinct from the other extracts in PC1 (variance 23.7%). There are five corresponding bins causing separation which belong to the diterpene xenibecin (**34**). In comparison to other extracts, the concentration of xenibecin in *X. umbellata* extracts treated with $CuSO_4$ was relatively high (Appendix 8). Furthermore, xenibellol B (**31**) was tentatively assigned as the compound responsible for the separation of extract from soft coral treated with *V. campbelli* based on the corresponding bins in the loadings plot.

The annotated metabolites detected in the extracts of *X. umbellata* are known compounds isolated from this species. The diterpenes xeniumbellal and umbellacin C are produced by *X. umbellata* in order to protect their body against predatory and stress environment, as well as by attachment of other organisms or molecules [221]. To keep the stability of their body and to stay markedly free of adhering, corals deposits some secondary

metabolites in their tissue, especially diterpenes and sterols which play vital roles in allelopathy [252, 253]. Furthermore, another diterpene detected in the *X. umbellata* extract after exposure to DMP was xenibecin, which exhibited cytotoxicity against P-388, HT-29, and A549 cells [28]. Therefore, we conclude that the increase of these compounds in the *X. umbellata* after treated with DMP is a result of the soft corals' stress response mechanisms.

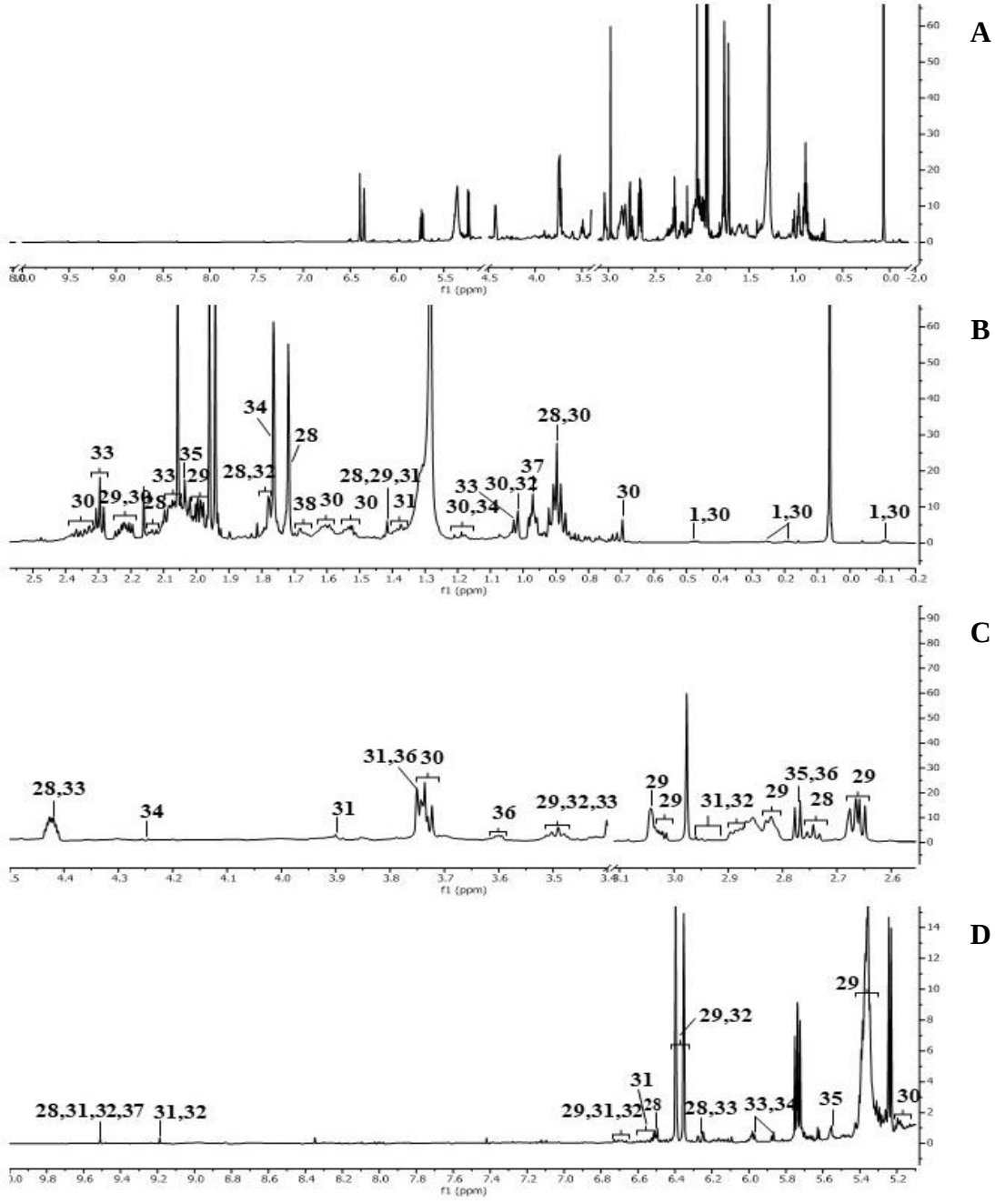

Figure 38 Full ^{1}H NMR spectrum (in CD_3OD) of *Xenia umbellata* extract (A), expanded region from -0.2-2.5 ppm (B), 2.5-4.5 ppm (C), and 5.1-10 ppm (D), marked with the assigned peaks (Appendix 5); numbers= number of tentative annotated compound listed in Appendix 5

c. LC-ESI-HRMS analysis

As a complement to ^{1}H-NMR analysis, which enables quantitative and comprehensive metabolite profiling of soft coral extracts, LC-ESI-HRMS provides better resolution of individual chemical composition into separate peaks and increases the opportunity of discovering novel metabolites of low abundance [254]. These two methods are an excellent combination in order to obtain comprehensive data on the soft coral metabolite constituents. To gain an overview of the chemical constituents in the extracts as well as to determine the optimal solvent for extracting the most metabolites, several solvents were initially tested, i.e. methanol, 80% aqueous methanol, ethyl acetate, *n*-hexane, and chloroform. In comparison to other solvents, methanol exhibited the maximum number of peaks in the LC-ESI-HRMS chromatogram that corresponded to their metabolites (Appendix 9). The optimal concentration of the extracts was determined by a linear dynamic range analysis with observation of dilution range of the quality control (QC) sample. As a result, 2 mg/mL of soft corals extracts in methanol provided the best results for detection of analytes with an intensity range of 10^{3}-10^{7}.

The analysis was conducted using LC-ESI-HRMS in positive ion mode due to a higher number of detected peaks and a better signal-to-noise ratio (S/N) in the total ion chromatogram (TIC). Umbelliferon (8 µg/mL) was used as an internal standard in order to observe the shifts of retention times and the external calibration of the instrument. This compound was not present in the extracts as well as did not overlap with other metabolites. In total, 81 samples of three soft corals species (*S. glaucum*, *L. crassum* and *X. umbellata*) treated with elicitors as well as control (untreated) were examined, and the total ion chromatogram (TIC) of the extracts from soft corals treated with various elicitors are shown at Figure 39.

The metabolites in the soft coral extracts were eluted based on their polarity. Polar compounds (e.g. organic acids) were detected early in the retention time range 0-2 minutes, followed by semi-polar and non-polar compounds detected near the end of the retention time range. Diterpenes and nitrogenous compounds (alkaloids and nitrogenous diterpenes) were eluted in the broad retention time range of 6-12 min. In addition, non polar compounds such as steroids, fatty acids, and lipids which were detected in high retention time (15-17 min).

Multivariate data analysis was used to determine the chemical variance of metabolites in each soft coral species following elicitation. This analysis, specifically principal component analysis (PCA) was used to examine heterogeneities on soft corals chemotaxonomy as well as the respons to elicitors in an untargeted manner. The raw TIC data were converted using ProteoWizard, and R program was used to generate the feature table. After aligning all data from three species, a total of 2681 features were generated. Additionally, 90 metabolites in the extracts were assigned tentatively based on their MS/MS fragmentation pattern and accurate mass. The list of tentatively assigned metabolites in *S. glaucum, L. crassum* and *X. umbellata* are shown in Table 9.

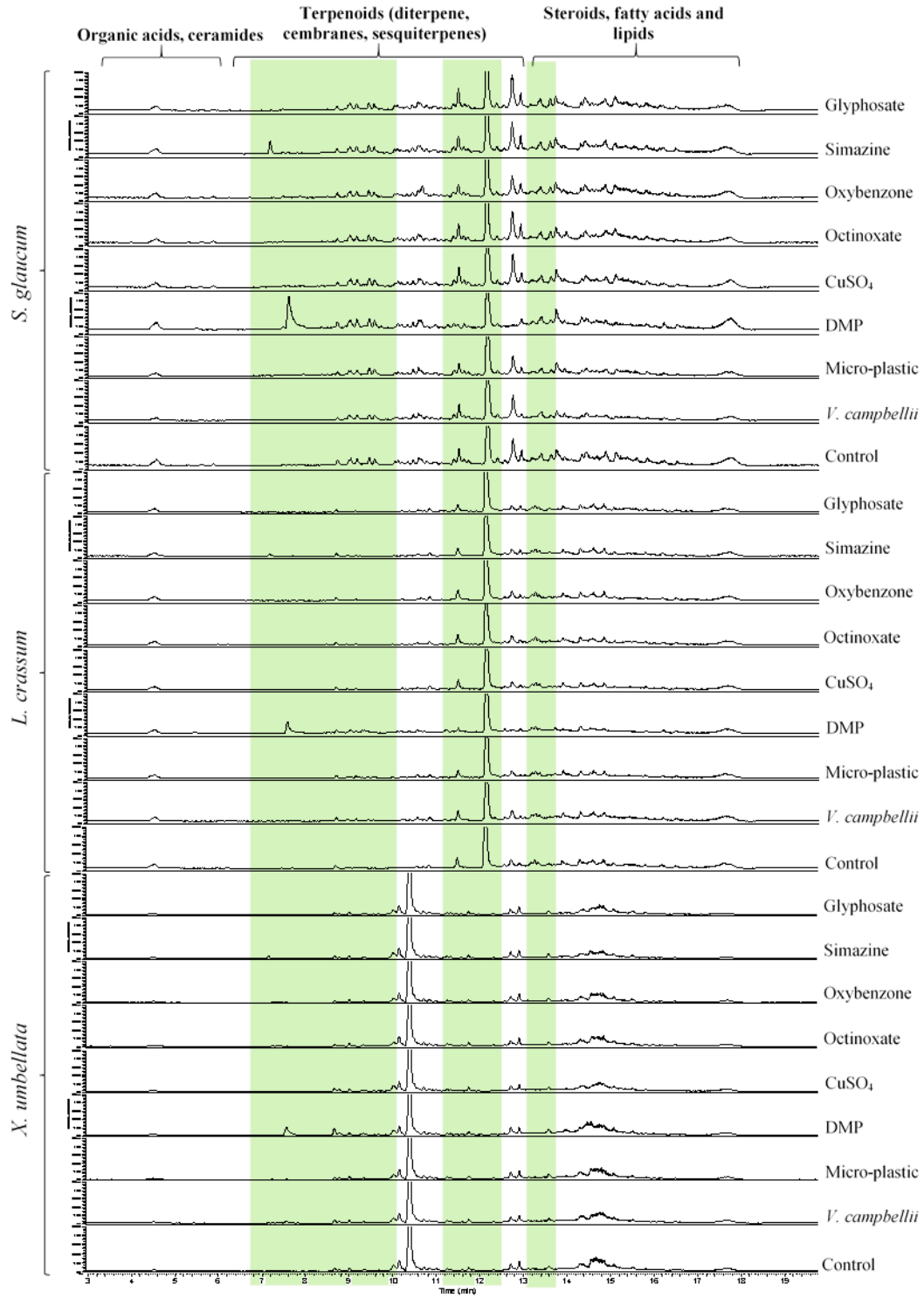

Figure 39 Total Ion Chromatogram (TICs, *m/z* 100-1500) in positive ion mode of soft corals extracts

Table 9 Metabolites (tentatively) annotated and responsible for separation of extracts in PCA from soft corals *S. glaucum*, *L. crassum*, and *X. umbellata* after elicitation; via HR-LC-MS^2 in positive ionization mode

Comp.	$[M+H]^+$ *m/z*	t_R (min)	Molecular formula	Δ (ppm)	MS^2 product ions, *m/z* (elemental composition, rel. intensity [%])	Identification of compound/class	Species
P.1	261.1494	1.43	$C_{16}H_{21}O_3$	1.273	243.1352 ($C_{16}H_{19}O_2$, **100**), 201.1274 ($C_{14}H_{17}O$, 49), 173.0960 ($C_{12}H_{13}O$, 11), 133.0640 (C_9H_9O, 8),	Sesquiterpene carboxylic acid	X
P.2	218.2112	6.11	$C_{12}H_{28}NO_2$	-1.951	200.2006 ($C_{12}H_{26}NO$, **100**), 174.1851 ($C_{10}H_{22}O_2$, 4), 106.0861 (C_8H_{10}, 27)	Amino alcohol	S
P.3	218.2109	6.16	$C_{12}H_{27}NO_2$	-1.716	200.2007 ($C_{12}H_{25}NO$, **100**), 177.0902 ($C_{11}H_{13}O_2$, 15), 123.0806 ($C_8H_{11}O$, 7), 106.0861 (C_8H_{10}, 34), 88.0755 ($C_4H_{10}NO$, 32)	Amino alcohol	L, X
P.4	321.2059	6.60	$C_{19}H_{29}O_4$	-2.133	303.1214 ($C_{19}H_{27}O_3$, **100**), 233.1149 ($C_{14}H_{17}O_3$, 19), 118.0732 (C_9H_{10}, 3)	Sesquiterpene	L
P.5	383.2631	7.47	$C_{25}H_{35}O_3$	-1.690	365.1964 ($C_{25}H_{33}O_2$, **100**), 339.2390 ($C_{23}H_{31}O_2$, 33), 265.1413 ($C_{19}H_{21}O$, 22), 251.1248 ($C_{18}H_{19}O$, 32), 133.0856 (C_9H_9O, 81)	Sesquiterpene	S, L
P.6	246.2425	7.56	$C_{14}H_{32}NO_2$	-0.836	246.2426 ($C_{14}H_{32}NO_2$, **100**), 228.2321 ($C_{14}H_{30}NO$, 41), 202.2159 ($C_{12}H_{26}O_2$, 2), 184.2058 ($C_{12}H_{24}O$, 5), 106.0860 (C_8H_{10}, 23)	Amino alcohol	S, L, X
P.7	427.2894	7.57	$C_{27}H_{39}O_4$	1.707	409.2244 ($C_{26}H_{33}O_4$, **100**), 391.2142 ($C_{26}H_{31}O_3$, 44), 309.1685 ($C_{21}H_{25}O_2$, 33), 295.1516 ($C_{20}H_{23}O_2$, 89), 269.1383 ($C_{18}H_{21}O_2$, 49)	Organic acid	S, L
P.8	195.0651	7.80	$C_{10}H_{11}O_4$	-0.079	177.1273 ($C_{10}H_9O_3$, **100**), 163.0389 ($C_9H_8O_3$, 37), 135.1167 ($C_8H_7O_2$, 18), 121.1010 ($C_7H_5O_2$, 18), 89.0596 (C_7H_5, 4)	Sesquiterpene carboxylic acid	S
P.9	344.2574	8.00	$C_{22}H_{34}NO_2$	-2.864	344.2526 ($C_{22}H_{46}NO_2$, 2), 326.2476 ($C_{22}H_{44}NO$, 13), 285.2211 ($C_{19}H_{27}NO$, 100), 229.1585 ($C_{16}H_{23}N$, 23), 177.1637 ($C_{13}H_{21}$, 16), 147.1168 ($C_{11}H_{15}$, 8)	Amino alcohol	L
P.10	192.1382	8.76	$C_{12}H_{18}NO$	-0.941	149.0963 ($C_{10}H_{13}O$, 1), 133.1021 ($C_{10}H_{13}$, 1), 119.0488 (C_9H_{11}, **100**)	Amino alcohol	X
P.11	274.2380	8.84	$C_{16}H_{36}NO_2$ $[M+Na]^+$	-0.824	256.2636 ($C_{16}H_{32}O_2$, **100**), 230.2477 ($C_{14}H_{30}O_2$, 7), 212.2376 ($C_{14}H_{28}O$, 1), 106.0862 (C_8H_{10}, 16)	Palmitic acid	L
P.12	290.1964	8.97	$C_{14}H_{28}NO_5$	-1.201	273.1326 ($C_{14}H_{25}O_5$, **100**), 255.1224 ($C_{13}H_{19}O_5$, 6), 227.1278 ($C_{12}H_{19}O_4$, 24), 185.1173 ($C_{10}H_{17}O_3$, 4), 169.0859 ($C_9H_{13}O_3$, 23), 122.0813 ($C_8H_{10}O_5$), 97.0651 (C_6H_9O, 1)	Amino alcohol	L, X
P.13	357.2034	9.36	$C_{22}H_{29}O_4$	-7.295	339.2144 ($C_{22}H_{27}O_3$, **100**), 321.2076 ($C_{22}H_{25}O_2$, 45), 269.2113 ($C_{19}H_{25}O$, 18), 251.2007 ($C_{19}H_{23}$, 29), 223.2059 ($C_{17}H_{19}$, 49), 171.1020 ($C_{13}H_{15}$, 5), 143.1070 ($C_{11}H_{11}$, 3)	Diterpene	L
P.14	321.2054	9.38	$C_{19}H_{29}O_4$	-1.949	303.1948 ($C_{19}H_{27}O_3$, **100**), 285.1843 ($C_{19}H_{25}O_2$, 29), 245.1534 ($C_{16}H_{21}O_2$, 3), 233.1512 ($C_{15}H_{21}O_2$, 1), 153.0906 ($C_9H_{13}O_2$, 2), 123.0797 ($C_8H_{11}O$, 2)	Diterpenoid	S
P.15	277.2006	9.53	$C_{14}H_{29}O_5$	-1.192	277.2010 ($C_{14}H_{29}O_5$, 1), 259.1901 ($C_{14}H_{27}O_4$, 1), 241.1797 ($C_{14}H_{25}O_3$, 1), 171.1377 ($C_{10}H_{19}O_2$, **100**), 99.0443 ($C_5H_7O_2$, 1)	Sesquiterpene	L
P.16	387.3210	9.56	$C_{26}H_{43}O_2$	3.370	387.2363 ($C_{26}H_{43}O_2$, 12), 369.3109 ($C_{26}H_{41}O$, **100**), 309.2717 ($C_{23}H_{33}$, 1), 255.1215 ($C_{19}H_{27}$, 4)	Fatty acid	S
P.17	315.1952	9.98	$C_{20}H_{27}O_3$	-0.797	315.1982 ($C_{20}H_{27}O_3$, 2), 297.1851 ($C_{20}H_{25}O_2$, **100**), 255.1739 ($C_{18}H_{23}O$, 16), 187.1115 ($C_{13}H_{15}O$, 20), 149.0957 ($C_{10}H_{13}O$, 5), 119.0862 (C_9H_{11}, 2)	Diterpene	S
P.18	494.3101	10.49	$C_{27}H_{44}NO_7$	-2.244	462.2852 ($C_{26}H_{40}NO_6$, 15), 434.2565 ($C_{24}H_{36}NO_6$, 3), 417.2261 ($C_{24}H_{33}O_6$, **100**), 357.2060 ($C_{22}H_{29}O_4$, 35), 279.1772 ($C_{20}H_{23}O$, 3), 251.1826 ($C_{19}H_{23}$, 3)	Diterpenoid alkaloid	X
P.19	349.2366	10.54	$C_{21}H_{33}O_4$	-2.107	348.1831 ($C_{21}H_{32}O_4$, 15), 331.2258 ($C_{21}H_{31}O_3$, 67), 291.1931 ($C_{18}H_{27}O_3$, 15), 257.1898 ($C_{17}H_{21}O_2$, **100**), 239.1799 ($C_{17}H_{19}O$, 17), 173.1318 ($C_{12}H_{13}O$, 10), 123.0802 ($C_8H_{11}O$, 6)	Xenia diterpenoid (metoxyacetal) [255]	X
P.20	528.3168	10.54	$C_{27}H_{46}NO_9$	0.117	511.2972 ($C_{27}H_{43}O_9$, 51), 493.2774 ($C_{27}H_{41}O_8$, **100**), 397.1628 ($C_{23}H_{25}O_6$, 17), 239.1825 ($C_{18}H_{23}$, 39)	Diterpenoid alkaloid	S
P.21	333.2053	10.55	$C_{20}H_{29}O_4$	-2.238	333.2421 ($C_{20}H_{29}O_4$, 4), 315.1954 ($C_{20}H_{27}O_3$, **100**), 297.1844 ($C_{20}H_{25}O_2$, 23), 269.1895 ($C_{19}H_{25}O$, 3), 255.1742 ($C_{18}H_{23}O$, 4), 135.0803 ($C_9H_{11}O$, 2)	3,4-dihydro-4β-hydroxy-Δ^2-sarcophine [248]	S, L
P.22	235.1690	10.90	$C_{15}H_{23}O_2$	-1.732	217.1587 ($C_{15}H_{21}O$, **100**), 203.1425 ($C_{14}H_{19}O$, 96), 163.1117 ($C_{11}H_{15}O$, 28), 123.0856 ($C_8H_{11}O$, 9), 95.0491 (C_6H_7O, 5),	Sesquiterpene	X

Comp.	$[M+H]^+$ *m/z*	t_R (min)	Molecular formula	Δ (ppm)	MS^2 product ions, *m/z* (elemental composition, rel. intensity [%])	Identification of compound/class	Species
P.23	237.1633	10.91	$C_{18}H_{21}$	-3.321	209.1324 ($C_{16}H_{17}$, 73), 195.1168 ($C_{15}H_{15}$, **100**), 181.1012 ($C_{14}H_{13}$, 54), 167.0855 ($C_{13}H_{11}$, 19), 155.0853 ($C_{12}H_{11}$, 7), 131.0856 ($C_{10}H_{11}$, 7)		X
P.24	317.2105	11.00	$C_{20}H_{29}O_3$	-1.927	317.1927 ($C_{20}H_{29}O_3$, 28), 299.2001 ($C_{20}H_{27}O_2$, **100**), 271.2059 ($C_{19}H_{27}O$, 12), 253.1948 ($C_{19}H_{25}$, 4)	Sarcophine [248]	S
P.25	339.1929	11.07	$C_{22}H_{27}O_3$	-2.669	321.2418 ($C_{22}H_{25}O_2$, **100**), 303.2432 ($C_{22}H_{23}O$, 9), 293.2481 ($C_{21}H_{25}O$, 4), 275.2369 ($C_{20}H_{19}O$, 12), 257.2263 ($C_{19}H_{13}O$, 5), 145.1225 ($C_{10}H_9O$, 3)	Diterpenoid	S
P.26	361.2204	11.12	$C_{23}H_{37}O_3$	-2.302	344.1800 ($C_{23}H_{36}O_2$, **100**), 299.2946 ($C_{21}H_{31}O$, 14), 269.2275 ($C_{19}H_{25}O$, 6), 203.1802 ($C_{14}H_{19}O$, 4), 151.0965 ($C_{10}H_{15}O$, 9), 133.0860 ($C_{10}H_{13}$, 16)	Diterpenoid	L
P.27	429.3358	11.67	$C_{28}H_{45}O_3$	-1.262	411.3015 ($C_{28}H_{43}O_2$, **100**), 385.2928 ($C_{26}H_{41}O_2$, 6), 369.2996 ($C_{26}H_{41}O$, 7), 267.2683 ($C_{18}H_{35}O$, 2), 187.1469 ($C_{14}H_{19}$, 6)	Steroid	S
P.28	361.2208	11.92	$C_{22}H_{33}O_4$	-1.084	343.2267 ($C_{22}H_{31}O_3$, **100**), 283.1547 ($C_{19}H_{23}O_2$, 7), 203.1055 ($C_{13}H_{15}O_2$, 4), 165.0913 ($C_{10}H_{13}O_2$, 6)	Cembranoid	S, L
P.29	443.3475	12.11	$C_{29}H_{47}O_3$	-0.997	425.3413 ($C_{29}H_{45}O_2$, 17), 357.2787 ($C_{24}H_{37}O_2$, 9), 291.2683 ($C_{20}H_{35}O$, 23), 165.0910 ($C_{10}H_{13}O_2$, **100**), 137.0962 ($C_9H_{13}O$, 3)	Steroid	L
P.30	518.4033	12.51	$C_{28}H_{56}NO_7$	-3.606	500.4815 ($C_{28}H_{54}NO_6$, **100**), 363.3077 ($C_{23}H_{41}NO_2$, 3)	*N*-Containing lipid	X
P.31	289.2543	12.59	$C_{20}H_{33}O$	-3.056	271.0674 ($C_{20}H_{31}$, 7), 229.1951 ($C_{17}H_{15}$, **100**), 191.1790 ($C_{14}H_{23}$, 2), 137.1325 ($C_{10}H_{17}$, 3)	Diterpene	S
P.32	303.2315	12.79	$C_{20}H_{31}O_2$	-1.770	285.2210 ($C_{20}H_{29}O$, **100**), 267.2108 ($C_{20}H_{27}$, 20), 227.1795 ($C_{17}H_{23}$, 7), 211.1481 ($C_{16}H_{19}$, 5), 133.1010 ($C_{10}H_{13}$, 4), 109.0645 (C_8H_{13}, 6)	Diterpene Sarcophytonin E	S
P.33	640.5460	12.83	$C_{38}H_{75}NO_4P$	4.103	623.5163 ($C_{38}H_{72}O_4P$, **100**), 567.4501 ($C_{34}H_{64}O_4P$, 15), 427.2897 ($C_{24}H_{44}O_4P$, 18), 285.2778 ($C_{21}H_{33}$, 10)	Phospholipid	S, L
P.34	355.2475	13.08	$C_{20}H_{35}O_5$	-2.669	337.1653 ($C_{20}H_{33}O_4$, 9), 319.2643 ($C_{20}H_{31}O_3$,5), 299.1611 ($C_{19}H_{23}O_3$, 50), 255.1351 ($C_{17}H_{19}O_2$, **100**), 199.0726 ($C_{14}H_{15}O$, 63)	Diterpene	S
P.35	363.3099	13.89	$C_{24}H_{43}O_2$	5.152	257.2473 ($C_{16}H_{33}O_2$, 22), 171.1748 ($C_{11}H_{23}O$, **100**), 133.0858 ($C_{10}H_{13}$, 24)	Fatty acid	S
P.36	319.2837	13.90	$C_{21}H_{35}O_2$	-1.961	257.2470 ($C_{16}H_{33}O_2$, 18), 213.2214 ($C_{14}H_{29}O$, 1), 151.0962 ($C_{10}H_{15}O$, **100**), 133.0857 ($C_{10}H_{13}$, 22), 107.0701 (C_8H_{11}, 1)	C21-hydrocarbon	S, L
P.37	301.2163	14.10	$C_{20}H_{29}O_2$	-1.682	283.2054 ($C_{20}H_{27}O$, **100**), 265.1945 ($C_{20}H_{25}$, 6), 227.2000 ($C_{17}H_{23}$, 23), 161.1328 ($C_{12}H_{17}$, 16), 135.1169 ($C_{10}H_{15}$, 20), 109.1011 (C_8H_{13}, 17),	Diterpene	X
P.38	648.3878	14.39	$C_{39}H_{54}NO_7$	-2.559	648.4225 ($C_{39}H_{54}NO_7$, 86), 631.3520 ($C_{38}H_{49}NO_7$, 100), 592.3627 ($C_{36}H_{50}NO_6$, 37), 536.3044 ($C_{32}H_{42}NO_6$, 13), 479.2348 ($C_{28}H_{33}NO_6$, 26), 423.1758 ($C_{25}H_{27}O_6$, 11)	Steroidal alkaloid	L
P.39	271.2416	14.69	$C_{16}H_{31}O_3$	2.658	270.3152 ($C_{16}H_{30}O_3$, 11), 243.2102 ($C_{14}H_{27}O_3$, 41), 229.1949 ($C_{13}H_{25}O_3$, 39), 215.1790 ($C_{12}H_{23}O_3$, 89), 201.1634 ($C_{11}H_{21}O_3$, **100**), 121.1010 (C_9H_{13}, 26), 95.0850 (C_7H_{11}, 19)	Fatty acid	S
P.40	794.6130	14.84	$C_{46}H_{84}NO_9$	-1.359	794.6025 ($C_{46}H_{84}NO_9$, 40), 735,5229 ($C_{42}H_{73}NO_9$, **100**), 630.5450 ($C_{40}H_{72}NO_4$, 37), 491.3972 ($C_{30}H_{53}NO_4$, 33), 283.2632 ($C_{18}H_{35}O_2$, 32)	Cerebroside	X
P.41	822.5728	15.24	$C_{53}H_{76}NO_6$	0.196	822.5161 ($C_{53}H_{76}NO_6$, **100**), 748.4594 ($C_{48}H_{62}NO_6$, 1), 416.2751 ($C_{25}H_{38}NO_4$, 1), 283.2632 ($C_{18}H_{35}O_2$, 7)	*N*-Containing lipid	L
P.42	536.4879	15.25	$C_{34}H_{66}NO_3$	-3.510	518.4612 ($C_{34}H_{64}NO_2$, **100**), 463.3989 ($C_{29}H_{53}NO_3$, 32), 357.3361 ($C_{21}H_{43}NO_3$, 15), 313.3100 ($C_{20}H_{41}O_2$, 18), 189.1486 ($C_{14}H_{21}$, 6)	Sphingolipid	S
P.43	347.3148	15.31	$C_{23}H_{39}O_2$	-2.120	285.2785 ($C_{18}H_{37}O_2$, 20), 241.2526 ($C_{16}H_{33}O$, 1), 197.2268 ($C_{13}H_{25}O$, 1), 151.0964 ($C_{10}H_{15}O$, **100**), 133.0858 ($C_{10}H_{13}$, 22)	C23-hydrocarbon	S
P.44	746.5757	15.32	$C_{41}H_{80}NO_{10}$	-2.685	746.5562 ($C_{41}H_{80}NO_{10}$, 9), 728.5447 ($C_{41}H_{78}NO_9$, 9), 552.4980 ($C_{34}H_{66}NO_4$, **100**), 466.3890 ($C_{28}H_{52}NO_4$, 13), 310.2735 ($C_{19}H_{36}NO_2$, 8), 283.2632 ($C_{18}H_{35}O_2$, 2)	Cerebroside	X
P.45	763.4381	15.70	$C_{45}H_{63}O_{10}$	4.421	763.4391 ($C_{45}H_{63}O_{10}$, 62), 703.4291 ($C_{43}H_{59}O_8$, 5), 515.2614 ($C_{29}H_{39}O_8$, **100**), 489.2454 ($C_{27}H_{37}O_8$, 75), 409.1866 ($C_{21}H_{29}O_8$, 15), 308.1716 ($C_{17}H_{24}O_5$, 11), 283.2640 ($C_{17}H_{31}O_3$, 10)	Sterol	X

Comp.	$[M+H]^+$ *m/z*	t_R (min)	Molecular formula	Δ (ppm)	MS^2 product ions, *m/z* (elemental composition, rel. intensity [%])	Identification of compound/class	Species
P.46	739.4382	15.73	$C_{43}H_{63}O_{10}$	-4.523	739.4340 ($C_{43}H_{63}O_{10}$, 63), 721.5070 ($C_{43}H_{61}O_9$, 94), 681.4858 ($C_{41}H_{61}O_8$, 10), 611.3942 ($C_{37}H_{55}O_7$, 24), 429.2630 ($C_{36}H_{37}O_5$, **100**), 371.2586 ($C_{24}H_{35}O_3$, 19), 263.1641 ($C_{16}H_{23}O_3$, 9)	Bisglaucumlide D/C	S
P.47	520.4928	15.79	$C_{34}H_{66}NO_2$	3.717	520.5052 ($C_{34}H_{66}NO_2$, 5), 503.4656 ($C_{34}H_{63}O_2$, **100**), 447.4034 ($C_{30}H_{55}O_2$, 11), 251.1855 ($C_{19}H_{23}$, 12)	Sphingolipid	X
P.48	650.5358	15.88	$C_{39}H_{72}NO_6$	0.545	634.4559 ($C_{39}H_{70}NO_5$, 67), 575.4329 ($C_{36}H_{61}O_5$, 10), 465.3103 ($C_{30}H_{41}O_4$, 3), 311.2945 ($C_{20}H_{39}O_2$, 18), 283.2630 ($C_{18}H_{35}O_2$, **100**), 269.2480 ($C_{17}H_{33}O_2$, 9)	Betaine lipid	L
P.49	405.3570	15.91	$C_{27}H_{49}O_2$	-1.137	361.3299 ($C_{24}H_{41}O_2$, 5), 299.2943 ($C_{19}H_{39}O_2$, 13), 255.2302 ($C_{16}H_{31}O_2$, 2), 195.1227 ($C_{13}H_{23}O$, **100**), 177.1122 ($C_{12}H_{17}O$, 10), 151.0965 ($C_{10}H_{15}O$, 3), 133.0858 (C10H13, 11)	Steroid	L
P.50	765.4551	15.97	$C_{45}H_{65}O_{10}$	-3.482	765.4541 ($C_{45}H_{65}O_{10}$, 1), 515.2615 ($C_{29}H_{39}O_8$, **100**), 489.2461 ($C_{27}H_{37}O_8$, 17), 243.0833 ($C_{11}H_{15}O_6$, 2)	Sterol	S, X
P.51	976.5975	16.00	$C_{53}H_{86}NO_{15}$	-1.769	779.5086 ($C_{39}H_{73}NO_{14}$, 17), 635.4667 ($C_{33}H_{65}NO_{10}$, **100**), 617.4559 ($C_{33}H_{63}NO_9$, 11), 495.2961 ($C_{27}H_{43}O_8$, 4), 359.2582 ($C_{23}H_{35}O_3$, 10), 333.2426 ($C_{21}H_{33}O_3$, 34)	*N*-Containing lipid	X
P.52	752.5647	16.05	$C_{43}H_{78}NO_9$	-3.202	752.5378 ($C_{43}H_{78}NO_9$, 5), 734.5543 ($C_{43}H_{76}NO_8$, 44), 572.5029 ($C_{37}H_{66}NO_3$, **100**), 554.4924 ($C_{37}H_{64}NO_2$, 13), 392.2919 ($C_{24}H_{40}O_4$, 23), 361.2731 ($C_{23}H_{37}O_3$, 7), 294.3172 ($C_{19}H_{34}O_2$, 4)	Cerebroside	S
P.53	774.5477	16.05	$C_{45}H_{76}NO_9$	-2.981	756.5576 ($C_{45}H_{74}NO_8$, 24), 594.4837 ($C_{39}H_{64}NO_3$, **100**), 455.3377 ($C_{29}H_{45}NO_3$, 11), 346.2715 ($C_{23}H_{38}O_2$, 14), 255.2332 ($C_{16}H_{31}O_2$, 5)	Cerebroside	S, L, X
P.54	734.5546	16.06	$C_{43}H_{76}NO_8$	-0.537	716.5409 ($C_{43}H_{74}NO_7$, 18), 572.5030 ($C_{37}H_{66}NO_3$, 93), 554.4923 ($C_{37}H_{64}NO_2$, **100**), 536.4824 ($C_{37}H_{62}NO$, 19), 394.3314 ($C_{28}H_{42}O$, 22), 280.2633 ($C_{19}H_{36}O$, 20)	Cerebroside	X
P.55	284.2944	16.12	$C_{18}H_{38}NO$	-1.377	283.2627 ($C_{18}H_{37}NO$, **100**), 267.1434 ($C_{18}H_{35}NO$, 26), 240.2317 ($C_{15}H_{30}NO$, 5), 178.1158 ($C_{11}H_{16}NO$, 5), 109.1014 (C_8H_{13}, 3), 95.0856 (C_7H_{11}, 3)	(2*S*,3*R*,*E*)-2-Aminooctadec-5-en-3-ol	S, L
P.56	760.4983	16.21	$C_{43}H_{70}NO_{10}$	-1.491	743.5497 ($C_{43}H_{69}NO_9$, 29), 581.4197 ($C_{32}H_{55}NO_8$, **100**), 563.4092 ($C_{32}H_{53}NO_7$, 14), 547.3329 ($C_{32}H_{53}NO_6$, 5), 333.2424 ($C_{21}H_{33}O_3$, 25), 305.2112 ($C_{19}H_{29}O_3$, 24)	Glyceroglycolipid	L, X
P.57	652.5735	16.27	$C_{43}H_{74}NO_3$	1.016	652.5720 ($C_{43}H_{74}NO_3$, 82), 635.3843 ($C_{43}H_{73}NO_2$, **100**), 341.3446 ($C_{23}H_{35}NO$, 24), 283.2665 ($C_{18}H_{35}O_2$, 40)	*N*-Containing lipid	L
P.58	749.5181	16.32	$C_{48}H_{77}O_6$	-2.261	749.5121 ($C_{48}H_{77}O_6$, **100**), 704.5839 ($C_{47}H_{76}O_4$, 7), 472.3636 ($C_{30}H_{48}O_4$, 16), 305.2684 ($C_{20}H_{33}O_2$, 2)	Glycerolipid	S, L, X
P.59	617.4597	16.36	$C_{41}H_{61}O_4$	3.633	617.4594 ($C_{41}H_{61}O_4$, **100**), 599.5419 ($C_{41}H_{60}O_3$, 6), 454.3645 ($C_{31}H_{50}O_2$, 3), 367.3282 ($C_{26}H_{39}O$, 2), 281.2472 ($C_{21}H_{29}$, 17)	Steroid	X
P.60	786.5149	16.44	$C_{45}H_{72}NO_{10}$	-0.234	751.4776 ($C_{44}H_{65}NO_9$, 14), 607.4357 ($C_{38}H_{73}NO_4$, **100**), 589.4264 ($C_{37}H_{67}NO_4$, 10), 515.3908 ($C_{32}H_{53}NO_4$, 7), 499.3389 ($C_{27}H_{49}NO_7$, 15), 333.2425 ($C_{21}H_{33}O_3$, 36)	Cerebroside	L, X
P.61	791.4705	16.44	$C_{47}H_{67}O_{10}$	-3.691	791.4703 ($C_{47}H_{67}O_{10}$, 5), 746.4661 ($C_{46}H_{66}O_8$, 3), 515.2615 ($C_{29}H_{39}O_8$, **100**)	Sterol	L
P.62	333.2416	16.45	$C_{21}H_{33}O_3$	-2.345	315.2315 ($C_{21}H_{31}O_2$, 5), 297.2189 ($C_{21}H_{29}O$, 4), 241.1951 ($C_{18}H_{25}$, **100**), 213.1635 ($C_{16}H_{21}$, 10), 185.1315 ($C_{14}H_{17}$, 11), 171.1167 ($C_{13}H_{15}$, 22), 105.0700 (C_8H_9, 10)	Steroid	X
P.63	802.6441	16.49	$C_{49}H_{86}NO_7$	4.581	756.6113 ($C_{47}H_{82}NO_6$, 43), 544.3632 ($C_{32}H_{50}NO_6$, **100**), 311.2948 ($C_{20}H_{39}O_2$, 17), 283.2630 ($C_{18}H_{35}O_2$, 23)	*N*-Containing lipid	S, L, X
P.64	680.5816	16.50	$C_{41}H_{78}NO_6$	-1.935	662.5602 ($C_{41}H_{76}NO_5$, **100**), 568.3259 ($C_{37}H_{46}NO_4$, 3), 552.3314 ($C_{37}H_{46}NO_3$, 2), 311.2960 ($C_{20}H_{39}O_2$, 1), 255.2316 ($C_{16}H_{31}O_2$, 2)	*N*-Containing lipid	L
P.65	768.5899	16.50	$C_{40}H_{82}NO_{12}$	-1.061	767.4736 ($C_{40}H_{81}NO_{12}$, 81), 606.4229 ($C_{38}H_{56}NO_5$, **100**), 586.5604 ($C_{38}H_{54}NO_4$, 17), 407.3135 ($C_{25}H_{43}O_4$, 19), 333.3484 ($C_{23}H_{41}O$, 7)	Cerebroside	L, X
P.66	524.4598	16.60	$C_{32}H_{63}NO_2P$	4.623	507.4250 ($C_{32}H_{60}O_2P$, **100**), 451.3626 ($C_{27}H_{50}NO_2P$, 42), 339.2375 ($C_{20}H_{36}O_2P$, 62), 189.1485 ($C_{14}H_21$, 9)	Phospholipid	S
P.67	808.6072	16.69	$C_{50}H_{82}NO_7$	-2.391	807.5228 ($C_{50}H_{81}NO_7$, **100**), 749.4773 ($C_{47}H_{73}O_7$, 1), 667.6021 ($C_{45}H_{79}O_3$, 4), 283.2650 ($C_{18}H_{35}O_2$, 1)	Betaine lipid	S

Comp.	$[M+H]^+$ *m/z*	t_R (min)	Molecular formula	Δ (ppm)	MS^2 product ions, *m/z* (elemental composition, rel. intensity [%])	Identification of compound/class	Species
P.68	812.5289	16.74	$C_{47}H_{74}NO_{10}$	1.097	811.7245 ($C_{47}H_{73}NO_{10}$, 5), 795.5023 ($C_{47}H_{73}NO_9$, 8), 633.4506 ($C_{44}H_{59}NO_2$, **100**), 615.4388 ($C_{44}H_{57}NO$, 9), 359.2582 ($C_{27}H_{35}$, 32), 331.2268 ($C_{25}H_{31}$, 37)	Cerebroside	X
P.69	794.5469	16.77	$C_{44}H_{76}NO_{11}$	6.372	793.5444 ($C_{44}H_{75}NO_{11}$, 24), 632.5968 ($C_{41}H_{78}NO_3$, 26), 614.5814 ($C_{41}H_{76}NO_2$, **100**), 452.4093 ($C_{32}H_{52}O$, 7), 356.3522 ($C_{26}H_{44}$, 4), 276.2686 ($C_{20}H_{36}$, 10)	Cerebroside	S, L, X
P.70	774.5883	16.83	$C_{46}H_{80}NO_8$	0.536	773.5734 ($C_{46}H_{79}NO_8$, 78), 731.4969 ($C_{43}H_{73}NO_8$, **100**), 715.5152 ($C_{43}H_{71}O_8$, 27), 633.5239 ($C_{39}H_{69}O_6$, 19), 309.2822 ($C_{20}H_{37}O_2$, 11)	Betaine lipid	X
P.71	747.4998	16.84	$C_{43}H_{71}O_{10}$	-3.112	747.4989 ($C_{43}H_{71}O_{10}$, **100**), 729.5436 ($C_{43}H_{69}O9$, 5), 548.3366 ($C_{31}H_{48}O_8$, 2), 497.3085 ($C_{27}H_{45}O_8$, 59), 309.2783 ($C_{20}H_{37}O_2$, 5), 281.2475 ($C_{18}H_{33}O_2$, 21)	Lipid	L
P.72	505.3887	16.86	$C_{31}H_{53}O_5$	-1.142	505.3514 ($C_{31}H_{53}O_5$, 53), 362.2219 ($C_{25}H_{30}O_2$, 16), 311.2939 ($C_{21}H_{27}O_2$, **100**), 177.1128 ($C_{12}H_{17}O$, 25)	Steroid	X
P.73	812.6617	16.95	$C_{47}H_{90}NO_9$	0.175	812.6627 ($C_{47}H_{90}NO_9$, 65), 794.6021 ($C_{47}H_{88}NO_8$, **100**), 551.5049 ($C_{35}H_{67}O_4$, 16), 285.2213 ($C_{20}H_{29}O$, 7)	*N*-Containing lipid	S
P.74	430.3806	17.06	$C_{25}H_{52}NO_4$	3.393	430.3813 ($C_{25}H_{52}NO_4$, **100**), 413.2167 ($C_{25}H_{51}NO_3$, 41), 257.1367 ($C_{16}H_{19}NO_2$, 25), 165.0901 ($C_{10}H_{13}O_2$, 11)	Unidentified steroidal alkaloid	L
P.75	397.3279	17.14	$C_{24}H_{45}O_4$	-7.516	397.3316 ($C_{24}H_{45}O_4$, **100**), 379.3582 ($C_{24}H_{43}O_3$, 23), 238.1936 ($C_{15}H_{26}O_2$, 2)	Fatty acid	S, L
P.76	676.5169	17.16	$C_{40}H_{70}NO_7$	2.296	675.5167 ($C_{40}H_{70}NO_7$, 2), 617.5153 ($C_{37}H_{61}O_7$, 11), 379.3369 ($C_{24}H_{43}O_3$, 3), 297.2794 ($C_{19}H_{37}O_2$, 17), 283.2635 ($C_{18}H_{35}O_2$, **100**), 269.2480 ($C_{17}H_{33}O_2$, 18), 255.2325 ($C_{16}H_{31}O_2$, 11)	Betaine lipid	S, L, X
P.77	910.7130	17.31	$C_{56}H_{96}NO_8$	-0.651	910.7133 ($C_{56}H_{96}NO_8$, 4), 747.5038 ($C_{46}H_{69}NO_7$, 11), 659.3611 ($C_{40}H_{51}O_8$, **100**), 497.3073 ($C_{34}H_{41}O_3$, 5), 283.2629 ($C_{18}H_{35}O_2$, 11)	Cerebroside	S, L
P.78	822.5836	17.33	$C_{50}H_{80}NO_8$	-2.831	821.5827 ($C_{50}H_{79}NO_8$, **100**), 805.5615 ($C_{49}H_{75}NO_8$, 6), 746.4717 ($C_{46}H_{66}O_8$, 15), 468.3611 ($C_{31}H_{48}O_3$, 4), 283.2634 ($C_{18}H_{35}O_2$, 71)	Betaine lipid	S, X
P.79	772.6141	17.34	$C_{47}H_{82}NO_7$	6.484	772.6025 ($C_{47}H_{82}NO_7$, 71), 755.5974 ($C_{47}H_{79}O_7$, **100**), 699.5283 ($C_{43}H_{71}O_7$, 27), 597.4538 ($C_{38}H_{61}O_5$, 17), 329.3047 ($C_{20}H_{41}O_3$, 40), 285.2791 ($C_{18}H_{37}O_2$, 35)	*N*-Containing lipid	L
P.80	800.6019	17.35	$C_{48}H_{82}NO_8$	-1.955	800.6032 ($C_{48}H_{82}NO_8$, 46), 756.6142 ($C_{47}H_{82}NO_6$, 4), 697.6123 ($C_{44}H_{73}O_6$, 9), 623.5079 ($C_{41}H_{67}O_4$, 4), 472.3637 ($C_{30}H_{48}O_4$, **100**), 283.2627 ($C_{18}H_{35}O_2$, 4)	Betaine lipid	S, L, X
P.81	353.3051	17.47	$C_{22}H_{41}O_3$	-1.331	353.3047 ($C_{22}H_{41}O_3$, **100**), 295.1526 ($C_{18}H_{31}O_3$, 35), 265.1402 ($C_{17}H_{29}O2$, 10), 159.1019 ($C_9H_{19}O_2$, 1)	Fatty acid	S
P.82	752.5591	17.54	$C_{43}H_{79}NO_7P$	-0.422	752.5997 ($C_{43}H_{79}NO_7P$, 1), 734.5480 ($C_{43}H_{77}NO_6P$, 11), 484.2823 ($C_{25}H_{43}NO_6P$, 3), 392.2924 ($C_{24}H_{40}O_4$, **100**), 361.2737 ($C_{23}H_{37}O_3$, 27), 294.3156 ($C_{19}H_{34}O_2$, 10)	Glycerphospholipid	L
P.83	806.6108	17.55	$C_{47}H_{84}NO_9$	-4.721	806.6019 ($C_{47}H_{84}NO_9$, 11), 788.5944 ($C_{47}H_{82}NO_8$, 13), 665.5858 ($C_{40}H_{75}NO_6$, 31), 538.3262 ($C_{32}H_{44}NO_6$, 3), 415.3207 ($C_{27}H_{43}O_3$, 54), 392.2923 ($C_{27}H_{38}NO$, **100**), 294.3156 ($C_{20}H_{38}O$, 12)	Cerebroside	L
P.84	816.5839	17.55	$C_{44}H_{82}NO_{12}$	0.245	815.6225 ($C_{44}H_{82}NO_{12}$, **100**), 757.5140 ($C_{41}H_{73}O_{12}$, 11), 547.3356 ($C_{35}H_{47}O_5$, 7), 309.1938 ($C_{14}H_{29}O_7$, 3), 283.2657 ($C_{18}H_{35}O_2$, 2)	Betaine lipid	L
P.85	794.5603	17.85	$C_{48}H_{76}NO_8$	-2.382	793.5598 ($C_{48}H_{75}NO_8$, 10), 632.5968 ($C_{40}H_{74}NO_4$, 26), 614.5464 ($C_{40}H_{72}NO_3$, **100**), 452.5093 ($C_{30}H_{60}O_2$, 7), 356.3522 ($C_{23}H_{48}O_2$, 4), 276.2686 ($C_{19}H_{32}O$, 10)	*N*-Containing lipid	S, L

Note: S= *S. glaucum*, L= *L. crassum*, X= *X. umbellata*

Variation in the metabolites of stress exposure soft corals was further analyzed by using principle component analysis; PCA. This analysis is a common method in metabolic profiling for determining the primary variance within a group as well as detecting outliers in a data set. The variations of the dataset are visualized in the principal components (PCs) score plot. In addition, the information of responsible features for clustering or differentiation of samples were visualized in the loadings plots of each PCA. In this study, batch effects were observed in the PCA score plots of all extracts. Thus, it was obvious that the primary variance is explained by the measurement conditions. These batch-to-batch differences are common in untargeted LC-MS metabolomics experiments. It is caused by unavoidable external influences on the chromatography and MS instrument. Therefore, a batch correction is necessary to ensure the comparability of samples from various batches.

The correction of batch effect by using "study samples" were performed for the data in this experiment. This method of correction was applied because of the assumption that all samples exhibit the same batch dependent effect due to proper randomization. This appears to be a benefit, as it allows the correction of a greater number of metabolites, including those that are undetectable in QCs due to dilution effects. After performing the samples correction, a satisfactory batch correction result was obtained, and this processing method was used for further data evaluation. The result of the PCA on the *S. glaucum* extract after treatment with the elicitors is depicted in Figure 40.

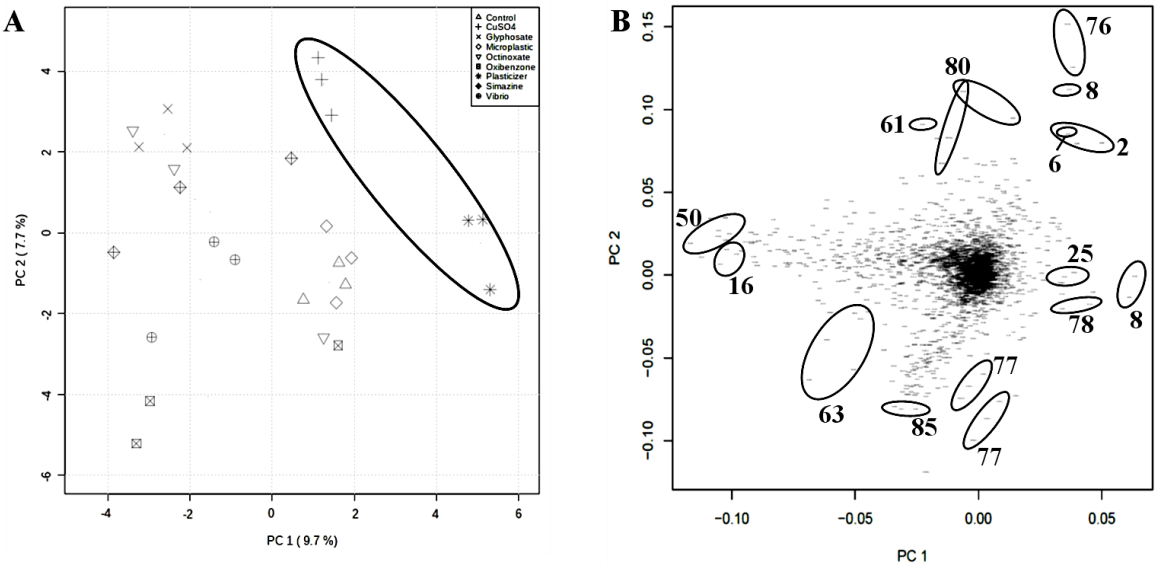

Note= Δ: Control, +: $CuSO_4$, ×: Glyphosate, ◇: Microplastic, ∇: Octinoxate, ⊠: Oxibenzone, ✳: Plasticizer, ⟐: Simazine, ⊕: Vibrio

Figure 40 PCA of LC-ESI-HRMS data of *Sarcophyton glaucum* extracts; scores plot (A) and loadings plot (B). Numbers correspond to compound number at Table 12

The variance of metabolites in the extracts of treated *S. glaucum* was low in both prime PCs (PC1 9.7% and PC2 7.7%). Nevertheless, the extracts of S. *glaucum* treated with plasticizer (DMP) were clearly discriminated from other extracts in principle component 1 (PC1). Moreover, extracts of soft coral treated with $CuSO_4$ and glyphosate clustered in the

positive direction of PC2, whereas oxybenzone distinct in the most negative direction of PC2. Afterwards, the evaluation of responsible features caused segregation were performed by evaluating the correspond loadings plot (Figure 40.B). As result, it was clear that extracts of *S. glaucum* treated with DMP in accordance with the results of NMR investigation were chemically distinct due to their fatty acid composition.

This separation is primarily caused by nitrogenous lipids, including betaine lipids cerebroside (P.**76**, P.**77**, P.**78**, P.**85** see Table 9), as well as short chain amino alcohol (P.**2** and P.**6**). Additionally, the other group of metabolites, such as diterpenoid (P.**25**) and sesquiterpene carboxylic acid (P.**8**), are also responsible for this separation. The nitrogenous metabolites with a high molecular weight including betaine lipids and cerebrosides are non-polar compounds eluted in the range of 16-17 min, while amino alcohol with a low molecular weight eluted in the range of 6-8 min. Similar to the soft coral extracts treated with DMP, the separation of extracts $CuSO_4$ treated coral was caused by betaine lipid (P.**80**) and an unidentified sterol (P.**61**).

In general, lipids and fatty acids were found as the major components causing the separation of all *S. glaucum* extracts in the PCA, which are observed in all PCs (in both positive and negative directions). Other components, e.g. steroids and cembrenes were not detected as responsible compounds for this segregation. The changing of lipid and fatty acid content in the soft coral body under stress conditions is related to their role as energy provider, as well as the "survival" mechanism of soft corals for protect their body [243, 244].

Moreover, multivariate data analysis was further performed on the LC-ESI-HRMS data of *L. crassum* (Figure 41). Similarly to the *S. glaucum* PCA result, the variance of metabolites in extracts of treated *L. crassum* was relatively low in both PCs (PC1 7.3% and PC2 7%). Nevertheless, the separation of extracts of *L. crassum* treated with DMP and $CuSO_4$ was observed in PC2. These groups were separated from other groups in the positive direction of PC2. The features causing this separation were tentatively identified as an unpolar compound nitrogenous lipids (P.**84**, P.**85**) with molecular formula $[M+H]^+$ $C_{44}H_{82}NO_{12}$ and $C_{48}H_{76}NO_8$, respectively, as well as a cerebroside (P.**83**), a steroid (P.**29**) and a steroidal alkaloid (P.**74**).

Lipids were tentatively identified as the responsible metabolites for segregation of some groups in the positive direction of PC1, e.g. extracts of soft coral treated with glyphosate, microplastic and *V. campbelli*. These lipids have been identified as glycerolipid (P.**58**), and nitrogenous lipids (P.**41**, P.**63**) with molecular formulas $[M+H]^+$ $C_{53}H_{76}NO_6$, $C_{49}H_{86}NO_7$, respectively. Two diterpenes (P.**32**, P.**37**) were identified as the responsible features causing the separation in the negative direction of PC2. These features are most likely the metabolites that caused the separation of the extracts from soft corals treated with glyphosate and *V. campbellii*. The presence of these metabolites is probably linked to the antibacterial activity of these extracts (shown at Chapter VI). Furthermore, features with a low molecular mass (*m/z* 430-490) were identified as responsible metabolites for the separation in the negative

direction of PC1. These features have been tentatively annotated as amino alcohols (P.**3**, P.**6**, P.**11**, P.**12**) with molecular formulas $[M+H]^+$ $C_{14}H_{32}NO_2$, $C_{16}H_{36}NO_2$, and $C_{14}H_{28}NO_5$, respectively.

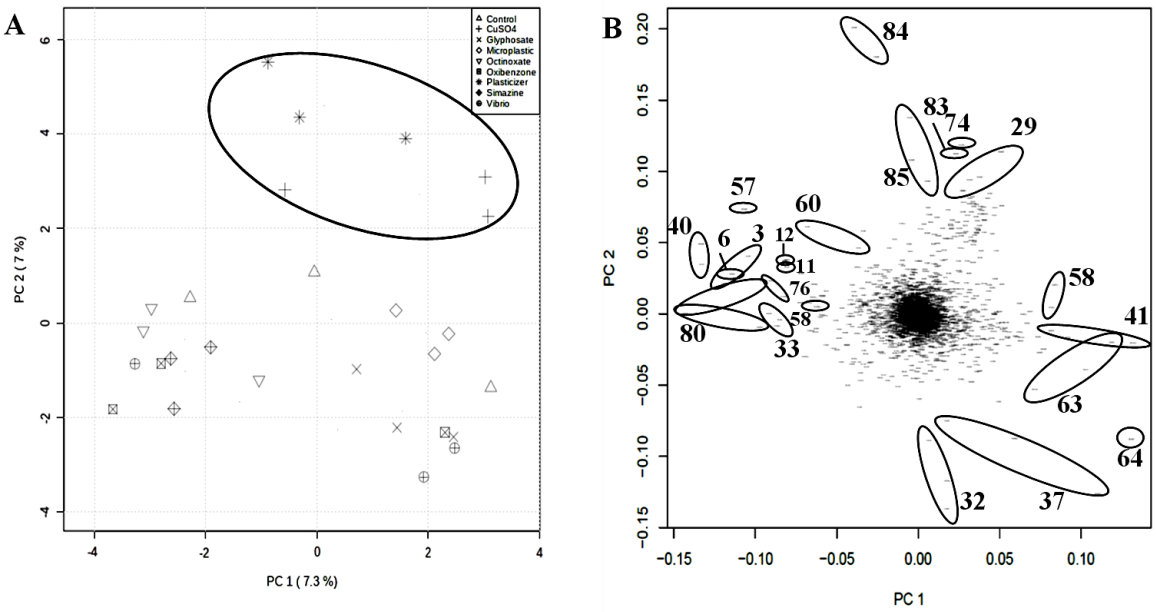

Note= Δ: Control, +: $CuSO_4$, ×: Glyphosate, ◇: Microplastic, ∇: Octinoxate, ⊠: Oxibenzone, ✳: Plasticizer, ◈: Simazine, ⊕: Vibrio

Figure 41 PCA of LC-ESI-HRMS data of *Lobophytum crassum* extracts; scores plot (A) and loadings plot (B). Numbers correspond to compound number at Table 12

Beside of the function as energy provider, these metabolites play a vital role in the defense mechanisms of all organisms, including soft corals and their symbiont. Microalgae, including zooxanthellae, produce certain metabolites such as cerebrosides, ceramides and fatty acids as a defense mechanism against stress and to protect themself against predator and other unfavorable conditions [256-258]. Therefore, this result confirmed that the stresses experienced by soft coral also affect their symbionts, which leads to production of some specialized metabolites. Additionally, to survive in stressful environments, coral with the help of zooxanthellae as symbionts will produce fatty acids and lipids which help the soft coral in maintaining its energy and skeleton [144, 145, 165].

Multivariate data analysis (PCA) for LC-ESI-HRMS data of *X. umbellata* extracts is shown in Figure 42. Similar to the PCA result of *L. crassum* extracts, the extracts of *X. umbellata* treated with plasticizer DMP and $CuSO_4$ were separated from other extracts. PC1 (7.8% variance) discriminated this two group in the positive direction, followed by the extracts of *X. umbellata* treated with *V. campbelii*. The responsible features caused this separation were tentatively identified base on the fragmentation pattern and literature. The composition of betaine lipids (P.**78**, P.**67**), cerebrosides (P.**52**, P.**60**), glycerolipid (P.**56**), steroids (P.**45**, P.**62**), fatty acid (P.**39**) and the low molecular mass metabolites such as amino alcohol (P.**6**) and sesquiterpene carboxylic acid (P.**1**) have a positive impact for the separation of DMP and $CuSO_4$ groups. In the negative direction of PC1, cerebroside (P.**65**),

steroid (P.**72**), and betaine lipid (P.**80**) were tentatively assigned as responsible compounds for the segregation.

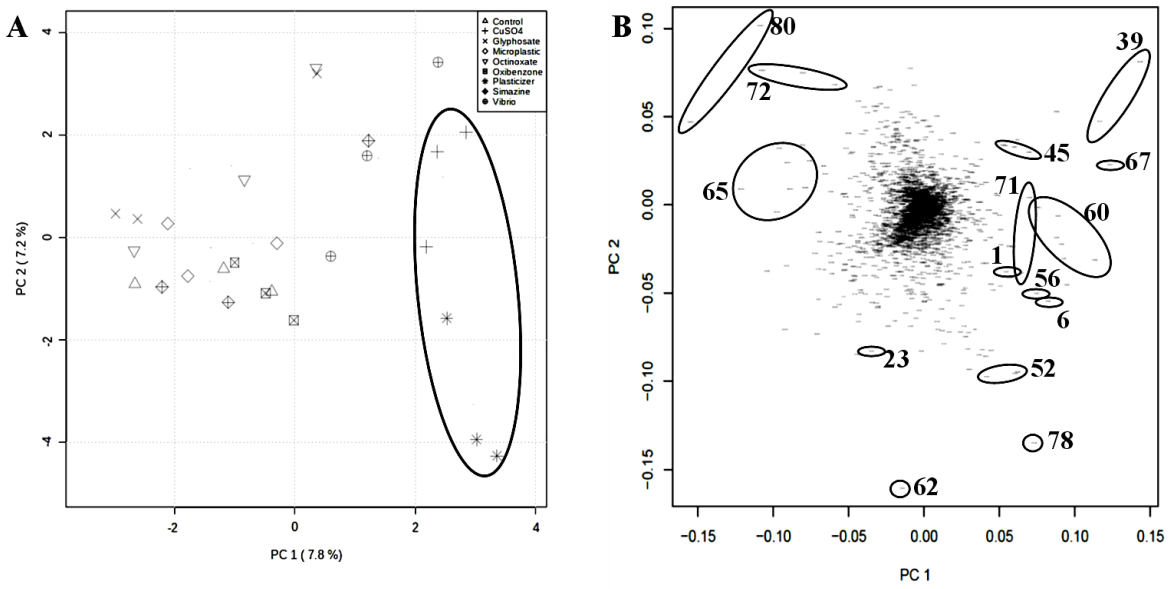

Note= Δ: Control, +: $CuSO_4$, ×: Glyphosate, ◇: Microplastic, ∇: Octinoxate, ⊠: Oxibenzone, ✳: Plasticizer, ◈: Simazine, ⊕: Vibrio

Figure 42 PCA of LC-ESI-HRMS data of *Xenia umbellata* extracts; scores plot (A) and loadings plot (B). Numbers correspond to compound number at Table 12

As previously described, fatty acids and lipids in the soft coral body play the role as the energy source for this organism. Furthermore, they are crucial for incorporation into phospholipids, the building blocks for the membrane lipid bilayer. In addition, fatty acids contribute to the hydrophobicity of the cell membranes and serve as a barrier between the cell contents and the extracellular medium by forming an impermeable barrier to water and polar molecules within the cells [144, 259]. Therefore, in order to protect their bodies and maintain their cell function during stressful conditions, soft coral or their symbionts produce more fatty acids and lipids compared to normal conditions.

e. Histology profiling of soft corals tissue after elicitation

Similarly to the MS imaging study (Chapter IV), histology profiling of soft coral was performed on two soft corals only, *S. glaucum* and *L. crassum*, because *X. umbellata* has no compact body structure, which complicates the embedding process. This experiment was conducted to determine the stress level of soft corals after treatments, as measured by the density of zooxanthellae and mucocyte cells in their bodies (especially in umbrella). The number of zooxanthellae and the density of mucocyte in the corals are two parameters used to assess their response to environmental conditions [260]. The corals (including soft corals) will initially response to stress by secreting large amounts of mucus from epidermal mucocyte cells, and further expelling or digesting their endosymbiont (zooxanthellae;

Symbiodinium spp.) [261-264]. Thus, by observing the production of mucus in the body of soft corals, we can ascertain the stress level of this organism.

The formation of mucus layers serves as a biomarker for coral stress [265]. Numerous studies have been conducted to determine this markers, however, each of these methods has limitations in terms of understanding and predicting the adaptation response of corals. However, methods for collecting coral mucus using artificial stressors have produced inconsistent results in terms of dissolved organic content when compared to mucus collected *in situ* [218, 266]. Therefore, histopathological methods that combine the detection of both indicators (zooxanthellae and mucocyte density) in soft coral tissue may be beneficial.

To address these questions, a novel technique combining the lectin histochemical stain wheat germ agglutinin (WGA) with high-resolution (200 nm) optical epifluorescence microscopy has been developed [263]. Auto-fluorescence of zooxanthellae chlorophyll was induced when the tissue sections were excited with laser diode 405/30 and HeNe 633. The fluorescence of mucocyte cells was then generated by excitation of the WGA-conjugated Alexa Fluor 647 with λ 633 nm light and chlorophyll with λ 405 nm light. After combining both images, a channel fluorescent image was created. These two channels obtained images that were artificially colored green (zooxanthellae) and red (mucus-WGA). Figure 43 depicts the outcome of tissue imaging for *S. glaucum* and Figure 44 for *L. crassum*.

According to the histology profiling results, the density of zooxanthellae cells in soft coral tissue varied between treatments. In general, the density of zooxanthellae cells in untreated tissue (control) was higher than in the tissue of treated soft corals. For *S. glaucum*, tissue sections of this coral treated with elicitors revealed that zooxanthellae cells were predominantly concentrated on the corals' surface, particularly around the tentacle area. In addition, during the observation under the microscope, damage of zooxanthellae cells was observed in the colony on the surface of the corals body. This condition was clearly visible in the tissue of soft coral treated with $CuSO_4$ and plasticizer DMP. Along with those elicitors ($CuSO_4$ and DMP), glyphosate exhibited an effect on the zooxanthellae in *L. crassum* that were found in lower density. Moreover, a high density of mucocyte cells was observed in *S. glaucum* tissue treated with *V. campbellii*, as well as in two other investigated soft corals after exposure to DMP and $CuSO_4$.

The density of zooxanthellae within the coral body depends on the condition of their host. Under normal condition, the migration of zooxanthellae from the coral body to the water column is relative low. However, under certain adverse conditions, such as high water temperature and salinity, as well as exposure to certain pollutants, zooxanthellae immigration is rapid [267-269]. Under stress condition, the coral will expell its symbiont, and on rare occasions, digest it into their body, specifically the gastrodermal cavity [233]. It could be an explanation for the localization of zooxanthellae in this study, which are detected in the tentacle area. From this result, it was also clearly shown that $CuSO_4$ and DMP are highly

toxic either for soft coral or their symbiont. These histological observation support the result obtained by counting zooxanthellae cells in the water column (previously described).

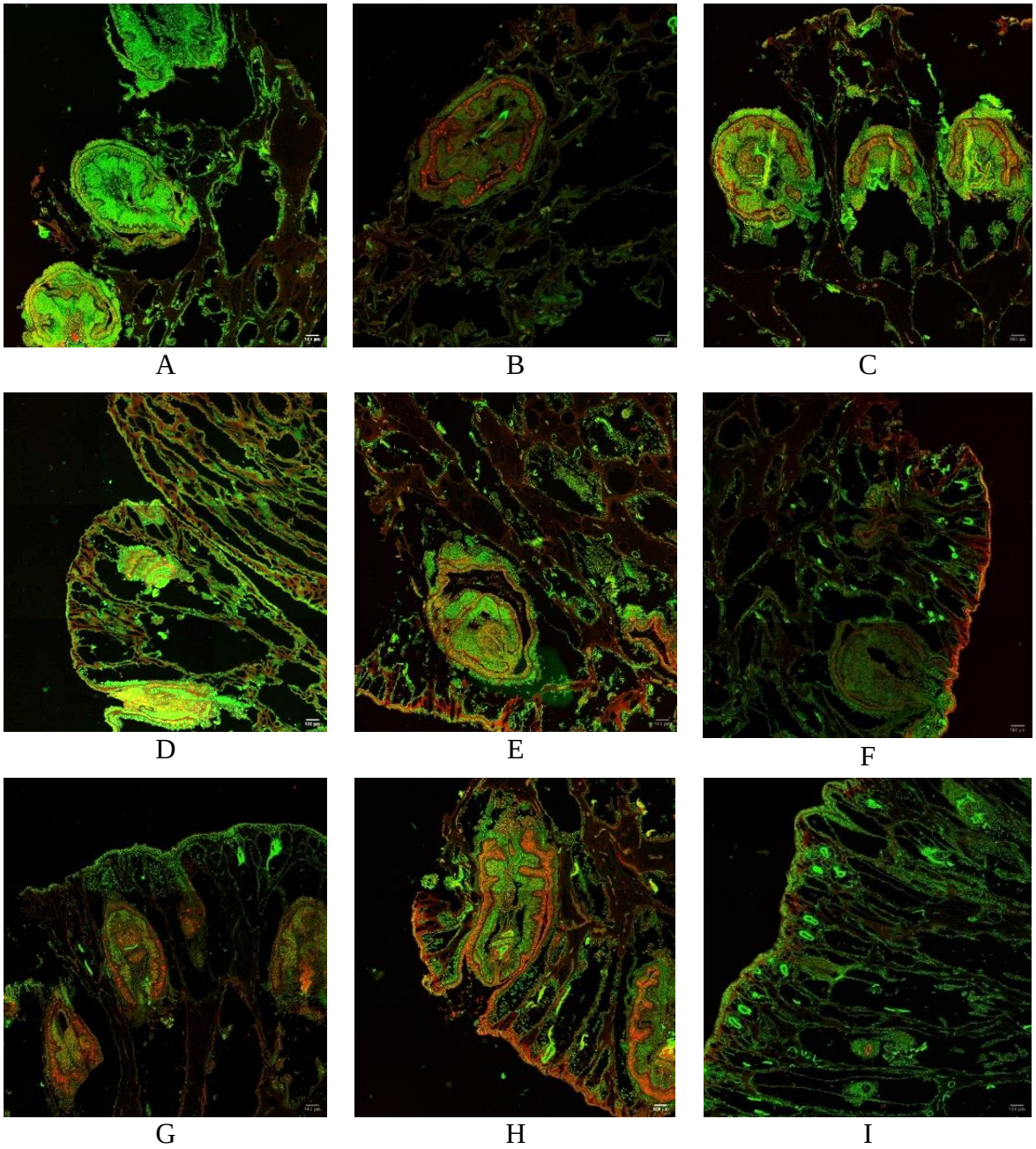

Figure 43 Histology imaging of the soft coral *Sarcophyton glaucum* after treatment with glyphosate (A), simazine (B), oxybenzone (C), octinoxate (D), $CuSO_4$ (E), DMP (F), microplastic (G), *Vibrio campbellii* (H), and without treatment (I); green = zooxanthellae, red = mucocite cells

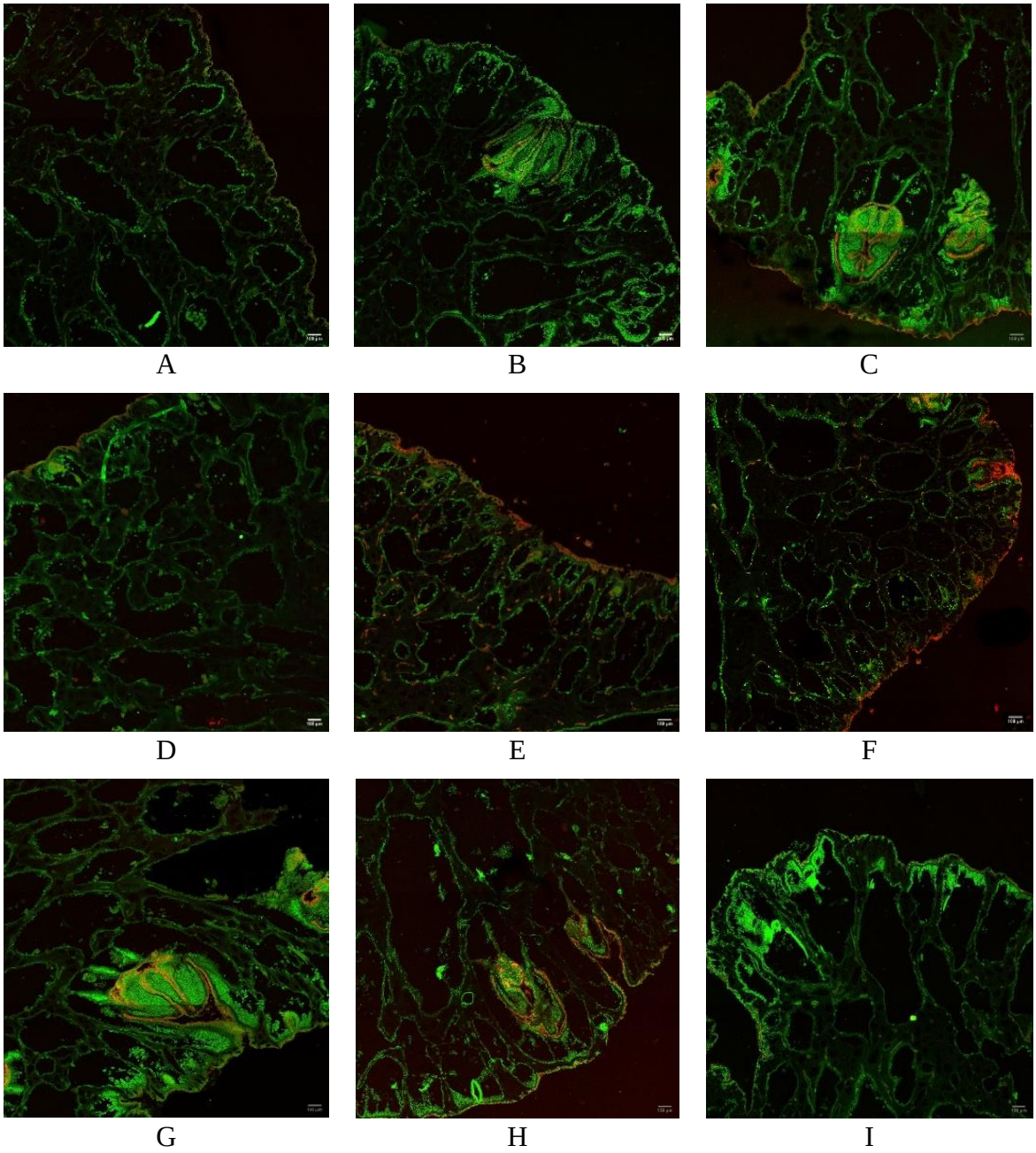

Figure 44 Histology imaging of the soft coral *Lobophytum crassum* after treatment with glyphosate (A), simazine (B), oxybenzone (C), octinoxate (D), $CuSO_4$ (E), DMP (F), microplastic (G), *Vibrio campbellii* (H), and without treatment (I); green = zooxanthellae, red = mucocite cells

Mucocytes were concentrated in the tentacle area of soft corals, which is also the location of the zooxanthellae. The zooxanthellae provide up to half of the photosynthetically fixed carbon required by corals to produce mucus [270, 271]. Therefore, the area where the zooxanthellae are concentrated also contains the colony of mucocyte cells and mucus. Coral mucus is a complex mixture of proteins and carbohydrates that is produced by mucocytes in the coral epidermal layer [272]. This substance acts as a defense against desiccation and pathogens [273]. As demonstrated here, after invasion by *V. campbellii*, *L. crassum* produces a high density of mucocytes. Therefore, it is clearly shown that mucus production is related to the pathogen infection. Beside of that, *Vibrio* are known for causing mucus production in the

corals [274]. Furthermore, the high concentration of mucus and mucocytes was also observed in the soft corals tissues treated with $CuSO_4$ and DMP. One possible explanation for this finding is that increased mucus production in corals enhances defense against pathogens as well as stress conditions in which other defense mechanisms may be compromised [275].

5.4. Conclusion

Exposure to the elicitors had a significant effect on the morphology and metabolite composition of *S. glaucum*, *L. crassum*, and *X. umbellata*. Our results provide insights on corals' responses to environmental stress at the metabolite level and define stress biomarkers in corals. $CuSO_4$ and DMP were found to be the most toxic elicitors to soft corals, followed by simazine, oxybenzone, and octinoxate. The retraction of tentacles for *S. glaucum* and *L. crassum* and necrosis of *X. umbellata* were observed after exposure to these elicitors. The number of associated zooxanthellae and PSII efficiency were also determined in order to monitor the occurrence of zooxanthellae-soft coral breakdown. The higher number of zooxanthellae in the water, the lower the PSII efficiency detected on the soft corals umbrella. However, this is not always the case; for example, in samples of *S. glaucum* treated with glyphosate at a concentration of 10 mg/L, the PSII efficiency was higher after treatment. There are two possible explanations: either glyphosate acts as a fertilizer for zooxanthellae at this concentration (due to the phosphorus content), or *S. glaucum* is a glyphosate-resistant organism.

Beside corals morphology, the effect of elicitors was also evident in the composition of their metabolites. The results of metabolite profiling in soft coral using untargeted ^{1}H-NMR and LC-MS metabolomics in combination with multivariate data analysis indicated that extracts of corals treated with $CuSO_4$ and DMP were distinct from other extracts. This separation is primarily due to the composition of fatty acids and nitrogenous lipids. The composition of these substances in the bodies of soft corals has been increased (based on ^{1}H-NMR data). The increase of fatty acids is related to energy demand during stress, since fatty acids are source of alternative energy under abiotic stress. Additionally, an unidentified steroidal alkaloid and a known ceramide, isogalbamide A, were detected as additional metabolites in *L. crassum* extracts treated with $CuSO_4$, resulting in the group being separated in LC-MS-PCA. Along with investigating the effect of elicitors on the morphology and chemical profiles of soft corals, mucus production can be used to determine their stress experienced. Histological examination using a novel technique combining the lectin histochemical stain WGA with high-resolution (200 nm) optical epifluorescence microscopy allows the investigation of mucus production in the corals tissue. Mucus was detected in high concentrations on the tissue of *Vibrio campbellii*-infected soft corals, as well as after exposure to DMP and $CuSO_4$. It strongly confirmed that this mucus is produced by corals in order to protect themselves from pathogens and under stress condition.

VI. Investigation of the bioactivity from elicitor-treated *Sarcophyton glaucum*, *Lobophyton crassum*, and *Xenia umbellata* extracts

Abstract

Soft corals produce a high diversity of metabolites with unique structures, which exhibit a broad spectrum of biological activities, i.e. antibacterial or cytotoxic properties. *Sarcophyton glaucum*, *Lobophytum crassum*, and *Xenia umbellata*, three soft coral species examined in this study had not yet been investigated for their antibacterial activity against *Allivibrio fischeri* and *Bacillus subtilis*. Therefore, we investigated the antibacterial activity of their methanolic crude extracts against these two bacteria, as well as their cytotoxicity to HT29-colon cancer and PC3-prostate cancer cell lines. A total of 54 samples were tested for each assay, including extracts of soft corals treated with glyphosate 10 mg/L, $CuSO_4$ 100 µg/L, and plasticizer 100 µg/L, as well as untreated soft corals. *S. glaucum* and *L. crassum* extracts tested at a very high concentration (500 µg/mL) inhibited *A. fischeri* completely (100%), whereas *X. umbellata* extracts at a lower concentration (50 µg/mL) acted as bacteriostatic for up to 9 hours. Interestingly, six extracts of *L. crassum* treated with glyphosate and $CuSO_4$ at both concentrations demonstrated high activity against *A. fischeri*, with average IC50 values of 7.60 µg/mL and 11.76 µg/mL, respectively. In comparison to *A. fischeri*, all extracts of the corresponding soft corals exhibited only weak to moderate antibacterial activity against *B. subtilis*. Furthermore, a low concentration of soft coral extracts (0.05 µg/mL) had no effect on the viability of both cell lines, while a higher concentration (50 µg/mL), they exhibited a strong inhibition, with a percentage of cell viability less than 3%.

6.1. Introduction

The marine environment is a rich source of bioactive metabolites. Until 2012, around 1200 new biochemical compounds were discovered from marine organisms [5, 276]. Over 3000 marine natural products have been identified from cnidarians alone, mostly in the last decade [277]. As cnidarians, soft corals are also well-known for producing a variety of diverse and complex secondary metabolites, including sesquiterpenes, diterpenes, cembranoids, steroids/steroidal glycosides, and fatty acids [278-287]. These metabolites possess a diverse spectrum of biological activities, such as antibacterial, cytotoxic, anti-inflammatory, and antifouling properties [288-294].

The three investigated soft coral species of this study also exhibited a broad spectrum of bioactivities. *Sarcophyton glaucum* is a prolific source of a wide variety of secondary metabolites, including cembranoids [288, 295], biscembranoids [281], terpenoids [278, 296, 297] and steroids [282, 286], as well as lipids and peptides [285]. For pharmacological research, several metabolites from this species have been shown to possess cytotoxic [281,

292, 298], antimicrobial [298, 299], neuroprotective [300], anti-inflammatory [281], and antifouling [294] activities. *Lobophytum crassum* is a species of soft coral found mainly in the Indo-Pacific and Red Seas. Several metabolites from this soft coral have been identified, i.e. cembranoids [287, 301, 302], cembrane diterpenes [303, 304], glycolipids [279], and sterols [284]. Various biological activities of these isolated metabolites have been also reported, including cytotoxicity [301, 305, 306], anti-inflammatory activity [293, 301], and HIV inhibition [307]. Beside of these mentioned activity above, the metabolites of *L. crassum* have a broad spectrum of antibacterial activity against Gram-positive and Gram-negative bacteria [283, 289, 308].

Furthermore, the xeniid soft coral in this study (*Xenia umbellata*) is well-known for its high diversity of terpenoids (particularly diterpenes) and steroids [8, 291, 309]. The diterpenoids from this species exhibited high cytotoxicity [290, 310, 311] and antibacterial activity [312]. These three soft corals have not yet been investigated for their antibacterial activity against Gram-negative *Aliivibrio fischeri* and Gram-positive *Bacillus subtilis* to date. Therefore, we investigated the antibacterial activity of *S. glaucum*, *L. crassum* and *X. umbellata* methanolic crude extracts against these two bacteria, as well as their cytotoxicity against several cancer cell lines.

6.2. Experimental

According to the metabolite profiling results (NMR and LC-MS) in Chapter V, the majority of samples contain similar metabolites as the control (untreated samples). Therefore, the antibacterial assay was conducted solely on the samples that differed from the control. Extracts of soft corals treated with glyphosate 10 mg/mL, $CuSO_4$ 100 µg/L, and plasticizer 100 µg/L, as well as untreated soft corals, were selected as the tested samples for bioactivity investigation. In total, 54 samples of three soft coral species were tested for each assay. The detailed procedure for these assays is describe in Chapter III.

6.3. Result and discussion

6.3.1. Antibacterial activity of soft coral extracts against Aliivibrio fischeri

Aliivibrio fischeri is a bioluminescent, Gram-negative bacterium living in marine environment. This bacterium lives free or in mutualistic association with squids and fishes. The antibacterial assay against the Gram-negative *A. fischeri* was determined using a luminescence based 96 well microtiter plate assay. This antibacterial assay was performed by applying two concentrations of the corresponding soft coral extracts, 50 µg/mL and 500 µg/mL, while chloramphenicol, a commercial antibiotic, was used as a positive control. At the concentration of 500 µg/mL, all extracts of *S. glaucum* and *L. crassum* inhibited bacteria growth completely, while the extracts of *X. umbellata* exhibited low activity against this bacterium. At a concentration of 50 µg/mL, almost all of soft coral extracts act as a growth promoter for *A. fischeri*. Interestingly, extracts of *L. crassum* (treated with glyphosate and

$CuSO_4$) at a concentration of 50 µg/mL exhibited activity against these bacteria. Figure 45 displays the results of antibacterial screening for all soft coral samples at two concentrations.

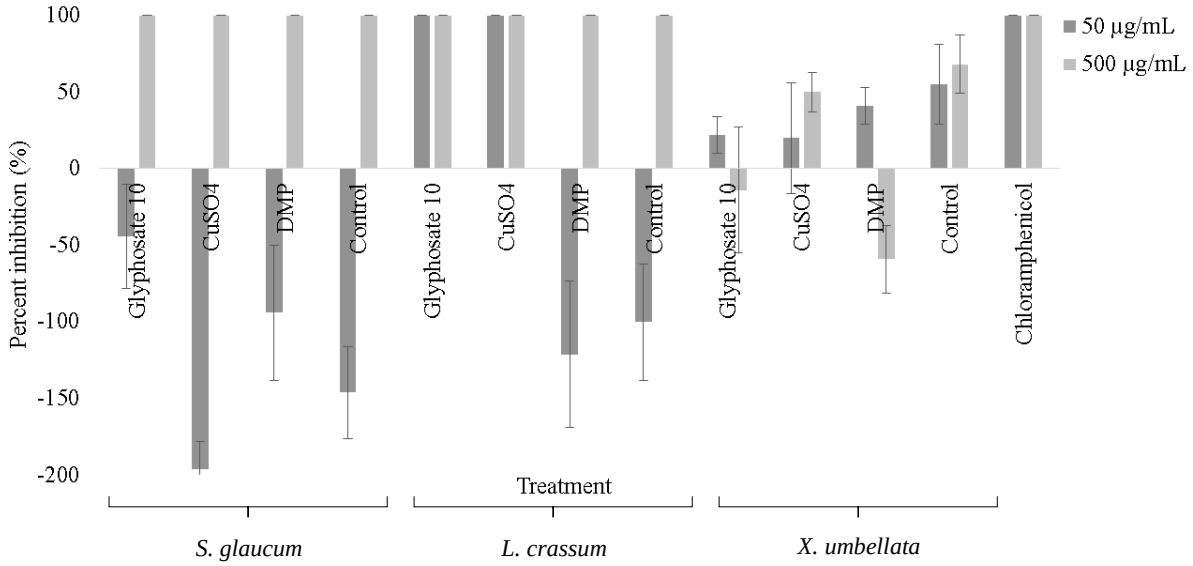

Figure 45 Antibacterial activity of methanolic crude extracts of treated soft corals and control against *Aliivibrio fischeri* (concentration 50 µg/mL and 500 µg/mL in DMSO, positive control chloramphenicol, negative control DMSO), technical replicates=2; All value is average of 3 biological replicates

Furthermore, those extracts from *L. crassum* treated with glyphosate at 10 mg/L and $CuSO_4$ 100 µg/L were chosen as exploratory samples for subsequent concentration tests. Eight different concentrations (500, 250, 125, 100, 50, 25, 10, 5 µg/mL) of the active samples were selected for this experiment. Three extracts of *L. crassum* treated with 100 µg/L $CuSO_4$ completely inhibited bacterial growth at concentrations less than 10 µg/mL, with IC50 values of 7.50 µg/mL, 7.72 µg/mL, and 7.86 µg/mL, respectively. Similar activity was observed in extracts of *L. crassum* treated with glyphosate 10 g/L which inhibited *A. fischeri* at concentrations lower than 25 µg/mL, with IC50 values of 11.26 µg/mL, 12.42 µg/mL, and 11.60 µg/mL, respectively (Figure 46).

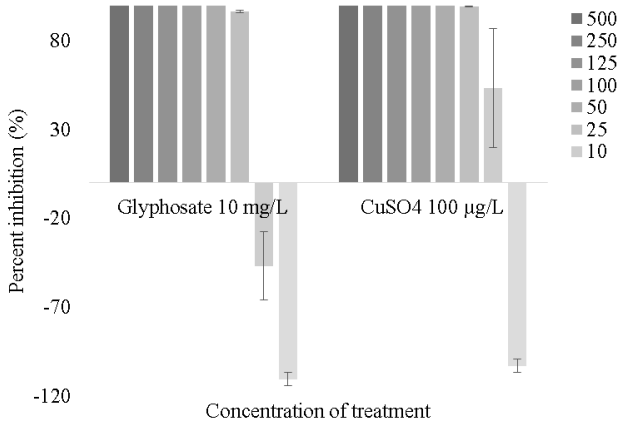

Figure 46 Antibacterial activity of crude extracts of *Lobophytum crassum* treated with glyphosate 10 mg/L and $CuSO_4$ 100 µg/L at different concentrations against *Aliivibrio fischeri*; All value are the average of 3 biological replicates

In fact, it is known that glyphosate inhibits the growth of certain bacteria, including *Escherichia coli* and *Salmonella enterica* [313-315]. Therefore, there is the possibility that the elicitors (glyphosate and $CuSO_4$) contributed to the antibacterial activity of these extracts against *A. fischeri*. To address this question, the antibacterial activity of these two substances was evaluated against *A. fischeri*. As a result (Appendix 10), neither elicitor, glyphosate nor $CuSO_4$, demonstrated antimicrobial activity against the tested bacterium. Thus, the activity of the *L. crassum* extracts treated with these two elicitors is clearly derived from the secondary metabolites produced by the soft corals in response to these stressors.

Furthermore, the antibacterial activity of *X. umbellata* crude extracts was determined over a range of incubation times. Interestingly, extracts of this soft coral demonstrated bacteriostatic activity against *A. fischeri* at a concentration of 500 µg/L. These extracts inhibited *A. fischeri* completely, but only for the first 9 hours. After 9 hours, these extracts serve as a growth promoter for tested bacteria (Figure 47). There are two possible explanations for this phenomenon: first, the bacterium experiences stress/shock after application of the extract then adapts to the environment, and further continues to grow. The second explanation is the extracts act as bacteriostatics, which keeps the bacteria in the stationary phase of growth for an extended period of time.

Numerous studies have been conducted to determine the antibacterial activity of soft coral compounds against Gram-negative bacteria. Terpenoids and cembranoids are a compound classes with broad antibacterial activity, including human pathogenic bacteria [316-318]. Moreover, isolated compounds from genus *Sarcophyton* and *Lobophytum* demonstrated antibacterial activity against *Vibrio* sp. [289, 319-322]. Certain cembranoid compounds as well as crude extract from *S. trocheliophorum*, demonstrated strong antibacterial activity against the (marine) bacterium *Vibrio cholera* [317, 323, 324]. A similar activity was reported for extracts of *Sarcophyton* sp. which exhibited the strong activity against several marine bacteria, i.e. the seaweed pathogens *Alteromonas* sp., *Cytophaga-Flavobacterium* and *Vibrio* sp. [325].

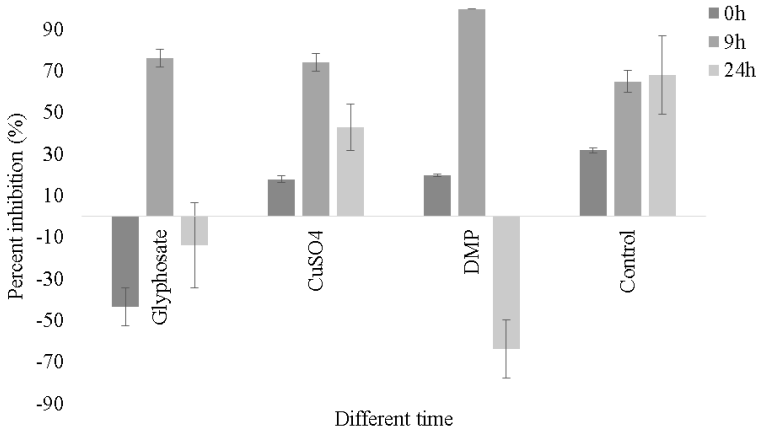

Figure 47 Antibacterial activity of crude extracts of *Xenia umbellata* against *Aliivibrio fischeri* after three different incubation times (concentration 500 µg/mL in 1% DMSO, positive control chloramphenicol, negative control 1% DMSO), technical replicates = 2; All value is average of 3 biological replicates

Similarly to the genus *Sarcophyton*, antibacterial activity against Gram-negative *Vibrio* sp. was discovered in the crude extract of *Lobophytum* genera [326], but still, not many studies performed similar investigation. Nevertheless, numerous studies have demonstrated that *L. crassum* produce a variety of potential antibacterial compounds against Gram-negative bacteria, such as cembranolides trans-fuseda-methylene-g-lactone and durumolides A–E which exhibited strong antibacterial activity against the human pathogen *Salmonella enteritidis* [327]. Additionally, the sesquiterpenes alismol isolated from *Lobophytum* sp. demonstrated significant inhibition of *Pseudomonas aeruginosa* [289].

6.3.2. Antibacterial activity of soft coral extracts against Bacillus subtilis

Beside Gram-negative bacteria, antibacterial assays against Gram-positive bacteria were performed on *Bacillus subtilis*. A turbidimetric assay was used to determine antibacterial activity of the crude methanolic extracts of all soft corals with chloramphenicol as a positive control. The antibacterial activity of the crude extracts was determined in two different concentrations, 50 µg/mL and 500 µg/mL. In comparison to Gram-negative bacteria, the corresponding soft coral extracts exhibited a low activity. At the concentration of 500 µg/mL, only extracts of all soft corals treated with glyphosate 10 mg/mL exhibited moderate antibacterial activity with 50% growth inhibition, while the remaining extracts have no activity to inhibit tested bacteria (Figure 48).

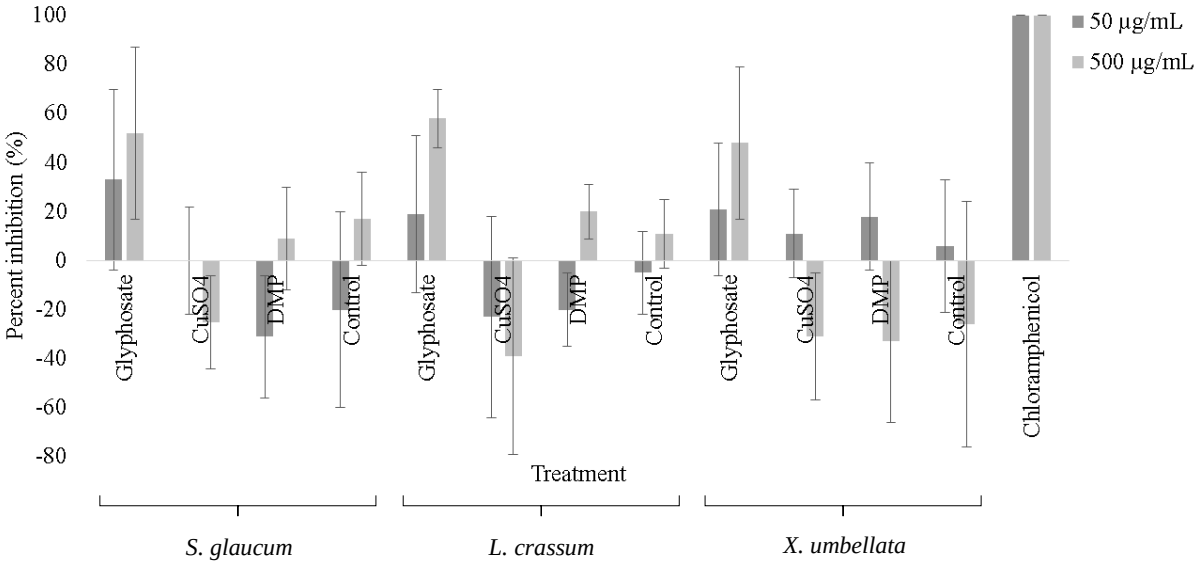

Figure 48 Antibacterial activity of methanolic crude extracts of treated soft coral and control against *Bacillus subtilis* (concentration 50 µg/mL and 500 µg/mL in DMSO, positive control chloramphenicol, negative control DMSO), technical replicates = 2; All values are averaged over 3 biological replicates

This finding contrasts with several previous studies, which revealed that extracts from *Sarcophyton* and *Lobophytum* possess antibacterial activity against *B. subtilis*. Some capnosane skeleton compounds such as trocheliophols as well as the steroid ahramycin B isolated from *S. trocheliophorum*, exhibited *B. subtilis* [318, 328]. Moreover, for a derivate of

the diterpene lobatrienetriol from *L. pauciflorum* antibacterial activity was shown against this bacterium [329]. This discrepancy in results is most likely due to the fact that the tested samples were crude extracts, whereas the activity reported in the literature was for isolated compounds. Therefore, it is possible that metabolites found in soft corals act as antibacterial compounds only in their pure form, rather than in mixtures.

Beside their antibacterial activity against *B. subtilis*, the secondary metabolites of those soft corals have antibacterial activity against other Gram-positive bacteria. Diterpenoids like 16-hydroxycembra-1,3,7,11-tetraene from *Sarcophyton* act as inhibitor to *Staphylococcus aureus* [330]. The isolated compounds from *Lobophytum* had activity against the Gram-positive human pathogenic bacteria *Staphylococcus aureus*, *Staphylococcus epidermidis*, and *Streptococcus pneumoniae* [289, 331]. In addition, Yan et al. [332, 333] discovered that novel biscembranoids from *L. pauciflorum*, namely lobophytones Q, T, and U, exhibited potent inhibitory activity against *S. aureus* and *S. pneumoniae*.

6.3.3. Cytotoxicity of soft coral extracts against cancer cell lines

The in-vitro cytotoxicity assay with two cancer cell lines (HT29-colon cancer and PC3-human prostate cancer) was determined at two corresponding concentrations (0.05, 50 µg/mL) of extracts following the method described by dos Santos et al. [334]. Cytotoxicity (MTT) of the soft coral extracts is shown in Figure 49. According to this cytotoxicity result, a low concentration of soft coral extracts (0.05 µg/mL) had no effect on the viability of both cell lines. However, all extracts in the high concentration (50 µg/mL) exhibited the strong inhibitory activity against the tested cell lines, with the percentage of cell viability less than 3%. Therefore, soft coral extracts and their isolated compounds have the potential to be developed for medicinal purposes.

The cytotoxicity of the soft coral extract is the result of high abundance of their secondary metabolites, such as cembranes and terpenoids. New isolated cembrane diterpenoids from *S. crassocaule*, namely sarcrassins A-E and emblide exhibited strong cytotoxic activity against the KB cell lines [335]. In addition, the biscembranoids glaucumolides A and B demonstrated significant cytotoxicity against two cancer cell lines, namely promyelocytic leukemia (HL-60) and leukemic lymphoblasts (CCRF-CEM) [281]. Interestingly, not just cytotoxic activity of the isolated compound, but the crude extract of *Sarcophyton* species also showed activity against HT29 and PC3 with IC50 value bellow 50 µg/mL [336].

As a potential source of cembrane-type metabolites, *Lobophytum* species have also been reported in many study as corals with high cytotoxic activity against various cancer cell lines. Several novel cembranoids and cembranolides have demonstrated moderate activity against tumor and cancer cell lines including HeLa cell, human lung cancer cell (A549), melanoma cell (B16-F10), and murine macrophage cell (RAW 264.7) [331, 337]. In addition, the diterpene 3β,11-dihydroxy-24-methylene-9,11-secocholestan-5-en-9-one isolated from

Lobophytum compactum exhibited potent cytotoxicity against a lung cancer cell line (A549) with an IC50 value < 5 µM [338]. Beside of cembranes and terpenes, the sterol 24-methylenecholest-5-ene-1α,3-1α,11α-triol-1-acetate exhibited HepG2, while 24-methylenecholest-5-ene-3β-ol isolated from *L. crassum* exhibited cytotoxicity against HepG2, Hep-2 and HCT-116 [339]. Therefore, the crude extract of these investigated soft corals has the potential to provide compounds with activity against cancer cell lines.

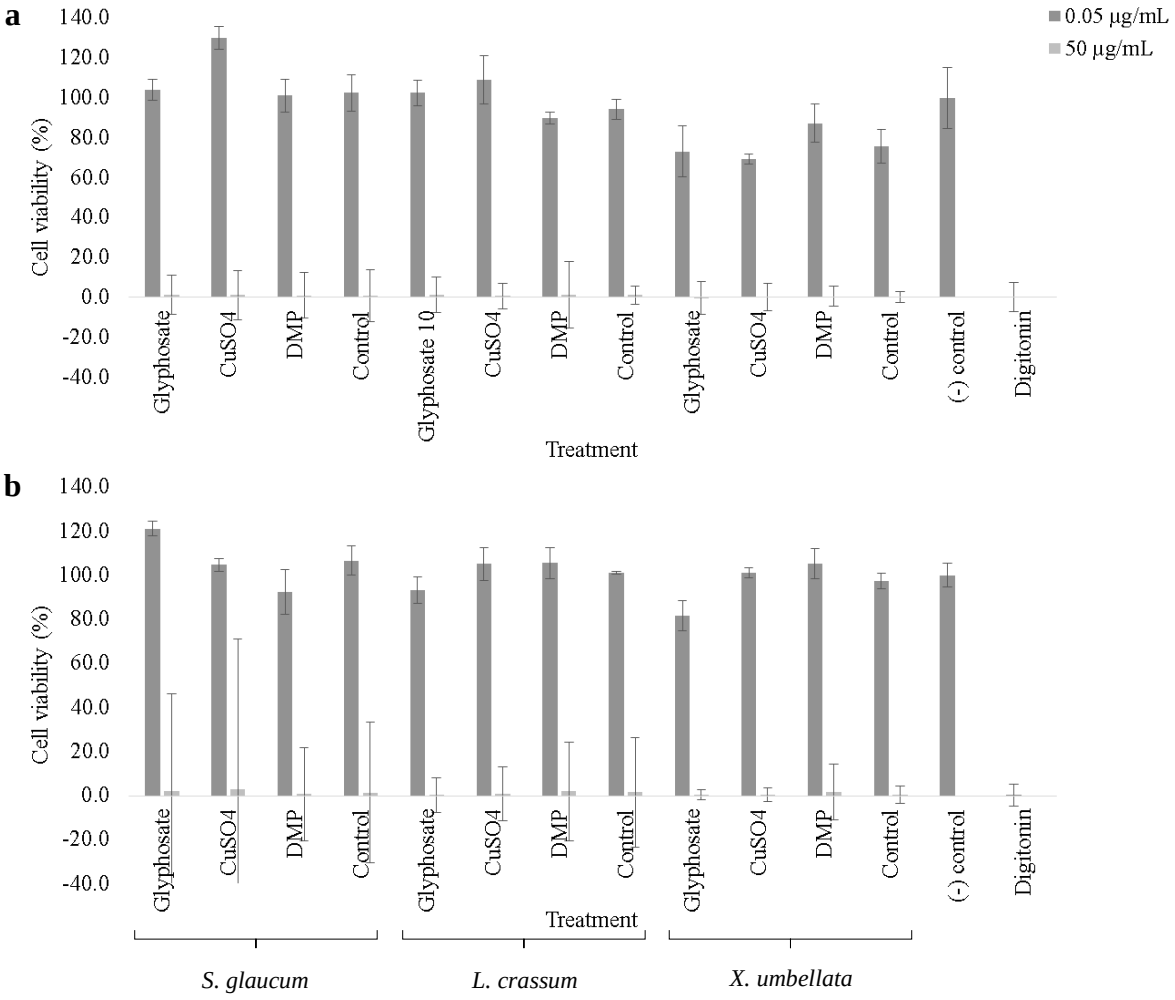

Figure 49 Cytotoxicity of soft coral extract for two cancer cell lines HT29 (a) and PC3 (b) (concentration 0.05 µg/mL and 50 µg/mL in DMSO, positive control chloramphenicol, negative control 1% DMSO), technical replicates = 2

6.4. Conclusion

This study evaluated the biological activity (antibacterial and cytotoxic) of methanolic extracts of three soft corals, *S. glaucum, L. crassum,* and *X. umbellata*. Two bacteria were chosen as representatives of Gram-negative and Gram-positive bacteria, namely *A. fischeri* and *B. subtilis*. All extracts of *S. glaucum* and *L. crassum* were found to be highly inhibitory against *A. fisheri*, particularly *L. crassum* elicited with glyphosate and $CuSO_4$. These extracts, even at the lowest tested concentration tested (50 g/mL) exhibited significant activity against

A. fischeri with an IC50 values less than 15 µg/mL. The antibacterial activity of the *L. crassum* extracts treated with these two elicitors is clearly derived from the secondary metabolites (diterpene content in the extracts; described at Chapter V) produced by the soft corals in response to these stressors, and not by the elicitors (glyphosate and $CuSO_4$). In contrast, *X. umbellata* exhibited negligible activity against both tested bacteria. Nonetheless, those extracts (500 g/mL) act as a bacteriostatic agent against *A. fischeri* for up to 9 hours. Some metabolites were not effective at inhibiting bacteria, but promoted their growth. Furthermore, to our knowledge, this is the first study documenting the antibacterial activity of soft corals against *A. fischeri*.

In comparison to *A. fischeri*, all extracts exhibited a lower activity against *B. subtilis*. In fact, natural products are typically more effective at inhibiting Gram-positive bacteria than Gram-negative bacteria, owing to Gram-negative bacteria having a double layer of cell membrane, which makes them more resistant. Notably, this phenomenon was not observed in this study. It is possible that the metabolites produced by soft corals in their capacity as marine organisms have specific defense mechanism against marine bacteria such as *A. fischeri*. Additionally, the cytotoxicity (MTT) of the soft coral extracts was active only at the highest tested concentration (50 µg/mL), which exhibited a high inhibitory activity against the tested cell lines, with a cell viability percentage less than 3%. Tests on isolated compounds may be required to substantiate this assertion.

VII. Effect of glyphosate on *Sarcophyton glaucum, Lobophytum crassum,* and *Xenia umbellata*

Abstract

Glyphosate-based herbicides (GBH) are the most used herbicides in the forestry and agricultural sectors. The widespread use of this herbicide may affect the aquatic organisms, including soft corals. However, there are not many studies reporting their effect on coral metabolites. Therefore, this study provides the first investigation regarding the effects of glyphosate on *S. glaucum*, *L. crassum*, and *X. umbellata*. The effects of glyphosate on soft corals were observed morphologically and chemically, i.e. color, tentacle behavior, density of zooxanthellae, and PSII efficiency, as well as the composition of secondary metabolites in soft corals. For five days, *S. glaucum*, *L. crassum*, and *X. umbellata* were exposed to various concentrations of glyphosate (1 g/L, 100 mg/L, 50 mg/L, 25 mg/L, 10 mg/L, and 5 mg/L, for *S. glaucum*, and four concentrations for two further corals. At high concentrations (1 g/L, 100 mg/L, and 50 mg/L), this herbicide was extremely toxic to soft corals, which was observed from the tentacle behavior and color of the polyp. Similarly to the morphology result, two glyphosate concentrations (1 g/L and 100 mg/L) affected metabolite composition of the corals. These extracts were clearly distinct from other extracts in PCA score plot. In addition, the extracts of *L. crassum* and *X. umbellata* treated with 50 mg/L were also separated from other extracts. In general, fatty acids were tentatively assigned as the metabolites responsible for group segregation in ^{1}H-NMR-PCA and LC-MS-PCA. Additionally, some diterpenes were detected as metabolites responsible for the separation of *L. crassum* extracts. The presence of diterpenes in soft coral species could be associated with their antibacterial activity. Extracts of *L. crassum* treated with 50 mg/L of glyphosate exhibited extremely strong activity against *A. fischeri*. Furthermore, according to MALDI-MSI result, glyphosate affected the spatial distribution of zooxanthellae pigments (canthaxanthin and diatoxanthin) within corals tissue. These pigments were detected at extremely low concentrations.

7.1. Introduction

In recent years, there has been increasing studies and concern about the pollutants and their effect in marine ecosystems, especially on their biota. Numerous pollutants have been discovered in the marine environment worldwide i.e. herbicides, which were detected in the water as a wide spectrum of pesticides [199, 340]. Glyphosate-based herbicides (GBH) are the most used herbicides in the forestry and agricultural sectors [341, 342]. Chemically, glyphosate or *N*-(phosphonomethyl)glycine is an organic derivative substance in phosphonomethyl glycine group [343]. This substance is a nonvolatile compound that appears as a white, odorless crystalline solid and contains one basic amino group and three

ionizable acidic sites [344]. The following table summarizes the chemical composition and physical properties of glyphosate.

Table 10 Physical and chemical properties of glyphosate

CAS number	1071-83-6
Molecular formula	$C_3H_8NO_5P$
Chemical structure	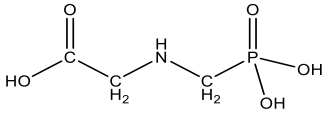
IUPAC name	N-(phosphonomethyl) glycine
Molecular weight (g/mol)	169.07
Water solubility	10.000 – 15.700 at 25 ºC
Melting point	200 – 230 ºC
Octanol-water coeff. (Kow)	-4.59 – -1.70
Half life of glyphosate	7 – 142 days

The application of glyphosate in agricultural and forestry fields has been reported to range between 0.9 and 4.27 kg acid equivalents (a.e.)/ha [345]. In several countries, including Australia, Canada, the United States, France, and Germany, this herbicide has been detected in high concentrations (up to to 5.4 mg/L) in the water column [198, 199, 204, 346-349]. In addition, a study conducted by Annett et al. [350] revealed that glyphosate contamination hotspots exist in South America, Europe, East and South Asia (Figure 50). The high usage of glyphosate leads to the increasing concentration of this substance in the environment, particularly the aquatic environment [198, 199, 204, 346]. Moreover, due to the broad spectrum of applications of glyphosate and its relatively long half-life (T½) in water (7-315 days, most commonly 45-60 days), this substance will remain persistent in coastal waters [351, 352].

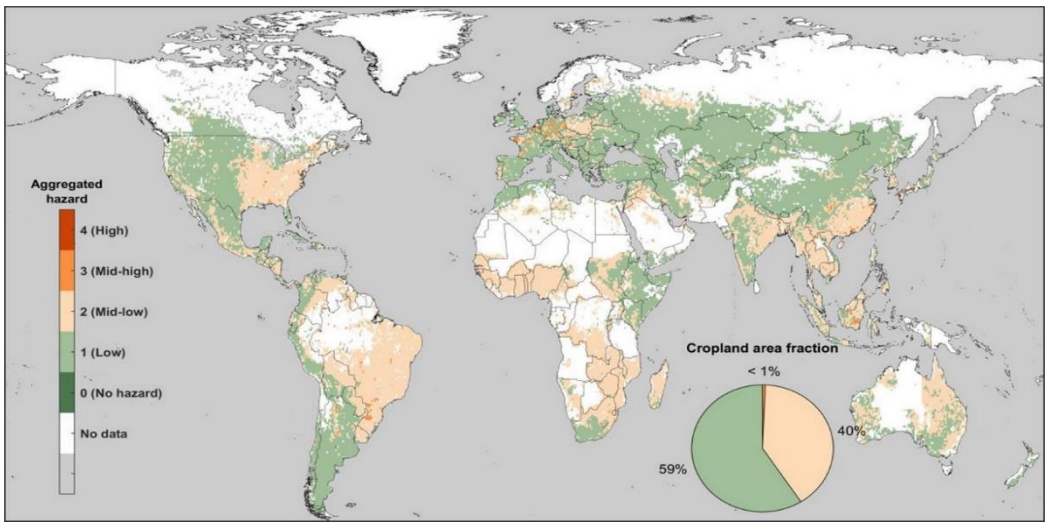

Figure 50 Geographic distribution of glyphosate and aminomethylphosphonic acid [350]

The persistence of glyphosate results in the production of its by-product such as aminomethylphosphonic acid (AMPA), which is toxic to aquatic organisms [345, 353]. However, only a few studies have been conducted to determine the precise concentration of these substances in the marine environment, for a variety of reasons, including analytical

difficulties, low molecular masses, ionic properties, and glyphosate's solubility in water [200, 348, 354]. Nevertheless, some pilot studies on the degradation of glyphosate in seawater have been conducted [352, 355].

The widespread use of glyphosate raises concerns about the chemical's adverse effect on aquatic organisms. The side effects of glyphosate and its derivate have been reported on aquatic organisms, including microalgae and diatoms, crustaceans, molluscs, amphibians [201, 356-365], and fishes [366-368]. On microalgae and other photosynthetic organisms in aquatic organism, this substance acts as a glycine analogue, inhibiting the shikimate pathway enzyme 5-enolpyruvyl-shikimate-3-phosphate synthase (EPSPS) [369-372]. Furthermore, due to the widespread use of glyphosate, this herbicide represent a hazard potential to polyp organisms such as corals. However, the effects of this substance on corals have received far less attention. One study in hard coral by Amid et al. (2018) revealed that the combination of glyphosate and elevated temperature caused the bleaching, including proportional loss in chlorophyll *a* and zooxanthellae of the branched coral *Acropora formosa* [181]. However, no study on soft coral has been conducted to date. To address this question, we investigated the effect of glyphosate at various concentrations on three species of soft coral. To our knowledge, this is the first study so far to investigate effects of glyphosate on soft corals.

7.2. Experimental

According to the findings in Chapter V, glyphosate at a concentration of 10 mg/L has no significant effect on the morphology and metabolites of soft corals, despite the fact that this concentration is much higher than the glyphosate concentrations detected in the marine environment (145 ng/L-5.4 mg/L) [196-204]. Therefore, we conducted this experiment to determine the maximum glyphosate tolerance of soft corals, as well as the changes in soft coral metabolites. *Sarcophyton glaucum*, *Lobophytum crassum*, and *Xenia umbellata* were investigated in this experiment. Six different concentrations of glyphosate (1 g/L, 100 mg/L, 50 mg/L, 25 mg/L, 10 mg/L, and 5 mg/L) were tested on *S. glaucum*, along with a control (no glyphosate exposure). However, due to limited coral material, *L. crassum* and *X. umbellata* were treated only with four concentrations of glyphosate (50 mg/L, 25 mg/L, 10 mg/L, and 5 mg/L). The experiments are described in detail in Chapter III.

7.3. Result and discussion

7.3.1. Physical effects of glyphosate on soft corals

Herein, in order to determine the physical effect of glyphosate on soft corals, their morphology including color, tentacle retraction, and the pumping rate of *Xenia umbellata*'s tentacles was observed. Additionally, the efficiency of Photosystem II (PSII) and the density of zooxanthellae cells were determined to ascertain the effect of this herbicide on soft coral symbionts. Daily observations of soft coral morphology were performed during a five-day exposure to glyphosate. Further, the following sections discusses the result regarding physical effects of glyphosate on three investigated soft coral species.

a. Morphology of soft corals before and after glyphosate exposure

The morphology of soft corals, specifically the color of the polyp, the behavior of the tentacles, and the polyp integrity, are the primary indicators of stress on corals. The coral retracts its tentacles as response to unfavorable environmental and stressful conditions [373], and the pale color of coral polyps is related to soft coral bleaching [92, 105, 184]. Therefore, these aspects are appropriate for observing the effect of stressors on the morphology of corals, especially for *S. glaucum* and *L. crassum*.

In addition, the stress of soft coral *Xenia umbellata* can be distinguished by its tentacle's pulsating rhythm. In the unfavorable condition, i.e. pollution in the water, they will reduce the pulsation of the tentacles to minimize pollutant intake and to maintain the body's osmoregulation [87]. Therefore, the pulsating rate of the tentacle of *X. umbellata* was quantified during this investigation (Figure 52). The morphology (color and tentacle behavior) of all soft corals after treated with various concentrations of glyphosate are shown in the Appendix 11. In addition, Figure 51 depicts the morphology of a representative soft coral (*S. glaucum*) after glyphosate exposure.

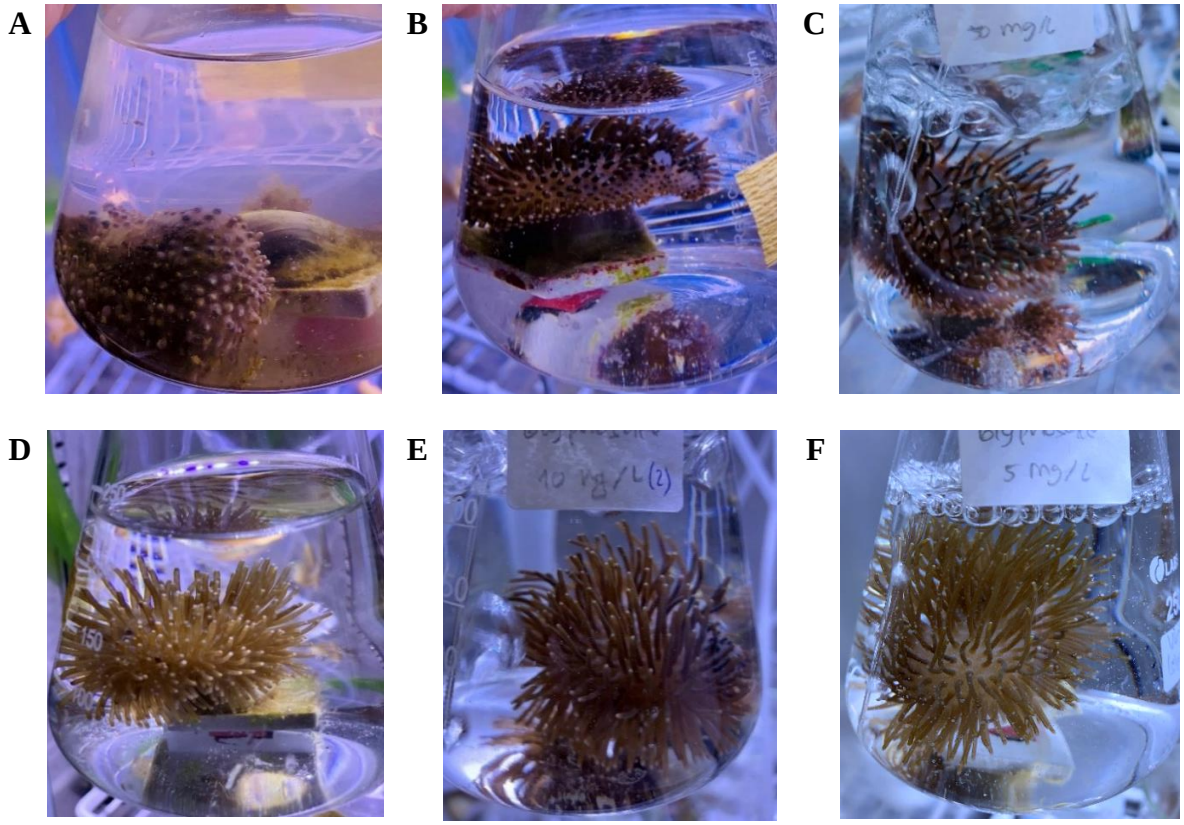

Figure 51 Morphology of *Sarcophyton glaucum* after treated with glyphosate in different concentration; A (1 g/L), B (100 mg/L), C (50 mg/L), D (25 mg/L), E (10 mg/L), F (5 mg/L)

The highest tested concentration in this experiment (1 g/L) was very toxic to *S. glaucum*. After two days of exposure to this concentration of glyphosate, *S. glaucum* lost its body integrity and died. At a concentration of 100 mg/L, severe stress was observed in this soft coral species, most notably in the major retraction of tentacles. In addition, an interesting

phenomenon was observed in the color of *S. glaucum*, which changed to a dark brown hue rather than fading. Further, after exposure to 50 mg/L of glyphosate, the tentacles of all investigated species were severely retracted (contracted for *X. umbellata*'s tentacles). In addition, the color on the top of *S. glaucum* umbrella became greenish. This phenomenon was observed only in *S. glaucum*, whereas the color of *L. crassum* was unaffected by the treatments.

In contrast to the three high concentrations described above, 25 mg/L, 10 mg/L, and 5 mg/L glyphosate had no significant effect on *S. glaucum* and *X. umbellata*, but did cause slight tentacle retraction in *L. crassum*. Moreover, the morphology of the three investigated soft corals after exposure to glyphosate at concentrations of 10 mg/L and 5 mg/L exhibited similar behavior to control coral (without glyphosate exposure), which is characterized by long expandable tentacles and a brown color. Nevertheless, there were some slight color changes in comparison to the control, e.g. the intensity of brown color in control coral was stronger than in the corals treated with both concentrations of glyphosate, respectively. Additionally, an interesting response was observed on *X. umbellata*, i.e. the tentacle behavior (color and their expansion) was normal and very similar to the control at lower concentration (<50 mg/L). Therefore, we could conclude that this species is most likely resistant to glyphosate.

As mentioned previously, the morphology changes of soft corals are associated with their stress response [218]. As a defense mechanism to water pollution (e.g. glyphosate), soft corals retract their tentacles to avoid absorbing toxic chemicals from the water column [87, 219]. The stress to the zooxanthellae which occurred during the exposure to glyphosate is probably due to the effect of this substance on their shikimic pathway. Glyphosate disrupts the shikimic acid pathway by inhibiting the enzyme 5-enolpyruvylshikimate-3-phosphate (EPSP) synthase, resulting in decreased levels of aromatic amino acids, which are required for protein synthesis and growth of algae/microalgae [374, 375]. As a result, some zooxanthellae may die and be expelled from the bodies of the host.

Furthermore, the color changes on soft coral tentacles and umbrellae were related to their symbiont zooxanthellae, as the brown color of soft corals is primarily due to pigments produced by this diatoms, e.g. carotenoids [95, 99]. In fact, glyphosate has an indirect effect on the decreasing of carotenoids contents in zooxanthellae. This herbicide influences photosynthetic processes which could be linked to glyphosate-induced reductions of plastoquinone (PQ) biosynthesis [376, 377] and chlorophyll concentrations [378]. Reducing of PQ biosynthesis leads to decreased carotenoid and xanthophyll levels in cells, because PQ acts as a cofactor for phytoene and ζ-carotene desaturase during carotenoid synthesis [379].

Moreover, glyphosate was proposed to interfere with photosynthesis by increasing ROS (reactive oxygen species) production in the mitochondria as a result of its inhibitory effect on the respiratory electron transport chain [208]. Once produced in the mitochondria, ROS enter the chloroplast, where they continue to cause oxidative damage to the photosynthesis

apparatus [208, 380, 381]. This could be an explanation for the intense brown and greenish color on the soft coral after exposure to glyphosate at concentrations of 100 mg/L and 50 mg/L, respectively. This intriguing phenomenon was probably caused by zooxanthellae responses to the high ROS level, which further leads to pigment (xanthophylls) production. These pigments contribute to ROS scavenging in their cells [382]. As a result, the concentration of xanthophylls in zooxanthellae increased, resulting in the dark brown coloration of their host body (umbrella and tentacles). The greenish coloration observed on soft coral treated with 50 mg/L glyphosate is most likely due to oxidative damage of the chloroplast and photosynthetic apparatus caused by ROS.

As a conclusion, an adverse effect of glyphosate was observed only at very "unnaturally" high experimental concentrations, whereas at low tested concentrations, the physiological properties of treated soft corals were comparable to control samples. All concentrations tested in this experiment are magnitudes higher than those detected in the marine environment (145 ng/L to 5.4 mg/L). However, considering that the duration of the experiment carried out in this study was only 5 days, this high concentration could be extremely harmful to soft corals within long-term exposure of glyphosate. Therefore, it is necessary to conduct additional research on glyphosate exposure over a long period of time, or minimum during half-life time of glyphosate persistence in the sea water.

b. Pulsation rate of Xenia umbellata tentacles before and after glyphosate exposure

To quantify the pulsation rate, five randomly chosen tentacles from each individual coral were counted manually. The pulsation rate of *Xenia umbellata*'s tentacles is shown in the Figure 52. In general, after exposure to glyphosate, the pulsating rate of *X. umbellata* was decreased. At the higher tested concentrations (50 mg/L and 25 mg/L), a significant decrease (P value <0.0001; Appendix 16) in tentacles pulsating up to 30% less was observed, while it was only slightly decreased after exposured to glyphosate at a concentration of 10 mg/mL. Interestingly, the pulsation rate after exposure to 5 mg/L glyphosate was similar to the control (with a very slight reduction of less than 5%). Therefore, at this concentration glyphosate has a negligible effect on *X. umbellata* tentacles (siphonozooids), as no significant difference in comparison to the control occurs.

The decrease in the pulsation rate of *X. umbellata* after exposure to high concentrations of glyphosate (50 mg/L and 25 mg/L), was the reaction of this soft coral to avoid ingesting toxic materials from the water column. Apart from the effect on the corals themselves, glyphosate is predicted to have an effect on their endosymbiont, zooxanthellae, which further affect the movement of their tentacles. The pulsation rate of the xeniid tentacle is related to zooxanthellae photosynthesis products [87]. During photosynthesis, zooxanthellae synthesize organic material to provide energy to their host [383, 384]. However, during stress condition, soft corals expel zooxanthellae, resulting in a decrease in organic matter and energy production on its body. This decrease is associated with the host corals' diminished energy

uptake [385]. As a result, the movement of coral tentacles decreased, as this movement requires a significant amount of energy [87]. In addition, for all organisms that host endosymbiotic zooxanthellae, particularly corals, movement of the holobiont may reduce their susceptibility to widespread physiological stress responses, such as zooxanthellae loss and further coral bleaching [99].

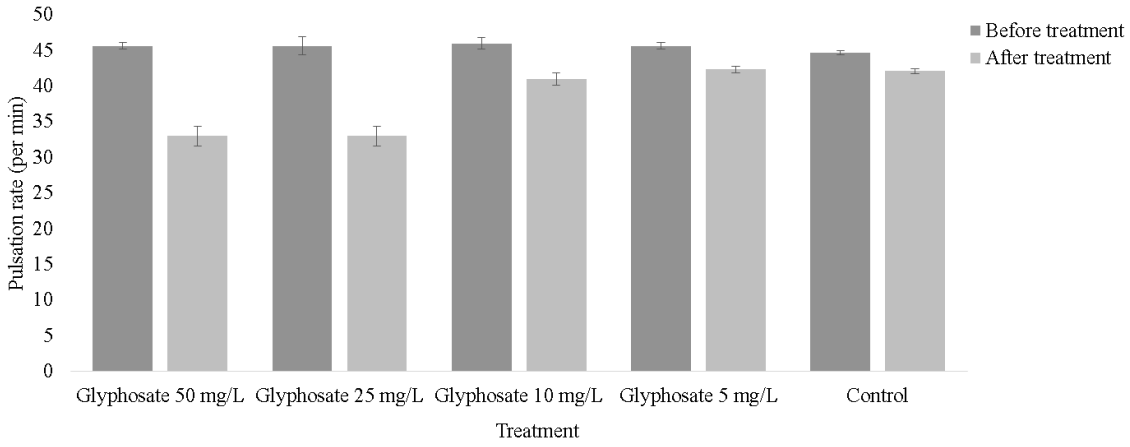

Figure 52 Pulsation rate of *Xenia umbellata*'s tentacles before and after exposure to glyphosate; statistical analysis by using Dunnett's multiple comparisons test is shown in Appendix 16

c. PSII efficiency of the zooxanthellae before and after treatments

PAM fluorometry has been extensively used to understand and monitor the effects of thermal irradiance damage and herbicides effects on the photosystem II (PSII) of photosynthetic organisms [95, 386-388]. In this study, the PSII efficiency was measured to investigate the effect of the herbicide glyphosate on three investigated soft corals. The PSII efficiency of the zooxanthellae inside of the soft coral after glyphosate exposure is shown in Figure 53.

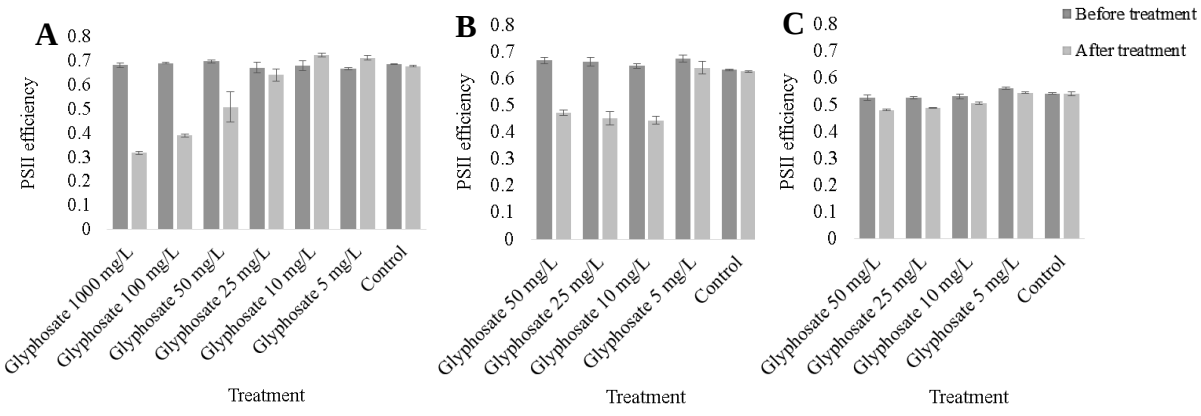

Figure 53 Photosystem II efficiency of soft coral *Sarcophyton glaucum* (A), *Lobophytum crassum* (B) and *Xenia umbellata* (C) containing zooxanthellae before and after exposure to glyphosate; statistical analysis (significance difference) by using Dunnett's multiple comparisons test is shown in Appendix 16

Similar to other analysis, glyphosate at higher concentration caused the significant decrease of PSII of corals and/or zooxanthellae (P value <0.0001; Appendix 16). Interestingly, PSII efficiency after exposure to glyphosate varied between the three

investigated species. For *S. glaucum*, PSII efficiency was concentration dependend significantly decreased after exposure to glyphosate at concentrations of 1 g/L, 100 mg/L, and 50 mg/L, whereas it was just slightly decreased after exposure to glyphosate at a concentration of 25 mg/L. Surprisingly, after exposure to glyphosate at 10 mg/L and 5 mg/L, the PSII of zooxanthellae in *S. glaucum* was increased. This phenomenon occurred exclusively in *S. glaucum*.

On *L. crassum*, glyphosate concentrations ranging from 50 mg/L to 10 mg/L reduced the PSII efficiency of zooxanthellae, while no significant difference was observed in the sample treated with 5 mg/L glyphosate (Appendix 15). This is expected, as high concentrations have a significant negative effect on soft corals and their endosymbionts in comparison to low concentrations. In contrast to the two other soft corals, the PSII efficiency of zooxanthellae in *X. umbellata* was relatively stable during glyphosate exposure, with only minor changes. However, the PSII efficiency of zooxanthellae in this coral species was found in the relative low in comparison to other investigated soft corals. It could be related to the fact that this species harbors a distinct zooxanthellae, as described in Chapter II, *Symbiodinium glynnii* (shown at Table 3). This zooxanthellae species is referred to as a more stress-tolerant symbiont that contributes to the coral holobiont's resilience to the conditions that caused the bleaching in the first place [389-394].

There are two possible explanations for the decrease in PSII efficiency in this study: first, stress on soft coral, which results in zooxanthellae expulsion from the coral bodies; and second, damage to the zooxanthellae cell itself [225-227]. In the case of glyphosate exposure, this herbicide is proposed to induce overproduction of ROS (reactive oxygen species), resulting in oxidative damage to the photosynthesis apparatus [380, 381]. Second, the increase of ROS caused the expulsion of zooxanthellae by their host in order to alleviate the body's oxidative stress [155, 395-397]. Thus, the decrease in PSII efficiency is a result of both, the reduction of zooxanthellae cells and the deterioration of the photosynthesis apparatus, or ROS directly effect the polyp.

The explanation to the intriguing phenomenon of *S. glaucum*'s PSII efficiency which increased after treated with 10 mg/L glyphosate is most likely related to the glyphosate's phosphorus content. Glyphosate is a phosphor-based herbicide that can act as a fertilizer for zooxanthellae. As this phenomenon was found just in the *S. glaucum* samples, there is the probability that the zooxanthellae in this soft coral belong to the group of glyphosate-resistant organisms and have a way to break down glyphosate to phosphate. However, there is no evidence to support this assumption. Therefore, additional analysis and studies are required. Further, as a result from this experiment we conclude that zooxanthellae's stress response, particularly in terms of photosystem II efficiency, is species-specific, whether on soft corals or endosymbiont zooxanthellae. Although the inhibition of PSII on zooxanthellae is reversible [209, 398], high concentrations or chronic glyphosate exposure can result in the

breakdown of coral symbiosis (bleaching), decreased reproductive output, and mortality [385, 398, 399].

d. Density of zooxanthellae cells in the water column

Coral stress, which includes bleaching, is typically defined by the expulsion of symbiotic zooxanthellae from the coral's body into the water column (environment) [400, 401]. There is a possibility that the abundance of zooxanthellae in the water column is related to the expulsion of zooxanthellae from the soft coral body. Therefore, to determine the density of this single cell organism, we collected and quantified the zooxanthellae in the incubation water. The result of zooxanthellae densities is shown in Figure 54.

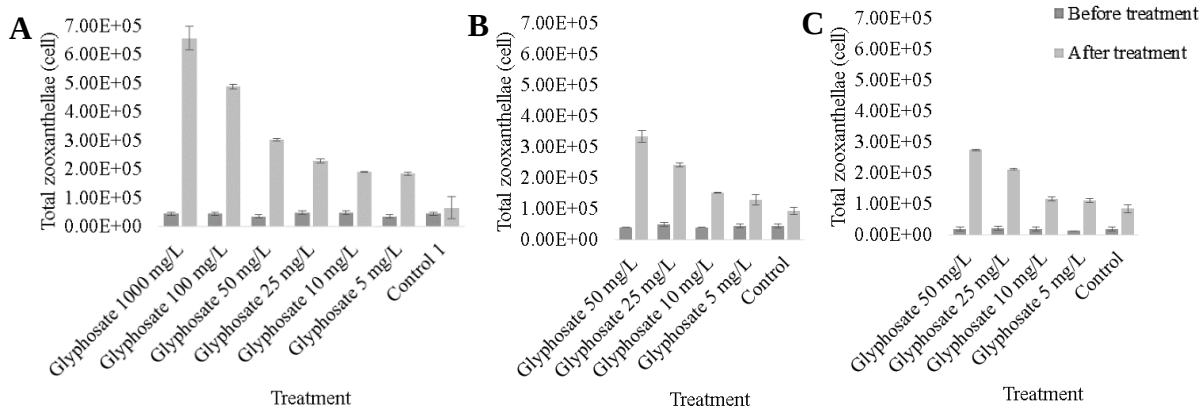

Figure 54 Zooxanthellae cell density in the water column before and after exposure to glyphosate; **A** (*Sarcophyton glaucum*), **B** (*Lobophytum crassum*), and **C** (*Xenia umbellata*); statistical analysis (significance difference) by using Dunnett's multiple comparisons test is shown in Appendix 16

According to the result above, glyphosate exposure significantly increased the density of zooxanthellae in the water column (P value <0.0001; Appendix 16), especially on the samples exposure to high concentration of glyphosate (1 g/L and 100 mg/L). The expulsion of zooxanthellae from soft corals confirmed all results described above. As a response to exposure of glyphosate, zooxanthellae expelled in concentration dependend manner their symbionts from the body. The reason for this was clearly stated above: glyphosate exposure indirectly increased the level of ROS in the soft coral body, which is toxic to soft corals. Thus, by expelling the symbiont (the source of excess ROS), the soft corals minimize their physiological damage [155, 397].

7.3.2. Metabolite profiling of soft corals treated with glyphosate

Apart from its effect on the morphology of soft corals *S. glaucum*, *L. crassum*, and *X. umbellata*, glyphosate may affect the composition of secondary metabolites in these organisms. Secondary metabolites in the soft corals act, e.g. as defense compounds, allowing corals to survive under stressful conditions [185, 186]. The exposure of soft corals to glyphosate is considered as stressor for this invertebrate because it altered their morphology (described in previous sections). Therefore, for further investigation, metabolite profiling of these three soft coral species is necessary. Two analytical techniques, namely ^{1}H-NMR and

LC-ESI-HRMS, were used to determine the effect of glyphosate on soft corals in term of their metabolites changing during elicitation process. The combination of these techniques can be a highly effective method for determining the secondary metabolome status of soft corals. In addition, it can be useful for monitoring corals and environmental-induced metabolic differences [56]. In this experiment, we observed changes in the metabolomes of *S. glaucum*, *L. crassum*, and *X.umbellata* after exposure to glyphosate at various concentrations (1 g/L, 100 mg/L, 50 mg/L, 25 mg/L, 10 mg/L, and 5 mg/L). To our knowledge, this is the first study to determine the effect of glyphosate on the soft corals metabolites.

a. ^{1}H-NMR analysis

^{1}H-NMR is an excellent technique for detection of changes in metabolites profiles of soft corals after exposure to stressors such as glyphosate. Due to the lack of significant differences in the ^{1}H-NMR profiles of extracts of *L. crassum* and *X. umbellata* treated with various concentrations of glyphosate (50 mg/L, 25 mg/L, 10 mg/L, and 5 mg/L), the metabolite profiling of soft corals by ^{1}H-NMR was limited to extracts of *S. glaucum*. The ^{1}H-NMR profiles of *S. glaucum* after treatment with eight different concentrations of glyphosate are depicted in Figure 55. For the comparison, the spectrum of pure glyphosate was stacked together with the spectra of extracts and highlighted in blue color.

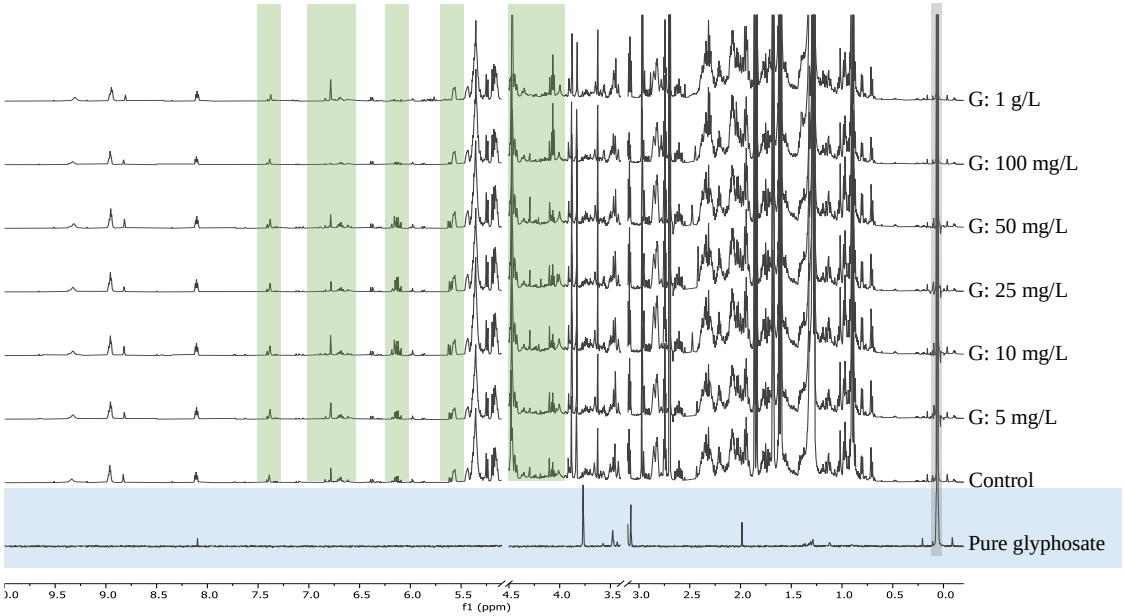

Figure 55 Stacked ^{1}H-NMR spectra (600 MHz, CD_3OD) of methanolic extracts of soft corals *Sarcophyton glaucum* after exposure to different concentrations of glyphosate. Solvent and elicitors signals are cut off (H_2O (4.50-5.10 ppm), CD_3OD (3.11-3.4 ppm), and the internal standard HMDS (δ=0.062 ppm) is highlighted in grey; G= Glyphosate

The ^{1}H-NMR spectra in Figure 55 display a diverse profile of *S. glaucum* extracts after exposure to different concentrations of glyphosate (highlighted in green color). After exposure to higher concentrations (1 g/L and 100 mg/L), the extracts of *S. glaucum* demonstrated a significant change in comparison to other extracts. Certain signals were absent in these extracts, including multiplets in the δ 6.06-6.20 ppm range, doublets of doublet signals in the δ 5.61 ppm range, and singlet in the δ 4.29 ppm. These signals

completely disappeared in the spectrum of extracts from coral treated with 1 g/L glyphosate, but were detected at extremely low intensities in the sample treated with 100 mg/L glyphosate. Additionally, one singlet in the δ 6.79 ppm region disappeared in the extract of *S. glaucum* treated with 100 mg/L. Apart from the loss of signals, some signals for example, in the area δ 4.05-4.11 ppm were detected at a high intensity in comparison to other extracts.

Furthermore, changes of ^{1}H-NMR profiles were noted in the remaining extracts. Two signals, a multiplet in the δ 6.06-6.20 ppm range and a doublet of a doublet signal in the 5.61 ppm range were detected at a higher intensity in extracts of *S. glaucum* exposed to glyphosate concentrations of 10 mg/L-50 mg/L. Out of the spectrum of *S. glaucum* extracts, ten major compounds responsible for the separation of glyphosate-treated extracts were tentatively assigned (Figure 57 and Table 11) based on NMR spectra and confirmed via 2D NMR analysis (HSQC) and database comparison. The changing of the signals described above is strongly correlated with the concentration of glyphosate exposure. This distinction was also apparent in multivariate data analysis, specifically in the PCA score plot (Figure 56.A). Extracts of *S. glaucum* treated with glyphosate at concentrations of 1 g/L and 100 mg/L were clearly separated from other extracts in the PC1 (35.8% variance). Fatty acids (**10**) are the primary components responsible for the separation of coral extracts treated with 100 mg/L. Along with fatty acids, sarcophytolol (**4**), sarcophytoxide (**3**), and ent-sarcophyolide E (**7**) were the metabolites responsible for separation in PC1. Sarcophine (**2**), a known cembranoid diterpene, and two unknown bins in the δ 2.69 and 2.71 ppm range were responsible for the separation of the control and extracts of soft coral treated with 25 mg/L of glyphosate. These unidentified bins are associated with a peak in the -CH_2 region, which belong to -CH_2 between two double bonds in polyunsaturated fatty acids. This indicates that these signals probably originate from the fatty acids in soft corals or their endosymbiont.

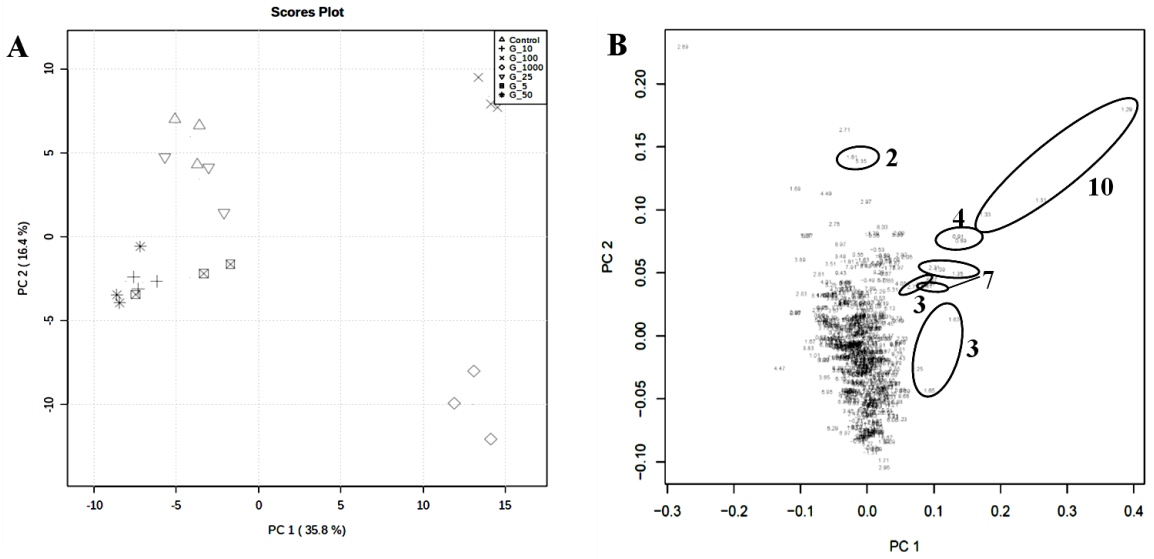

Note= Δ: Control, ◇: 1 g/L, ×: 100 mg/L, ✱: 50 mg/L, ∇: 25 mg/L, +: 10 mg/L, ⊠: 5 mg/L

Figure 56 PCA of ^{1}H-NMR of extracts from *Sarcophyton glaucum* exposed to different concentrations of glyphosate; scores plot (a) and loadings plot (b)

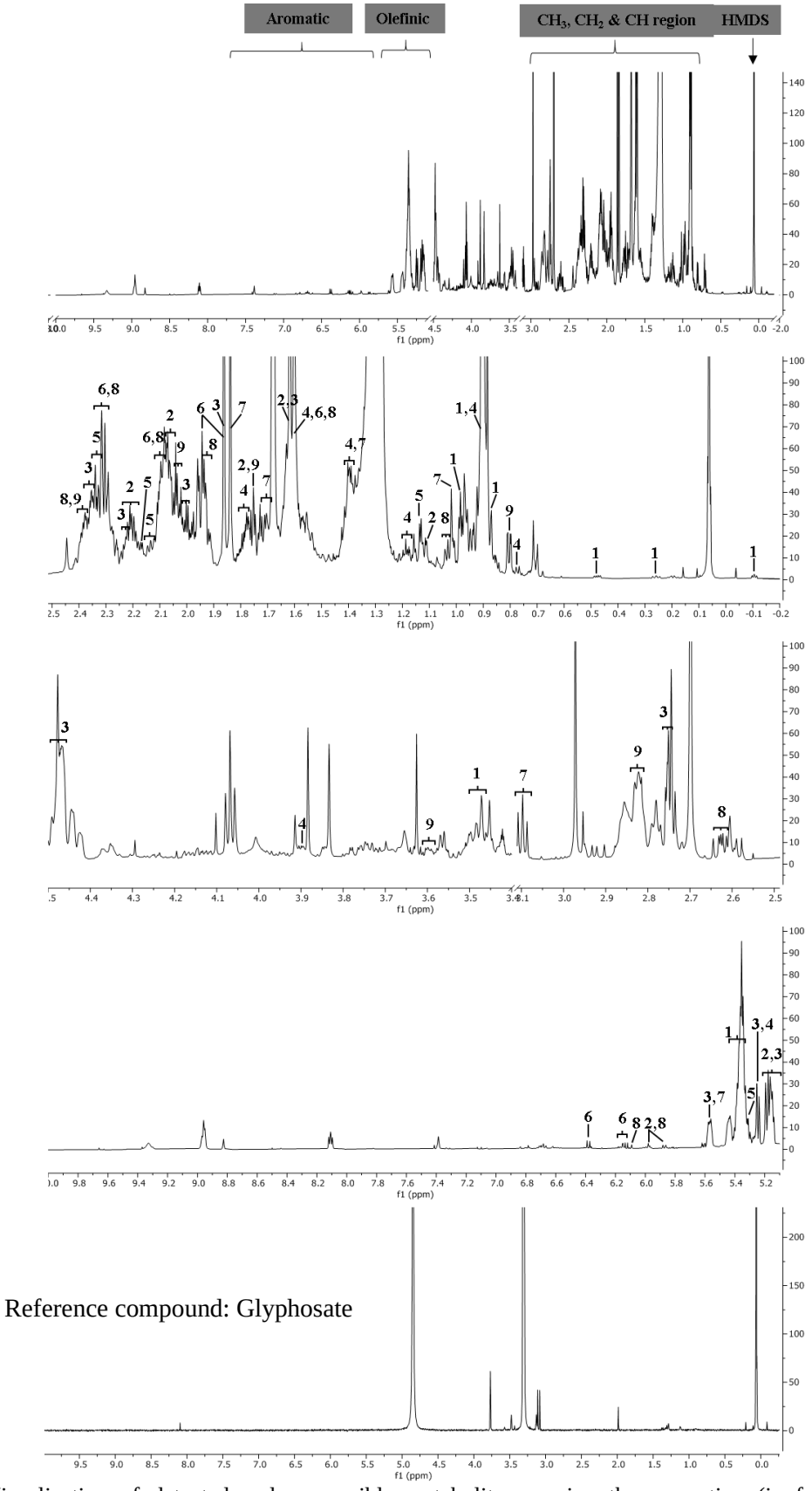

Figure 57 Visualization of detected and responsible metabolites causing the separation (in full ^{1}H-NMR spectrum) of *Sarcophyton glaucum* extract after exposure to glyphosate; numbers= number of tentative annotated compound listed in Table 10

Unfortunately, the visualized signals in Figure 55, which change after exposure to two high concentrations of glyphosate, were not detected in the loadings plot as responsible metabolites causing the segregation. In addition, some signals, such as the multiplets in area δ 6.06 and 6.20 ppm, the signals which changes during glyphosate exposure, as well as two additional signals at δ 5.61 and 4.29 ppm remain unknown. Unfortunately, due to the degradation of metabolites belonging to these signals, the 2D NMR measurement was not successful. Therefore, it is still an open question, and the elucidation of this metabolite is required. In comparison to other extracts, extracts of *S. glaucum* treated with 100 mg/L glyphosate contained significantly more fatty acids (Appendix 12). The increase of fatty acids in the coral's body is associated with the biological function of this metabolites as an energy source for soft corals [144, 402]. Corals require energy to survive in a stressful environment. Therefore, they increase the fatty acids production in order to survive.

Moreover, all of the metabolites that caused segregation in the PCA after glyphosate exposure to *S. glaucum* are marker metabolites (isolated metabolites) of this coral species. Regrettably, there is no evidence of changes in zooxanthellae metabolites during glyphosate-induced stress, despite the fact that glyphosate's primary effect is known to be on the soft coral endosymbiont (zooxanthellae) as a photosynthetic organism. This is probably because the concentration of zooxanthellae metabolites in the soft coral's extracts was extremely low, which causes the low detection in ^{1}H-NMR analysis. Nevertheless, by using a complementary techniques (e.g. LC-ESI-HRMS), the metabolites of zooxanthellae could be detected in the extract, as well as their spatial distribution within the soft coral tissue, using MS Imaging.

Table 11 Resonance tentative assignments of detected metabolites in the extracts of *Sarcophyton glaucum* after exposure to glyphosate with ^{1}H- and ^{1}H/^{13}C- NMR spectra (at 600 MHz; solvent methanol-d4)

Metabolite	Position	^{1}H, δ [ppm] multiplicity	^{13}C δ [ppm] HSQC
Gorgosterol (**1**) 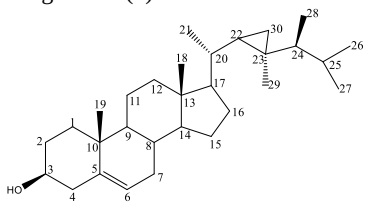	3	3.47 m	72.7
	6	5.37 m	129.3
	21	1.03 s	21.7
	22	0.26 m	30.8
	26	0.98 s	22.7
	27	0.87 s	20.9
	29	0.90	14.5
	30	0.48 dd	*n.d.*
		-0.11 t	
Sarcophine (**2**) 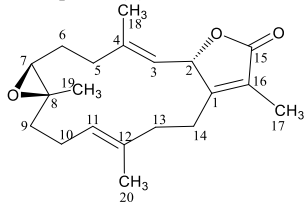	3	5.35 dd	122.6
	5	2.19 m	35.9
	6	2.23 m	24.1
	7	2.75	64.1
	11	5.35	122.6
	16	1.11 d	25.9
	18	1.62 s	15.3
	19	1.26 s	16.7
Sarcophytoxide (**3**) † 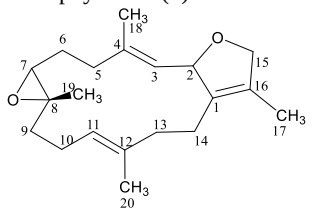	2	5.44	86.6
	3	5.25	126.3
	5	2.19 m	35.9
	6	2.23 m	26.1
	7	2.75	64.1
	16	4.46 m	79.1
	18	1.62 s	15.3
	19	1.26 s	16.7
	20	1.86 br s	18.1

Sarcophytolol (**4**) 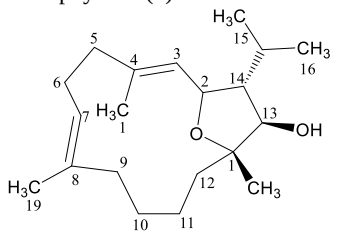	1	1.40 m	30.2
	2	4.50 dd	74.8
	3	5.34[b] d	122.6
	7	5.16 dd	124.8
	11	1.78 m	28.7
	14	3.89 d	70.4
	15	1.18 m	30.0
	17	0.77 d	20.2
	19	1.60 s	16.2
	20	0.90 s	14.5
Glaucumolide A/B (**5**) 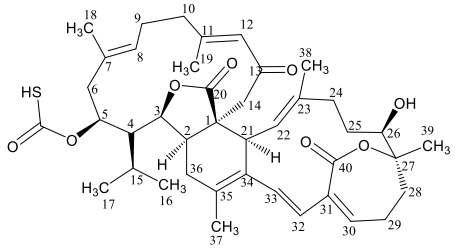	2	2.35 m	38.6
	6	2.22 m 2.14 m	43.0
	8	5.24 dd	126.8
	12	5.87 dd	122.4
	15	2.23 m	24.1
	17	1.11 d	26.1
	19	2.15 s	30.7
	22	5.16[c]	124.9
	37	1.84 s	20.9
Sarglaucol (**6**) 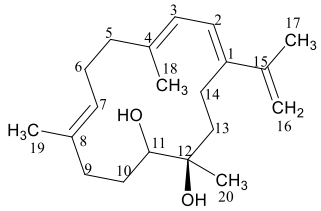	2	6.38 d	120.0
	3	6,14 d	117.6
	5	2.23 m 2.00 m	24.2
	7	5.18 t	127.4
	9	2.19 m	35.9
	16	5.16[c] s	124.9
	17	1.94 s	24.4
	18	1.62 s	15.8
	19	1.60[c] s	16.2
Ent-Sarcophyolide E (**7**) 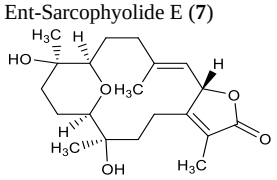	2	5.57 d	85.3
	3	4.96	126.3
	5	2.19[b]	35.9
	10	1.39 m 1.70 m	28.8
	11	3.21 d	75.8
	13	1.70 m 1.35[a] m	27.1
	17	1.68[e] s	10.2
	18	1.84 s	17.8
	19	1.02 s	19.9
Sarcophytol A (**8**) 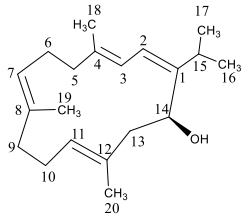	2	4.95 m	*n.d.*
	3	2.19 m 2.37 m	35.9
	5	5.17[bc] m	124.8
	6	2.08 m	28.1
	7	1.93 m	39.5
	13	5.97 d	125.5
	14	6.13 d	117.3
	17	1.11 d	25.9
	18	1.60 s	15.6
	20	1.71 s	15.2
Bisglaucumlide (**9**) 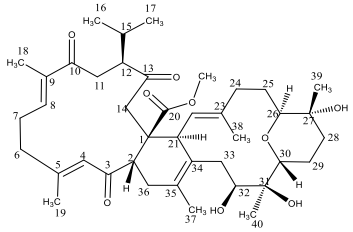	2	3.90	49.3
	4	5.96[b] d	122.4
	11	2.05	39.9
	16	0.81 d	18.0
	17	0.99 d	22.7
	18	1.75 s	17.8
	24	2.34[d]	24.6
	30	3.60 m	70.3
	36	2.83 br d	26.6
	38	1.86 s	18.1
	40	1.16 s	17.2
Fatty acid (**10**) Arachdonic acid (AHA), eicosapentaenoic acid (EPA), docosahexaenoid acid	$(CH_2$-$)n$ CH_3 terminal CH-5/6-8/9-11/12-14/15-17/18	1.29-1.31 0.90 5.32-5.40 m	30.8 14.5

[a] Corresponds to overlapping NMR signals in fatty acids signal
[b] Corresponds to overlapping NMR signals in 2
[c] Corresponds to overlapping NMR signals in 3
[d] Corresponds to overlapping NMR signals in 5
[e] Corresponds to overlapping NMR signals in 7

b. LC-ESI-HRMS analysis

To address the issue regarding the ^{1}H-NMR analysis, which is unable to detect some metabolites due to their low concentration in the extracts, LC-ESI-HRMS analysis in positive ion mode was performed. The high sensitivity of this method provides the possibility to detect extremely low concentrations of compounds with respect to their ionization properties [403]. In this experiment, the chemical constituents of three soft coral species exposed to eight different glyphosate concentrations were separated using reversed-phase UHPLC, resulting in the representative total ion chromatograms shown in Figure 58. Furthermore, mass spectral fragmentation studies using data-dependent HR-MS/MS experiments were performed for the peak assignment. In total, 75 metabolites responsible for the separation of group in PCA score plot have been tentatively annotated (Table 12) by using MS/MS fragmentation data and further comparison to the literatures and data bases.

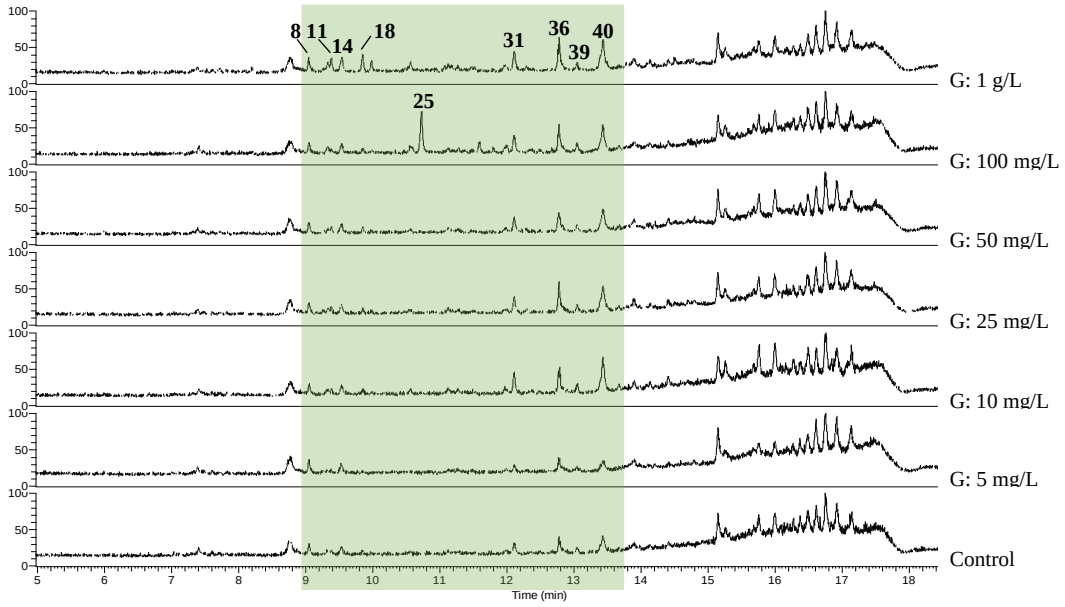

Figure 58 Total Ion Chromatogram (TICs, m/z 100-1500) in positive ion mode of *Sarcophyton glaucum* extracts after exposure to different concentrations of glyphosate

Similar to ^{1}H-NMR profiles result, chromatograms of *S. glaucum* extracts exposed to glyphosate at concentrations of 1 g/L and 100 mg/L displayed distinct profiles in comparison to other extracts (highlighted with green color). Certain metabolites with retention time of 9-11 minutes appeared to be more intense in *S. glaucum* extracts treated with 1 g/L. In addition, a single intense peak with a retention time of 10.72 min was observed in extracts of *S. glaucum* exposed to 100 mg/L.

Table 12 Metabolites annotated (tentatively) of metabolites responsible for separation of extracts from soft coral *Sarcophyton glaucum*, *Lobophytum crassum*, and *Xenia umbellata* after exposure to glyphosate; via HR-LC-MS^2 in positive ionization mode

Comp	$[M+H]^+$ *m/z*	t_R (min)	Molecular formula	Δ (ppm)	MS^2 product ions, *m/z* (elemental composition, rel. intensity [%])	Identification of class/compound	Species
P.1	272.2156	6.50	$C_{15}H_{26}NO_2$	7.951	224.1277 ($C_{13}H_{22}NO_2$, 3), 196.1257 ($C_{11}H_{18}NO_2$, **100**), 163.1187 ($C_{11}H_{15}O$, 7), 149.0966 ($C_{10}H_{13}O$, 13), 118.0651 (C_9H_{10}, 10)	Amino alcohol	S
P.2	218.2111	6.76	$C_{12}H_{27}NO_2$	-1.716	200.2012 ($C_{12}H_{25}NO$, **100**), 177.0912 ($C_{11}H_{13}O_2$, 15), 123.0808 ($C_8H_{11}O$, 7), 106.0761 (C_8H_{10}, 34), 88.0765 ($C_4H_{10}NO$, 32)	Amino alcohol	X
P.3	251.2007	6.84	$C_{16}H_{27}O_2$	-0.400	233.1529 ($C_{15}H_{21}O_2$, 4), 195.1223 ($C_{12}H_{19}O_2$, **100**), 177.1117 ($C_{12}H_{17}O$, 33), 133.0856 (C_9H_9O, 44), 117.0906 (C_9H_9, 2)	Sesquiterpene	S
P.4	274.2170	8.22	$C_{18}H_{28}NO$ $[M+NH_4]^+$	-1.390	257.1909 ($C_{18}H_{25}O$, **100**), 229.1587 ($C_{16}H_{21}O$, 28), 215.1436 ($C_{15}H_{19}O$, 15), 161.0962 ($C_{11}H_{13}O$, 15), 133.1007 ($C_{10}H_{13}$, 4)	Sesquiterpene	S, L
P.5	192.1381	8.43	$C_{12}H_{18}NO$	-1.201	174.1272 ($C_{12}H_{16}N$, 7), 146.1039 ($C_{10}H_{12}N$, 6), 119.0889 (C_9H_{11}, **100**)	1-(Pyridin-2-yl)heptan-1-one	S, L, X
P.6	328.2862	8.92	$C_{19}H_{38}NO_3$	2.740	310.2832 ($C_{19}H_{36}NO_2$, 1), 268.2629 ($C_{17}H_{34}NO$, **100**), 210.1996 ($C_{14}H_{26}O$, 11), 134.1190 ($C_{10}H_{14}$, 1)	Ceramide	L
P.7	219.1387	9.05	$C_{14}H_{19}O_2$	0.892	201.1636 ($C_{14}H_{17}O$, **100**), 175.1179 ($C_{12}H_{15}O$, 44), 161.0920 ($C_{11}H_{13}O$, 44), 121.1012 (C_9H_{13}, 15), 107.0855 (C_8H_{11}, 34)	Sesquiterpene	S, L, X
P.8	357.2068	9.13	$C_{22}H_{29}O_4$	0.601	339.1923 ($C_{22}H_{27}O_3$, **100**), 327.1924 ($C_{21}H_{27}O_3$, 47), 299.1615 ($C_{19}H_{23}O_3$, 19), 217.1379 ($C_{14}H_{17}O_2$, 1)	Diterpenoid	L
P.9	376.2480	9.19	$C_{22}H_{34}NO_4$	-2.379	358.2766 ($C_{22}H_{32}NO_3$, **100**), 340.2652 ($C_{22}H_{30}NO_2$, 32), 312.2892 ($C_{20}H_{26}NO_2$, 48), 295.1620 ($C_{20}H_{23}O_2$, 15), 241.1591 ($C_{17}H_{21}O$, 11), 166.1223 ($C_{11}H_{18}O$, 13), 133.1006 ($C_{10}H_{13}$, 7)	Cembranoid	L
P.10	387.2177	9.22	$C_{23}H_{31}O_5$	-1.421	369.2105 ($C_{23}H_{29}O_4$, **100**), 351.3002 ($C_{23}H_{27}O_3$, 21), 289.1432 ($C_{18}H_{25}O_3$, 5), 275.1657 ($C_{17}H_{23}O_3$, 4), 157.0967 ($C_{12}H_{13}$, 2)	Diterpenoid	L, S
P.11	221.1531	9.37	$C_{14}H_{21}O_2$	-2.774	203.1426 ($C_{14}H_{19}O$, **100**), 193.1006 ($C_{12}H_{17}O_2$, 7), 179.1065 ($C_{11}H_{15}O_2$, 20), 165.0907 ($C_{10}H_{13}O_2$, 42), 109.1008 (C_8H_{13}, 12), 95.0854 (C_7H_{11}, 5)	Diacetylene	S
P.12	315.1952	9.39	$C_{20}H_{27}O_3$	-2.602	297.1829 ($C_{20}H_{25}O_2$, **100**), 254.1621 ($C_{18}H_{22}O$, 20), 189.1206 ($C_{13}H_{17}O$, 7), 163.1154 ($C_{11}H_{15}O$, 6), 135.0800 ($C_9H_{11}O$, 3), 109.0649 (C_7H_9O, 2)	Diterpene	S
P.13	299.1829	9.51	$C_{16}H_{27}O_5$	-4.260	298.1888 ($C_{16}H_{26}O_5$, 2), 280.1774 ($C_{16}H_{24}O_4$, **100**), 254.1619 ($C_{14}H_{22}O_4$, 29), 240.1461 ($C_{13}H_{20}O_4$, 18), 214.1307 ($C_{11}H_{18}O_4$, 8), 196.1203 ($C_{11}H_{16}O_3$, 7)	Sesquiterpene	L, X
P.14	360.2530	9.63	$C_{22}H_{34}NO_3$	-1.084	343.2265 ($C_{22}H_{31}O_3$, **100**), 325.2156 ($C_{22}H_{29}O_2$, 22), 283.1647 ($C_{19}H_{23}O_2$, 7), 165.0913 ($C_{11}H_{17}O$, 6)	Diterpene alkaloid	S, L
P.15	374.2692	9.71	$C_{23}H_{36}NO_3$	-2.326	356.2579 ($C_{23}H_{34}NO_2$, **100**), 329.2177 ($C_{21}H_{29}O_3$, 5), 311.2049 ($C_{21}H_{27}O_2$, 8), 283.1921 ($C_{19}H_{23}O_2$, 4)	Diterpene alkaloid	L
P.16	257.1860	9.76	$C_{16}H_{33}O_2$	1.733	256.2628 ($C_{16}H_{32}O_2$, 10), 239.1794 ($C_{16}H_{31}O$, 35), 228.1824 ($C_{14}H_{28}O_2$, 56), 214.1667 ($C_{13}H_{26}O_2$, 54), 200.1513 ($C_{12}H_{24}O_2$, **100**), 130.1221 ($C_8H_{18}O$, 12), 116.1071 ($C_7H_{16}O$, 26), 95.0853 (C_7H_{11}, 15)	Fatty acid	S
P.17	330.2997	9.84	$C_{19}H_{40}NO_3$	-1.213	312.2889 ($C_{19}H_{38}NO_2$, **100**), 294.2782 ($C_{19}H_{36}NO$, 5), 256.2437 ($C_{16}H_{32}O_2$, 5), 166.0995 ($C_{10}H_{14}O_2$, 1)	Fatty acid	L
P.18	235.1693	9.89	$C_{15}H_{23}O_2$	-2.152	217.1581 ($C_{15}H_{21}O$, **100**), 203.1419 ($C_{14}H_{19}O$, 83), 163.1112 ($C_{11}H_{15}O$, 22), 123.0851 ($C_8H_{11}O$, 7)	Sesquiterpene	S, X
P.19	397.2001	10.14	$C_{24}H_{29}O_5$	-3.521	379.1886 ($C_{24}H_{27}O_4$, **100**), 337.1768 ($C_{22}H_{25}O_3$, 3), 297.1856 ($C_{20}H_{25}O_2$, 7), 251.1799 ($C_{19}H_{23}$, 4), 209.1324 ($C_{16}H_{17}$, 3), 131.0848 ($C_{10}H_{11}$, 1)	Diterpenoid	L
P.20	341.2685	10.15	$C_{20}H_{37}O_4$	-2.016	341.2700 ($C_{20}H_{37}O_4$, 2), 323.2691 ($C_{20}H_{35}O_3$, 27), 283.2055 ($C_{20}H_{27}O$, **100**), 243.1744 ($C_{17}H_{23}O$, 13), 165.1270 ($C_{11}H_{17}O$, 9)	Diterpenoid	S, L
P.21	376.2480	10.32	$C_{22}H_{34}NO_4$	-2.379	358.2766 ($C_{22}H_{32}NO_3$, **100**), 340.2652 ($C_{22}H_{30}NO_2$, 8), 312.2092 ($C_{21}H_{28}O_2$, 48), 294.1986 ($C_{21}H_{26}O$, 15), 278.3473 ($C_{20}H_{22}O$, 2), 173.1021 ($C_{12}H_{14}O$, 1)	Cembranoid	L
P.22	374.3039	10.12	$C_{24}H_{40}NO_2$	1.806	356.3031 ($C_{24}H_{38}NO$, **100**), 332.2928 ($C_{22}H_{38}NO$, 67), 314.1824 ($C_{22}H_{34}O$, 75), 268.2182 ($C_{20}H_{28}$, 45), 214.1301 ($C_{16}H_{22}$, 5)	Diterpene alkaloid	X
P.23	335.2213	10.56	$C_{20}H_{31}O_4$	-2.791	317.2082 ($C_{20}H_{29}O_3$, **100**), 273.2161 ($C_{18}H_{25}O_2$, 22), 247.2027 ($C_{16}H_{23}O_2$, 97), 231.1708 ($C_{15}H_{19}O_2$, 1), 175.1487 ($C_{12}H_{15}O$, 1), 122.1374 ($C_8H_{10}O$, 1)	Diterpene	L
P.24	513.2084	10.90	$C_{26}H_{34}O_9Na$ $[M+Na]^+$	-2.209	453.1873 ($C_{24}H_{30}O_7Na$, **100**), 371.1844 ($C_{22}H_{27}O_5$, 42), 311.1638 ($C_{20}H_{23}O_3$, 3), 293.1533 ($C_{20}H_{23}O_2$, 1), 265.1584 ($C_{19}H_{21}O$, 1), 195.1168 ($C_{15}H_{15}$, 2)	Xeniolide O †	X
P.25	530.3323	11.06	$C_{27}H_{48}NO_9$	-1.142	512.3228 ($C_{27}H_{46}NO_8$, 1), 484.2909 ($C_{25}H_{42}NO_8$, 1), 389.2677 ($C_{24}H_{37}O_4$, **100**), 330.2797 ($C_{21}H_{30}O_3$, 1), 203.1790 ($C_{15}H_{23}$, 2)	Nitrogenous fatty acid	S, L

Comp	$[M+H]^+$ *m/z*	t_R (min)	Molecular formula	Δ (ppm)	MS^2 product ions, *m/z* (elemental composition, rel. intensity [%])	Identification of class/compound	Species
P.26	495.2232	11.22	$C_{25}H_{35}O_{10}$	0.356	439.1960 ($C_{22}H_{31}O_9$, 1), 354.1612 ($C_{18}H_{26}O_7$, **100**), 323.1483 ($C_{17}H_{23}O_6$, 12), 253.1070 ($C_{13}H_{17}O_5$, 10), 235.0960 ($C_{13}H_{15}O_4$, 5), 195.1011 ($C_{11}H_{15}O_3$, 7)	Diterpenoid	L
P.27	415.2109	11.33	$C_{24}H_{31}O_6$	-2.801	397.1988 ($C_{24}H_{29}O_5$, 1), 355.1891 ($C_{22}H_{27}O_4$, 27), 313.1787 ($C_{20}H_{25}O_3$, 16), 295.1682 ($C_{20}H_{23}O_2$, **100**), 277.1577 ($C_{20}H_{21}O$, 11), 207.1165 ($C_{16}H_{15}$, 3), 169.1007 ($C_{13}H_{13}$, 1)	Steroid	X
P.28	482.3763	11.45	$C_{28}H_{52}NO_5$	1.849	464.3702 ($C_{28}H_{50}NO_4$, 88), 405.3005 ($C_{25}H_{41}O_4$, **100**), 211.2162 ($C_{14}H_{27}O$, 13), 184.0732 ($C_9H_{12}O_4$, 10)	Betaine lipid	S, X
P.29	444.3629	11.54	$C_{25}H_{50}NO_5$	-4.491	426.3594 ($C_{25}H_{48}NO_4$, 12), 408.3288 ($C_{25}H_{46}NO_3$, 10), 368.3272 ($C_{23}H_{44}O_3$, **100**), 336.3053 ($C_{22}H_{40}O_2$, 31), 242.1669 ($C_{17}H_{22}O$, 3), 135.0495 ($C_9H_{11}O$, 1)	Nitrogenous fatty acid	S
P.30	345.2055	11.59	$C_{21}H_{29}O_4$	-0.046	327.2098 ($C_{21}H_{27}O_3$, **100**), 253.1900 ($C_{18}H_{21}O$, 9), 113.0916 ($C_7H_{13}O$, 5)	Cembranoid	S
P.31	433.2584	11.94	$C_{25}H_{37}O_6$	-1.418	416.2557 ($C_{25}H_{36}O_5$, 29), 397.2339 ($C_{25}H_{33}O_4$, **100**), 351.1979 ($C_{23}H_{27}O_3$, 11), 271.1623 ($C_{18}H_{23}O_2$, 13), 192.1118 ($C_{12}H_{16}O_2$, 55), 147.0799 ($C_{10}H_{11}O$, 21)	Diterpenoid	L
P.32	430.3878	12.32	$C_{25}H_{52}NO_4$	-4.263	412.3866 ($C_{25}H_{50}NO_3$, **100**), 398.3788 ($C_{25}H_{50}O_3$, 5), 311.2941 ($C_{19}H_{35}O_3$, 11), 285.2380 ($C_{17}H_{33}O_3$, 11), 219.1677 ($C_{15}H_{23}O$, 4), 175.0765 ($C_{12}H_{15}O$, 12)	Steroidal alkaloid	L
P.33	418.2742	12.36	$C_{28}H_{36}NO_2$	-0.973	418.1071 ($C_{28}H_{36}NO_2$, 1), 403.2507 ($C_{27}H_{33}NO_2$, 1), 286.2138 ($C_{19}H_{28}NO$, **100**), 247.2231 ($C_{17}H_{27}O$, 5), 218.1513 ($C_{15}H_{22}O$, 2), 150.0884 ($C_{10}H_{14}O$, 1)	Sphingolipid	S
P.34	470.2924	12.62	$C_{28}H_{40}NO_5$	-2.941	452.3039 ($C_{28}H_{38}NO_4$, **100**), 411.3464 ($C_{25}H_{31}O_5$, 16), 313.3299 ($C_{21}H_{29}O_2$, 5)	Betaine lipid	S
P.35	504.3413	12.74	$C_{27}H_{54}NO_7$	-6.612	503.2445 ($C_{27}H_{53}NO_7$, 1), 444.3098 ($C_{24}H_{44}O_7$, **100**), 426.2977 ($C_{24}H_{42}O_6$, 1), 283.2632 ($C_{18}H_{35}O_2$, 7)	Betaine lipid	S
P.36	484.2538	12.82	$C_{24}H_{38}NO_9$	-1.773	466.2312 ($C_{24}H_{36}NO_8$, 1), 419.2356 ($C_{23}H_{33}NO_6$, 7), 360.1528 ($C_{20}H_{24}O_6$, **100**), 308.3748 ($C_{20}H_{20}O_3$, 3), 147.0047 ($C_{10}H_{11}O$, 1)	Betaine lipid	S, X
P.37	310.2027	12.99	$C_{17}H_{28}NO_4$	2.791	309.1672 ($C_{17}H_{27}NO_4$, **100**), 296.1579 ($C_{16}H_{26}NO_4$, 80), 281.1311 ($C_{15}H_{23}NO_4$, 25), 161.0959 ($C_{11}H_{13}O$, 7)	Hydroxyamides	S
P.38	394.3312	13.06	$C_{24}H_{44}NO_3$	-2.331	377.3087 ($C_{24}H_{41}O_3$, **100**), 349.2748 ($C_{22}H_{37}O_3$, 35), 309.2681 ($C_{19}H_{33}O_3$, 7), 275.1669 ($C_{17}H_{23}O_3$, 13), 171.1167 ($C_{13}H_{15}$, 3)	Steroidal alkaloid	X
P.39	501.3585	13.10	$C_{31}H_{49}O_5$	1.019	500.4808 ($C_{31}H_{48}O_5$, 2), 483.3442 ($C_{31}H_{47}O_4$, 89), 468.3187 ($C_{30}H_{44}O_4$, 2), 440.2878 ($C_{28}H_{40}O_4$, 2), 321.1855 ($C_{20}H_{33}O_3$, **100**), 262.1923 ($C_{17}H_{26}O_2$, 28), 161.1291 ($C_{12}H_{17}$, 3)	Steroid	L
P.40	537.5619	13.57	$C_{36}H_{73}O_2$	1.570	536.5799 ($C_{36}H_{72}O_2$, 1), 518.4919 ($C_{35}H_{66}O_2$, **100**), 488.4806 ($C_{33}H_{60}O_2$, 5), 284.2944 ($C_{19}H_{40}O$, 5)	Fatty acid/lipid	S
P.41	746.5598	14.06	$C_{41}H_{81}NO_8P$	-3.037	728.4558 ($C_{41}H_{79}NO_7P$, 1), 585.4426 ($C_{33}H_{64}NO_5P$, 1), 492.3627 ($C_{29}H_{51}NO_3P$, 12), 475.3316 ($C_{29}H_{48}O_3P$, **100**), 363.2360 ($C_{25}H_{31}O_2$, 1), 243.1733 ($C_{17}H_{23}O$, 1)	Phospholipid	S
P.42	687.4787	14.14	$C_{48}H_{63}O_3$	1.421	669.4737 ($C_{48}H_{61}O_2$, 34), 641.4774 ($C_{47}H_{61}O$, 14), 615.4607 ($C_{45}H_{59}O$, 6), 517.3557 ($C_{38}H_{45}O$, 3), 371.2321 ($C_{27}H_{31}O$, 37), 355.2471 ($C_{27}H_{31}$, **100**), 339.2116 ($C_{26}H_{27}$, 16)	Steroid	S
P.43	403.3215	14.28	$C_{26}H_{43}O_3$	0.692	385.3087 ($C_{26}H_{42}O_2$, **100**), 283.2645 ($C_{19}H_{23}O_2$, 2), 183.2123 ($C_{11}H_{19}O_2$, 1), 169.1964 ($C_{10}H_{17}O_2$, 1)	Steroid	L
P.44	538.3511	15.32	$C_{33}H_{48}NO_5$	-3.028	520.3405 ($C_{33}H_{46}NO_4$, **100**), 502.3296 ($C_{33}H_{44}NO_3$, 10), 444.2711 ($C_{29}H_{34}NO_3$, 4), 302.1902 ($C_{19}H_{26}O_3$, 16), 216.1536 ($C_{15}H_{20}O$, 13), 202.1596 ($C_{14}H_{18}O$ 2)	Sphingolipid	S
P.45	676.4212	14.41	$C_{41}H_{58}NO_7$	-0.192	657.4116 ($C_{41}H_{56}NO_6$, 43), 617.4744 ($C_{38}H_{49}O_7$, **100**), 493.2746 ($C_{34}H_{37}O_3$, 21), 341.2094 ($C_{25}H_{25}O$, 7)	Betaine lipid	L
P.46	554.5128	14.44	$C_{34}H_{68}NO_4$	-3.672	536.5026 ($C_{34}H_{66}NO_3$, **100**), 518.4918 ($C_{34}H_{64}NO_2$, 10), 379.4885 ($C_{26}H_{51}O$, 1), 284.2942 ($C_{19}H_{40}O$, 1)	Sphingolipid	L
P.47	680.6190	14.48	$C_{42}H_{82}NO_5$	3.966	603.5574 ($C_{39}H_{73}NO_3$, 3), 424.3221 ($C_{28}H_{42}NO_2$, 7), 396.3104 ($C_{27}H_{40}O_2$, **100**), 366.2631 ($C_{25}H_{34}O_2$, 7), 267.1624 ($C_{19}H_{23}O$, 3)	Sphingolipid	X
P.48	654.5648	14.66	$C_{39}H_{76}NO_6$	.3.761	528.5067 ($C_{31}H_{62}NO_5$, 2), 475.4509 ($C_{27}H_{57}NO_5$, 6), 398.3261 ($C_{23}H_{44}NO_4$, 18), 339.2525 ($C_{20}H_{35}O_4$, **100**), 283.1903 ($C_{16}H_{27}O_4$, 15), 269.1745 ($C_{15}H_{25}O_4$, 14), 219.2104 ($C_{14}H_{19}O_2$, 14)	Betaine lipid	S
P.49	538.3511	14.80	$C_{33}H_{48}NO_5$	-3.028	520.3405 ($C_{33}H_{46}NO_4$, **100**), 502.3296 ($C_{33}H_{44}NO_3$, 10), 444.2711 ($C_{30}H_{36}O_3$, 4), 216.1736 ($C_{12}H_{24}O_3$, 13)	*N*-Containing lipid	S
P.50	794.6130	14.84	$C_{46}H_{84}NO_9$	-2.023	745.5407 ($C_{43}H_{75}O_9$, **100**), 632.4311 ($C_{37}H_{60}O_8$, 35), 483.4935 ($C_{28}H_{51}O_6$, 16), 283.2632 ($C_{18}H_{35}O_2$, 17)	Betaine lipid	X
P.51	823.5152	15.01	$C_{52}H_{71}O_8$	0.371	764.5137 ($C_{50}H_{68}O_6$, **100**), 720.4828 ($C_{48}H_{64}O_5$, 8), 569.3070 ($C_{37}H_{45}O_5$, 2), 495.2901 ($C_{34}H_{39}O_3$, 1), 409.2559 ($C_{30}H_{33}O$, 1)	Steroid	L
P.52	568.5090	15.57	$C_{38}H_{66}NO_2$	-0.681	551.4808 ($C_{38}H_{63}O_2$, **100**), 495.4278 ($C_{34}H_{55}O_2$, 60), 451.3608 ($C_{31}H_{47}O_2$, 6), 383.2628 ($C_{26}H_{39}O_2$, 91), 301.2731 ($C_{21}H_{33}O$, 37), 189.1484 ($C_{14}H_{21}$, 11)	*N*-Containing fatty acid	L
P.53	816.6408	15.69	$C_{50}H_{74}NO_8$	1.239	757.4676 ($C_{47}H_{65}O_8$, **100**), 655.4206 ($C_{39}H_{59}O_8$, 2), 569.3075 ($C_{33}H_{45}O_8$, 12), 489.2450 ($C_{27}H_{37}O_8$, 75), 407.2514 ($C_{23}H_{35}O_6$, 5), 283.2623 ($C_{18}H_{35}O_2$, 5)	Betaine lipid	X, L

Comp	$[M+H]^+$ *m/z*	t_R (min)	Molecular formula	Δ (ppm)	MS^2 product ions, *m/z* (elemental composition, rel. intensity [%])	Identification of class/compound	Species
P.54	872.6029	15.90	$C_{54}H_{82}NO_8$	-1.712	828.6116 ($C_{53}H_{82}NO_6$, 27), 593.2750 ($C_{36}H_{51}NO_6$, 43), 562.3329 ($C_{35}H_{48}NO_5$, 14), 544.3429 ($C_{35}H_{46}NO_4$, **100**), 485.2905 ($C_{32}H_{39}NO_3$, 3), 389.2551 ($C_{27}H_{33}O_2$, 1), 307.2403 ($C_{23}H_{31}$, 1)	*N*-Containing lipid	S, X
P.55	725.4984	15.91	$C_{44}H_{69}O_8$	-1.168	707.5051 ($C_{44}H_{68}O_7$, 3), 545.5085 ($C_{37}H_{69}O_2$, **100**), 368.2781 ($C_{25}H_{36}O_2$, 5), 262.2531 ($C_{18}H_{30}O$, 8)	Glyceroglycolipid	L
P.56	566.4409	15.96	$C_{33}H_{60}NO_6$	3.778	565.4280 ($C_{33}H_{59}NO_6$, 8), 507.3698 ($C_{30}H_{51}O_6$, **100**), 432.3169 ($C_{27}H_{44}O_4$, 5), 355.2437 ($C_{23}H_{31}O_3$, 8), 233.1360 ($C_{15}H_{21}O_2$, 7), 175.1479 ($C_{13}H_{19}$, 5)	Betaine lipid	L
P.57	893.5543	15.99	$C_{56}H_{77}O_9$	-2.702	847.5130 ($C_{54}H_{71}O_8$, 1), 615.3968 ($C_{36}H_{55}O_8$ 11), 539.3410 ($C_{33}H_{47}O_6$, **100**), 492.3224 ($C_{32}H_{44}O_4$), 333.2792 ($C_{22}H_{37}O_2$, 1)	Unknown	L, X
P.58	749.5175	16.07	$C_{43}H_{73}O_{10}$	0.842	705.4571 ($C_{40}H_{65}O_{10}$, 2), 659.3177 ($C_{39}H_{47}O_9$, 3), 497.3077 ($C_{34}H_{41}O_3$, **100**), 368.2603 ($C_{25}H_{36}O_2$, 5), 313.2769 ($C_{22}H_{33}O$, 3)	Glyceroglycolipid	S, L, X
P.59	814.5451	16.10	$C_{47}H_{76}NO_{10}$	-2.331	796.5365 ($C_{47}H_{74}NO_9$, 10), 635.4653 ($C_{41}H_{65}NO_4$, **100**), 558.3769 ($C_{37}H_{50}O_4$, 21), 405.2623 ($C_{28}H_{37}O_2$, 5), 359.2674 ($C_{27}H_{35}$, 16), 333.2586 ($C_{25}H_{33}$, 51)	Cerebroside	L
P.60	820.5860	16.12	$C_{47}H_{83}NO_8P$	0.448	752.5237 ($C_{42}H_{75}NO_8P$, 2), 659.3576 ($C_{36}H_{54}NO_8P$, 2), 544.2985 ($C_{30}H_{43}NO_6P$, 85), 517.2664 ($C_{30}H_{40}O_6P$, **100**), 436.2616 ($C_{28}H_{36}O_4$, 5), 333.2424 ($C_{21}H_{33}O_3$, 3)	Ethanolamine glycerophospholipids	S, L
P.61	672.5128	16.26	$C_{41}H_{71}NO_4P$	-1.084	655.4836 ($C_{41}H_{68}O_4P$, 13), 637.4755 ($C_{41}H_{66}O_3P$, **100**), 483.3629 ($C_{35}H_{47}O$, 50), 467.3743 ($C_{35}H_{47}$, 35), 263.2784 ($C_{19}H_{35}$, 13)	Phospholipid	L
P.62	786.5149	16.44	$C_{45}H_{72}NO_{10}$	-0.234	751.4776 ($C_{44}H_{65}NO_9$, 14), 607.4357 ($C_{38}H_{73}NO_4$, **100**), 589.4264 ($C_{37}H_{67}NO_4$, 10), 515.3908 ($C_{32}H_{53}NO_4$, 7), 499.3389 ($C_{27}H_{49}NO_7$, 15), 333.2425 ($C_{21}H_{33}O_3$, 36)	Cerebroside	L, X
P.63	800.6041	16.49	$C_{48}H_{82}NO_8$	4.581	800.6013 ($C_{48}H_{82}NO_8$, 46), 756.6092 ($C_{47}H_{82}NO_6$, 4), 697.6113 ($C_{44}H_{73}O_6$, **100**), 623.5062 ($C_{41}H_{67}O_4$, 4), 472.3614 ($C_{30}H_{48}O_4$, 6), 283.2603 ($C_{18}H_{35}O_2$, 4)	Betaine lipid	L
P.64	768.5899	16.50	$C_{40}H_{82}NO_{12}$	-1.061	767.4736 ($C_{40}H_{81}NO_{12}$, 81), 606.4229 ($C_{38}H_{56}NO_5$, **100**), 586.5604 ($C_{38}H_{54}NO_4$, 17), 407.3135 ($C_{25}H_{43}O_4$, 19), 333.3484 ($C_{23}H_{41}O$, 7)	Cerebroside	L, X
P.65	748.5854	16.17	$C_{41}H_{83}NO_8P$	-0.312	749.5986 ($C_{41}H_{84}NO_8P$, **100**), 748.5824 ($C_{41}H_{83}NO_8P$, 16), 704.5923 ($C_{40}H_{83}NO_6P$, 3), 492.3244 ($C_{32}H_{44}O_4$, 8), 413.2880 ($C_{30}H_{37}O$, 5)	Glycerophospholipid	X
P.66	812.5305	16.74	$C_{40}H_{79}NO_{13}P$	1.962	795.5048 ($C_{40}H_{76}O_{13}P$, 9), 777.4929 ($C_{40}H_{74}O_{12}P$, 31), 633.4506 ($C_{41}H_{61}O_5$, **100**), 615.4410 ($C_{41}H_{59}O_4$, 10), 541.4008 ($C_{38}H_{53}O_2$, 5), 331.2263 ($C_{25}H_{31}$, 35), 239.1824 ($C_{18}H_{23}$, 2)	Serine glycerophospholipids	X
P.67	817.4889	16.78	$C_{49}H_{69}O_{10}$	-0.215	758.5248 ($C_{47}H_{66}O_8$, 32), 655.4333 ($C_{43}H_{59}O_5$, **100**), 543.2924 ($C_{35}H_{43}O_5$, 7), 515.2610 ($C_{33}H_{39}O_5$, 5), 353.2089 ($C_{23}H_{29}O_3$, 2), 297.1827 ($C_{20}H_{25}O_2$, 1)	Lipid	X
P.68	917.5764	16.78	$C_{55}H_{81}O_{11}$	-1.625	899.5670 ($C_{55}H_{79}O_{10}$, 3), 885.5511 ($C_{54}H_{77}O_{10}$, **100**), 799.5532 ($C_{51}H_{75}O_7$, 4), 621.3795 ($C_{40}H_{45}O_6$, 4), 607.2544 ($C_{39}H_{43}O_6$, 13)	Lipid	L
P.69	910.7130	17.31	$C_{56}H_{96}NO_8$	-0.651	910.7133 ($C_{56}H_{96}NO_8$, 4), 747.5038 ($C_{46}H_{69}NO_7$, 11), 659.3611 ($C_{40}H_{51}O_8$, **100**), 497.3073 ($C_{34}H_{41}O_3$, 5), 283.2629 ($C_{18}H_{35}O_2$, 11)	Cerebroside	S
P.70	772.6221	17.34	$C_{44}H_{87}NO_7P$	0.114	755.5974 ($C_{44}H_{84}O_7P$, **100**), 699.5283 ($C_{40}H_{76}O_7P$, 27), 597.4538 ($C_{35}H_{66}O_5P$, 17), 329.3047 ($C_{20}H_{41}O_3$, 40), 285.2791 ($C_{18}H_{37}O_2$, 35)	Phospholipid	S, X
P.71	735.5166	17.36	$C_{46}H_{71}O_7$	-2.938	717.5049 ($C_{46}H_{69}O_6$, 16), 675.4652 ($C_{43}H_{63}O_6$, **100**), 637.4437 ($C_{40}H_{61}O_6$, 10), 623.4276 ($C_{39}H_{59}O_6$, 17), 563.4058 ($C_{37}H_{55}O_4$, 5), 467.3491 ($C_{31}H_{47}O_3$, 2), 294.2950 ($C_{20}H_{38}O$, 1)	Lipid	X
P.72	938.5377	17.36	$C_{56}H_{76}NO_{11}$	-2.522	879.4658 ($C_{53}H_{67}O_{11}$, 16), 775.4537 ($C_{50}H_{63}O_7$, 17), 661.4653 ($C_{46}H_{61}O_3$, **100**), 498.3126 ($C_{34}H_{42}O_3$, 6), 301.2897 ($C_{22}H_{37}$, 3)	Betaine lipid	X
P.73	822.5859	17.39	$C_{50}H_{80}NO_8$	-3.031	821.5827 ($C_{50}H_{79}NO_8$, **100**), 805.5615 ($C_{49}H_{75}NO_8$, 6), 746.4722 ($C_{46}H_{66}O_8$, 15), 468.3607 ($C_{31}H_{48}O_3$, 4), 283.2634 ($C_{18}H_{35}O_2$, 71)	Betaine lipid	X
P.74	806.6108	17.55	$C_{47}H_{84}NO_9$	-4.721	806.6019 ($C_{47}H_{84}NO_9$, 11), 788.5944 ($C_{47}H_{82}NO_8$, 13), 665.5858 ($C_{40}H_{75}NO_6$, 31), 538.3262 ($C_{32}H_{44}NO_6$, 3), 415.3207 ($C_{27}H_{43}O_3$, 54), 392.2923 ($C_{27}H_{38}NO$, **100**), 294.3156 ($C_{20}H_{38}O$, 12)	Cerebroside	L
P.75	794.5603	17.85	$C_{48}H_{76}NO_8$	-2.382	793.5598 ($C_{48}H_{75}NO_8$, 10), 632.5968 ($C_{40}H_{74}NO_4$, 26), 614.5464 ($C_{40}H_{72}NO_3$, **100**), 452.5093 ($C_{30}H_{60}O_2$, 7), 356.3522 ($C_{23}H_{48}O_2$, 4), 276.2686 ($C_{19}H_{32}O$, 10)	*N*-Containing lipid	S, L

Note: S= *S. glaucum*, L= *L. crassum*, X= *X. umbellata*

The appearance of the peaks results in the separation of *S. glaucum* extracts treated with higher concentration of glyphosate in multivariate data analysis result (e.g., PCA score plot) (Figure 59, Figure 61, and Figure 62). Moreover, the metabolites of *L. crassum* and *X. umbellata* treated with high glyphosate concentrations (50 mg/L and 25 mg/L, respectively) were significantly different from those of soft coral extracts treated with low glyphosate concentrations.

The variation in metabolites between extracts can be observed in the multivariate data analysis results (i.e. PCA). PCA can assist in the reduction of large datasets derived from extracts, and visualize clusters and outliers. As previously stated, extracts of *S. glaucum* treated with the highest glyphosate concentrations (100 mg/L and 1 g/L) were distinct from other extracts. It is also visible in the PCA score plot (Figure 59.A) which indicates that both groups were separated from other extracts in PC1 (34.8% variance). According to the analysis of correspond loadings plot (Figure 59.B) this separation is caused by several groups of metabolites, such as lipids, including betaine lipids (P.**28**, P.**35**, P.**48**), phospholipids (P.**41**, P.**58**, P.**60**, P.**70**), sphingolipid (P.**33**), as well as nitrogenous fatty acid (P.**25**). The metabolites with lower molecular mass were also caused this separation, such as diterpenoids (P.**30** and P.**31**).

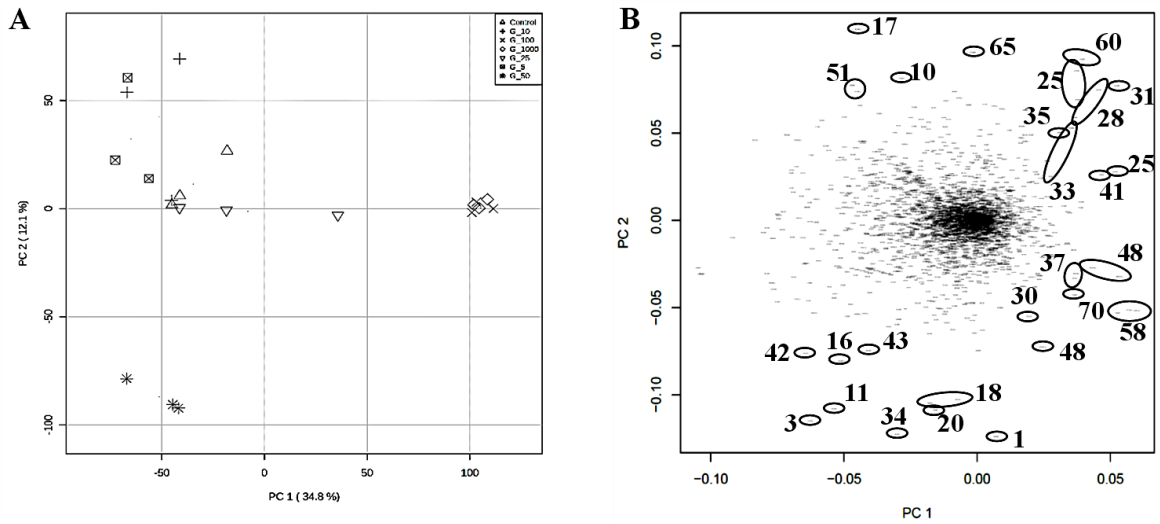

Note= Δ: Control, ◇: 1 g/L, ×: 100 mg/L, ✱: 50 mg/L, ∇: 25 mg/L, +: 10 mg/L, ⊠: 5 mg/L

Figure 59 PCA of LC-ESI-HRMS data extracts of *Sarcophyton glaucum* after exposure to different concentration of glyphosate; scores plot (a) and loadings plot (b). Numbers correspond to Table 12

In addition, the clear segregation of the coral extracts treated with 50 mg/L glyphosate was also observed in PC2 (12.1% variance). The features responsible for this separation were tentatively annotated as the group of amino alcohol (P.**1**), sesquiterpenes (P.**3**, P.**18**), cembrane (P.**20**), a low chain betaine lipid (P.**34**), and steroids (P.**42**, P.**43**). In general, lipids are responsible for the separation of each group. These substances were detected in high concentration in comparison to other group of extracts (Figure 60). It is probably due the coral itself or its endosymbiont, zooxanthellae. This argument is based on the presence of

fatty acids, phospholipids, and betaine lipids, all of which are predominantly produced by zooxanthellae and then transferred to their host [404-406]. Nevertheless, fatty acids and lipids are produced by soft corals in order to provide the energy for survival under adverse conditions [407, 408].

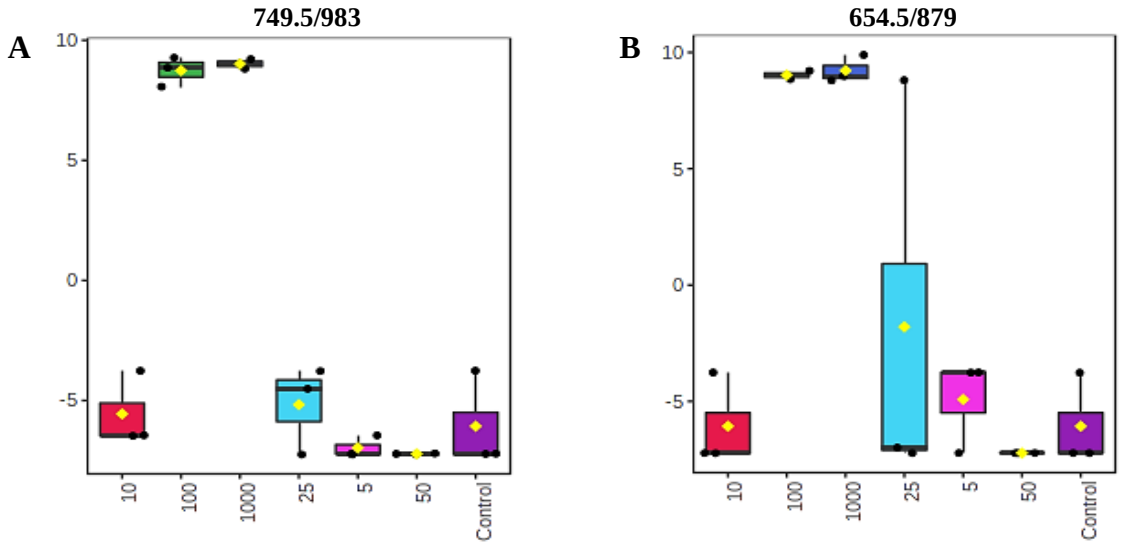

Figure 60 Box plot of glyceroclycolipid (P.**58**) (A) and lipid (P.**40**) (B) composition in *S. glaucum* extracts

Further, the multivariate data analysis was applied to determine the variance in extracts of *L. crassum* after exposure to various concentrations of glyphosate. The outcome of this analysis is depicted in Figure 61. According to the PCA score plot, group of *L. crassum* treated with the lowest concentration of glyphosate (5 mg/L) along with the control were clearly distinct from other extracts in PC1 (35.1% variance). The segregation of this group is expected since the lowest concentration of glyphosate have no effect on *L. crassum*, as evidenced by their morphology. The responsible features causing this separation were then identified based on the loadings plot in the direction of these groups.

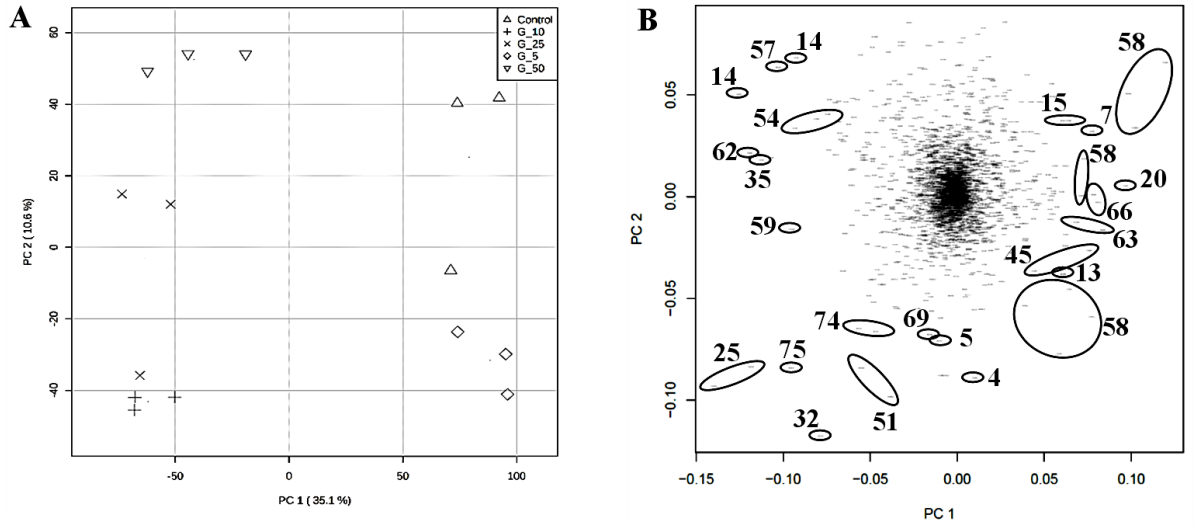

Note= ∆: Control, ∇: 50 mg/L, ×: 25 mg/L, +: 10 mg/L, ◇: 5 mg/L

Figure 61 PCA of LC-ESI-HRMS data extracts of *Lobophytum crassum* after exposure to different concentration of glyphosate; scores plot (a) and loadings plot (b). Numbers correspond to Table 12

The responsible features for this separation were tentatively annotated as glyceroglycolipid (P.**58**, P.**65**), betaine lipids (P.**45**, P.**63**), sesquiterpene (P.**13**), diterpene alkaloid (P.**15**), sesquiterpene (P.**7**), and diterpenoid (P.**20**). In general, lipids are the main component causing this separation. According to the visual inspection (morphology investigation), there was no sign of coral stress itself. Therefore, the changing of lipids composition in the extracts was most likely due to the stress occur on zooxanthellae. Furthermore, the separation of extracts of soft corals treated with the highest concentration (50 mg/L) were observed in the positive direction of PC2 (10.6% variance). This separation is primarily due to cerebroside compounds (P.**59** and P.**62**), diterpene (P.**25**) and N-containing diterpene (P.**14**) along with an unknown feature with *m/z* 893.5543, $[M+H]^+$ $C_{56}H_{77}O_9$. These diterpenes were detected in relative higher concentrations than in other extracts. In addition, steroids compounds (P.**32** and P.**51**) along with cerebrosides (P.**69** and P.**74**) were tentatively annotated as the features caused the separation of the extracts of *L. crassum* treated with 10 mg/L of glyphosate.

The analysis of variation of soft coral metabolites after exposure to glyphosate was also performed on *X. umbellata* extracts. Similar to *L. crassum*, as expected, extracts of corals treated with 5 mg/L of glyphosate were distinct together with the control in PC1 (22% variance) (Figure 62). This separation is caused by several features, which have been tentatively annotated as lipids, including betaine lipids (P.**50**, P.**53**, P.**68**, P.**72**), amino alcohol (P.**5**), and cerebroside (P.**62**); these metabolites are known as metabolites produced by microalgae, including zooxanthellae. The concentration of these metabolites were relative high in comparison to other extracts. This indicates that exposure to high concentrations of glyphosate (> 5 mg/L) tended to affect zooxanthellae associated, as indicated by the composition of their metabolites.

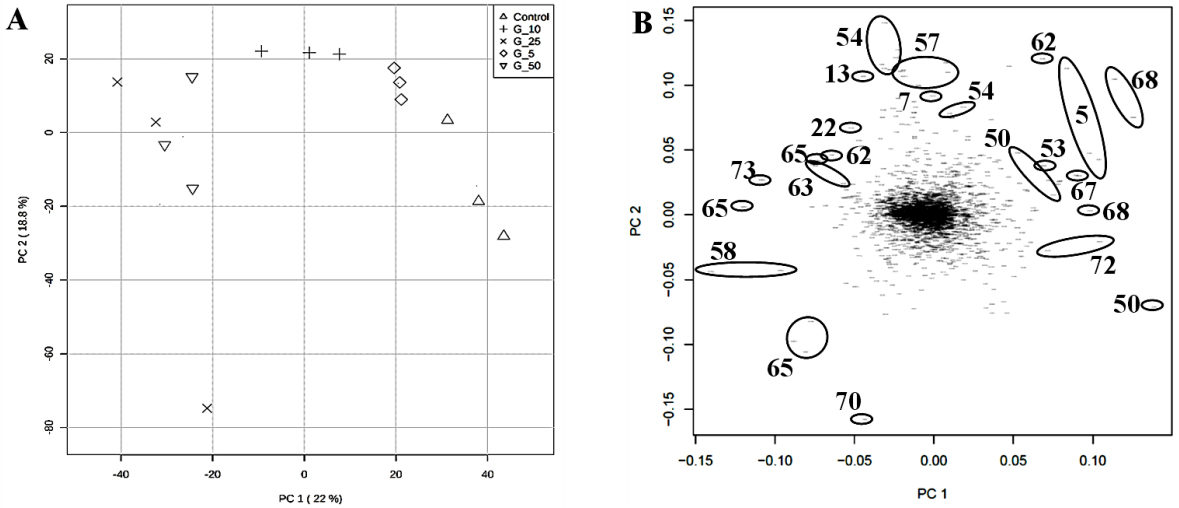

Note= Δ: Control, ∇: 50 mg/L, ×: 25 mg/L, +: 10 mg/L, ◇: 5 mg/L

Figure 62 PCA of LC-ESI-HRMS data extracts of *Xenia umbellata* after exposure to different concentration glyphosate; scores plot (a) and loadings plot (b). Numbers correspond to Table 12

Furthermore, the high concentrations of glyphosate (25 mg/L and 50 mg/L) had an effect on the metabolite composition of *X. umbellata*. These group of extracts were clustered in the opposite direction of PC1 from control samples. The responsible features for this separation mainly belong to the unpolar metabolites, including phospholipids (P.**65**, P.**70**), betaine lipids (P.**63**, P.**73**), glyceroglycolipid (P.**58**), and cerebroside (P.**62**). Along with these unpolar components, two metabolites, including sesquiterpene (P.**13**) and diterpene alkaloid (P.**22**) were tentatively annotated as the responsible features for this separation. The separation of groups in the PCA score plots of each extract from soft corals were mainly due to the composition of lipids. As mentioned above, this substances act as the energy producers for soft corals in unfavorable conditions. On the other hand, the endosymbiont of soft corals, zooxanthellae, contribute to the composition of these substances in the extracts.

As diatoms, these organisms are known as producers of lipids and fatty acids [166, 404, 409, 410]. In most cases, these metabolites are produced more abundantly when diatoms are stressed [411-414], which can also occur when these organisms are exposed to glyphosate. Cruz et al. discovered that glyphosate significantly increased the production of lipids and fatty acids in marine diatoms [369]. Further, zooxanthellae produced fatty acids and lipids, which were then transferred to their host soft corals [404, 409, 410]. Therefore, the increase of fatty acid composition in the extracts are mostly related to the production of these substances by zooxanthellae.

Moreover, some diterpenes were tentatively assigned as the metabolites responsible for the separation, particularly in extracts of *L. crassum* exposed to the highest glyphosate concentration. Diterpene production is associated with defense mechanisms in soft corals and their symbionts [221]. This class of secondary metabolites is produced by a variety of marine organisms as a defense mechanism against predators and under adverse (stress) conditions [185, 415-417]. Soft corals, especially in genera *Lobophytum*, produce promising diterpenes with broad bioactivities such as antibacterial, antifouling, and antiinflamation [418-424]. Therefore, we conclude that glyphosate at very high concentration is a source of stress for soft corals and zooxanthellae, as well as an inducer of the production of certain metabolites in these organisms.

c. Spatial distribution of soft coral metabolites after treatment with glyphosate

The glyphosate exposure on corals is known to have an effect on their endosymbiont as a photosynthetic organism, including the composition of their metabolites (based on the result described above). However, the metabolites produced by zooxanthellae are extremely difficult to detect due to their low concentration in crude extracts of soft corals. MS-Imaging (e.g. MALDI-MSI) enables the detection of zooxanthellae marker metabolites, particularly their spatial distribution within the soft coral body. Beside the observation of the distribution of metabolites, this analysis may aid in determining the effect of stressors (e.g. glyphosate) on zooxanthellae metabolites as well as on their host. As described in Chapter IV, MALDI-

MSI were were performed only for two soft coral species, *S. glaucum* and *L. crassum*, due to the difficulties encountered during the *X. umbellata* embedding process.

To examine the effect of glyphosate on the metabolites of the investigated soft corals and their endosymbiont, the tissue was embedded in CMC and then sprayed with DHB matrix, allowing for the ionization of metabolites in the tissue. The positive ion mode was used to measure the sprayed soft coral tissue. To begin, the analysis of detected metabolites in coral tissue was limited to zooxanthellae marker metabolites. Four known pigments from zooxanthellae, namely phaeophytin A (*m/z* 871.5711), diatoxanthin (*m/z* 567.4182), (3*S*,4*R*,3´*R*)-4-hydroxyalloxanthin (*m/z* 581.3981), and canthaxanthin (*m/z* 565.4056) were selected and their appearance in the tissue manually checked using MSI Reader software. Along with these four pigments, distribution of zooxanthellae can be distinguished by the brownish color of their microscopic image (optical image). Figure 63 depicts the spatial distribution of four corresponding zooxanthellae metabolites as well as an optical image of soft coral tissue (control and glyphosate-induced sample).

The spatial distribution of pigments produced by zooxanthellae as determined by MALDI-MSI clearly demonstrates that these metabolites were concentrated in the areas where zooxanthellae are localized, which is mostly in the umbrella part of soft corals. Interestingly, these pigments were distributed differently throughout the body of soft corals. Phaeophytin A and (3*S*,4*R*,3´*R*)-4-hydroxyalloxanthin were distributed in the same location, whereas diatoxanthin and canthaxanthin were found in a different location from these two pigments. It was evident in both soft corals, but was more pronounced in *S. glaucum* tissue. The distribution of these pigments is related to the location and function of zooxanthellae within the body soft corals. As previously stated in Chapter IV, the presence of phaeophytin A and (3*S*,4*R*,3´*R*)-4-hydroxyalloxanthin was clearly associated with the presence of zooxanthellae, as evidenced by the brown coloration of zooxanthellae under microscopic observation. Therefore, it is obvious that these pigments are marker metabolites produced by this endosymbiont.

In contrast to those two pigments, diatoxanthin and canthaxanthin were not detected in the region exhibiting the brown color. These metabolites were primarily detected in the vesicles at the bottom of siphonozooids (tentacles), which belong to gastrodermal cells of the coral host. It was also observed in *L. crassum*, in which the zooxanthellae were collocated in the barrier of umbrella and stem. According to the anatomy structure of this coral, this part is the gastrodermal area of coral polyp. As an explanation for this situation, some zooxanthellae are located in siphonozooids of soft coral in order to acclimate the light during photosynthesis [155]. During this process in siphonozooids, zooxanthellae convert the xanthophyll diadinoxanthin to diatoxanthin as well as other carotenoids such as canthaxanthin in their body [156, 157]. Further, zooxanthellae cells migrated to gastrodermal compartments (symbiosomes) as a result of siphonozooids movement during food intake [158-160]. As a result, these pigments were abundantly detected in this region.

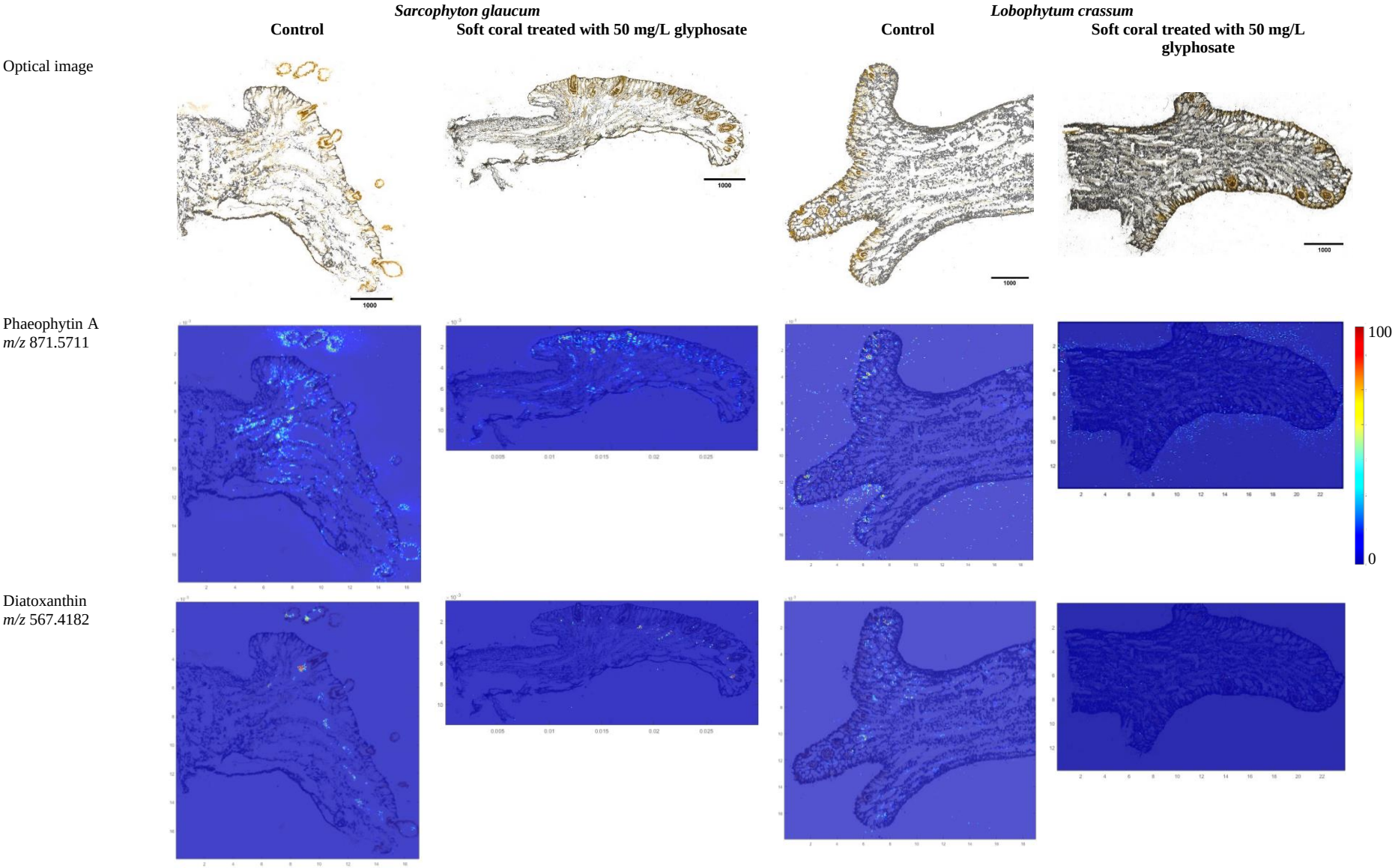
Sarcophyton glaucum
Lobophytum crassum
Control
Soft coral treated with 50 mg/L glyphosate
Control
Soft coral treated with 50 mg/L glyphosate
Optical image
Phaeophytin A
m/z 871.5711
Diatoxanthin
m/z 567.4182
1000
100
0

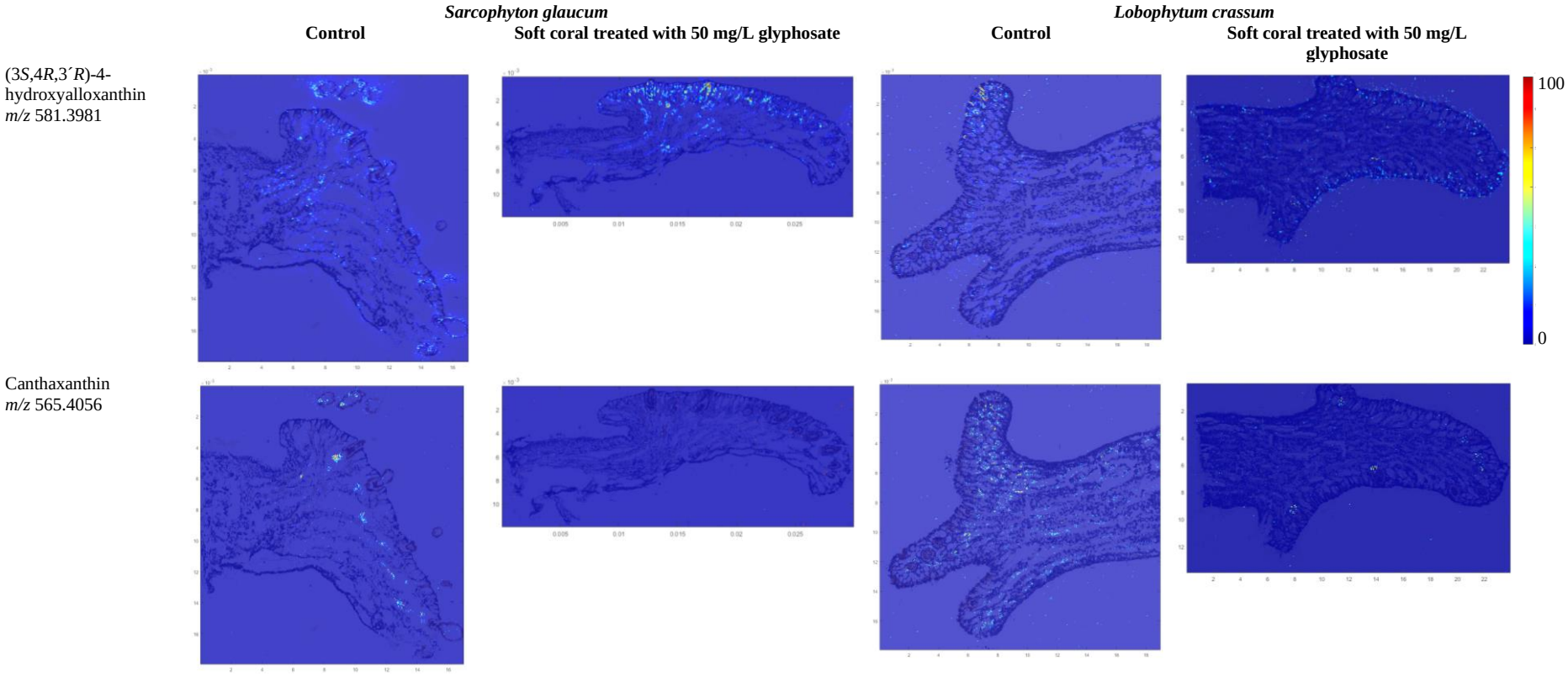

Figure 63 AP-MALDI-MSI of soft coral *Sarcophyton glaucum* and *Lobophytum crassum* after treated with glyphosate with the spatial distribution of zooxanthellae marker metabolites with *m/z* $[M+H]^+$ 871.5711, 567.4182, 581.3981, 565.4056, and full imaging without microscopic image overlay

Regarding glyphosate's effect on zooxanthellae metabolites, some evidence was observed, most notably on the appearance of pigments in the coral tissue which is related to the their endosymbiont, zooxanthellae. The presence of each pigment varied between the investigated species. Canthaxanthin was detected in extremely low concentrations in *L. crassum* exposed to glyphosate 50 mg/L, while not detected in treated *S. glaucum*. Diatoxanthin, a related pigment, was detected only in treated *S. glaucum* as well as in control. Different with other pigments, phaeophytin A was detected predominantly on the outer body of both soft corals treated with glyphosate. Furthermore, (3*S*,4*R*,3'*R*)-4-hydroxyalloxanthin was detected in the coral body in the same location where the phaeophytin A localized.

The reduction of the pigments canthaxanthin in *L. crassum* and diatoxanthin in *S. glaucum* are most likely the response of zooxanthellae to glyphosate exposure. Since glyphosate has been shown to impair the photosynthetic organism's ability to produce chlorophyll and carotenoids [374, 425-427]. Several studies revealed that exposure to glyphosate at sub-lethal concentrations reduced the chlorophyll and carotenoid content on terrestrial plants and algae [374, 427, 428]. As discussed previously, glyphosate has an indirect effect on the depletion of carotenoids and xanthophyll in zooxanthellae. This herbicide impacted photosynthetic processes, which may be related to glyphosate-induced reductions of plastoquinone (PQ) biosynthesis [376, 377] which further leads to decrease of carotenoid and xanthophyll in the cells [379]. This may account for the low concentrations of these two carotenoids in soft coral tissue. However, as the role of carotenoids is to protect the photosynthetic apparatus of the zooxanthellae from excessive ROS production, the reduction in carotenoid contents associated with glyphosate exposure remains debatable.

In the normal case, glyphosate exposure is proposed to result in an increase of reactive oxygen species (ROS) in plant cells [381], probably including zooxanthellae cells as photosynthetic organism. Further, as a response to a high level of ROS, zooxanthellae produce more carotenoids such as xanthophyll, which contribute to ROS scavenging [382]. Increased pigment production (carotenoids) may result in an increase in their concentration in zooxanthellae cells. These mechanisms have been discovered in microalgae, for example in *Phaeodactylum tricornutum* [425]. Therefore, the findings in this study suggest that glyphosate's effect on zooxanthellae is primarily related to the disturbance of photosynthetic processes of this organism in terms of carotenoid production, rather than to the relation of ROS overproduction induced by glyphosate.

The glyphosate effect on the endosymbionts of soft corals, particularly on zooxanthellae pigments was remarkable by using MALDI-MS imaging. This method, however, did not allow for observation of metabolites changing after glyphosate exposure. There were no remarkable differences in the distribution or detection of stress-related metabolites on soft corals tissue in comparison to the control (untreated) sample. For detail, spatial distributions of soft coral-marker metabolites in two soft corals (*S. glaucum* and *L. crassum*) are shown in Appendix 14.

d. Biological activity of the extracts of soft coral treated with glyphosate

In addition to the physical and chemical analysis, the biological activity of methanolic extracts of *S. glaucum, L. crassum,* and *X. umbellata* treated with glyphosate was evaluated. The antibacterial activity was perfomed against the gram-negative bacterium *Aliivibrio fischeri* and the gram-positive bacterium *Bacillus subtilis*, while cytotoxicity was determined against several cancer cell lines. This antibacterial assay was conducted using two different concentrations of the corresponding soft coral extracts, 500 µg/mL and 50 µg/mL, with chloramphenicol as a positive control. Additionally, for each biological replicate, this assay was performed twice in triplicate. The averaged activities per sample against *A. fischeri* and *B. subtilis* are compiled in Figure 64 and Figure 65 respectively.

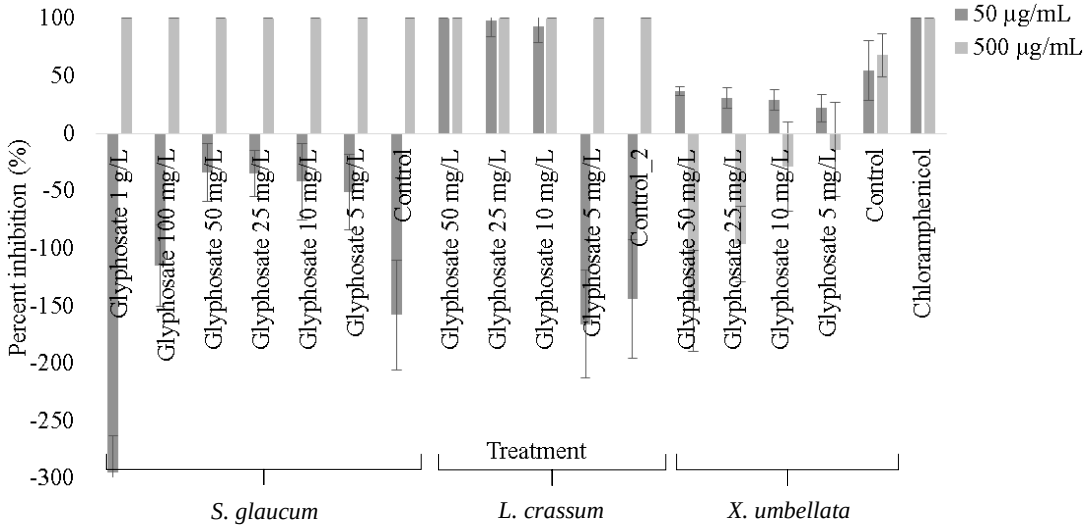

Figure 64 Antibacterial activity of methanolic crude extracts of three soft coral species exposed to different concentration of glyphosate against *Aliivibrio fischeri* (concentration 50 µg/mL and 500 µg/mL in DMSO, positive control chloramphenicol, negative control DMSO), technical replicates = 2

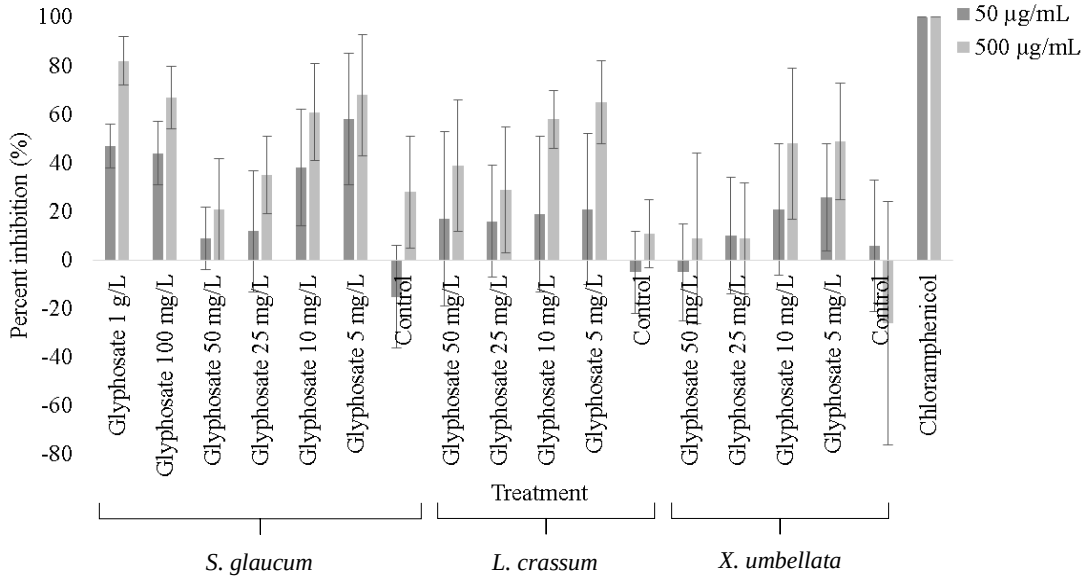

Figure 65 Antibacterial activity of methanolic crude extracts of three soft coral species exposed to different concentration of glyphosate against *Bacillus subtillis* (concentration 50 µg/mL and 500 µg/mL in DMSO, positive control chloramphenicol, negative control DMSO), technical replicates = 2

In general, at the highest concentration (500 µg/mL), all extracts of *S. glaucum* and *L. crassum* completely inhibited the growth of *A. fischeri*. In comparison to the extracts of the other two soft corals, *X. umbellata* extracts exhibited moderate activity against the tested bacterium. Moreover, interesting behaviour was observed in the extracts of *L. crassum* treated with glyphosate at high concentrations (>5 mg/L). In both tested concentrations (500 µg/mL and 50 µg/mL), the extracts of these corresponding soft corals exhibited a strong inhibitory effect against *A. fischeri*. Glyphosate at these concentrations may induce the formation of chemical constituents of the extracts which could cause the production of metabolites that are highly active against *A. fischeri*. However, it remains as an open question.

Furthermore, extracts of *S. glaucum* treated with the highest glyphosate concentrations (1 g/L and 100 mg/L) as well as the lowest glyphosate concentrations (10 mg/L and 5 mg/L) exhibited moderate antibacterial activity against *B. subtilis*. Interestingly, extracts of this coral exposed to glyphosate at 25 mg/L and 50 mg/L had negligible activity against the tested bacteria. In addition, extracts of *L. crassum* and *X. umbellata* treated with glyphosate at concentration of 10 mg/L and 5 mg/L in the highest concentration (500 g/mL) exhibited moderate to strong activity against *B. subtilis*. This activity was even stronger than activity of untreated soft coral extracts (control sample).

As mentioned in Chapter VI, glyphosate is known as inhibitor to several bacteria, e.g. *E. coli* and *S. enterica* [313-315]. This substance may act in the same way on bacteria of this study (*A. fischeri* and *B. subtilis*). Therefore, in order to address this question, the antibacterial activity of glyphosate was evaluated against *A. fischeri* and *B. subtilis*. As a result (Appendix 10), this herbicide shows no antibacterial activity against the tested bacteria up to concentration of 100 µM. Thus, the activity of the soft coral extracts treated with glyphosate is clearly derived from the secondary metabolites produced by the corals themself in response to the stressor.

Further, cytotoxic assays were performed on all soft coral extracts treated with glyphosate. The cytotoxicity against two cancer cell lines (HT29 colon cancer and PC3 human prostate cancer) was determined in-vitro using extracts at two corresponding concentrations (0.05 and 50 µg/mL). Cytotoxicity (MTT) of the soft corals extracts is shown in Figure 66. Based on the result, low concentrations of soft coral extracts (0.05 µg/mL) had no effect on the viability of both cell lines. However, all extracts at a higher concentration (50 µg/mL) demonstrated a significant inhibitory activity against the tested cell lines, with a percentage of cell viability less than 5%. These results are similar to a study conducted by Farag et al. (2017), which confirmed that the crude extract of *Sarcophyton* species exhibited significant activity against the two cell lines HT29 and PC3, with an IC50 value less than 50 µg/mL [336].

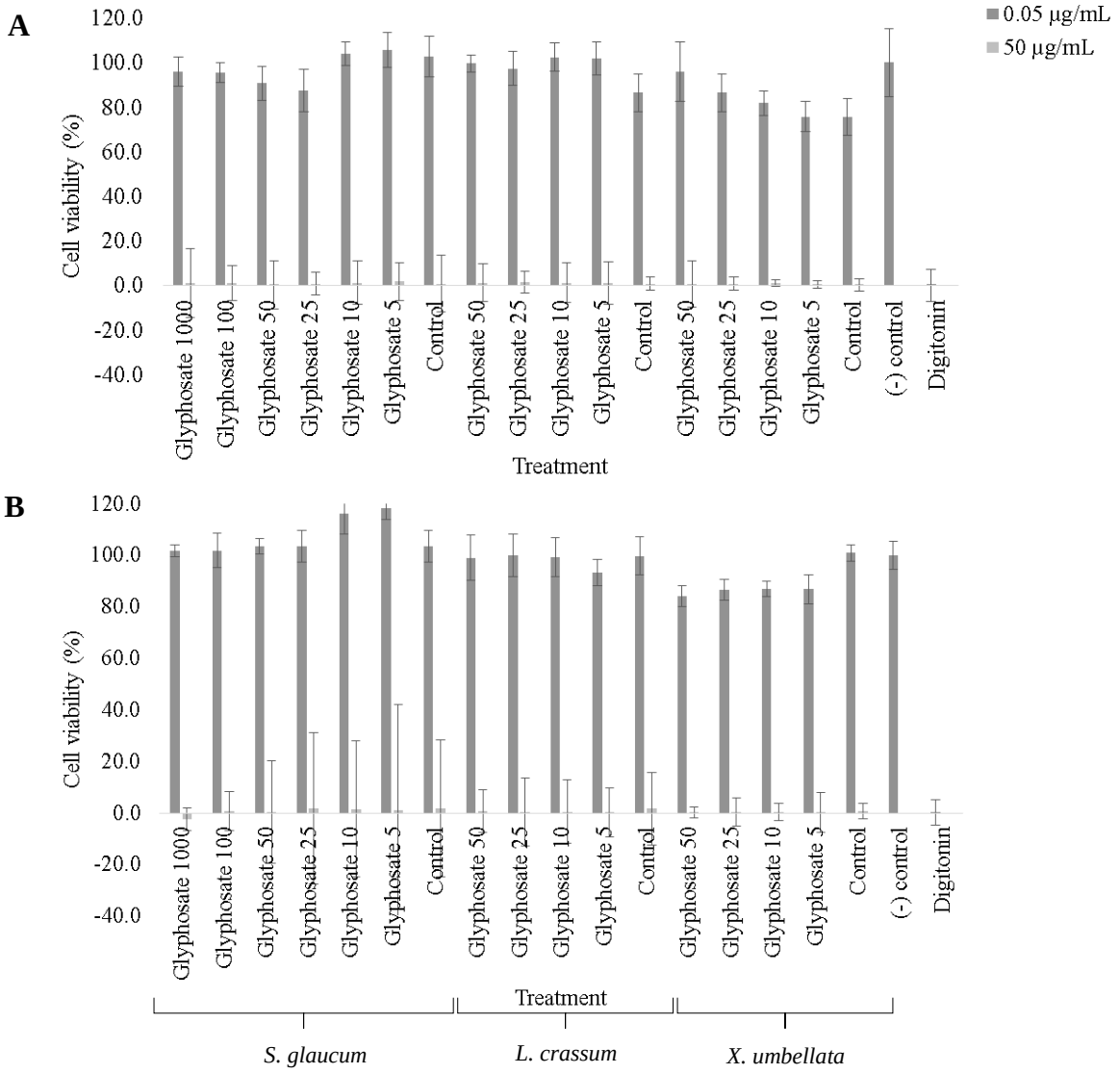

Figure 66 Cytotoxicity of soft coral extracts against the two cancer cell lines HT29 (a) and PC3 (b) (concentration 0.05 µg/mL and 50 µg/mL in DMSO; positive control digitonin; negative control DMSO)

7.4. Conclusion

The effect of glyphosate was specifically investigated in this experiment on *S. glaucum*, *L. crassum*, and *X. umbellata*. To the best of our knowledge, this is the first study to document the effect of glyphosate on soft corals in detail, including the morphology and metabolites that change as response to glyphosate exposure. The effect of glyphosate exposure on soft corals was initially observed in terms of polyp color and tentacle behavior. This herbicide was deadly to *S. glaucum* only at the "unnaturally" highest concentration (1 g/L). Additionally, an interesting phenomenon was observed in samples treated with 100 mg/L glyphosate, which is the color of *S. glaucum* changed to a dark brown hue rather than fading, became greenish after exposure to 50 mg/L of glyphosate. This case could be explained by glyphosate-induced damage to the photosynthetic apparatus and increased

carotenoid production for ROS scavenging. In fact, the concentrations of glyphosare are extremely high in comparison to the concentration detected in the natural environment.

Furthermore, to conduct an in-depth analysis of the metabolites that changed in soft corals after glyphosate exposure were performed by using two analytical methods ^{1}H-NMR and LC-ESI-HRMS. Similarly to the morphology result, the highest glyphosate concentrations (1 g/L and 100 mg/L) affected metabolite composition of the soft corals. Fatty acids, sarcophytolol, deoxosarcophine, and ent-Sarcophyolide E were tentatively assigned as metabolites responsible for the differentiation of *S. glaucum*, according to ^{1}H-NMR-PCA, result. Unfortunately, some signals, such as the multiplets in area δ 6.06 and 6.20 ppm, the signals which changes during glyphosate exposure, remain unknown. Therefore, the elucidation of this metabolite is required. Moreover, there is no evidence of changes in zooxanthellae metabolites during glyphosate-induced stress, despite the fact that glyphosate's primary effect is known to be on zooxanthellae as a photosynthetic organism.

Similar to the ^{1}H-NMR result, lipids were tentatively assigned as the metabolites responsible for group segregation in LC-MS-PCA. Lipid act as the energy producers for soft corals in unfavorable conditions. On the other hand, the zooxanthellae contribute to the composition of these substances in the extracts. Additionally, some diterpenes were detected as metabolites responsible for the separation of *L. crassum* (exposure to 50 mg/L glyphosate) extracts, which was increased after glyphosate exposure. The presence of diterpene in soft coral species could be associated with their antibacterial activity against *A. fischeri*. *L. crassum* extracts treated with glyphosate at this concentration exhibited extremely strong activity against *A. fischeri* at both concentrations tested, which could be a result of the chemical constituents of the extracts (diterpenes constituents).

MALDI-MSI was also used to determine the effect of glyphosate on zooxanthellae. There was some evidence, most notably in the appearance of pigments, i.e. canthaxanthin and its related pigment, diatoxanthin. These pigments were detected in the low concentration in both soft corals, *S. glaucum* and *L. crassum* after exposure to 50 mg/mL of glyphosate. Reduced levels of pigments in soft coral body were associated with glyphosate-induced damage to the photosynthesis apparatus and the organism's ability to produce pigments, including carotenoids. Based on the results, this MALDI-MSI had the disadvantage of not allowing for the detection of secondary metabolite changes in the investigated soft coral after glyphosate exposure.

VIII. General discussion and conclusions

Secondary metabolites produced by marine invertebrates, including corals are extremely diverse. These metabolites, referred to as marine natural products, regularly display extraordinary chemical and pharmacological properties [429]. Soft corals specifically, contribute a diverse range of metabolites with structural diversity, which exhibit a broad spectrum of biological activities. This could be explained by the necessity of these organisms to release secondary metabolites as their own chemical defense to survive in unfavorable and stress conditions [430]. Numerous studies have been conducted to determine the effect of some stressors (physical stress), such as rising seawater temperatures, acidification of seawater, and low salinity, on soft corals, resulting in the alteration of their secondary metabolites [59, 431, 432]. In addition to these physical stressors, chemicals derived from terrestrial activities and products used by humans have an effect on soft corals, and lead to changes in their metabolites. Not only corals, but their endosymbionts, zooxanthellae, will be impacted. These dinoflagellates are the "life partners" of corals, providing up to 90% of the nutritional requirements of the coral [433]. By introducing stressors, the break down between the soft coral-zooxanthellae relationship may occur. Therefore, the objective of this study was to investigate the effect of stressors on the composition of secondary metabolites in soft corals and their endosymbionts. In addition, physical effects on corals were also investigated, such as changes of morphology (color, tentacle movement, and pulsation of tentacles), zooxanthellae density, and PSII efficiency of zooxanthellae.

Since it was not possible to obtain corals from the natural environment, soft coral species from the aquarium culture were used in collaboration with the Leibniz Center for Marine Tropical Research (ZMT) in Bremen for the studies described here. Three species were chosen for this study based on their viability in ZMT and a variety of scientific criteria, including their morphology, abundance in the marine organism, and status as representative species in at least two families. *Sarcophyton glaucum* and *Lobophytum crassum* (family Alcyoniidae), along with *Xenia umbellata* (family Xeniidae) were selected. However, because the soft corals used in this experiment are long-lived aquarium strains, it was difficult to ensure that their response to elicitors was identical to the response of wild-strain soft corals. The disparity between wild and aquarium corals might be attributable to ecological differences, as aquarium corals may have lost or interrupted their fitness to produce these chemicals that act as defenses against predators, which are not found in the aquarium [434]. Furthermore, due to the complexity of soft corals as invertebrates, the response of a single individual would be meaningful enough. Therefore, we fragmented soft corals (ca.1.5-2 cm^2) from a single adult individual species and cultured them at the same time and under the same conditions to minimize error.

Regarding the elicitors/stressors, we included appropiate elicitors, with respect to their potential for accumulation in the ocean. Two pesticides (glyphosate and simazine) were

selected as the representatives from agriculture activity. Since glyphosate has been widely used as a pesticide worldwide for years, it was noteworthy to investigate its effect on corals. To the best of our knowledge, this is the first study to examine the glyphosate effect on soft corals, particularly on their metabolite profiles. Moreover, two sun-blocker components were used in this experiment, namely oxybenzone and octinoxate, because of their common occurrence as an ingredient in sun-blocker products. These substances, once used by humans, will precipitate into the ocean, where they are proposed to have an adverse effect on corals and other benthic organisms. $CuSO_4$, a plasticizer (dimethyl phthalate, DMP), and microplastic were chosen as elicitors to represent industrial activity.

At the beginning of each study, the appropriate elicitor concentration on the investigated soft corals was determined. The criteria chosen for an appropriate concentration was that the soft corals are in a clearly impaired state, but without dying off, as evidenced by their morphology and metabolite compositions. The concentrations of elicitors used in this study are much higher than those found in the natural environment. However, the duration of exposure in this study was only 5 days, while corals in nature are exposed to the stressors for years. The higher elicitor concentration with shortened exposure time may simultate natural condition to some extent. Therefore, a comprehensive study under real environmental conditions, i.e. lower trigger concentration at much longer exposure times, would have to be performed in continuing work.

In total, 81 individual soft corals (3 soft coral species, 3 biological replicates, 8 elicitors + 1 control) were investigated. The morphology of these soft corals was examined over a five-days period of elicitation (Chapter V). Stressed corals can be identified by their tentacles being retracted (in the case of *S. glaucum* and *L. crassum*) or contracted/no longer pulsating (for *X. umbellata*). Additionally, we could differentiate them visually based on their color. $CuSO_4$ and DMP were the most toxic compounds to soft corals, followed by simazine, oxybenzone, and octinoxate. Not only the morphology was observed, but the organisms were evaluated also in terms of the number of zooxanthellae associated and the PSII efficiency. These approaches were used to monitor the occurrence of zooxanthellae-soft corals break down. The first stage of zooxanthellae-coral break down occurs when corals expel zooxanthellae from their bodies, resulting in a high density of zooxanthellae cells in the water column. The more zooxanthellae are expelled into the water, the lower the PSII efficiency detected on the soft corals umbrella. However, this is not always the case; for example, in samples of *S. glaucum* treated with glyphosate at a concentration of 10 mg/L, the PSII efficiency was higher after treatment than before treatment. Also, the morphology of soft corals exposed to glyphosate at a concentration of 10 mg/L resembled untreated corals. Corals treated with this concentration of glyphosate showed an appearance similar to healthy corals. There are two possible explanations: either glyphosate at this concentration acts as a fertilizer for zooxanthellae (due to the phosphorus content), or *S. glaucum* belongs to a

glyphosate-resistant organism. Therefore, to address this question, additional experiments with various concentrations of glyphosate were conducted (described in Chapter VII).

Furthermore, the biggest physical effect of microplastic was observed on *X. umbellata*, as its particles adhered to the tentacles of this soft coral species, resulting in tentacle damage. In *S. glaucum*, the effect of microplastics was evident from the coloration of the tentacles. It was clearly seen that the tentacles had lost their brown color, which is characteristic of zooxanthellae. Microplastic particles can attach to corals and may disrupt their symbiont's habitat, and further lead to zooxanthellae expulsion. However, further detailed testing is required to confirm this preliminary result.

After a five-day elicitation period, the individual soft corals were harvested to study their metabolite profiles. Untargeted ^{1}H-NMR and/or LC-MS metabolomics coupled with multivariate data analysis has been used as an appropriate analysis method. ^{1}H-NMR, for instance, is an effective technique for detecting and quantifying the major constituents of natural resource extracts, including primary and secondary metabolites. However, the low sensitivity precludes the detection of trace amounts of chemicals. In the studies presented here, only the change in the main metabolites could be detected by ^{1}H-NMR. It was able only to detect changes in fatty acids and/or lipids, as well as a few major components belonging to major species-specific compounds (Chapter IV). As complementary method to ^{1}H-NMR, the high sensitivity of LC-HRMS provides the detection of wide variety of secondary metabolites. However, certain compounds, even major ones, can have their ion formation suppressed during LC-MS analysis, while others can be easily ionized. Thus, the excessive visibility is primarily a limitation of MS. In addition, this method has other disadvantages including lack of quantifiability, low reproducibility and the possibility of batch effects in the data set. In this study (Chapter V), batch effects occurred during measurement due to technical reasons. These effects actually can be corrected by post-processing via batch correction, but this is an additional processing step, which has the possibility of introducing errors. Nevertheless, the combination of these techniques (^{1}H-NMR and LC-HRMS) is a powerful tool that enables a comprehensive assessment of soft coral metabolites following elicitation.

The principal component analysis (PCA) was used first to analyze the variation in metabolites between different soft coral species (Chapter IV), as well as the changes in metabolites in each soft coral after elicitor exposure (Chapter V and VII). PCA can assist in the reduction of large datasets (^{1}H-NMR and LC-HRMS data) derived from extracts and in the visualization of clusters and outliers. Furthermore, the PCA loading plot enables the determination of the NMR or MS signals of compounds that exhibit differences between groups. As previously stated (Chapter IV), *X. umbellata* is the most discriminated species based on ^{1}H-NMR-PCA and LC-MS-PCA analyses, and does not cluster with *S. glaucum* or *L. crassum*. This is to be expected, as this soft coral belongs to a different family (the phylogenetic data is shown in chapter II). Besides belonging to the different coral family,

other zooxanthellae associated with *X. umbellata* than with the other two coral species studied (Chapter II). *Symbiodinium glynnii* is the zooxanthellae species harbored in *X. umbellata*. This species is known as more stress-tolerant symbiont that contributes to the resilience of coral holobiont to the bleaching conditions in the first place [389-394]. As demonstrated in Chapter VII, the harbored zooxanthellae had a significant effect on the PSII efficiency measured in their host (*X. umbellata*) after glyphosate exposure, where by the PSII efficiency of these species was only slightly decreased in comparison to the two other soft coral species. Therefore, we conclude that the stress response of zooxanthellae, particularly in terms of photosystem II efficiency, is species-specific, whether caused by endosymbiont zooxanthellae or soft corals.

Due to the fact that *X. umbellata* is a member of a different family, and harbors zooxanthellae that are also different, it has a different metabolite profile (greater number of peaks) compared to *S. glaucum* and *L. crassum* (Chapter IV). Nitrogenous compounds, which include diterpene alkaloids, amino alcohol, ceramides, and betaine lipids were the predominant metabolites in *X. umbellata* extracts. Surprisingly, little research on the nitrogenous compounds in *X. umbellata* has been conducted. Therefore, this species is expected to contain novel natural products and should be prioritized for phytochemical research. The major compounds detected in *S. glaucum* (based on the LC-MS and ^{1}H-NMR and 2D NMR) were tentatively annotated as two diastereomers of sarcophytoxide, one of these also occurred in *L. crassum*, while in *X. umbellata* was a xeniolide O diterpene containing a 9-membered ring along with the betaine derivates

^{1}H-NMR- and LC-MS-PCA were performed to analyze the effect of elicitors on the metabolite composition of coral (Chapter V). For all three investigated coral specis, the extracts of soft corals after treated with DMP are clearly separated from the other extracts in the ^{1}H-NMR-based PCA. Besides DMP, the extracts of all soft corals treated with $CuSO_4$ were also significantly different from other extracts in the LC-MS-PCA. The composition of fatty acids and lipids, including phospholipids and betaine lipids, are the primary reason for this separation. The content of these substances in soft coral bodies were increased (based on ^{1}H-NMR data). The increase in the fatty acid content of corals' bodies during stress is related to the increased energy demand. Fatty acids and amino acids can be produced as an energy source for organisms under abiotic stress [144, 407, 435]. In both analyses, the major metabolites detected during the elicitation process were only fatty acids and lipids. A diterpene and steroidal alkaloid were detected as additional metabolites in *L. crassum* extracts treated with $CuSO_4$, which also resulted in separation of this group in LC-MS-PCA. The presence of these metabolites is probably linked to the antibacterial properties of this extracts. Extracts of *L. crassum* especially those after treated with $CuSO_4$ exhibited a strong activity even in low tested concentration against *A. fischeri* with an average IC50 value of 7.70 µg/mL (Chapter VI). This activity is classified as a relatively high activity for crude extracts,

which probably due to the content of the diterpene and steroidal alkaloid, which is already known as the antibacterial compounds.

More specifically, we evaluated the extract's growth inhibitory activity against *A. fischeri* and *B. subtilis*, as well as its cytotoxic activity against HT29 colon cancer and PC3 human prostate cancer cell lines (Chapter VI). According to the metabolite profiling results in Chapter IV, the majority of samples contain similar metabolites to the control (untreated samples). Therefore, the antibacterial assay was performed only on samples that were distinct from the control, which are samples treated with glyphosate, $CuSO_4$, and plasticizer. Along with untreated (control) soft corals extracts, these extracts were tested against both bacteria as well as on cancer cell lines. In contrast to the activity of *L. crassum* extracts described previously, *X. umbellata*, which exhibited a diverse array of peaks in the LC-HRMS spectra, demonstrated low activity against both tested bacteria. Nevertheless, those extracts act as a bacteriostatic agent against *A. fischeri* for up to 9 hours. It is possible that this coral contained contrasting metabolites that were on one hand extremely effective at inhibiting bacteria, but on the other hand served as growth promoter for them. However, the exact metabolites caused this activity is remain unknown. Therefore, further research, e.g. bioactivity guide isolation of secondary metabolites in this species of soft coral is northworthy.

In comparison to *A. fischeri* (Gram-negative bacteria), all extracts have a lower activity against *B. subtillis* (Gram-positive). In most cases, natural products are more effective at inhibiting Gram-positive bacteria than Gram-negative bacteria, owing to the fact that Gram-negative bacteria has two layer of cell membrane, making them more resistant. Interestingly, this phenomenon did not occur in this study. It is possible that the metabolites produced by soft corals, which are marine organisms, serve as a defense mechanism specifically against marine bacteria such as *A. fischeri*. To our knowledge, this is the first study to document the antibacterial properties of soft corals against the marine bacteria *A. fischeri*. However, the activity could be lower for fractions or isolated compounds. In most cases, the antibacterial and cytotoxic activity of fractions and isolated compounds is not as high as suggested by the activity of crude extracts [436, 437], or can be higher if caused by one compound. This could be due to additive or synergetic effects between the constituents in extracts, but other possible explanations cannot be ruled out. To substantiate this assertion, a test on isolated compounds from living soft corals would be noteworthy.

Glyphosate is used extensively worldwide, raising concerns about its toxicity to aquatic organisms, including corals and microalgae. Even though this herbicides have a negligible effect on humans, they continue to be a source of contention in society and among scientists in general. The effects of glyphosate on soft corals and their endosymbionts were investigated in detail for the first time in this thesis. According to the result in Chapter V, glyphosate has no effect on soft corals at a concentration of 10 mg/mL. Indeed, this concentration is already extremely high in comparison to the glyphosate concentration detected in the marine environment (ranged from 145 ng/L to 5.4 mg/L). Therefore, a more comprehensive study

was conducted to ascertain the concentration at which glyphosate was toxic to soft corals (Chapter VII). Six different glyphosate concentrations were tested on the soft coral *S. glaucum*, but only four lower concentrations on the other two soft coral species, as the consequence of limited coral materials. As a result, after two days of exposure, glyphosate at a concentration of 1 g/L killed the corals. Interestingly, the color of *S. glaucum* changed to a dark brown hue instead of fading after exposure to 100 mg/L, while the color changed to greenish after exposure to 50 mg/L. This is more likely due to the pigment production by zooxanthellae. However, the question arose: how are zooxanthellae able to produce pigments in response to two different concentrations of glyphosate (100 mg/L – dark brown; 50 mg/mL – greenish)? Glyphosate-induced damage to the photosynthetic apparatus and increased carotenoid production for ROS (reactive oxygen species) scavenging can be an explanation for this case, illustrated in the Figure 67.

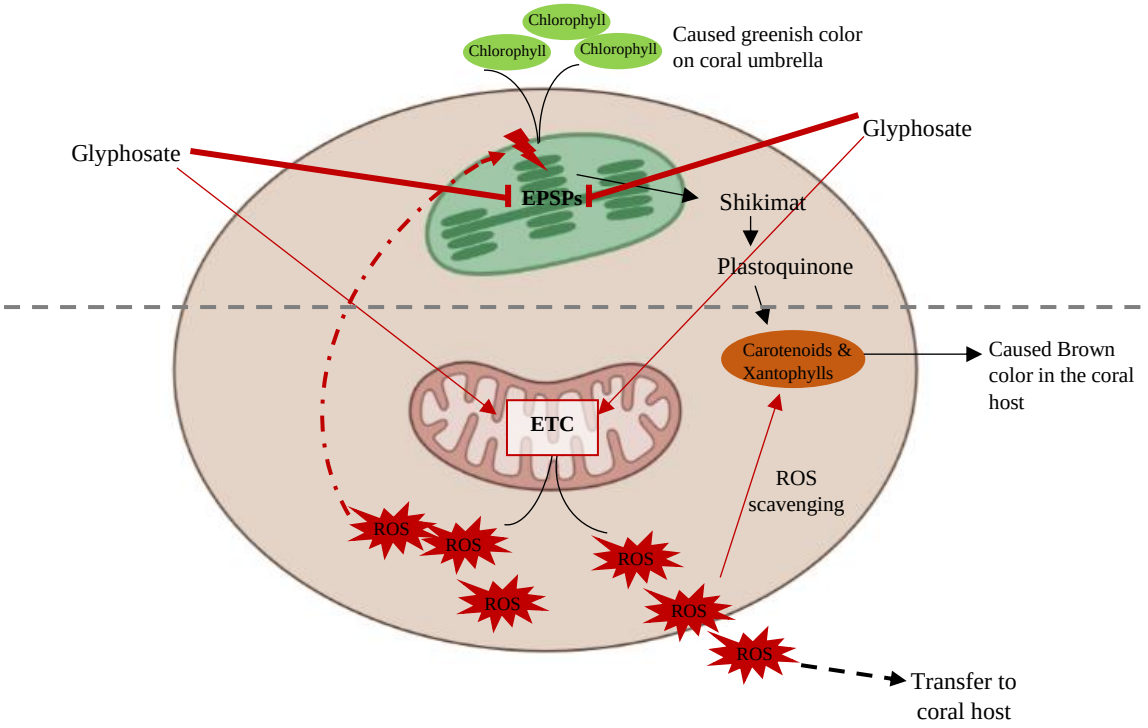

Figure 67 Illustration of glyphosate effects on the ROS and carotenoid level in a zooxanthellae cell

During exposure to glyphosate, the herbicide inhibits the mitochondrial electron transport chain, resulting in the formation of reactive oxygen species (ROS). ROS enter the chloroplast after being produced in the mitochondria and continue to cause oxidative damage to the photosynthesis apparatus. When the chloroplast is damaged, some of the chlorophyll in zooxanthellae cells is released and accumulates in the outer part of the cells, which was detected in the host tissue (umbrella part; the location of zooxanthellae). On the other hand, increase of ROS levels in the cell stimulates the production of carotenoids, which act as ROS scavengers to protect the cell. As a result, excessive carotenoids may be produced in the cells, and these substances are then transferred to the coral host body, where they are visualized as an intense brown color. In contrast to this, the pale color of soft corals can also be explained

by this mechanism. Apart from causing the death of zooxanthellae cells, glyphosate has an indirect effect on the carotenoid and xanthophyll levels in zooxanthellae. This process could be related to glyphosate-induced decreases in plastoquinone (PQ) biosynthesis as a result of inhibition of 5-enolpyruvylshikimate-3-phosphate (EPSP) synthase. Reduced PQ biosynthesis lead to decrease in the levels of carotenoid and xanthophyll in cells [379].

Furthermore, a variance in the metabolites composition of soft corals treated with different concentrations of glyphosate was observed. Due to the lack of difference in *L. crassum* and *X. umbellata* extracts exposed to glyphosate as determined by ^{1}H-NMR-PCA, multivariate analysis of ^{1}H-NMR data was performed only on *S. glaucum* data. According to ^{1}H-NMR-PCA, fatty acids, sarcophytolol, sarcophytoxide, and ent-sarcophyolide E were tentatively assigned as metabolites responsible for the differentiation of *S. glaucum* extracts treated with high glyphosate concentrations (1 g/L and 100 mg/L). Thus, this result is comparable to the one obtained using LC-HRMS. Similar to the ^{1}H-NMR result, lipids were tentatively assigned as the metabolites responsible for group segregation in LC-MS-PCA. Additionally, some diterpenes were detected as metabolites responsible for the separation of *L. crassum* extracts, which were increased after glyphosate exposure. The presence of diterpenes in soft coral species could be associated with their antibacterial activity against *A. fischeri*. Extracts of *L. crassum* treated with glyphosate at concentration of 50 mg/L exhibited extremely strong activity against *A. fischeri* at both concentrations tested (Chapter VII), which could be a result of the diterpene constituents of the extracts.

In addition to the investigation of the effect of elicitors on the physical and chemical profiles of soft corals, the stress experienced by soft corals following elicitation can be observed through histological examination (Chapter V). Corals, with the assistance of their endosymbiont, produce mucus as a defense mechanism during times of stress. Mucus was found in high concentrations on the tissue of soft corals infected with *Vibrio campbellii,* as well as after exposure to DMP and $CuSO_4$. It has been strongly confirmed that this mucus is produced by corals in order to protect themselves against pathogens and under adverse conditions. Furthermore, a similar approach was used to examine the spatial distribution of metabolites from soft corals and zooxanthellae within the coral body. Instead of the conventional histological profiling, the modern method, MALDI-MS Imaging were used in this study (Chapter IV). This is the first study utilizing MS-Imaging in order to investigate the distribution of soft corals and zooxanthellae metabolites within corals body. However, the experiment's process with soft corals was extremely difficult. First, not all three species of soft corals are suitable for embedding. We were unable to embed *X. umbellata* due to the non-compact characteristic of their body. Therefore, only *S. glaucum* and *L. crassum* were used in both studies. Second, difficulties occurred during the process of sectioning. The sclerites within the soft coral tissue were responsible for the damage to the slide during tissue section. Instead of forming a thin layer of tissue, the tissue section became powdered as a result of the severe damage. Finally, tissue sections with a thickness of 50 µm were the first

that did not cause structural damage. However, this tissue thickness is relatively high in comparison to other MALDI-MSI studies (thicknesses between 10 µm - 25 µm) [151-153]. As a compromise to the high thickness of the tissue, the double concentration of the DHB matrix (2,5-dihydroxybenzoic acid) was applied to facilitate metabolite ionization. In order to validate the performance of the experiment (i.e. no artifacts, good ionization, and clearly visible distribution of metabolites), the detection of zooxanthellae-specific metabolites in *S. glaucum* tissue was performed. By observing the pigment (pheophytin A and diatoxanthin) distribution in combination with microscopic images, we confirmed the suitability of the adapted method in this study, i.e. the tissue thickness, concentration of the matrix, as well as the chosen parameters for MALDI-MSI measurement.

In total 7 known compounds from soft corals and 4 known compounds from zooxanthellae were detected in the samples. The spatial distribution of each metabolite could also be distinguished. Utilizing this method may prove to be extremely beneficial as a guide for the isolation of targeted compounds within the body of soft corals. Additionally, by determining the spatial distribution of metabolites in the body of soft corals, we are able to know which metabolites are produced by soft corals or their symbiont and which metabolites are the "symbiosis product" of these two organisms. Such investigations may contribute to a better understanding of the interaction between soft corals and zooxanthellae, particularly in the biosynthesis of their secondary metabolites.

From the research presented here, there are still many unanswered questions that need to be addressed. In addition, there are a few points that need to be modified for further (future) research, including: 1) The coral used should have been grown in the ocean, as aquarium corals may have lost the ability to make defense metabolites against predators. 2) A thorough study under real environmental conditions, i.e., the duration of elicitation could be longer than five days at a reasonable concentration, 3) Isolation of metabolites (bioactivity guide isolation) of secondary metabolites for soft corals being studied, especially *Xenia umbellata*; 4) Method development for LC-HRMS analysis (negative ion mode) and MALDI-MSI, particularly for the sectioning process, in order to prevent smearing and damage to the coral tissue.

Nevertheless, this thesis contributes to major understanding of the complexity of soft corals-zooxanthellae relationship, focusing on their secondary metabolites in response to environmental stressors. The application of advanced analytical techniques, such as NMR and LC-MS, in conjunction with multivariate data analysis, provides in-depth insight into the various levels of metabolites produced by stress in soft corals. The methods described in this work can also be used to analyze other natural sources of metabolites. The information contained in this thesis can be used to ascertain the valuable properties of soft coral extracts, determine marker compounds that distinguish soft corals from zooxanthellae, and to identify targets for future coral-chemistry investigations.

References

1. Blunt, J.W., B.R. Copp, R.A. Keyzers, M.H.G. Munroa, and M.R. Prinsep, Marine natural products. *Natural Product Reports*, 2012. 29(2): p. 144-222.
2. Christensen, V., D. Pauly, and X. He, Coral reef and other tropical fisheries, in *Encyclopedia of Ocean Sciences* (Third Edition), J.K. Cochran, H.J. Bokuniewicz, and P.L. Yager, Editors. 2019, Academic Press: Oxford. p. 320-323.
3. Chanmethakul, T., H. Chansang, and S. Watanasit, Soft coral (Cnidaria: Alcyonacea) distribution patterns in Thai waters. *Zoological Studies*, 2010. 49: p. 72-84.
4. Rocha, J., R. Calado, and M. Leal, Marine bioactive compounds from Cnidarians, in *Springer Handbook of Marine Biotechnology*, S.-K. Kim, Editor. 2015, Springer Berlin Heidelberg: Berlin, Heidelberg. p. 823-849.
5. Blunt, J.W., B.R. Copp, R.A. Keyzers, M.H. G. Munroa, and M.R. Prinsep, Marine natural products. *Natural Product Reports*, 2014. 31(2): p. 160-258.
6. Ahmed, A.F., A.F. Ahmed, Y. Chen, C. Huang, Y. Tseng, C. Lin , C. Dai, Y. Wu, and J. Sheu, Isolation and structure elucidation of cembranoids from a Dongsha Atoll soft coral *Sarcophyton stellatum*. *Marine Drugs*, 2018. 16(6).
7. Al-Lihaibi, S.S., A. Abdel-Lateff, W.M. Alarif, H.S. Alorfi, Y. Nogata, and T. Okino, Environmentally friendly antifouling metabolites from Red Sea organisms. *Journal of Chemistry*, 2019. 2019.
8. Bawakid, N.O., W.M. Alarif, and A. Abdel-Lateff, Rare norisodinosterol derivatives from *Xenia umbellata*: Isolation and anti-proliferative activity. *Open Chemistry*, 2021. 19(1).
9. Chao, C.-H., H.C. Huang, Y. Wu, C.K. Lu, C.F. Dai, and J.H Sheu, Glycolipids from the formosan soft coral *Lobophytum crassum*. *Chemical and Pharmaceutical Bulletin*, 2007. 55(12).
10. Chao, C.-H., W.-L. Li, C.-Y. Huang, A.F. Ahmed, C.-F. Dai, Y.C. Wu, M.C. Lu, C.C. Liaw, and J.H. Sheu, Isoprenoids from the soft coral *Sarcophyton glaucum*. *Marine Drugs*, 2017. 15(7).
11. Cheng, S.-Y., S.-K. Wang, S.-F. Chiou, C.-H. Hsu, C.-F. Dai, et al., Cembranoids from the Octocoral *Sarcophyton ehrenbergi*. *Journal of Natural Products*, 2010. 73(2).
12. Cheng, S.-Y., Z.-H. Wen, S.-F. Chiou, C.-W. Tsai, S.-K. Wang, and C.Y. Duh, Ceramide and cerebrosides from the Octocoral *Sarcophyton ehrenbergi*. *Journal of Natural Products*, 2009. 72(3).
13. Cuong, N.X., N.P. Thao, B.T.T. Luyen, N.T.T. Ngan, D.T.T. Thuy, S.B. Song, N.H. Nam, P.V. Kiem, Y.H. Kim, and C.V. Minh, Cembranoid diterpenes from the soft coral *Lobophytum crassum* and their anti-inflammatory activities. *Chemical and Pharmaceutical Bulletin*, 2014. 62(2).
14. El-Gamal, A.A.H., S.-K. Wang, and C.-Y. Duh, Umbellactal, a novel diterpenoid from the formosan soft coral *Xenia umbellata*. *Tetrahedron Letters*, 2005. 46(36).
15. El-Gamal, A.A.H., S.-K. Wang, and C.-Y. Duh, Xenibellal, a novel norditerpenoid from the formosan soft coral *Xenia umbellata*. *Tetrahedron Letters*, 2005. 46(26): p. 4499-4500.
16. Iwagawa, T., K. Hashimoto, H. Okamura, J.-I Kurawaki, M. Nakatani, D.X. Hou, M. Fujii, M. Doe, Y. Morimoto, and K. Takemura, Biscembranes from the soft coral *Sarcophyton glaucum*. *Journal of Natural Products*, 2006. 69(8).
17. Kashman, Y., E. Zadock, and L. Néeman, Some new cembrane derivatives of marine origin. *Tetrahedron Letters*, 1974. 30(19).
18. Kobayashi, M., T. Hayashi, K. Hayashi, M. Tanabe, T. Nakagawa, and H. Mitsuhashi, Marine Sterols. XI. Polyhydroxysterols of the soft coral *Sarcophyton glaucum*: Isolation and Synthesis of 5α;-Cholestane-1β, 3β, 5, 6β-tetrol. *Chemical and Pharmaceutical Bulletin*, 1983. 31(6).
19. Peng, B.-R., M.-C. Lu, M. El-Shazly, S.-L. Wu, K.-H. Lai, and J.H. Su, Aquaculture soft coral *Lobophytum crassum* as a producer of anti-proliferative cembranoids. *Marine Drugs*, 2018. 16(1).

20. Thao, N.P., B.T.T. Luyen, N.T.T. Ngan, S.B. Song, N.X. Cuong, N.H. Nam, P.V. Kiem, Y.H. Kim, and C.V. Minh , New anti-inflammatory cembranoid diterpenoids from the Vietnamese soft coral *Lobophytum crassum*. *Bioorganic and Medicinal Chemistry Letters*, 2014. 24(1).
21. Yin, S.-W., Y.-P. Shi, X.-M. Li, and B.-G. Wang, A new cembranoid diterpene and other related metabolites from the South-China-Sea soft coral *Lobophytum crassum*. *Helvetica Chimica Acta*, 2006. 89(3).
22. Zhang, C.-X., X.-X. He, J. Zhang, Q. Guo, L.-F. Lei, et al., New precursor of tetraterpenoids from the soft coral *Sarcophyton glaucum*. *Natural Product Research*, 2013. 27(9).
23. Liang, L.F. and Y.W. Guo, Terpenes from the soft corals of the genus *Sarcophyton*: Chemistry and biological activities. *Chemistry and Biodiversity*, 2013. 10(12).
24. Lai, K.-H., W.-J. You, C-C. Lin, M. El-Shazly, Z.-J. Liao, and J.H. Su, Anti-inflammatory cembranoids from the soft coral *Lobophytum crassum*. *Marine Drugs*, 2017. 15(10).
25. Ng, S., C.-S. Phan, T. Ishii, T. Kamada, T. Hamada, and C.S. Vairappan, Terpenoids from marine soft coral of the Genus *Xenia* in 1977 to 2019. *Molecules*, 2020. 25.
26. Abou El-Kassem, L.T., U.W. Hawas, S.K. El-Desouky, and R. Al-Farawati, Sesquiterpenes from the Saudi Red Sea: *Litophyton arboreum* with their cytotoxic and antimicrobial activities. *Zeitschrift für Naturforschung*, 2018. 73(1-2).
27. Ben, H., Y. Sawall, A. Abdullah, A.A. Al-Sofyani, and M. Wahl, Chemical versus structural defense against fish predation in two dominant soft coral species (Xeniidae) in the Red Sea. *Aquatic Biology*, 2015. 23.
28. Duh, C.-Y., A.A.H. El-Gamal, C.-Y. Chiang, C.-J. Chu, S.-K. Wang, and C.F. Dai, New cytotoxic xenia diterpenoids from the formosan soft coral *Xenia umbellata*. *Journal of Natural Products*, 2002. 65(12).
29. Lages, B.G., B.G. Fleury, C.E.L. Ferreira, and R.C. Pereira., Chemical defense of an exotic coral as invasion strategy. *Journal of Experimental Marine Biology and Ecology*, 2006. 328(1).
30. Hoegh-Guldberg, O., P.J. Mumby, A.J. Hooten, R.S. Steneck, P. Greenfield, E. Gomez, C.D. Harvell, P.F. Sale, A.J. Edwards, K. Caldeira, N. Knowlton, C.M. Eakin, R. Iglesias-Prieto, N. Muthiga, R.H. Bradbury, A. Dubiand, and M.E. Hatziolos, Coral reefs under rapid climate change and ocean acidification. *Science*, 2007. 318(5857).
31. Knowlton, N., R.E. Brainard, R. Fisher, M. Moews, L. Plaisance, and M.J. Caley, Coral reef biodiversity, Chapter 4: Coral reef biodiversity, in life in the world's oceans. 2010. p. 65-78.
32. Knowlton, N. and C. Jackson, The Ecology of coral reefs. 2001. P.395-422.
33. Hughes, T.P., K.D. Anderson, S.R. Connolly, S.F.Heron, J.T. Kerry, Spatial and temporal patterns of mass bleaching of corals in the Anthropocene. *Science*, 2018. 359(6371).
34. Spalding, M. and B. Brown, Warm-water coral reefs and climate change. *Science*, 2015. 350.
35. Spalding, M., C. Ravilious, and E.P. Green, World atlas of coral reefs. 2001.
36. van Dam, J., A.P. Negri, S. Uthicke, and J.F. Mueller, Chemical pollution on coral reefs: Exposure and ecological effects. 2011. 25. p. 187-211
37. Downs, C.A., E. Kramarsky-Winter, R. Segal, J. Fauth, S. Knutson, O. Bronstein, F.R. Ciner, R. Jeger, Y. Lichtenfeld, C.M. Woodley, P. Pennington, K. Cadenas, A. Kushmaro, and Y. Loya, Toxicopathological effects of the sunscreen UV Filter, oxybenzone (benzophenone-3), on coral planulae and cultured primary cells and its environmental contamination in Hawaii and the U.S. Virgin Islands. *Archives of Environmental Contamination and Toxicology*, 2016. 70(2).
38. Giokas, D.L., A. Salvador, and A. Chisvert, UV filters: From sunscreens to human body and the environment. *Trends in Analytical Chemistry*, 2007. 26(5).
39. NOAA, Skincare Chemicals and Coral Reefs. 2021. Access: January 2022
40. Lewis, S.E., J. E. Brodie, Z.T. Bainbridge, K.W. Rohde, A.M. Davis, B. L. Masters, M. Maughan, M.J. Devlin, J.F. Mueller, and B. Schaffelke, Herbicides: a new threat to the Great Barrier Reef. *Environmental Pollution*, 2009. 157(8-9).
41. Mitchell, C., J. Brodie, and I. White, Sediments, nutrients and pesticide residues in event flow conditions in streams of the Mackay Whitsunday Region, Australia. *Marine Pollution Bulletin*, 2005. 51(1-4).

42. Ali, A.-h.A.M., M.A. Hamed, and H. Abd El-Azim, Heavy metals distribution in the coral reef ecosystems of the Northern Red Sea. *Helgoland Marine Research*, 2011. 65(1).
43. Hwang, J.-S., H.-U. Dahms, K.L. Huang, M.-Y. Huang, X.-J. Liu, J.S. Khim, and C.K. Wong, Bioaccumulation of trace metals in octocorals depends on age and tissue compartmentalization. *PLOS ONE*, 2018. 13(4).
44. Hall, N., K.L.E. Berry, L. Rintoul, and M.O. Hoogenboom, Microplastic ingestion by scleractinian corals. *Marine Biology*, 2015. 162.
45. Hankins, C., A. Duffy, and K. Drisco, Scleractinian coral microplastic ingestion: Potential calcification effects, size limits, and retention. *Marine pollution bulletin*, 2018. 135.
46. Saliu, F., S. Montano, B. Leoni, M. Lasagni, and P. Galli, Microplastics as a threat to coral reef environments: Detection of phthalate esters in neuston and scleractinian corals from the Faafu Atoll, Maldives. *Marine Pollution Bulletin*, 2019. 142.
47. Nice, E.C., Challenges for omics technologies in the implementation of personalized medicine. *Expert Review of Precision Medicine and Drug Development*, 2018. 3(4).
48. Ning, M. and E.H. Lo, Opportunities and challenges in omics. *Translational Stroke Research*, 2010. 1(4).
49. Pinu, F.R., S.A. Goldansaz, and J. Jaine, Translational metabolomics: Current challenges and future opportunities. *Metabolites*, 2019. 9(6).
50. Joyce, A.R. and B.Ø. Palsson, The model organism as a system: integrating 'omics' data sets. *Nature Reviews Molecular Cell Biology*, 2006. 7(3).
51. Álvarez-Sánchez, B., F. Priego-Capote, and M.D.L. de Castro, Metabolomics analysis I. Selection of biological samples and practical aspects preceding sample preparation. *Trends in Analytical Chemistry*, 2010. 29(2).
52. Bundy, J.G., M.P. Davey, and M.R. Viant, Environmental metabolomics: a critical review and future perspectives. *Metabolomics*, 2008. 5(1).
53. Viant, M.R., Recent developments in environmental metabolomics. *Molecular BioSystems*, 2008. 4(10).
54. Larsen, P.E. and Y. Dai, Metabolome of human gut microbiome is predictive of host dysbiosis. *Gigascience*, 2015. 4.
55. Trivedi, D.K., K.A. Hollywood, and R. Goodacre, Metabolomics for the masses: The future of metabolomics in a personalized world. *New Horizons in Translational Medicine*, 2017. 3(6).
56. Farag, M.A., A. Porzel, M.A. Al-Hammady, M.-E. F. Hegazy, A. Meyer, T.A. Mohamed, H. Westphal, and L.A. Wessjohann, Soft corals biodiversity in the Egyptian Red Sea: A comparative MS and NMR metabolomics approach of wild and aquarium grown species. *Journal of Proteome Research*, 2016. 15(4).
57. Santacruz, L., D.X. Hurtado, R. Doohan, O.P. Thomas, M. Puyana, and E. Tello, Metabolomic study of soft corals from the Colombian Caribbean: PSYCHE and ^{1}H-NMR comparative analysis. *Scientific Reports*, 2020. 10(1).
58. Farag, M.A., D.A. Al-Mahdy, A. Meyer, H. Westphal, and L.A. Wessjohann, Metabolomics reveals biotic and abiotic elicitor effects on the soft coral *Sarcophyton ehrenbergi* terpenoid content. *Scientific Reports*, 2017. 7(1).
59. Farag, M.A., A. Meyer, and S.E. Ali, Bleaching effect in *Sarcophyton* spp. soft corals-is there a correlation to their diterpene content. *Environmental Science and Pollution Research (international)*, 2021. 28(20).
60. Farag, M.A., A.A. Maamoun, A. Meyer, and L.A. Wessjohann, Salicylic acid and its derivatives elicit the production of diterpenes and sterols in corals and their algal symbionts: a metabolomics approach to elicitor SAR. *Metabolomics*, 2018. 14(10).
61. van der Greef, J., P. Stroobant, and R. van der Heijden, The role of analytical sciences in medical systems biology. *Current Opinion in Chemical Biology*, 2004. 8(5).
62. Patel, K.N., J.K. Patel, M.P. Patel, G.C. Rajput, and H.A. Patel, Introduction to hyphenated techniques and their applications in pharmacy. *Pharmaceutical Methods*, 2010. 1(1).
63. Worley, B. and R. Powers, Multivariate analysis in metabolomics. *Current Metabolomics*, 2013. 1(1).

64. Fingas, M., Chapter 5 - Remote sensing for marine management, in World Seas: an Environmental evaluation (Second edition), C. Sheppard, Editor. 2019, Academic Press. p. 103-119.
65. Reaka-Kudla, M.L., D.E. Wilson, and E. Wilson. The global biodiversity of coral reefs: A comparison with rain forests. 1997.
66. Kusumoto, B., M.J. Costello, Y. Kubota, T. Shiono, C.-L. Wei, M. Yasuhara, and A. Chao, Global distribution of coral diversity: Biodiversity knowledge gradients related to spatial resolution. *Ecological Research*, 2020. 35.
67. Veron, J.E.N., Corals of the world. Townsville: *Australian Institute of Marine Science*, 2000. 1-3.
68. Hughes, T.P., J.T. Kerry, M. Álvarez-Noriega, J.G. Álvarez-Romero, K.D. Anderson, et al., Global warming and recurrent mass bleaching of corals. *Nature*, 2017. 543(7645).
69. Hoegh-Guldberg, O., Low coral cover in a high-CO_2 world. *Journal of Geophysical Research: Oceans*, 2005. 110(C9).
70. Hoegh-Guldberg, O., E.V. Kennedy, H.L. Beyer, C. McClennen, H.P. Possingham, Securing a long-term future for coral reefs. *Trends in Ecology and Evolution*, 2018. 33(12).
71. Wilkinson, C., Status of coral reefs of the world: 2000. 2000: *Australian Institute of Marine Science*.
72. Costanza, R., R. d'Arge, R. de Groot, S. Farber, M. Grasso, B. Hannon, K. Limburg, S. Naeem, R.V. O'Neill, J. Paruelo, R.G. Raskin, P. Sutton, and M. van den Belt, The value of the world's ecosystem services and natural capital. *Nature*, 1997. 387(6630).
73. Rivera, H., A. Chan, and V. Luu, Coral reefs are critical for our food supply, tourism, and ocean health. We can protect them from climate change. *MIT Science Policy Review*, 2020. 1.
74. Woodhead, A.J., C.C. Hicks, A.V. Norström, G.J. Williams, and N.A.J. Graham, Coral reef ecosystem services in the Anthropocene. *Functional Ecology*, 2019. 33(6).
75. Fabricius, K. and P. Alderslade, Soft corals and sea fans: A comprehensive guide to the tropical shallow water genera of the central-west Pacific, the Indian Ocean and the Red Sea. 2001.
76. Benayahu, Y. Reproduction and developmental pathways of Red Sea Xeniidae (Octocorallia, Alcyonacea). in Coelenterate Biology: Recent Research on Cnidaria and Ctenophora. 1991. Dordrecht: Springer Netherlands.
77. Benayahu, Y. and Y. Loya, Life history studies on the Red Sea soft coral *Xenia macrospiculata* Gohar, 1940. II. Planulae shedding and post larval development. The Biological bulletin, 1984. 166.
78. Fabricius, K. and M. Dommisse, Depletion of suspended particulate matter over coastal reef communities dominated by zooxanthellate soft corals. *Marine Ecology-progress Series*, 2000. 196.
79. Ribes, M., R. Coma, and J.-M. Gili, Heterotrophic feeding by gorgonian corals with symbiotic zooxanthella. *Limnology and Oceanography*, 1998. 43(6).
80. Muller-Parker, G., C.F. D'Elia, and C.B. Cook, Interactions between corals and their symbiotic algae, in coral reefs in the Anthropocene, C. Birkeland, Editor. 2015, Springer Netherlands: Dordrecht. p. 99-116.
81. Yellowlees, D., T.A. Rees, and W. Leggat, Metabolic interactions between algal symbionts and invertebrate hosts. *Plant, Cell, and Environment*, 2008. 31(5).
82. Verseveldt, Revision of the genus *Sarcophyton* Lesson (Octocorallia, Alcyonacea). 1982, Leiden, The Netherlands: Brill.
83. Aratake, S., T. Tomura, S. Saitoh, R. Yokokura, Y. Kawanishi, R. Shinjo, J.D. Reimer, J. Tanaka, and H. Maekawa, Soft coral *Sarcophyton* (Cnidaria: Anthozoa: Octocorallia) species diversity and chemotypes. *PLOS ONE*, 2012. 7(1).
84. Chavanich, S., V. Viyakarn, T. Loyjiw, P. Pattaratamrong, and A. Chankong, Mass bleaching of soft coral, *Sarcophyton* spp. in Thailand and the role of temperature and salinity stress. *ICES Journal of Marine Science*, 2009. 66(7).
85. Rao, D. and K. Devi, Studies on the soft corals (Octocorallia: Alcyonacea) of Andaman Islands, Bay of Bengal. *Records of Zoological Survey of India* (Occasional Paper No.), 2003. 206.

86. Tentori, E. and L.P. van Ofwegen, Patterns of distribution of calcite crystals in soft corals sclerites. *Journal of Morphology*, 2011. 272(5).
87. Kremien, M., U. Shavit, T.Mass, and A. Genin, Benefit of pulsation in soft corals. *Proceedings of the National Academy of Sciences*, 2013. 110(22).
88. Halász, A., C.S. McFadden, R. Toonen, and Y. Benayahu, Re-description of type material of *Xenia* Lamarck, 1816 (Octocorallia: Xeniidae). *Zootaxa*, 2019. 4652(2): p. zootaxa.4652.2.1.
89. Kumar, S., G. Stecher, M. Li, C. Knyaz, and K. Tamura, MEGA X: Molecular evolutionary genetics analysis across computing platforms. *Molecular Biology and Evolution*, 2018. 35(6).
90. Ateweberhan, M., D.A. Feary, S. Keshavmurthy, A. Chen, M.H. Schleyer, and C.R.C. Shepparda, Climate change impacts on coral reefs: synergies with local effects, possibilities for acclimation, and management implications. *Marine Pollution Bulletin*, 2013. 74(2).
91. Brodie, J. and M. Landos, Pesticides in Queensland and Great Barrier Reef waterways - potential impacts on aquatic ecosystems and the failure of national management. *Estuarine, Coastal and Shelf Science*, 2019. 230.
92. Danovaro, R., L. Bongiorni, C. Corinaldesi, D. Giovannelli, E. Damiani, P. Astolfi, L. Greci, and A. Pusceddu, Sunscreens cause coral bleaching by promoting viral infections. *Environmental Health Perspectives*, 2008. 116(4).
93. Doney, S.C., V.J. Fabry, R.A. Feely, and J.A. Kleypas, Ocean Acidification: The other CO_2 problem. *Annual Review of Marine Science*, 2009. 1(1).
94. Ianora, A. and A. Miralto, Toxigenic effects of diatoms on grazers, phytoplankton and other microbes: a review. *Ecotoxicology*, 2010. 19(3).
95. Jones, R.J., O. Hoegh-Guldberg, A.W.D. Larkum, and U. Schreiber, Temperature-induced bleaching of corals begins with impairment of the CO_2 fixation mechanism in zooxanthellae. *Plant, Cell, and Environment*, 1998. 21(12).
96. Dawson, T.P., S.T. Jackson, J.I. House, I.C. Prentice, and G.M. Mace, Beyond predictions: biodiversity conservation in a changing climate. *Science*, 2011. 332(6025).
97. Hughes, T.P., J.T. Kerry, A.H. Baird, S.R. Connolly, A. Dietzel, et al., Global warming transforms coral reef assemblages. *Nature*, 2018. 556(7702).
98. Doney, S.C., M. Ruckelshaus, J.E. Duffy, J.P. Barry, F. Chan, C.A. English, H.M. Galindo, J.M. Grebmeier, A.B. Hollowed, N. Knowlton, J. Polovina, N.N. Rabalais, W.J. Sydeman, and L.D. Talley, Climate change impacts on marine ecosystems. *Annual Review of Marine Science*, 2012. 4(1).
99. Hoegh-Guldberg, O., Climate change, coral bleaching and the future of the world's coral reefs. *Marine and Freshwater Research*, 1999. 50(8).
100. Hoegh-Guldberg, O., The Ocean. In: Climate Change 2014: Impacts, Adaptation, and Vulnerability. Part B: Regional Aspects. Contribution of Working Group II to the Fifth Assessment Report of the Intergovernmental Panel on Climate Change [Barros, V.R., C.B. Field, D.J. Dokken, M.D. Mastrandrea, K.J. Mach, T.E. Bilir, M. Chatterjee, K.L. Ebi, Y.O. Estrada, R.C. Genova, B. Girma, E.S. Kissel, A.N. Levy, S. MacCracken, P.R. Mastrandrea, and L.L. White (eds.)]. Cambridge University Press, Cambridge, United Kingdom and New York, NY, USA, 2014: p. 1655-1731.
101. de Putron, S.J., D.C. McCorkle, A.L. Cohen, and A.B. Dillon, Seawater carbonate chemistry and weight of two Atlantic corals Favia Frau and Porites astreoides during experiments, 2011, in Supplement to: de Putron, SJ et al. (2011): The impact of seawater saturation state and bicarbonate ion concentration on calcification by new recruits of two Atlantic corals. Coral Reefs, 30(2), 321-328. 2011, Pangaea.
102. Pandolfi, J.M., S.R. Connolly, D.J. Marshall, and A.L. Cohen, Projecting coral reef futures under global warming and ocean acidification. *Science*, 2011. 333(6041).
103. Ries, J., A. Cohen, and D. McCorkle, Marine calcifiers exhibit mixed responses to CO_2-induced ocean acidification. *Geology*, 2009. 37.
104. Rodolfo-Metalpa, R., S. Martin, C. Ferrier-Pagès, and J.-P. Gattuso, Response of the temperate coral *Cladocora caespitosa* to mid- and long-term exposure to pCO_2 and temperature levels projected for the year 2100 AD. *Biogeosciences Discussions*, 2009. 6.
105. Hoadley, K.D., D. T. Pettay, A.G. Grottoli, W.-J. Cai, T.F. Melman, V. Schoepf, X. Hu, Q. Li, H. Xu, Y. Wang, Y. Matsui, J.H. Baumann, and M.E. Warner, Physiological response to

elevated temperature and pCO_2 varies across four Pacific coral species: Understanding the unique host+symbiont response. *Scientific Reports*, 2015. 5(1).
106. Bruno, J.F. and E.R. Selig, Regional decline of coral cover in the Indo-Pacific: Timing, extent, and subregional comparisons. *PLOS ONE*, 2007. 2(8).
107. De'ath, G., K.E. Fabricius, H. Sweatman, and M. Puotinen, The 27–year decline of coral cover on the Great Barrier Reef and its causes. *Proceedings of the National Academy of Sciences*, 2012. 109(44).
108. Kroon, F.J., B. Schaffelke, and R. Bartley, Informing policy to protect coastal coral reefs: Insight from a global review of reducing agricultural pollution to coastal ecosystems. *Marine Pollution Bulletin*, 2014. 85(1).
109. Müller, J., S. Duquesne, J.C. Ng, G.K. Eaglesham, K. Krrishnamohan, K. Manonmanii, M. Hodge, and G.K. Eaglesham, Pesticides in sediments from Queensland irrigation channels and drains. *Marine Pollution Bulletin*, 2000. 41(7).
110. Haynes, D., J. Mueller, and S. Carter, Pesticide and herbicide residues in sediments and seagrasses from the Great Barrier Reef World Heritage Area and Queensland Coast. *Marine Pollution Bulletin*, 2000. 41.
111. Schaffelke, B., J. Mellors, and N. Duke, Water quality in the Great Barrier Reef region: Responses of mangrove, seagrass and macroalgal communities. *Marine pollution bulletin*, 2005. 51.
112. Ainsworth, T.D., L. Krause, T. Bridge, G. Torda, J.-B. Raina, et al., The coral core microbiome identifies rare bacterial taxa as ubiquitous endosymbionts. *The ISME Journal*, 2015. 9(10).
113. Thompson, J.R., H.E. Rivera, C.J. Closek, and M. Medina, Microbes in the coral holobiont: partners through evolution, development, and ecological interactions. *Frontiers in Cellular and Infection Microbiology*, 2015. 4(176).
114. Rosenberg, E., O. Koren, L. Reshef, R. Efrony, and I. Zilber-Rosenberg, The role of microorganisms in coral health, disease and evolution. *Nature Reviews Microbiology*, 2007. 5(5).
115. Randall, C.J. and R. van Woesik, Contemporary white-band disease in Caribbean corals driven by climate change. *Nature Climate Change*, 2015. 5(4).
116. Raymundo, L.J., C.D. Harvell, and T.L. Reynolds, Porites ulcerative white spot disease: description, prevalence, and host range of a new coral disease affecting Indo-Pacific reefs. *Diseases of Aquatic Organisms*, 2003. 56(2).
117. Ritchie, K. and G. Smith, Preferential carbon utilization by surface bacterial communities from water mass, normal, and white-band diseased *Acropora cervicornis*. *Molecular marine biology and biotechnology*, 1995. 4.
118. Sheridan, C., E. Kramarsky-Winter, M. Sweet, A. Kushmaro, and M.C. Leal, Diseases in coral aquaculture: causes, implications and preventions. *Aquaculture*, 2013. 396-399.
119. Sussman, M., B.L. Willis, S. Victor, and D.G. Bourne, Coral pathogens identified for white syndrome (WS) epizootics in the Indo-Pacific. *PLOS ONE*, 2008. 3(6).
120. Cambiaghi, A., M. Ferrario, and M. Masseroli, Analysis of metabolomic data: tools, current strategies and future challenges for omics data integration. *Briefings in Bioinformatics*, 2017. 18(3).
121. Roberts, L.D., A.L. Souza, R.E. Gerszten, and C.B. Clish, Targeted Metabolomics. *Current Protocols in Molecular Biology*, 2012. 98(1).
122. Dunn, S.R., M.C. Thomas, G.W. Nette, and S.G. Dove, A lipidomic approach to understanding free fatty acid lipogenesis derived from dissolved inorganic carbon within cnidarian-dinoflagellate symbiosis. *PLOS ONE*, 2012. 7(10).
123. Sogin, E.M., H. Putnam, P. Anderson, and R.D. Gates, Metabolomic signatures of increases in temperature and ocean acidification from the reef-building coral, *Pocillopora damicornis*. Metabolomics, 2016. 12(4).
124. Wolfender, J.-L., G. Marti, A. Thomas, and S. Bertrand, Current approaches and challenges for the metabolite profiling of complex natural extracts. *Journal of Chromatography A*, 2015. 1382.

125. Goodacre, R., D. Broadhurst, A.K. Smilde, B.S. Kristal, J.D. Baker, et al., Proposed minimum reporting standards for data analysis in metabolomics. *Metabolomics*, 2007. 3(3).
126. Gika, H.G., I.D. Wilson, and G.A. Theodoridis, LC-MS-based holistic metabolic profiling. Problems, limitations, advantages, and future perspectives. *Journal of Chromatography B: Analytical Technologies in the Biomedical and Life Sciences*, 2014. 966.
127. Kim, H.K., Y.H. Choi, and R. Verpoorte, NMR-based plant metabolomics: where do we stand, where do we go? *Trends in Biotechnology*, 2011. 29(6).
128. France, S.C. and L.L. Hoover, DNA sequences of the mitochondrial COI gene have low levels of divergence among deep-sea octocorals (Cnidaria: Anthozoa). *Hydrobiologia*, 2002. 471(1).
129. Sánchez, J.A., C.S. McFadden, S.C. France, and H.R. Lasker, Molecular phylogenetic analyses of shallow-water Caribbean octocorals. *Marine Biology*, 2003. 142(5).
130. Kearse, M., R. Moir, A. Wilson, S. Stones-Havas, M. Cheung, S. Sturrock, S. Buxton, A. Cooper, S. Markowitz, C. Duran, T. Thierer, B. Ashton, P. Meintjes, and A. Drummond, Geneious Basic: an integrated and extendable desktop software platform for the organization and analysis of sequence data. *Bioinformatics*, 2012. 28(12).
131. Katoh, K., J. Rozewicki, and K.D. Yamada, MAFFT online service: multiple sequence alignment, interactive sequence choice and visualization. *Briefings in Bioinformatics*, 2017. 20(4).
132. LaJeunesse, T.C. and D.J. Thornhill, Improved resolution of reef-coral endosymbiont (Symbiodinium) species diversity, ecology, and evolution through psbA non-coding region genotyping. *PLOS ONE*, 2011. 6(12).
133. Matsuo, K., H. Ota, T. Akamatsu, A. Sugiyama, and T. Katsuyama, Histochemistry of the surface mucous gel layer of the human colon. *Gut*, 1997. 40(6).
134. Corrêa dos Santos, C.H., M.G. Carvalho, K. Franke, and L.A. Wessjohann, Dammarane-type triterpenoids from the stem of Ziziphus glaziovii Warm. (Rhamnaceae). *Phytochemistry*, 2019. 162.
135. Porzel, A., M.A. Farag, J. Mülbradt, and L.A. Wessjohann, Metabolite profiling and fingerprinting of *Hypericum* species: a comparison of MS and NMR metabolomics. *Metabolomics*, 2014. 10(4).
136. Shaaban, M., M.A. Ghani, and K.A. Shaaban, Unusual pyranosyl cembranoid diterpene from *Sarcophyton trocheliophorum*. *Zeitschrift für Naturforschung B*, 2016. 71(12).
137. Abdelkarem, F.M., E.K. Desoky, A.M. Nafady, A.E. Allam, A. Mahdy, M. Nagata, T. Miyamoto, and K. Shimizu, Isolation of new secondary metabolites from gorgonian soft coral *Heteroxenia fuscescens* collected from Red Sea. *Phytochemistry Letters*, 2020. 36.
138. Duh, C.-Y., S.-C. Chien, P.-Y. Song, S.-K. Wang, A.A.H. El-Gamal, and C.F. Dai, New cadinene sesquiterpenoids from the formosan soft coral *Xenia puerto*-galerae. *Journal of Natural Products*, 2002. 65(12).
139. Edrada, R.A., V. Wray, L. Witte, L. van Ofwegen and P. Proksch, Bioactive terpenes from the soft coral *Heteroxenia* sp. from Mindoro, Philippines. Z*eitschrift für Naturforschung C*, 2000. 55(1-2).
140. Elshamy, A.I. and M.I. Nassar, Xenia terpenoids as anticancer promoters. *Journal of Biologically Active Products from Nature*, 2015. 5(2).
141. Mohammed, R., M.A.E. Seliem, T. Mohammed, and A.A. El Fatah, Bioactive secondary metabolites from the Red Sea soft coral *Heteroxenia fuscescens*. *International Journal of Applied Research in Natural Products*, 2012. 4.
142. Shen, Y.-C., Y.-R. Wu, J.-J. Lin, K.-L. Lo, Y.-C.Kuo, and A.T. Khalil, Eight new diterpenoids from soft coral *Cespitularia hypotentaculata*. *Tetrahedron*, 2007. 63(45).
143. Bergé, J.-P. and G. Barnathan, Fatty Acids from lipids of marine organisms: Molecular biodiversity, rolesas biomarkers, biologically active compounds, and economical aspects, in Marine Biotechnology I, R. Ulber and Y. Le Gal, Editors. 2005, Springer Berlin Heidelberg: Berlin, Heidelberg. p. 49-125.
144. Burri, L., N. Hoem, S. Banni, and K. Berge1, Marine omega-3 phospholipids: metabolism and biological activities. *International journal of molecular sciences*, 2012. 13(11).

145. Lee, Y.J., D.C. Perdian, Z. Song, E.S. Yeung, and B.J. Nikolau, Use of mass spectrometry for imaging metabolites in plants. *Plant Journal*, 2012. 70(1).
146. Römpp, A. and B. Spengler, Mass spectrometry imaging with high resolution in mass and space. *Histochemistry and Cell Biology*, 2013. 139(6).
147. Spengler, B., Mass spectrometry imaging of biomolecular information. *Analytical Chemistry*, 2015. 87(1).
148. Gabelica, V., E. Schulz, and M. Karas, Internal energy build-up in matrix-assisted laser desorption/ionization. *Journal of Mass Spectrometry*, 2004. 39(6).
149. Schulz, E., M. Karas, F. Rosu, and V. Gabelic, Influence of the Matrix on analyte fragmentation in atmospheric pressure MALDI. *Journal of the American Society for Mass Spectrometry*, 2006. 17(7).
150. Dong, Y., B. Li, S. Malitsky, I. Rogachev, A. Aharoni, F. Kaftan, A. Svatoš, and P. Franceschi, Sample preparation for mass spectrometry imaging of plant tissues: A Review. *Frontiers in Plant Science*, 2016. 7.
151. Fujino, Y., T. Minamizaki, H. Yoshioka, M. Okada, and Y. Yoshiko, Imaging and mapping of mouse bone using MALDI-imaging mass spectrometry. *Bone Reports*, 2016. 5.
152. Gorzolka, K., J. Kölling, T.W. Nattkemper, and K. Niehaus, Spatio-temporal metabolite profiling of the barley germination process by MALDI MS imaging. *PLOS ONE*, 2016. 11(3).
153. Wooldridge, S., Breakdown of the coral-algae symbiosis: Towards formalising a linkage between warm-water bleaching thresholds and the growth rate of the intracellular zooxanthellae. *Biogeosciences Discussions*, 2012. 9.
154. Smith, D., D. Suggett, and N. Baker, Is photoinhibition of zooxanthellae photosynthesis the primary cause of thermal bleaching in corals. *Global Change Biology*, 2005. 11.
155. Brown, B., I. Ambarsari, M.E. Warner, W.K. Fitt, and D.G. Cummings, Diurnal changes in photochemical efficiency and xanthophyll concentrations in shallow water reef corals: Evidence for photoinhibition and photoprotection. *Coral Reefs*, 1999. 18.
156. Falkowski, P.G., Z. Dubinsky, L. Muscatine, and J.W. Porter, Light and the bioenergetics of a symbiotic coral. *BioScience*, 1984. 34(11).
157. Lichtenberg, M., A.W.D. Larkum, and M. Kühl, Photosynthetic acclimation of symbiodinium in hospite depends on vertical position in the tissue of the scleractinian coral *Montastrea curta*. *Frontiers in Microbiology*, 2016. 7(230).
158. Trevor, T., J.E. Parkinson, and V.M. Weis, Host and Symbiont cell cycle coordination is mediated by symbiotic state, nutrition, and partner identity in a model cnidarian-dinoflagellate symbiosis. *mBio*, 2020. 11(2).
159. Wangpraseurt, D., A.W.D. Larkum, P.J. Ralph, and M. Kühl, Light gradients and optical microniches in coral tissues. *Frontiers in Microbiology*, 2012. 3(316).
160. Chao, C.-H., Z.-H. Wen, Y.-C. Wu, H.-C. Yeh, and J.-H. Sheu, Cytotoxic and anti-inflammatory cembranoids from the soft coral *Lobophytum crassum*. *Journal of Natural Products*, 2008. 71(11).
161. González, Y., D. Torres-Mendoza, G.E. Jones, and P.L. Fernandez, Marine diterpenoids as potential anti-inflammatory agents. *Mediators of Inflammation*, 2015. 2015.
162. Li, Y. and G. Pattenden, Novel macrocyclic and polycyclic norcembranoid diterpenes from *Sinularia* species of soft coral: Structural relationships and biosynthetic speculations. *Natural Product Reports*, 2011. 28(2).
163. Nurrachma, M.Y., D. Sakaraga, A.Y. Nugraha, S.I. Rahmawati, A. Bayu, L. Sukmarini, A. Atikana, A. Prasetyoputri, F. Izzati, M.F. Warsito, and M. Y. Putra, Cembranoids of soft corals: Recent updates and their biological activities. *Natural Products and Bioprospecting*, 2021. 11(3).
164. Lordan, R., A. Tsoupras, and I. Zabetakis, Phospholipids of animal and marine origin: structure, function, and anti-inflammatory properties. *Molecules* (Basel, Switzerland), 2017. 22(11).
165. Haq, M., S. Suraiya, S. Ahmed, and B.-S. Chun, Phospholipids from marine source: Extractions and forthcoming industrial applications. *Journal of Functional Foods*, 2021. 80.

166. Sabater, M.G. and H.T. Yap, Long-term effects of induced mineral accretion on growth, survival and corallite properties of *Porites cylindrica* Dana. *Journal of Experimental Marine Biology and Ecology*, 2004. 311(2).
167. Digby, P.S.B., Photosynthesis and respiration in the coralline algae, *Clathromorphum circumscriptum* and *Corallina officinalis* and the metabolic basis of calcification. *Journal of the Marine Biological Association of the United Kingdom*, 1977. 57(4).
168. Gómez-Lemos, L.A., C. Doropoulos, E. Bayraktarov, and G. Diaz-Pulido, Coralline algal metabolites induce settlement and mediate the inductive effect of epiphytic microbes on coral larvae. *Scientific Reports*, 2018. 8(1).
169. Jorissen, H., P.E. Galand, I. Bonnard, S. Meiling, D. Raviglione, A. Meistertzheim, L. Hédouin, B. Banaigs, C.E. Payri, and M.M. Nugues, Coral larval settlement preferences linked to crustose coralline algae with distinct chemical and microbial signatures. *Scientific Reports*, 2021. 11(1).
170. Petersen, L.-E., M.Y. Kellermann, S. Nietzer, and P.J. Schupp, Photosensitivity of the bacterial pigment cycloprodigiosin enables settlement in coral larvae—Light as an understudied environmental factor. *Frontiers in Marine Science*, 2021. 8(1599).
171. Sneed, J.M., K.H. Sharp, K.B. Ritchie, and V.J. Paul, The chemical cue tetrabromopyrrole from a biofilm bacterium induces settlement of multiple Caribbean corals. *Proceedings of the Royal Society B: Biological Sciences*, 2014. 281(1786).
172. Ahmed, A.F., Y.-W. Chen, C.-Y. Huang, Y.-J. Tseng, C.-C. Lin, C.-F. Dai, Y.-C. Wu, and J-H, Sheu, Isolation and structure elucidation of cembranoids from a Dongsha Atoll soft coral *Sarcophyton stellatum*. *Marine Drugs*, 2018. 16(6).
173. Huang, T.-Y., C.-Y. Huang, S.-R. Chen, J.-R. Weng, T.-H. Tu, Y.-B. Cheng, S.-H. Wu, and J.-H. Sheu, New hydroquinone monoterpenoid and cembranoid-related metabolites from the soft coral *Sarcophyton tenuispiculatum*. *Marine Drugs*, 2021. 19(1).
174. Ren, L., X. Leng, T. Li, J. Liu, W. Wang, X. Yan, X. Yan, and S. He, Four new cembranoids from the South China Sea soft coral *Sarcophyton trocheliophorum*. *Natural Product Research*, 2021.
175. Ciereszko, L.S., Sterol and diterpenoid production by zooxanthellae in coral reefs: A Review. *Biological Oceanography*, 1989. 6(3-4).
176. Kokke, W.C., S. Epstein, S.A. Look, G.H. Rau, W. Fenical, and C. Djerassi, On the origin of terpenes in symbiotic associations between marine invertebrates and algae (zooxanthellae). Culture studies and an application of 13C/12C isotope ratio mass spectrometry. *Journal of Biological Chemistry*, 1984. 259(13).
177. Michalek-Wagner, K., D. Bourne, and B. Bowden, The effects of different strains of zooxanthellae on the secondary-metabolite chemistry and development of the soft-coral host *Lobophytum compactum*. *Marine Biology*, 2001. 138.
178. Mydlarz, L.D., R.S. Jacobs, J. Boehnlein, and R.G. Kerr, Pseudopterosin biosynthesis in *Symbiodinium* sp., the dinoflagellate symbiont of *Pseudopterogorgia elisabethae*. *Chemistry & Biology*, 2003. 10(11).
179. Boehnlein, J., L. Santiago-Vazquez, and R. Kerr, Diterpene biosynthesis by the dinoflagellate symbiont of the Caribbean gorgonian *Pseudopterogorgia bipinnata*. *Marine Ecology-progress Series*, 2005. 303.
180. Amid, C., M. Olstedt, J.S. Gunnarsson, H.L. Lan, H.T.T. Minh, P.J. Van den Brink, M. Hellström, and M. Tedengren, Additive effects of the herbicide glyphosate and elevated temperature on the branched coral *Acropora formosa* in Nha Trang, Vietnam. *Environmental Science and Pollution Research*, 2018. 25(14).
181. Roche, H., B. Salvat, and F. Ramade. Assessment of the pesticides pollution of coral reefs communities from french Polynesia. 2011.
182. He, T., M.M.P. Tsui, C.J. Tan. C.Y. Ma, S.K.F. Yiu, L.H. Wang, T.H. Chen, T.Yung. Fan, P.K.S.Lam, and M.B. Murphy, Toxicological effects of two organic ultraviolet filters and a related commercial sunscreen product in adult corals. *Environmental Pollution*, 2019. 245.
183. Sully, S., D.E. Burkepile, M.K. Donovan, G. Hodgson, and R. van Woesik, A global analysis of coral bleaching over the past two decades. *Nature Communications*, 2019. 10(1).

184. Changyun, W., L. Haiyan, S. Changlun, W. Yanan, L. Liang, and g. Huashi, Chemical defensive substances of soft corals and gorgonians. *Acta Ecologica Sinica*, 2008. 28.
185. Fleury, B., J.C. Coll, and P. Sammarco, Complementary (secondary) metabolites in a soft coral: Sex-specific variability, inter-clonal variability, and competition. *Marine Ecology*, 2006. 27.
186. DeCarlo, T.M., A.L. Cohen, G. Wong, and K.A. Davis, Mass coral mortality under local amplification of 2 °C ocean warming. *Scientific Reports*, 2017. 7(1).
187. Depczynski, M., J. P. Gilmour, T. Ridgway, H. Barnes, A.J. Heyward, T.H. Holmes, J.A.Y. Moore, B.T. Radford, D.P. Thomson, P. Tinkler, and S. K. Wilson, Bleaching, coral mortality and subsequent survivorship on a West Australian fringing reef. *Coral Reefs*, 2013. 32(1).
188. Gissi, F., J. Stauber, A. Reichelt-Brushett, P.L. Harrison, and D.F. Jolley, Inhibition in fertilisation of coral gametes following exposure to nickel and copper. *Ecotoxicology and Environmental Safety*, 2017. 145.
189. Reichelt-Brushett, A.J. and K. Michalek-Wagner, Effects of copper on the fertilization success of the soft coral *Lobophytum compactum*. *Aquatic Toxicology*, 2005. 74(3).
190. Schwarz, J.A., C.L. Mitchelmore, R. Jones, A. O'Dea, and S. Seymour, Exposure to copper induces oxidative and stress responses and DNA damage in the coral *Montastraea franksi*. *Comparative Biochemistry and Physiology Part C: Toxicology & Pharmacology*, 2013. 157(3).
191. Huang, W., M. Chen, B. Song, J. Deng, M. Shen, Q. Chen, G. Zeng, and J. Liang, Microplastics in the coral reefs and their potential impacts on corals: A mini-review. *Science of The Total Environment*, 2021. 762.
192. Montano, S., D. Seveso, D. Maggioni, P. Galli, S. Corsarini, and F. Saliu, Spatial variability of phthalates contamination in the reef-building corals *Porites lutea*, *Pocillopora verrucosa* and *Pavona varians*. *Marine Pollution Bulletin*, 2020. 155.
193. Cervino, J.M., B. Hauff, J.A. Haslun, K. Winiarski-Cervino, M. Cavazos, P. Lawther, A.M. Wier, K. Hughen, and K.B. Strychar, Ulcerated yellow spot syndrome: implications of aquaculture-related pathogens associated with soft coral *Sarcophyton ehrenbergi* tissue lesions. *Diseases of Aquatic Organisms*, 2012. 102(2).
194. Munn, C.B., H.K. Marchant, and A.J. Moody, Defences against oxidative stress in vibrios associated with corals. *FEMS Microbiology Letters*, 2008. 281(1).
195. Avigliano, E. and N.F. Schenone, Human health risk assessment and environmental distribution of trace elements, glyphosate, fecal coliform and total coliform in Atlantic Rainforest mountain rivers (South America). *Microchemical Journal*, 2015. 122.
196. Battaglin, W.A., M.T. Meyer, K.M. Kuivila, and J.E. Dietze, Glyphosate and Its Degradation Product AMPA Occur Frequently and Widely in U.S. Soils, Surface Water, Groundwater, and Precipitation. *JAWRA Journal of the American Water Resources Association*, 2014. 50(2).
197. Coupe, R.H., S.J. Kalkhoff, P.D. Capel, and C. Gregoire, Fate and transport of glyphosate and aminomethylphosphonic acid in surface waters of agricultural basins. *Pest Management Science*, 2012. 68(1).
198. Davis, A.M., P.J. Thorburn, S.E. Lewis, Z.T. Bainbridge, S.J. Attard, R. milla, and J.E. Brodie, Environmental impacts of irrigated sugarcane production: Herbicide run-off dynamics from farms and associated drainage systems. *Agriculture, Ecosystems & Environment*, 2013. 180.
199. Hanke, I., H. Singer, and J. Hollender, Ultratrace-level determination of glyphosate, aminomethylphosphonic acid and glufosinate in natural waters by solid-phase extraction followed by liquid chromatography–tandem mass spectrometry: performance tuning of derivatization, enrichment and detection. *Analytical and Bioanalytical Chemistry*, 2008. 391(6).
200. Matozzo, V., M. Munari, L. Masiero, L. Finos, and M.G. Marin, Ecotoxicological hazard of a mixture of glyphosate and aminomethylphosphonic acid to the mussel *Mytilus galloprovincialis* (Lamarck 1819). *Scientific Reports*, 2019. 9(1).
201. Peruzzo, P.J., A.A. Porta, and A.E. Ronco, Levels of glyphosate in surface waters, sediments and soils associated with direct sowing soybean cultivation in north pampasic region of Argentina. *Environmental Pollution*, 2008. 156(1).

202. Solomon, K.R. and D.G. Thompson, Ecological risk assessment for aquatic organisms from over-water uses of glyphosate. *Journal of Toxicology and Environmental Health, Part B*, 2003. 6(3).
203. Struger, J., D. Thompson, B. Staznik, P. Martin, T. McDaniel, and C. Marvin, Occurrence of glyphosate in surface waters of Southern Ontario. Bu*lletin of Environmental Contamination and Toxicology*, 2008. 80(4).
204. Fuerst, E.P. and M.A. Norman, Interactions of Herbicides with photosynthetic electron transport. *Weed Science*, 1991. 39(3).
205. Dabney, B.L. and R. Patiño, Low-dose stimulation of growth of the harmful alga, *Prymnesium parvum*, by glyphosate and glyphosate-based herbicides. *Harmful Algae*, 2018. 80.
206. Droppa, M., G. Horváth, I. Vass, and S. Demetera, Mode of action of photosystem II herbicides studied by thermoluminescence. *Biochimica et Biophysica Acta (BBA) - Bioenergetics*, 1981. 638(2).
207. Gomes, M.P. and P. Juneau, Temperature and light modulation of herbicide toxicity on algal and cyanobacterial physiology. *Frontiers in Environmental Science*, 2017. 5(50).
208. Jones, R. and A. Kerswell, Phytotoxicity of photosystem II (PSII) herbicides to coral. *Marine Ecology-progress Series*, 2003. 261.
209. Coles, S.L. and B.E. Brown, Coral bleaching--capacity for acclimatization and adaptation. *Advances in Marine Biology*, 2003. 46.
210. Gohar, H. and H.M. Roushdy, On the physiology of the neuromuscular system of *Heteroxenia* (Alcyonaria). *Publications of the Marine Biological Station, Ghardaqa (Red Sea)*, 1959. 10.
211. Horridge, G.A., The Responses of *Heteroxenia* (Alcyonaria) to stimulation and to some inorganic ions. *Journal of Experimental Biology*, 1956. 33(3).
212. Simancas-Giraldo, S.M., N. Xiang, M.M. Kennedy, R. Nafeh, E. Zelli, and C. Wild, Photosynthesis and respiration of the soft coral Xenia umbellata respond to warming but not to organic carbon eutrophication. *PeerJ*, 2021. 9.
213. Vollstedt, S., N. Xiang, S.M. Simancas-Giraldo, and C. Wild, Organic eutrophication increases resistance of the pulsating soft coral *Xenia umbellata* to warming. *PeerJ*, 2020. 8.
214. Jantzen C, W.C., Rasheed M, El-Zibdah M, and Richter C, Enhanced pore-water nutrient fluxes by the upside-down jellyfish *Cassiopea* sp. in a Red Sea coral reef. *Marine Ecology Progress Series*, 2010. 411.
215. Vopel, K., D. Thistle, J. Ott, M. Bright, and H. Røy, Wave-induced H2S flux sustains a chemoautotrophic symbiosis. *Limnology and Oceanography*, 2005. 50(1).
216. Schneider, S.L. and H.W. Lim, Review of environmental effects of oxybenzone and other sunscreen active ingredients. *Journal of the American Academy of Dermatology*, 2019. 80(1).
217. Dellisanti, W., J.T.H. Chung, C.F.Y. Chow, J. Wu1, M.L. Wells, and L.L. Chan, Experimental techniques to assess coral physiology in situ under global and local stressors: Current approaches and novel insights. *Frontiers in Physiology*, 2021. 12(594).
218. Goldberg, W., coral food, feeding, nutrition, and secretion: A Review. 2018.
219. Banin, E., T. Israely, A. Kushmaro, Y. Loya, E. Orr, and E. Rosenberg, Penetration of the coral-bleaching bacterium *Vibrio shiloi* into *Oculina patagonica*. *Applied and environmental microbiology*, 2000. 66(7).
220. Changyun, W., L. Haiyan, S. Changlun, W. Yanan, L. Liang, and G. Huashi, Chemical defensive substances of soft corals and gorgonians. *Acta Ecologica Sinica*, 2008. 28(5).
221. Munn Colin, B. and M. Sadowsky, The role of vibrios in diseases of corals. *Microbiology Spectrum*, 2015. 3(4).
222. Brown, B., The significance of pollution in eliciting the "bleaching" response in symbiotic cnidarians. *International Journal of Environment and Pollution*, 2000. 13.
223. Jones, R.J., Zooxanthellae loss as a bioassay for assessing stress in corals. *Marine Ecology Progress Series*, 1997. 149(1/3).
224. Warner, M.E., W.K. Fitt, and G.W. Schmidt, Damage to photosystem II in symbiotic dinoflagellates: A determinant of coral bleaching. *Proceedings of the National Academy of Sciences*, 1999. 96(14).

225. Bhagooli, R. and M. Hidaka, Comparison of stress susceptibility of in hospite and isolated zooxanthellae among five coral species. *Journal of Experimental Marine Biology and Ecology*, 2003. 291(2).
226. Jones, R.J., S. Ward, A.Y. Amri, and O. Hoegh-Guldberg, Changes in quantum efficiency of photosystem II of symbiotic dinoflagellates of corals after heat stress, and of bleached corals sampled after the 1998 Great Barrier Reef mass bleaching event. *Marine and Freshwater Research*, 2000. 51(1).
227. Tyohemba, R.L., M.S. Humphries, M.H. Schleyer, and S.N. Porter, Accumulation of commonly used agricultural herbicides in coral reef organisms from iSimangaliso Wetland Park, South Africa. *Environmental Pollution*, 2022. 294.
228. Jones, R.J. and O. Hoegh-Guldberg, Diurnal changes in the photochemical efficiency of the symbiotic dinoflagellates (Dinophyceae) of corals: photoprotection, photoinactivation and the relationship to coral bleaching. *Plant, Cell & Environment*, 2001. 24(1): p. 89-99.
229. Marshall, P. and A. Baird, Bleaching of corals on the Great Barrier Reef: Differential susceptibilities among taxa. *Coral Reefs*, 2000. 19.
230. Fitt, W.K., B.E. Brown, M.E. Warner, and R.P. Dunne, Coral bleaching: interpretation of thermal tolerance limits and thermal thresholds in tropical corals. *Coral Reefs*, 2001. 20(1).
231. Winters, G., R. Holzman, A. Blekhman, S. Beer, and Y. Loya, Photographic assessment of coral chlorophyll contents: Implications for ecophysiological studies and coral monitoring. *Journal of Experimental Marine Biology and Ecology*, 2009. 380(1).
232. Fujise, L., H. Yamashita, G. Suzuki, K. Sasaki, L.M. Liao, and K. Koike, Moderate thermal stress causes active and immediate expulsion of photosynthetically damaged zooxanthellae (*Symbiodinium*) from corals. *PLOS ONE*, 2014. 9(12).
233. Baghdasarian, G. and L. Muscatine, Preferential expulsion of dividing algal cells as a mechanism for regulating algal-cnidarian symbiosis. *Biology Bulletin*, 2000. 199(3).
234. Jones, R.J., Coral bleaching, bleaching-induced mortality, and the adaptive significance of the bleaching response. *Marine Biology*, 2008. 154(1).
235. Gledhill, M., M. Nimmo, S.J. Hill, and M.T. Brown, The toxicity of copper(II) species to marine algae, with particular reference to macroalgae. *Journal of Phycology*, 1997. 33(1).
236. Krämer, U. and S. Clemens, Functions and homeostasis of zinc, copper, and nickel in plants, in Molecular Biology of Metal Homeostasis and Detoxification: From Microbes to Man, M.J. Tamas and E. Martinoia, Editors. 2006, Springer Berlin Heidelberg: Berlin, Heidelberg. p. 215-271.
237. Fan, J., L. Ho, P. Hobsonb, and J. Brookes, Evaluating the effectiveness of copper sulphate, chlorine, potassium permanganate, hydrogen peroxide and ozone on cyanobacterial cell integrity. *Water Research*, 2013. 47(14).
238. Reichert, J., J. Schellenberg, P. Schubert, and T. Wilke, Responses of reef building corals to microplastic exposure. *Environmental Pollution*, 2018. 237.
239. Okubo, N., S. Takahashi, and Y. Nakano, Microplastics disturb the anthozoan-algae symbiotic relationship. *Marine Pollution Bulletin*, 2018. 135.
240. Su, Y., K. Zhang, Z. Zhou, J. Wang, X. Yang, J. Tang, H. Li, and S. Lin, Microplastic exposure represses the growth of endosymbiotic dinoflagellate *Cladocopium goreaui* in culture through affecting its apoptosis and metabolism. *Chemosphere*, 2020. 244.
241. Syakti, A.D., J.V. Jaya, A. Rahman, N.V. Hidayati, T.S. Raza'I, F. Idris, M. Trenggono, P. Doumenq, and L.M. Chou, Bleaching and necrosis of staghorn coral (*Acropora formosa*) in laboratory assays: Immediate impact of LDPE microplastics. *Chemosphere*, 2019. 228.
242. Harland, A.D., J.C. Navarro, P.S. Davies, and L.M. Fixter, Lipids of some Caribbean and Red Sea corals: total lipid, wax esters, triglycerides and fatty acids. *Marine Biology*, 1993. 117(1).
243. Parrish, C., Lipids in Marine Ecosystems. *ISRN Oceanography*, 2013. 2013.
244. Chen, H.-K., L.-H. Wang, S.-N. Song, and A.B. Mayfield, A compartmental comparison of major lipid species in a coral-*Symbiodinium* endosymbiosis: Evidence that the coral host regulates lipogenesis of its cytosolic lipid bodies. *PLOS ONE*, 2015. 10(7).
245. Tonetti Botana, M., The role of *Symbiodinium* membrane lipids in response to heat shock: implications for coral bleaching. 2019.

246. Tang, C.-H., L.-S. Fang, T.-Y. Fan, L.-H. Wang, C.-Y. Lin, S.H. Lee, and W.H. Wang, Cellular membrane accommodation to thermal oscillations in the coral *Seriatopora caliendrum*. *PLOS ONE*, 2014. 9(8).
247. Chao, C.-H., W.-L. Li, C.-Y. Huang, A.F. Ahmed, C.-F. Dai, Y.-C. Wu, M.-C. Lu, C.-C. Liaw, and J.-H. Sheu, Isoprenoids from the soft coral *Sarcophyton glaucum*. *Marine Drugs*, 2017. 15(7).
248. Katsuyama, I., H. Fahmy, J.K. Zjawiony, S.I. Khalifa, R.W. Kilada, T. Konoshima, M. Takasaki, and H. Tokuda, Semisynthesis of new sarcophine derivatives with chemopreventive activity. *Journal of Natural Products*, 2002. 65(12).
249. Kashman, Y., S. Carmely, and A. Groweiss, Further cembranoid derivatives from the Red Sea soft corals *Alcyonium flaccidum* and *Lobophytum crassum*. *The Journal of Organic Chemistry*, 1981. 46(18).
250. Liao, Z.-J., H.-J. Su, Y.-C. Shyue, Z.-H. Wen, J.-H. Sheu, and J.-H. Su, Two new cembranoids from the soft coral *Lobophytum crassum*. Bulle*tin of the Chemical Society of Japan*, 2011. 84(6).
251. Clare, A.S., Marine natural product antifoulants: Status and potential. *Biofouling*, 1996. 9(3).
252. Fang, F., T. Yan, and Q. Liu, Application of chemical ecology in controlling marine fouling organisms. *Ying Yong Sheng Tai Xue Bao*, 2005. 16(10).
253. Farag, M.A., A. Porzel, M.A. Al-Hammady, M.F. Hegazy, A. Meyer, T. A. Mohamed, H. Westphal, and L.A. Wessjohann, Soft corals biodiversity in the Egyptian Red Sea: A comparative MS and NMR Metabolomics approach of wild and aquarium grown species. *Journal of Proteome Research*., 2016. 15(4).
254. Iwagawa, T., A. Yasuhisa, H. Tsunao, and S. Motoo, New xenia diterpenoids from a soft coral, xenia species. *Tetrahedron*, 1995. 51(41).
255. Liu, B. and C. Benning, Lipid metabolism in microalgae distinguishes itself. *Current Opinion in Biotechnology*, 2013. 24(2).
256. Nikolova-Karakashian, M.N. and K.A. Rozenova, Ceramide in stress response. *Advances in Experimental Medicine and Biology*, 2010. 688.
257. Sun, X.-M., L.-J. Ren, Q.-Y. Zhao, X.-J. Ji, and H. Huang, Microalgae for the production of lipid and carotenoids: a review with focus on stress regulation and adaptation. *Biotechnology for Biofuels*, 2018. 11(1).
258. Parzanini, C., C.C. Parrish, J.-F. Hamel, and A. Mercier, Functional diversity and nutritional content in a deep-sea faunal assemblage through total lipid, lipid class, and fatty acid analyses. *PLOS ONE*, 2018. 13(11).
259. Wild, C., M. Huettel, A. Klueter, S.G. Kremb, M.Y.M. Rasheed, and B.B. Jørgensen, Coral mucus functions as an energy carrier and particle trap in the reef ecosystem. *Nature*, 2004. 428(6978).
260. Peters, E.C., A survey of cellular reactions to environmental stress and disease in Caribbean scleractinian corals. *Helgoländer Meeresuntersuchungen*, 1984. 37(1).
261. Peters, E.C. and M.E.Q. Pilson, A comparative study of the effects of sedimentation on symbiotic and asymbiotic colonies of the coral *Astrangiadanae M*ilne Edwards and Haime 1849. *Journal of Experimental Marine Biology and Ecology*, 1985. 92(2).
262. Piggot, A.M., B.W. Fouke, M. Sivaguru, R.A. Sanford, and H.R. Gaskins, Change in zooxanthellae and mucocyte tissue density as an adaptive response to environmental stress by the coral, *Montastraea annularis*. *Marine Biology*, 2009. 156(11).
263. Vargas-Angel, B., E.C. Peters, E. Kramarsky-Winter, D.S. Gilliam, and R.E. Dodge, Cellular reactions to sedimentation and temperature stress in the Caribbean coral *Montastraea cavernosa*. *Journal of invertebrate pathology*, 2007. 95(2).
264. Wright, R.M., M.E. Strader, H.M. Genuise, and M. Matz, Effects of thermal stress on amount, composition, and antibacterial properties of coral mucus. *PeerJ*, 2019. 7.
265. Tanaka, Y., T. Miyajima, Y. Umezawa, T. Hayashibara, H. Ogawa, and i. Koike, Net release of dissolved organic matter by the scleractinian coral *Acropora pulchra*. *Journal of Experimental Marine Biology and Ecology*, 2009. 377.

266. Bhagooli, R. and M. Hidaka, Release of zooxanthellae with intact photosynthetic activity by the coral *Galaxea fascicularis* in response to high temperature stress. *Marine Biology*, 2004. 145.
267. Sammarco, P.W. and K.B. Strychar, Effects of climate change/global warming on coral reefs: Adaptation/exaptation in corals, evolution in zooxanthellae, and biogeographic shifts. *Environmental Bioindicators*, 2009. 4(1).
268. Sammarco, P.W. and K.B. Strychar, Responses to high seawater temperatures in zooxanthellate octocorals. *PLOS ONE*, 2013. 8(2).
269. Crossland, C.J., In situ release of mucus and DOC-lipid from the corals *Acropora variabilis* and *Stylophora pistillata* in different light regimes. *Coral Reefs*, 1987. 6(1).
270. Davies, P.S., The role of zooxanthellae in the nutritional energy requirements of *Pocillopora eydouxi*. *Coral Reefs*, 1984. 2(4).
271. Brown, B.E. and J.C. Bythell, Perspectives on mucus secretion in reef corals. *Marine Ecology Progress Series*, 2005. 296.
272. Shnit-Orland, M. and A. Kushmaro, Coral mucus-associated bacteria: a possible first line of defense. *FEMS Microbiology Ecology*, 2009. 67(3).
273. Banin, E., T. Israely, M. Fine, Y. Loya, and E. Rosenberg, Role of endosymbiotic zooxanthellae and coral mucus in the adhesion of the coral-bleaching pathogen *Vibrio shiloi* to its host. *FEMS Microbiology Letters*, 2001. 199(1).
274. Palmer, C.V., J.C. Bythell, and B.L. Willis, Levels of immunity parameters underpin bleaching and disease susceptibility of reef corals. *The FASEB Journal*, 2010. 24(6).
275. Martins, A., H. Vieira, H. Gaspar, and S. Santos, Marketed marine natural products in the pharmaceutical and cosmeceutical industries: Tips for success. *Marine Drugs*, 2014. 12(2).
276. Rocha, J., L. Peixe, N.C.M. Gomes, and R. Calado, Cnidarians as a source of new marine bioactive compounds--an overview of the last decade and future steps for bioprospecting. *Marine drugs*, 2011. 9(10).
277. Al-Lihaibi, S.S., W.M. Alarif, A. Abdel-Lateff, S.N. Ayyad, A.B. Abdel-Naim, F.F. El-Senduny, and F.A.Badria, Three new cembranoid-type diterpenes from Red Sea soft coral *Sarcophyton glaucum*: Isolation and antiproliferative activity against HepG2 cells. *European Journal of Medicinal Chemistry*, 2014. 81.
278. Chao, C.-H., H.-C. Huang, Y.-C. Wu, C.-K. Lu, C.-F. Dai, and J.-H. Sheu, Glycolipids from the formosan soft coral *Lobophytum crassum*. *Chemical & pharmaceutical bulletin*, 2007. 55 12.
279. Feller, M., A. Rudi, N.Berer, I. Goldberg, Z. Stein, Y. Benayahu, M. Schleyer, and Y. Kashman, Isoprenoids of the soft coral *Sarcophyton glaucum*: Nyalolide, a new biscembranoid, and other terpenoids. *Journal of Natural Products*, 2004. 67(8).
280. Huang, C.-Y., P.-J. Sung, C. Uvarani, J.-H. Su, M.-C. Lu, T.-L. Hwang, C.-F. Dai, S.-L. Wu, and J.-H. Sheu, Glaucumolides A and B, biscembranoids with new structural type from a cultured soft coral *Sarcophyton glaucum*. *Scientific Reports*, 2015. 5(1).
281. Kobayashi, M., T. Hayashi, F. Nakajima, and H. Mitsuhashi, Marine sterols. IX. Occurrence of 24 xi-methylcholestane-1 beta, 3 beta, 5 alpha, 6 beta, 25-pentol 25-monoacetate in the soft coral, *Sarcophyton glaucum*. *Steroids*, 1979. 34(3).
282. Matthée, G.F., G.M. König, and A.D. Wright, Three new diterpenes from the marine soft coral *Lobophytum crassum*. *Journal of Natural Products*, 1998. 61(2).
283. Nguyen, P.T., N.H. Nam, N.X.Cuong, and N.X. Nhiem, A new sterol from the soft coral *Lobophytum crassum*. *Bulletin of The Korean Chemical Society*, 2013. 34.
284. Quah, Y., N.I.M. Ismail, J.L.S. Ooi, Y.A. Affendi, F.A.Manan, L.-K. Teh, F.-C. Wong, T.-T. Chai, Purification and identification of novel cytotoxic oligopeptides from soft coral *Sarcophyton glaucum*. *Journal of Zhejiang University-Science B*, 2019. 20(1).
285. Wang, Z., H. Tang, P. Wang, W. Gong, M. Xue, H. Zhang, T. Liu, B. Liu, Y. Yi, and W. Zhang, Bioactive polyoxygenated steroids from the South China sea soft coral, *Sarcophyton* sp. *Marine drugs*, 2013. 11(3).
286. Yin, F.-Z., L.-G. Yao, Z.-Y. Zhang, J.-R. Wang, H. Wang, and Y.-W. Guo, Polyoxygenated cembranoids from the Hainan soft coral *Lobophytum crassum*. *Tetrahedron*, 2021. 90.

287. Abou El-Ezz, R.F., S.A. Ahmed, M.M. Radwan, N.A. Ayoub, and M.S. Afifi, , Bioactive cembranoids from the Red Sea soft coral *Sarcophyton glaucum*. *Tetrahedron Letters*, 2013. 54(8).
288. Al-Footy, K., W.M. Alarif, M.S. Zubair, M.A. Ghandourah, and M.M. Aly, Antibacterial and cytotoxic properties of isoprenoids from the Red Sea soft coral, *Lobophytum* sp. *Tropical Journal of Pharmaceutical Research*, 2016. 15.
289. Alarif, W., M.A. Ghandourah, A.A. Lateff, N.O. Bawakid, A.A. Alotaibi, M.Y. Alfaifi, and S.E.I. Elbehairi, Two new xeniolide diterpenes from the soft coral *Xenia umbellata*; displayed anti proliferative effects. *Pharmacognosy Magazine*, 2020. 16(72).
290. Althagbi, H.I., F. Budiyanto, A. Abdel-Lateff, K.O. Al-Footy, N.O. Bawakid, M.A. Ghandourah, M.Y. Alfaifi, S.E.I. Elbehairi, and W.M. Alarif, Antiproliferative isoprenoid derivatives from the Red Sea Alcyonacean *Xenia umbellata*. *Molecules* (Basel, Switzerland), 2021. 26(5).
291. Hegazy, M.E., A.A. El-Beih, A.Y. Moustafa, A.A. Hamdy, M.A. Alhammady et al., Cytotoxic cembranoids from the Red Sea soft coral *Sarcophyton glaucum*. *Natural Product Communications*, 2011. 6(12).
292. Lai, K.-H., W.-J. You, C.-C. Lin, M. El-Shazly, Z.-J.Liao, and J.-H. Su, Anti-inflammatory dembranoids from the soft coral *Lobophytum crassum*. *Marine drugs*, 2017. 15(10).
293. Zhang, J., X. Tang, X. Han, D. Feng, X. Luo, L. van Ofwegen, P. Li, and G. Li, Sarcoglaucins A-I, new antifouling cembrane-type diterpenes from the South China Sea soft coral *Sarcophyton glaucum*. *Organic Chemistry Frontiers*, 2019. 6(12).
294. Hegazy, M.E., A.M.G. Eldeen, A.A. Shahat, F.F. Abdel-Latif, T.A. Mohamed, B.R. Whittlesey, and P.W. Paré, Bioactive hydroperoxyl cembranoids from the Red Sea soft coral *Sarcophyton glaucum*. *Marine Drugs*, 2012. 10(1).
295. Fridkovsky, E., A. Rudi, Y. Benayahu, Y. Kashman, and M. Schleyer, Sarcoglane, a new cytotoxic diterpene from *Sarcophyton glaucum*. Tetrahedron Letters, 1996. 37(38).
296. Zhang, C.X., X.-X. He, J. Zhang, Q. Guo, L.-F. Lei, J.-Y. Su, and L.-M. Zeng, New precursor of tetraterpenoids from the soft coral *Sarcophyton glaucum*. *Natural Product Research*, 2013. 27(9).
297. Abdel-Lateff, A., W.M. Alarif, S.-E.N. Ayyad, S.S. Al-Lihaibi, and S.A. Basaif, New cytotoxic isoprenoid derivatives from the Red Sea soft coral *Sarcophyton glaucum*. *Natural Product Research*, 2015. 29(1).
298. Al-Footy, K.O., W.M. Alarif, F. Asiri, M.M. Aly, and S.-E.N. Ayyad, Rare pyrane-based cembranoids from the Red Sea soft coral *Sarcophyton trocheliophorum* as potential antimicrobial–antitumor agents. *Medicinal Chemistry Research*, 2015. 24(2).
299. Badria, F.A., A.N. Guirguis, S. Perovic, R. Steffen, W.E. Müller, and H.C. Schröder, Sarcophytolide: a new neuroprotective compound from the soft coral *Sarcophyton glaucum*. *Toxicology*, 1998. 131(2-3).
300. Chao, C.H., Z.-H. Wen, Y.-C. Wu, H.-C. Yeh, and J.-H. Sheu, Cytotoxic and anti-inflammatory cembranoids from the soft coral *Lobophytum crassum*. *Journal of Natural Products*, 2008. 71(11).
301. Yeh, Y.-T., S.-C. Lin, G.-H. Lee, and Z.-H. Wen, Cembranoids from Octocoral *Lobophytum crassum* (von Marenzeller, 1886). *Marine Drugs*, 2021. 19(3).
302. Mohamed, T.A., A.I. Elshamy, T.A. Hussien, J.-H. Su, J.-H. Sheu, and M.E.F. Hegazy, Lobophylins F-H: three new cembrene diterpenoids from soft coral *Lobophytum crassum*. *Journal of Asian Natural Products Research*, 2017. 19(3).
303. Zhao, M., S. Cheng, W. Yuan, Y. Xi, and X. Li, Cembranoids from a Chinese Collection of the soft coral *Lobophytum crassum*. *Marine drugs*, 2016. 14(6).
304. Aboutabl, E.A., N.M. Selim, S.M. Azzam, C.G. Michel, M.F. Hegazy, and A.M. Ali, Polyhydroxy sterols isolated from the Red Sea soft coral *Lobophytum crassum* and their cytotoxic activity. *Natural Product Communications*, 2017. 12(2).
305. Lee, N.-L. and J.-H. Su, Tetrahydrofuran cembranoids from the cultured soft coral *Lobophytum crassum*. *Marine drugs*, 2011. 9(12).

306. Rashid, M.A., K.R. Gustafson, and M.R. Boyd, HIV-inhibitory cembrane derivatives from a Philippines collection of the soft coral *Lobophytum* species. *Journal of Natural Products*, 2000. 63(4).
307. Zhao, M., J. Yin, W. Jiang, M. Ma, X. Lei, Z. Xiang, J. Dong, K. Huang, and P. Yan, Cytotoxic and antibacterial cembranoids from a South China Sea soft coral, *Lobophytum* sp. *Marine drugs*, 2013. 11(4).
308. El-Gamal, A.A., S.-K. Wang, and C.-Y. Duh, Umbellactal, a novel diterpenoid from the formosan soft coral *Xenia umbellata*. *Tetrahedron letters*, 2005. 46(36).
309. Duh, C.Y., A.A.H. El-Gamal, C.-Y. Chiang, C.-J. Chu, S.-K. Wang, and C.-F. Dai, New cytotoxic xenia diterpenoids from the formosan soft coral *Xenia um*bellata. *Journal of Natural Products*, 2002. 65(12).
310. El-Gamal, A.A., S.K. Wang, and C.Y. Duh, Cytotoxic xenia diterpenoids from the soft coral *Xenia umbellata*. *Journal of Natural Products*, 2006. 69(3).
311. Ayyad, S.-E.N., W.M. Alarif, K.O. Al-Footy, E.A. Selim, M,A, Ghandourah, M.M. Aly, and H.S. Alorfi, Isolation, antimicrobial and antitumor activities of a new polyhydroxysteroid and a new diterpenoid from the soft coral *Xenia umbellata*. *Zeitschrift für Naturforschung C*, 2017. 72(1-2).
312. Bote, K., J. Pöppe, R. Merle, O. Makarova, and U. Roesler, Minimum inhibitory concentration of glyphosate and of a glyphosate-containing herbicide formulation for *Escherichia coli* isolates – differences between pathogenicand non-pathogenic isolates and between host species. *Frontiers in Microbiology*, 2019. 10.
313. Pöppe, J., K. Bote,1 R. Merle, O. Makarova, and U. Roesler, Minimum inhibitory concentration of glyphosate and a glyphosate-containing herbicide in *Salmonella enterica* isolates originating from different time periods, hosts, and serovars. *European journal of microbiology and immunology*, 2019. 9(2).
314. Raoult, D., L. Hadjadj, S.A. Baron, and J.-M. Rolain, Role of glyphosate in the emergence of antimicrobial resistance in bacteria?. *Journal of Antimicrobial Chemotherapy*, 2021. 76(7).
315. Blunt, J.W., B.R. Copp, R.A. Keyzers, M.H.G. Munro, and M.R. Prinsep, Marine natural products. *Natural Product Reports*, 2012. 29(2).
316. Gomaa, M.N., K. Soliman, A. Ayesh, A.A. and El-Wahed, Antibacterial effect of the red sea soft coral *Sarcophyton trocheliophorum*. *Natural Product Research*, 2016. 30(6).
317. Liu, Z., W. Cheng, D. Liu, L. van Ofwegen, P. Proksch, and W. Lin, Capnosane-type cembranoids from the soft coral *Sarcophyton trocheliophorum* with antibacterial effects. *Tetrahedron*, 2014. 70(45): p. 8703-8713.
318. Abu El-Regal, M. and F. A.Z, Antibacterial activity of some red sea soft corals, Egypt. 2016.
319. Gomaa, M.N., K. Soliman, A. Ayesh, A. A. El-Wahed, Z. Hamza, H.M. Mansour, S.A.M. Khalifa, H.B.M.Ali, and H.R. El-Seedi, Antibacterial effect of the red sea soft coral *Sarcophyton trocheliophorum*. *Natural Product Research*, 2016. 30(6).
320. Liang, L.-F., L.-F. Lan, O. Taglialatela-Scafati, and Y.-W. Guo, Sartrolides A–G and bissartrolide, new cembranolides from the South China Sea soft coral *Sarcophyton trocheliophorum* Marenzeller. *Tetrahedron*, 2013. 69(35).
321. Liu, Z., W. Cheng, D. Liu, L. van Ofwegen, P. Proksch, and W. Lin, Capnosane-type cembranoids from the soft coral *Sarcophyton troche* with antibacterial effects. *Tetrahedron*, 2014. 70.
322. Putra, M.Y., A. Saparhadi, F. Karim, T. Murniasih, and R.T. Swasono, Bioassay-guided isolation of an antibacterial compound from the indonesian soft coral *Sarcophyton trocheliophorum*. *Bulletin of Marine and Fischeries Postharvest and Biotechnology*. 2016. 11(2).
323. Zubair, M., W. Alarif, K. Al-Footy, M. Ph, and M. Ali, New antimicrobial biscembrane hydrocarbon and cembranoid diterpenes from the soft coral *Sarcophyton trocheliophorum*. *Turkish Journal of Chemistry*, 2016. 40(3).
324. Kamada, T., I.I. Zanil, C.-S. Phan, and C.S. Vairappan, A new cembrane, from soft coral genus *Sarcophyton* in Borneo. *Natural Product Communications*, 2018. 13(2).

325. Putra, M.Y., T. Murniasih, R.T. Swasono, J.T. Wibowo, and A.N.C. Saputri, Secondary metabolites and their biological activities in Indonesian soft coral of the genus *Lobophytum*. *Asian Pacific Journal of Tropical Biomedicine*, 2016. 6(11).
326. Cheng, S.-Y., Z.-H. Wen, S.-F. Chiou, C.-H.Hsu, S.-K.Wang, C.-F. Dai, M.-Y. Chiang, and C.-Y.Duh, Durumolides A–E, anti-inflammatory and antibacterial cembranolides from the soft coral *Lobophytum durum*. *Tetrahedron*, 2008. 64(41).
327. Shaaban, M., M.A. Ghani, and K. Shaaban, Zahramycins A-B, Two New steroids from the coral *Sarcophyton trocheliophorum*. *ChemInform*, 2013. 44.
328. Edrada, R.A., P. Proksch, V. Wray, L. Witte, and L. van Ofwegen, Four new bioactive lobane diterpenes of the soft coral *Lobophytum pauciflorum* from Mindoro, Philippines. *Journal of Natural Products*, 1998. 61(3).
329. Kamada, T., C.-S. Phan, H.-S. Tin, C.S. Vairappan, and T.S.T. Muhammad, 16-Hydroxycembra-1,3,7,11-tetraene, a new cembrane diterpene from Malaysian soft coral genus *Sarcophyton*. *Natural Product Communications*, 2016. 11(8).
330. Zhao, M., J. Yin, W. Jiang, M. Ma, and X. Lei, Cytotoxic and antibacterial cembranoids from a South China Sea soft coral, *Lobophytum* sp. *Marine Drugs*, 2013. 11(4).
331. Yan, P., Z. Deng, L. van Ofwegen, P. Proksch, and W.Lin, Lobophytones O-T, new biscembranoids and cembranoid from soft coral *Lobophytum pauciflorum*. *Marine Drugs*, 2010. 8(11).
332. Yan, P., Z. Deng, L. van Ofwegen, P. Proksch, and W. Lin, Lobophytones U - Z_1, biscembranoids from the Chinese soft coral *Lobophytum pauciflorum*. *Chemistry and Biodiversity*, 2011. 8(9).
333. dos Santos, C.H.C., M.G. Carvalho, K. Franke, and L. Wessjohann, Dammarane-type triterpenoids from the stem of *Ziziphus glaziovii* Warm. (Rhamnaceae). *Phytochemistry*, 2019. 162.
334. Zhang, C., J. Li, J. Su, Y. Liang, X. Yang, K. Zheng, and L. Zeng, Cytotoxic diterpenoids from the soft coral *Sarcophyton crassocaule*. *Journal of Natural Products*, 2006. 69(10).
335. Farag, M.A., M.I. Fekry, M. A. Al-Hammady, M.N. Khalil, H.R. El-Seedi, A. Meyer, A. Porzel, H. Westphal, L.A. Wessjohann, Cytotoxic effects of *Sarcophyton* sp. Soft corals—Is there a correlation to their NMR fingerprints?. *Marine Drugs*, 2017. 15(7).
336. Roy, P.K., S. Roy, and K. Ueda, New cytotoxic cembranolides from an Okinawan soft coral, *Lobophytum* sp. Fitoterapia, 2019. 136.
337. Minh, C.V., V.K. Phan, X.N. Nguyen, X.C. Nguyen, P.T. Nguyen, H.N. Nguyen, L.T.A. Hoang, C.T. Do, D.T.T. Thuy, H.-K. Kang, H.-D. Jang, and Y.H. Kim, Cytotoxic and antioxidant activities of diterpenes and sterols from the Vietnamese soft coral *Lobophytum compactum*. *Bioorganic and Medicinal Chemistry Letters*, 2011. 21(7).
338. Aboutabl, E.A., N.M. Selim, S.M. Azzam, C.G. Michel, M.F. Hegazy, and A.M. Ali, Polyhydroxy sterols isolated from the Red Sea soft coral *Lobophytum crassum* and their cytotoxic activity. *Natural Product Communications*, 2017. 12(2).
339. Brodie, J.E., F.J. Kroon, B. Schaffelke, E.C. Wolanski, S.E. Lewis, M.J. Devlin, I.C. Bohnet, Z.T. Bainbridge, J. Waterhouse, A.M. Davis, Terrestrial pollutant runoff to the Great Barrier Reef: An update of issues, priorities and management responses. *Marine Pollution Bulletin*, 2012. 65(4-9).
340. Carretta, L., A. Cardinali, E. Marotta, G. Zanin, and R. Masin, A new rapid procedure for simultaneous determination of glyphosate and AMPA in water at sub μg/L level. *Journal of Chromatography A*, 2019. 1600.
341. Lupi, L., F. Bedmar, M. Puricelli, D. Marino, V.C. Aparicio, and D. Wunderlin, Glyphosate runoff and its occurrence in rainwater and subsurface soil in the nearby area of agricultural fields in Argentina. *Chemosphere*, 2019. 225.
342. Dill, G.M., R.D. Sammons, P.C.C. Feng, F. Kohn, K. Kretzmer, A. Mehrsheikh, M. Bleeke, J.L. Honegger, D. Farmer, D. Wright, and E.A. Haupfear, Glyphosate: discovery, development, applications, and properties, in Glyphosate Resistance in Crops and Weeds. 2010.

343. Kanissery, R., B. Gairhe, D. Kadyampakeni, O. Batuman, and F. Alferez, Glyphosate: Its environmental persistence and impact on crop health and nutrition. *Plants* (Basel, Switzerland), 2019. 8(11).
344. Giesy, J.P., S. Dobson, and K.R. Solomon, Ecotoxicological risk assessment for Roundup® herbicide, in Reviews of Environmental Contamination and Toxicology: Continuation of Residue Reviews, G.W. Ware, Editor. 2000, Springer New York: New York, NY. p. 35-120.
345. Aurelie, V., S. Larroudé, and J.-F. Humbert, Herbicide contamination of freshwater ecosystems: Impact on microbial communities. pesticides - formulations, effects, fate, 2011.
346. Carles, L., H. Gardon, L. Joseph, J. Sanchís, M. Farré, and J. Artigas, Meta-analysis of glyphosate contamination in surface waters and dissipation by biofilms. *Environment International*, 2019. 124.
347. Skeff, W., C. Neumann, and D.E. Schulz-Bull, Glyphosate and AMPA in the estuaries of the Baltic Sea method optimization and field study. *Marine Pollution Bulletin*, 2015. 100(1).
348. Swanson, N., A.F. Leu, J. Abrahamson, and B.C. Wallet, Genetically engineered crops, glyphosate and the deterioration of health in the United States of America. *Journal of Organic Systems*, 2014. 9.
349. Maggi, F., D. Cecilia, Fiona.H.M. Tang, and A. McBratney, The global environmental hazard of glyphosate use. *Science of The Total Environment*, 2020. 717.
350. Annett, R., H.R. Habibi, and A. Hontela, Impact of glyphosate and glyphosate-based herbicides on the freshwater environment. *Journal of Applied Toxicology*, 2014. 34(5).
351. Mercurio, P., F. Flores, J.F. Mueller, S. Carter, and A.P. Negri, Glyphosate persistence in seawater. *Marine Pollution Bulletin*, 2014. 85(2).
352. Antunes, A.M., T.L. Rocha, F.S. Pires, M.A. de Freitas, V.R.M. Cruz Leite, S. Arana, P.C. Moreira, and S.M.T. Sabóia-Morais, Gender-specific histopathological response in guppies *Poecilia reticulata* exposed to glyphosate or its metabolite aminomethylphosphonic acid. *Journal of Applied Toxicology*, 2017. 37(9).
353. Skeff, W., C. Recknagel, and D.E. Schulz-Bull, The influence of salt matrices on the reversed-phase liquid chromatography behavior and electrospray ionization tandem mass spectrometry detection of glyphosate, glufosinate, aminomethylphosphonic acid and 2-aminoethylphosphonic acid in water. *Journal of Chromatography A*, 2016. 1475.
354. Janßen, R., W. Skeff2, J. Werner, M.A. Wirth, B.Kreikemeyer, D. Schulz-Bull, and M. Labrenz, A Glyphosate pulse to brackish long-term microcosms has a greater impact on the microbial diversity and abundance of planktonic than of biofilm assemblages. *Frontiers in Marine Science*, 2019. 6(758).
355. Avigliano, L., I.S. Canosa, D.A. Medesani, and E.M. Rodríguez, Effects of glyphosate on somatic and ovarian growth in the estuarine crab *Neohelice granulata*, during the pre-reproductive period. *Water, Air, & Soil Pollution*, 2018. 229.
356. Baier, F., E. Gruber, T. Hein, E. Bondar-Kunze, and M. Ivanković, Non-target effects of a glyphosate-based herbicide on common toad larvae (Bufo bufo, Amphibia) and associated algae are altered by temperature. *PeerJ*, 2016. 4.
357. Canosa, I.S., M.Zanitti, N. Lonné, D.A. Medesani, L.S.L. Greco, and E.M. Rodríguez, Imbalances in the male reproductive function of the estuarine crab *Neohelice granulata*, caused by glyphosate. *Ecotoxicology and Environmental Safety*, 2019. 182.
358. de Brito Rodrigues, L., R. de Oliveira, F.R. Abe, L.B. Brito, and D.S. Moura, Ecotoxicological assessment of glyphosate-based herbicides: Effects on different organisms. *Environmental Toxicology and Chemistry*, 2017. 36(7).
359. de Melo, M.S., T.P.G. dos Santos, M. Jaramillo, L. Nezzi, Y.M.R. Muller, and E.M. Nazari, Histopathological and ultrastructural indices for the assessment of glyphosate-based herbicide cytotoxicity in decapod crustacean hepatopancreas. *Aquatic Toxicology*, 2019. 210.
360. Osterberg, J.S., K.M. Darnell, T.M. Blickley, J.A. Romano, and D. Rittschof, Acute toxicity and sub-lethal effects of common pesticides in post-larval and juvenile blue crabs, Callinectes sapidus. *Journal of Experimental Marine Biology and Ecology*, 2012. 424-425.
361. Parlapiano, I., F. Biandolino, A. Grattagliano, A. Ruscito, G. Libralato, and E. Prato, Effects of commercial formulations of glyphosate on marine crustaceans and implications for risk assessment under temperature changes. *Ecotoxicology and Environmental Safety*, 2021. 213.

362. Séguin, A., A. Mottier, C. Perron, J.M. Lebel, A. Serpentini, and K. Costil, Sub-lethal effects of a glyphosate-based commercial formulation and adjuvants on juvenile oysters (*Crassostrea gigas*) exposed for 35days. *Marine Pollution Bulletin*, 2017. 117(1-2).
363. Silva, P.M.d., Toxicological evaluation of the herbicide glyphosate in the cultured oyster Crassostrea gasar. *Journal of Aquaculture & Marine Biology*, 2018. 7.
364. Tsui, M.T.K. and L.M. Chu, Aquatic toxicity of glyphosate-based formulations: comparison between different organisms and the effects of environmental factors. *Chemosphere*, 2003. 52(7).
365. Lushchak, O.V., O.I. Kubrak, J.M. Storey, K.B. Storey, and V.I. Lushchak, Low toxic herbicide Roundup induces mild oxidative stress in goldfish tissues. *Chemosphere*, 2009. 76(7).
366. Muhammad, U.A., N.A. Yasid, H.M. Daud, and M.Y. Shukor, Glyphosate herbicide induces changes in the growth pattern and somatic indices of crossbred red tilapia (*O. niloticus* × *O. mossambicus*). *Animals*, 2021. 11(5).
367. Webster, T.M.U., L.V. Laing, H. Florance, and E.M. Santos, Effects of glyphosate and its formulation, roundup, on reproduction in zebrafish (*Danio rerio*). *Environmental Science and Technology*, 2014. 48(2).
368. Cruz de Carvalho, R., E. Feijão, A.R. Matos, M.T. Cabrita, S.C. Novais, and M.F. Lemos, Glyphosate-based herbicide toxicophenomics in marine diatoms: Impacts on primary production and physiological fitness. *Applied Sciences*, 2020. 10.
369. Steinrücken, H.C. and N. Amrhein, The herbicide glyphosate is a potent inhibitor of 5-enolpyruvyl-shikimic acid-3-phosphate synthase. *Biochemical and Biophysical Research Communications*, 1980. 94(4).
370. van Bruggen, A.H.C., M.M. He, K. Shin, V. Mai, K.C. Jeong, M.R. Finckh, and J.G. Morris Jr, Environmental and health effects of the herbicide glyphosate. *Science of The Total Environment*, 2018. 616-617.
371. Wong, P.K., Effects of 2,4-D, glyphosate and paraquat on growth, photosynthesis and chlorophyll–a synthesis of *Scenedesmus quadricauda* Berb 614. *Chemosphere*, 2000. 41(1).
372. Chen, Y., M. Jun, H. Huang, P. Chen, F. and Chao, Effects of temperature, pH, ammonia nitrogen content and salinity on coral (*Acropora millepora* & *Palythoa* sp.) bleaching. *Agricultural Biotechnology*; Cranston, 2017. 6(6).
373. Kaeoboon, S., R. Suksungworn, and N. Sanevas, Toxicity response of *Chlorella* microalgae to glyphosate herbicide exposure based on biomass, pigment contents and photosynthetic efficiency. *Plant Science Today*, 2021. 8.
374. Singh, S., V. Kumar, J.P.K. Gill, S. Datta, S. Singh, V. Dhaka, D. Kapoor, A.B. Wani, D. Dhanjal, M. Kumar, S.L. Harikumar, and J. Singh, Herbicide glyphosate: Toxicity and microbial degradation. *International journal of environmental research and public health*, 2020. 17(20).
375. Cobb, A.H. and J.P.H. Reade, The inhibition of amino acid biosynthesis, *Herbicides and Plant Physiology*. 2010.
376. Gomes, M.P., S.G.L. Manac'h, L. Hénault-Ethier, M. Labrecque, M. Lucotte, and P. Juneau, Glyphosate-dependent inhibition of photosynthesis in willow. *Frontiers in Plant Science*, 2017. 8.
377. Gomes, M.P., S.G.L. Manac'h, S. Maccario, M. Labrecque, M. Lucotte, and P. Juneau, Differential effects of glyphosate and aminomethylphosphonic acid (AMPA) on photosynthesis and chlorophyll metabolism in willow plants. *Pesticide Biochemistry and Physiology*, 2016. 130.
378. Sandmann, G., S. Römer, and P.D. Fraser, Understanding carotenoid metabolism as a necessity for genetic engineering of crop plants. *Metabolic Engineering*, 2006. 8(4).
379. Gomes, M., F.V. da Silva Cruz, E.M. Bicalho, F.V. Borges, and M.B. Fonseca, Effects of glyphosate acid and the glyphosate-commercial formulation (Roundup) on *Dimorphandra wilsonii* seed germination: Interference of seed respiratory metabolism. *Environmental Pollution*, 2018. 220.

380. Gomes, M.P. and P. Juneau, Oxidative stress in duckweed (*Lemna minor* L.) induced by glyphosate: Is the mitochondrial electron transport chain a target of this herbicide?. *Environmental Pollution*, 2016. 218.
381. Havaux, M., Carotenoids as membrane stabilizers in chloroplasts. *Trends in Plant Science*, 1998. 3(4).
382. Burriesci, M.S., T.K. Raab, and J.R. Pringle, Evidence that glucose is the major transferred metabolite in dinoflagellate-cnidarian symbiosis. *The Journal of experimental biology*, 2012. 215(Pt 19).
383. Leletkin, V.A., The energy budget of coral polyps. *Russian Journal of Marine Biology*, 2000. 26(6).
384. Cantin, N., A. Negri, and B. Willis, Photoinhibition from chronic herbicide exposure reduces reproductive output of reef-building corals. *Marine Ecology Progress Series*, 2007. 344.
385. Flores, F., C.J. Collier, P. Mercurio, and A.P. Negri, Phytotoxicity of four photosystem II herbicides to tropical seagrasses. *PLOS ONE*, 2013. 8(9).
386. Ralph, P., Herbicide toxicity of *Halophila ovalis* assessed by chlorophyll a fluorescence. *Aquatic Botany*, 2000. 66.
387. Slattery, M., M.S. Pankey, and M.P. Lesser, Annual thermal stress increases a soft coral's susceptibility to bleaching. *Scientific Reports*, 2019. 9(1).
388. Berkelmans, R. and M.J.H. van Oppen, The role of zooxanthellae in the thermal tolerance of corals: a 'nugget of hope' for coral reefs in an era of climate change. *Proceedings of the Royal Society B: Biological Sciences*, 2006. 273(1599).
389. Ghavam M.P., S.M.R. Fatemi, M.H. Shahhosseiny, O. Hoegh-Guldberg, and W.K.W. Loh, Predominance of clade D *Symbiodinium* in shallow-water reef-building corals off Kish and Larak Islands (Persian Gulf, Iran). *Marine Biology*, 2007. 153(1).
390. Guest, J.R., J. Low, K. Tun, B. Wilson, C. Ng, D. Raingeard, K.E. Ulstrup, J.T.I. Tanzil, P.A. Todd, T.C. Toh, L.M. Chou, and P.D. Steinberg, Coral community response to bleaching on a highly disturbed reef. *Scientific Reports*, 2016. 6(1).
391. LaJeunesse, T.C., D.C. Wham, D.T. Pettay, J.E. Parkinson, S. Keshavmurthy, and C.A. Chen, Ecologically differentiated stress-tolerant endosymbionts in the dinoflagellate genus *Symbiodinium* (Dinophyceae) Clade D are different species. *Phycologia*, 2014. 53(4).
392. Silverstein, R.N., R. Cunning, and A.C. Baker, Change in algal symbiont communities after bleaching, not prior heat exposure, increases heat tolerance of reef corals. *Global Change Biology*, 2015. 21(1).
393. Stat, M. and R. Gates, Clade D Symbiodinium in scleractinian corals: A "Nugget" of hope, a selfish opportunist, an ominous sign, or all of the above?. *Journal of Marine Biology*, 2011. 2011.
394. Downs, C.A., J.E. Fauth, J.C. Halas, P. Dustan, J. Bemiss, and C.M. Woodley, Oxidative stress and seasonal coral bleaching. *Free Radical Biology and Medicine*, 2002. 33(4).
395. Nielsen, D.A., K. Petrou, and R.D. Gates, Coral bleaching from a single cell perspective. *The ISME journal*, 2018. 12(6).
396. Weis, V.M., Cellular mechanisms of Cnidarian bleaching: stress causes the collapse of symbiosis. *Journal of Experimental Biology*, 2008. 211(Pt 19).
397. Jones, R., J. Muller, D. Haynes, and U. Schreiber, Effects of herbicides diuron and atrazine on corals of the Great Barrier Reef, Australia. *Marine Ecology Progress Series*, 2003. 251.
398. Negri, A., C. Vollhardt, C. Humphrey, A. Heyward, R. Jones, G. Eaglesham, K. Fabricius, Effects of the herbicide diuron on the early life history stages of coral. *Marine Pollution Bulletin*, 2005. 51(1).
399. Jones, R., Zooxanthellae loss as a bioassay for assessing stress in corals. *Marine Ecology Progress Series*, 1997. 149.
400. Li, S., K.F. Yu, Q. Shi, T.R. Chen, M.X. Zhao, and J.X. Zhao, Interspecies and spatial diversity in the symbiotic zooxanthellae density in corals from northern South China Sea and its relationship to coral reef bleaching. *Chinese Science Bulletin*, 2008. 53.
401. Gurr, M.I., J.L. Harwood, and K.N. Frayn, Lipid biochemistry. 2002. 409: Springer.
402. Xiao, J.F., B. Zhou, and H.W. Ressom, Metabolite identification and quantitation in LC-MS/MS-based metabolomics. *Trends in analytical chemistry*: TRAC, 2012. 32.

403. Imbs, A., I. Yakovleva, and Q.-L. Pham, Distribution of lipids and fatty acids in the zooxanthellae and host of the soft coral *Sinularia* sp. *Fisheries Science*, 2010. 76.
404. Luo, Y.-J., L.-H. Wang, W.-N.U. Chen, S.-E. Peng, J.T.-C. Tzen, Y.-Y. Hsiao, H.-J. Huang, L.-S. Fang, and C.-S. Chen, Ratiometric imaging of gastrodermal lipid bodies in coral–dinoflagellate endosymbiosis. *Coral Reefs*, 2009. 28(1).
405. Patton, J., S. Abraham, and A.A. Benson, Lipogenesis in the intact coral *Pocillopora capitata* and its isolated zooxanthellae: evidence for a light-driven carbon cycle between symbiont and host. *Marine Biology*, 1977. 44(3).
406. Groppa, M.D. and M.P. Benavides, Polyamines and abiotic stress: recent advances. *Amino Acids*, 2008. 34(1).
407. Treignier, C., R. Grover, C. Ferrier-Pagés, and I. Tolosa, Effect of light and feeding on the fatty acid and sterol composition of zooxanthellae and host tissue isolated from the scleractinian coral *Turbinaria reniformis*. *Limnology and oceanography*, 2008. 53.
408. Imbs, A., M. Yakovleva, N.A. Latyshev, and L.Q. Pham, Biosynthesis of polyunsaturated fatty acids in zooxanthellae and polyps of corals. *Russian journal of marine biology*, 2010. 36(6).
409. Imbs, A.B., I. Yakovlevaet, T. Dautova, and L.H. Bui, Diversity of fatty acid composition of symbiotic dinoflagellates in corals: evidence for the transfer of host PUFAs to the symbionts. *Phytochemistry*, 2014. 101.
410. Almeyda, M., P.G.S. Bilbao, C.A. Popovich, D. Constenla, and P.I. Leonardi, Enhancement of polyunsaturated fatty acid production under low-temperature stress in *Cylindrotheca closterium*. *Journal of Applied Phycology*, 2020. 32.
411. Cointet, E., G. Wielgosz-Collin, G. Bougaran, V. Rabesaotra, O. Gonçalves, and V. Méléder, Effects of light and nitrogen availability on photosynthetic efficiency and fatty acid content of three original benthic diatom strains. *PLOS ONE*, 2019. 14(11).
412. de Jesús-Campos, D., J.A. López-Elías, Luis.Á. Medina-Juarez, G. Carvallo-Ruiz, D. Fimbres-Olivarria, and C. Hayano-Kanashiroa, Chemical composition, fatty acid profile and molecular changes derived from nitrogen stress in the diatom *Chaetoceros muelleri*. *Aquaculture Reports*, 2020. 16.
413. Sayanova, O., V. Mimouni, L. Ulmann, A. Morant-Manceau, V. Pasquet, B. Schoefs, J.A. Napier, Modulation of lipid biosynthesis by stress in diatoms. P*hilosophical Transactions of the Royal Society B: Biological Sciences*, 2017. 372(1728).
414. Da Gama, B., E. Plouguerné, and R. Pereira, The antifouling defence mechanisms of marine macroalgae. 2014.
415. de Sousa, I.P., M.V. Sousa Teixeira, and N.A. An overview of biotransformation and toxicity of diterpenes. *Molecules* (Basel, Switzerland), 2018. 23(6).
416. Pawlik, J.R., Marine invertebrate chemical defenses. *Chemical Reviews*, 1993. 93(5).
417. Chan, Y.S., C.W. Ong, B.L. Chuah, K.S. Khoo, F.Y. Chye, and N. Sit, Antimicrobial, antiviral and cytotoxic activities of selected marine organisms collected from the coastal areas of Malaysia. *Journal of Marine Science and Technology* (Taiwan), 2018. 26.
418. Cheng, S.-Y., Z.-H. Wen, S.-K. Wang, S.-F. Chiou, and C.-H. Su, Anti-inflammatory cembranolides from the soft coral *Lobophytum durum*. *Bioorganic & Medicinal Chemistry*, 2009. 17(11).
419. Hassan, A., R. Mohammed, H. Hetta, A, Abdelaziz, O. El-Gendy, and A. Sleim, Biological and chemical investigation of the soft coral *Lobophytum pauciflorum* collected from the Egyptian Red Sea. *International Journal of Pharmacognosy and Phytochemical Research*, 2016. 8.
420. Raveendran, T.V., V.P. Limna Mol, and P.S. Parameswaran, Natural product antifoulants from the octocorals of Indian waters. *International Biodeterioration and Biodegradation*, 2011. 65(1).
421. Roy, P.K., R. Ashimine, H. Miyazato, J. Taira, and K. Ueda, New casbane and cembrane diterpenoids from an okinawan soft coral, *Lobophytum* sp. *Molecules*, 2016. 21(5).
422. Wang, S.-K. and C.-Y. Duh, New cytotoxic cembranolides from the soft coral *Lobophytum michaelae*. *Marine Drugs*, 2012. 10(2).

423. Yamada, K., K. Ryu, T. Miyamoto, and R. Higuchi, Bioactive terpenoids from octocorallia. 4. Three new cembrane-type diterpenoids from the soft coral *Lobophytum schoedei*. *Journal of Natural Products*, 1997. 60(8).
424. Cruz de Carvalho, R., E. Feijão, A.R. Matos, M.T. Cabrita, and S.C. Novais, Glyphosate-based herbicide toxicophenomics in marine diatoms: Impacts on primary production and physiological fitness. *Applied Sciences*, 2020. 10(21).
425. Hernando, F., M. Royuela, A. Muñoz-Rueda, and C. Gonzalez-Murua, Effect of glyphosate on the greening process and photosynthetic metabolism in *Chlorella pyrenoidosa*. *Journal of Plant Physiology*, 1989. 134(1).
426. Doddaiah, K.M, A. Narayan, R.G. Aswathanarayana, and S. Ravi, Effect of metabolic inhibitors on growth and carotenoid production in *Dunaliella bardawil*. *Journal of food science and technology*, 2013. 50(6).
427. Percival, G.C., The influence of glyphosate on carotenoid pigments, reactive oxygen species scavenging enzymes and secondary stress metabolites within leaf tissue of three Acer species. *Urban Forestry and Urban Greening*, 2017. 24.
428. Sawadogo, W.R., R. Boly, C. Cerella, M.H. Teiten, M. Dicato, and M. Diederich, A survey of marine natural compounds and their derivatives with anti-cancer activity reported in 2012. *Molecules*, 2015. 20(4).
429. Abraham, I., K. El-Sayed, Z.-S. Chen, and H. Guo, Current status on marine products with reversal effect on cancer multidrug resistance. *Marine drugs*, 2012. 10(10).
430. Farag, M.A., A. Meyer, S.E. Ali, M.A. Salem, P. Giavalisco, H. Westphal, and L.A. Wessjohann, Comparative metabolomics approach detects stress-specific responses during coral bleaching in soft corals. *Journal of Proteome Research*, 2018. 17(6).
431. Kuanui, P., S. Chavanich, V. Viyakarn, M. Omori, and C. Lin, Effects of temperature and salinity on survival rate of cultured corals and photosynthetic efficiency of zooxanthellae in coral tissues. *Ocean Science Journal*, 2015. 50.
432. Muscatine, L. and J.W. Porter, Reef Corals: Mutualistic symbioses adapted to nutrient-poor environments. *BioScience*, 1977. 27(7).
433. Coll, J.C., The chemistry and chemical ecology of octocorals (Coelenterata, Anthozoa, Octocorallia). *Chemical Reviews*, 1992. 92(4).
434. Hayat, S., Q. Hayat, M.N. Alyemeni, A.S. Wani, J. Pichtel, and A. Ahmad, Role of proline under changing environments: A Review. *Plant Signaling and Behavio*, 2012. 7(11).
435. Galma, W., M. Endale, E. Getaneh, R. Eswaramoorthy, T. Assefa, and Y. Melaku, Antibacterial and antioxidant activities of extracts and isolated compounds from the roots extract of *Cucumis prophetarum* and in silico study on DNA gyrase and human peroxiredoxin 5. *BMC chemistry*, 2021. 15(1).
436. de Lima, C., K.M.T. Caffaro, M.G.S. Araújo, M.L. de Bastos, C. Lucia, and E. Barreto, Antibacterial and cytotoxic activity of extracts and isolated compounds from *Myrciaria ferruginea* (Myrtaceae). *Records of Natural Products***,** 2017.

Appendix

Appendix 1 Gene sequences used for the identification of the octocoral species from this study

Table A.1. Gene sequences used for the identification of the octocoral species (*Sarcophyton glaucum*, *Lobophytum crassum*, and *Xenia umbellata*) used in this study

Species with identical sequences	**Museum voucher**	**Accession No. mutS**	**Accession No. COI**	**Accession No. 28S**
Xenia umbellata	ZMTAU:36792	KT590460.1	KT590441.1	MK400153.1
X. umbellata	ZMTAU:36791	-	KT590440.1	KY442370.1
X. umbellata	ZMTAU:37034	KT590459.1	-	-
X. umbellata	ZMTAU:36790	KT590458.1	KT590439.1	KY442369.1
X. umbellata	ZMTAU:36788	KT590457.1	KT590438.1	KY442367.1
X. umbellata	ZMTAU:36883	KT590456.1	-	-
X. umbellata	ZMTAU:36877	KT590455.1	-	-
X. umbellata	ZMTAU:36780	KT590454.1	KT590437.1	KY442359.1
X. umbellata	ZMTAU:36784	KT590453.1	KT590436.1	-
X. umbellata	ZMTAU:36783	KT590452.1	KT590435.1	KY442362.1
X. umbellata	USNM:1202016	KC864921.1	KC864990.1	KY442391.1
X. umbellata	USNM:1202005	KC864912.1	KC864981.1	KM201437.1
X. hicksoni	ZMTAU:Co34073	MK396705.1	MK396749.1	MK400170.1
X. hicksoni	ZMTAU:Co34072	GQ342529.1	GQ342463.1	JX203759.1
Lobophyton crassum	RMNH:Coel. 40954	KF915643.1	KF955112.1	KF915408.1
L. crassum	ZMTAU:Co36321	MH516609.1	MH516361.1	-
L. crassum	ZMTAU:Co35325	MH516601.1	MH516352.1	-
L. crassum	ZMTAU:Co35370	MH516604.1	MH516551.1	-
L. crassum	isolate KE-216	-	-	MG583546.1
L. crassum	isolate KE-210	-	-	MG583545.1
L. crassum	isolate KE-207	-	-	MG583544.1
L. crassum	isolate KE-193	-	-	MG583543.1
L. crassum	isolate KE-144	-	-	MG583542.1
L. crassum	isolate KE-136	-	-	MG583541.1
L. crassum	isolate KE-132	-	-	MG583540.1
L. crassum	isolate KE-125	-	-	MG583539.1
L. crassum	isolate KE-116	-	-	MG583537.1
L. crassum	isolate KE-63	-	-	MG583534.1
L. borbonicum	NTM-C005514D	DQ280555.1	-	-
Sarcophyton glaucum	RMNH:Coel. 41008	KF915701.1	-	-
S. glaucum	RMNH:Coel._41009	KF915702.1	-	-
S. glaucum	RMNH:Coel. 41028	KF915709.1	-	-
S. glaucum	RMNH:Coel._41030	KF915710.1	-	-
S. glaucum	RMNH:Coel._41036	KF915713.1	-	-
S. glaucum	NTM-C013877	DQ280527.1	-	-

Appendix 2 Linear dynamic range (dilution range) experiment on soft corals extract

Table A.2. Selected concentration of *Sarcophyton glaucum* extracts for determination of the linear dynamic range (the suitable concentration) for LC-HRMS measurement

No.	Dilution range	Concentration (mg/mL)
1.	1 to 0	8
2.	1/1	4
3.	1/2	2
4.	1/3	1
5.	1/4	0.5

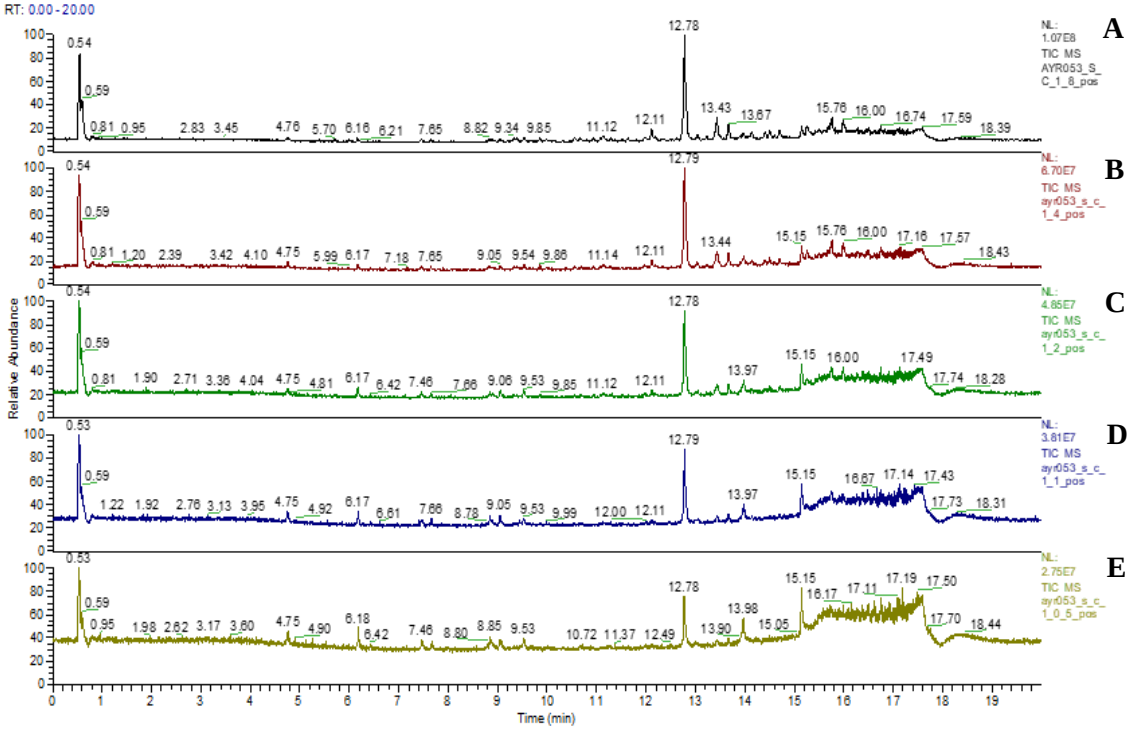

Figure A.1. LC-HRMS spectra of *S. glaucum* extracts in different concentration; 8 mg/mL (**A**), 4 mg/mL (**B**), 2 mg/mL (**C**), 1 mg/mL (**D**), 0.5 mg/mL (**E**)

The LC-HRMS spectra of all samples were then evaluated with the Xcalibur software 2.2 SP1 (Thermo Fisher Scientific) to process the linear dynamic range for metabolic profiling. To check the linear range of MS peak intensity, nine representative masses (*m/z*) with different intensity were selected (Table bellow). The data were then analyzed using statistical regression analysis.

Table A.3. Molecular mass $[M+H]^+$ of the selected peaks (ion) for determination of the linear dynamic range in positive ion mode of *S. glaucum* extracts

Molecular mass (*m/z*) $[M+H]^+$	Relative intensity	Retention time
285.2209	1.34 E7	12.78
510.3809	1.76 E6	13.44
553.3306	1.99 E6	13.97
466.3285	3.03 E5	13.44
631.3609	2.35 E5	13.67
394.2579	2.25 E5	9.86
331.1899	1.89 E4	9.85
438.2975	2.0 E4	12.11
494.3594	4.7 E4	12.67

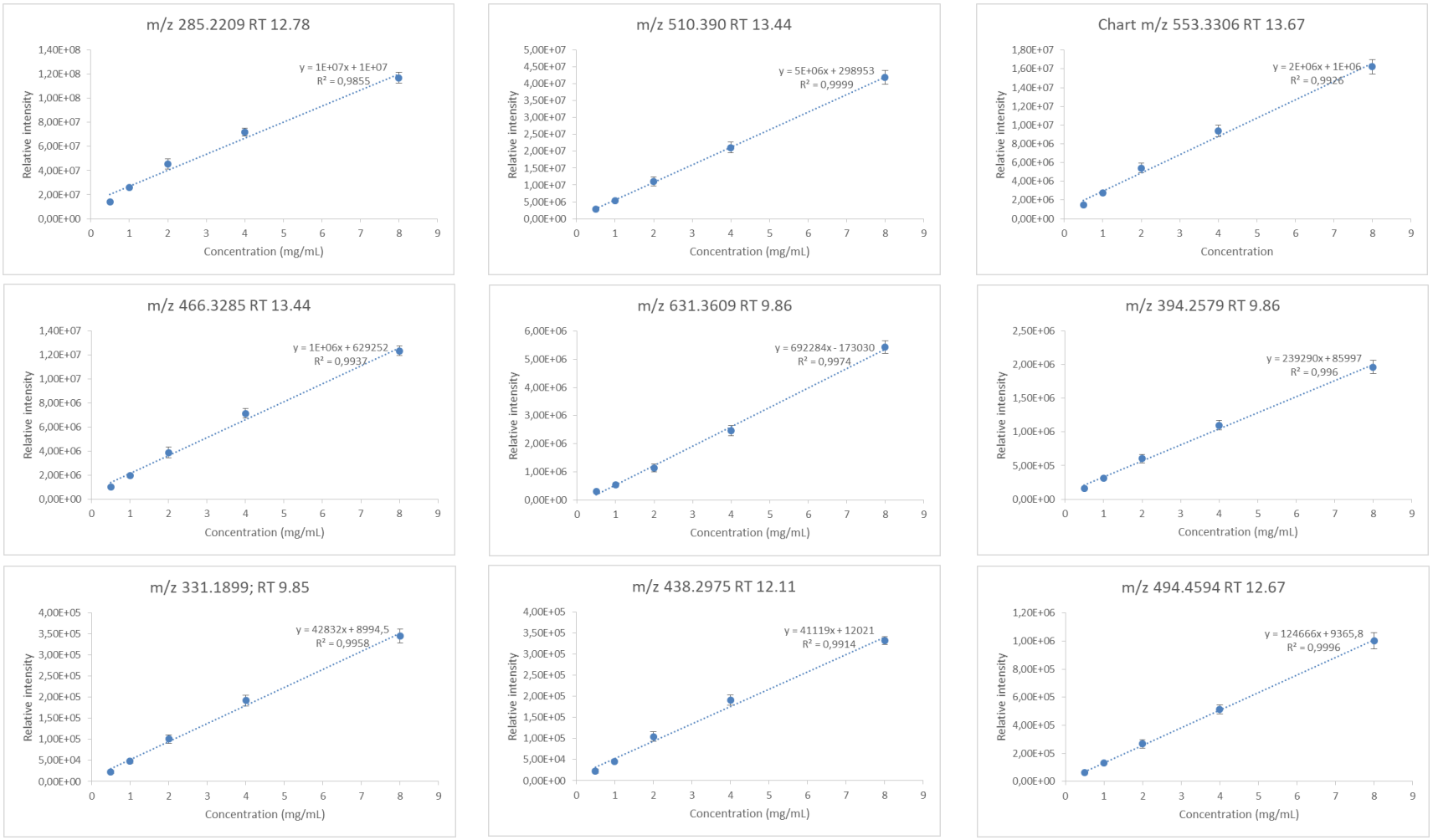

Figure A.2. Diagram of regression analysis data for linear dynamic range *S. glaucum* extract

As result, a concentration of 2 mg freeze dried material per mL will be used for the next experiments to avoid losing the peaks at the lower concentration, as well as the saturated of the highest peaks.

Appendix 3 ^{1}H-NMR spectra of elicitors

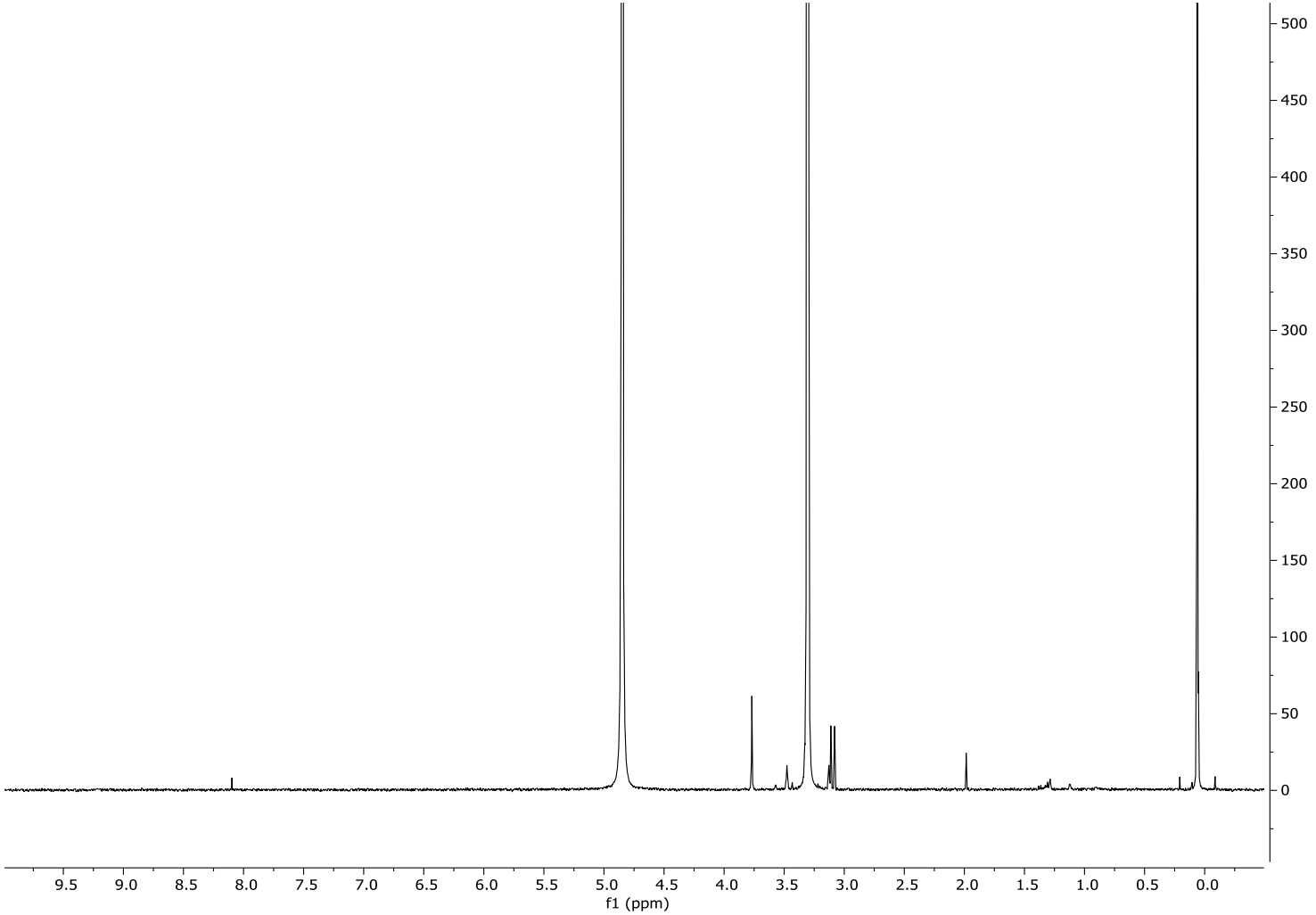

Figure A.3. ^{1}H NMR spectra of glyphosate in CD_3OD

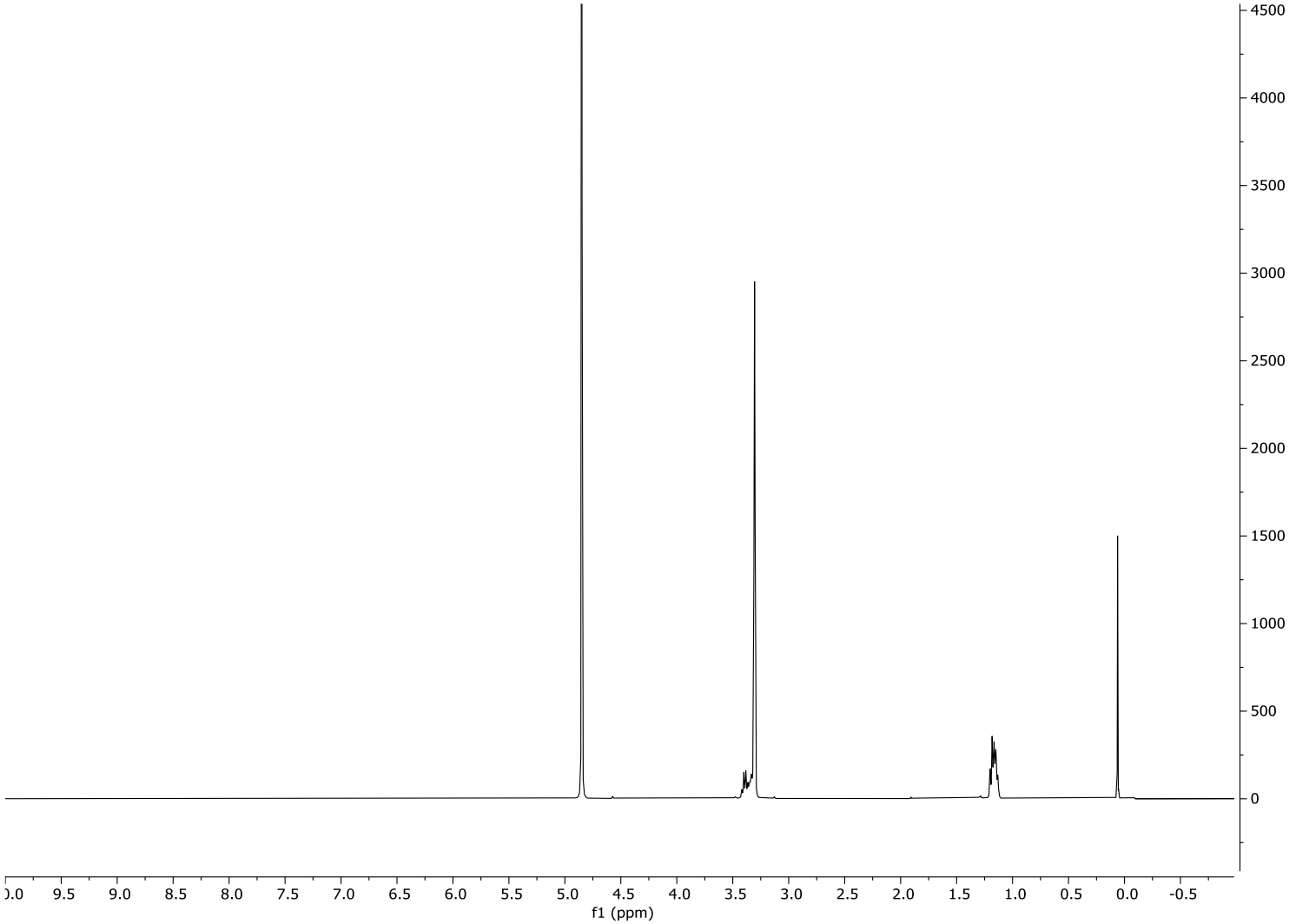

Figure A.4. ^{1}H NMR spectra of simazine in CD_3OD

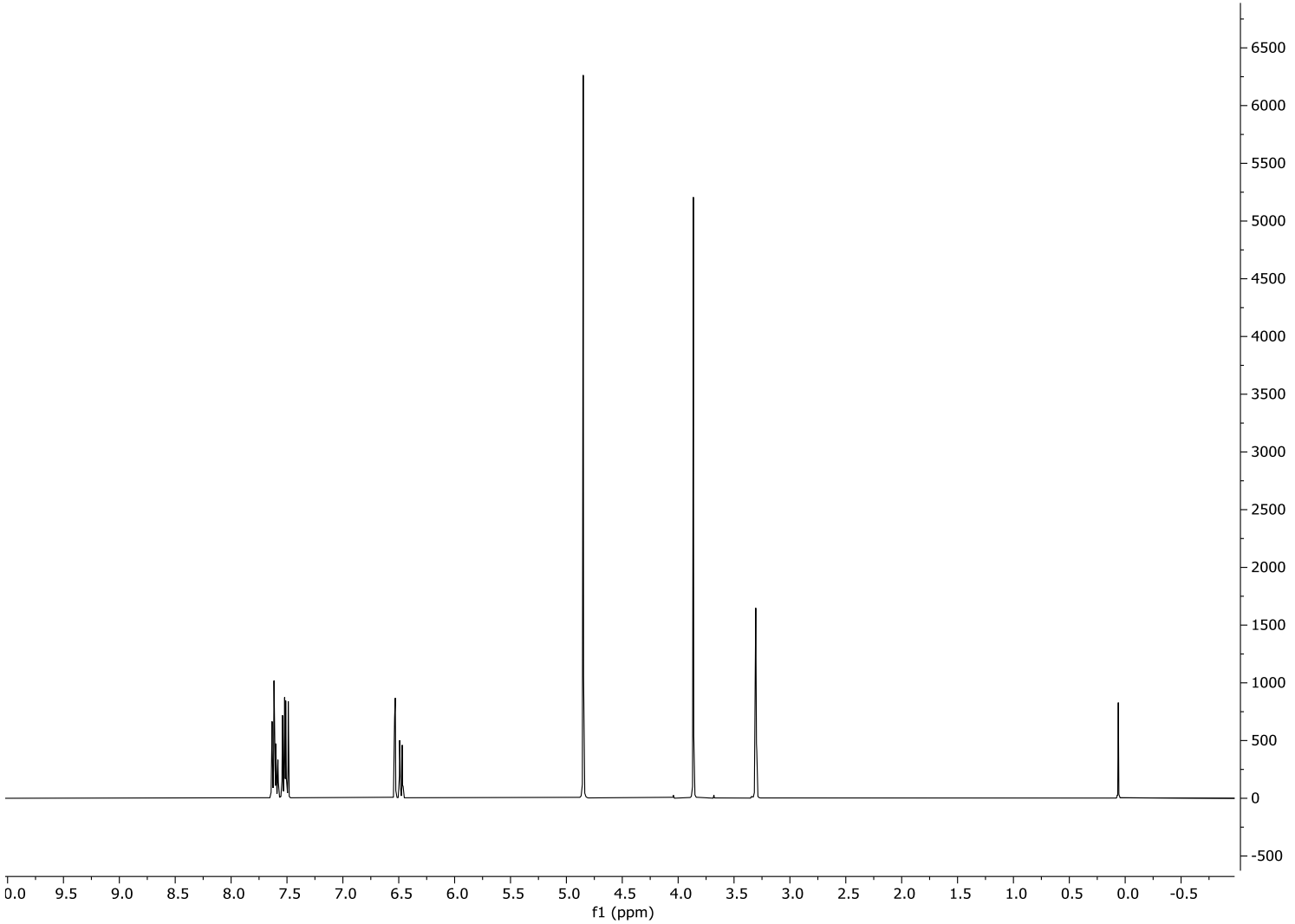

Figure A.5. ^{1}H NMR spectra of oxybenzone in CD_3OD

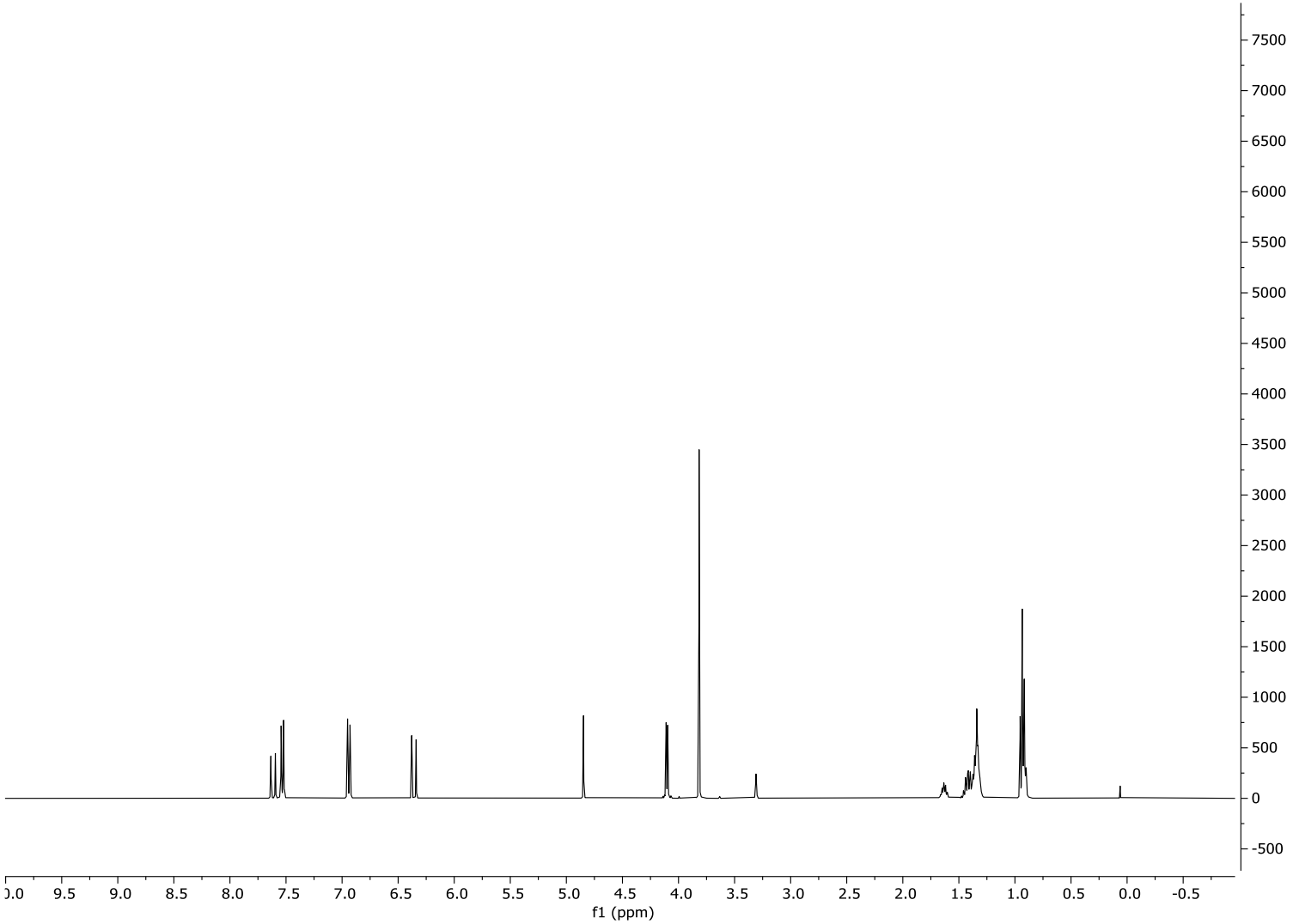

Figure A.6. ^{1}H NMR spectra of octinoxate in CD_3OD

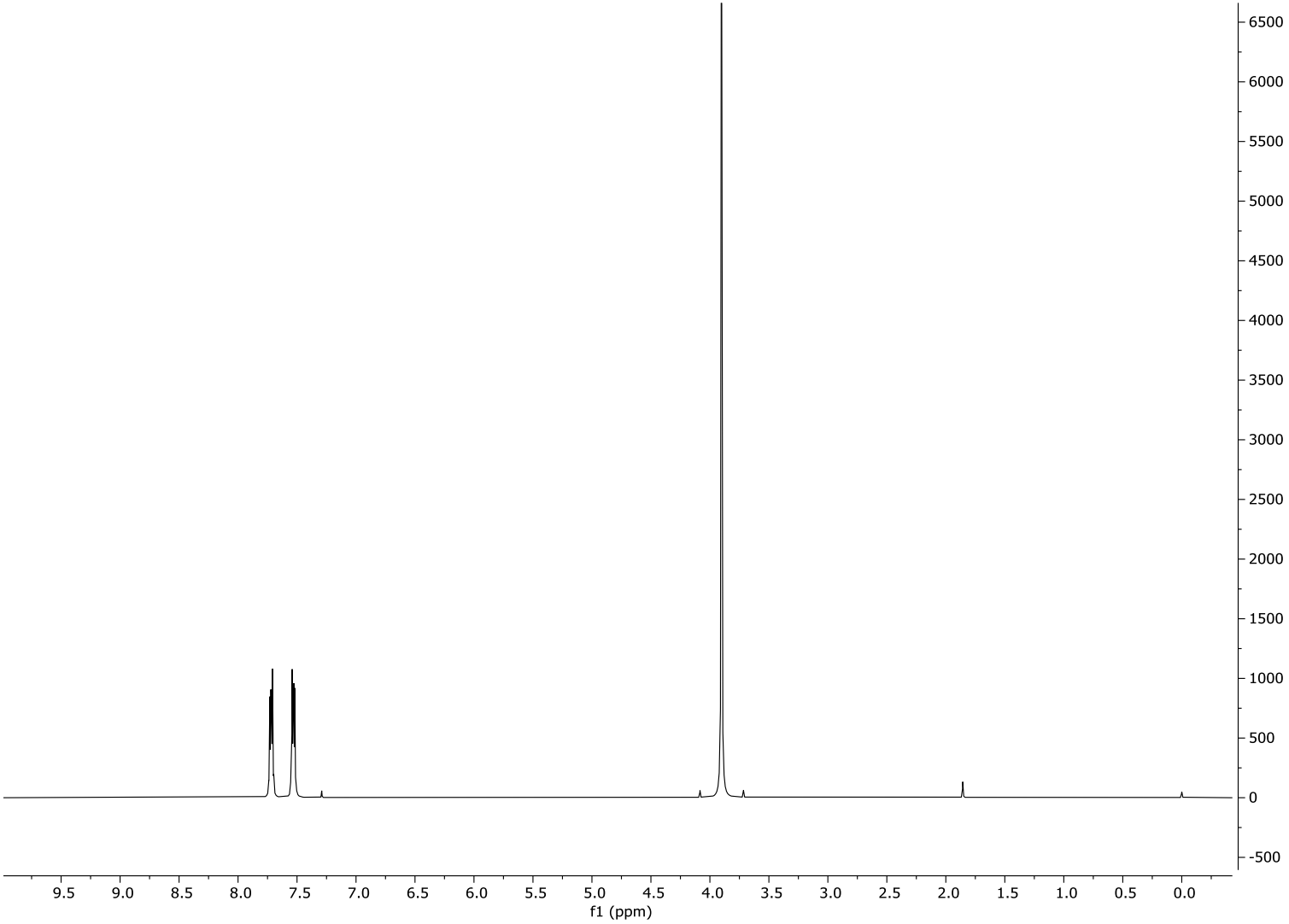

Figure A.7. ^{1}H NMR spectra of dimethyl phthalate in CD_3OD

Appendix 4 Selected known compounds and their spatial distribution in the body of *S. glaucum* and *L. crassum*

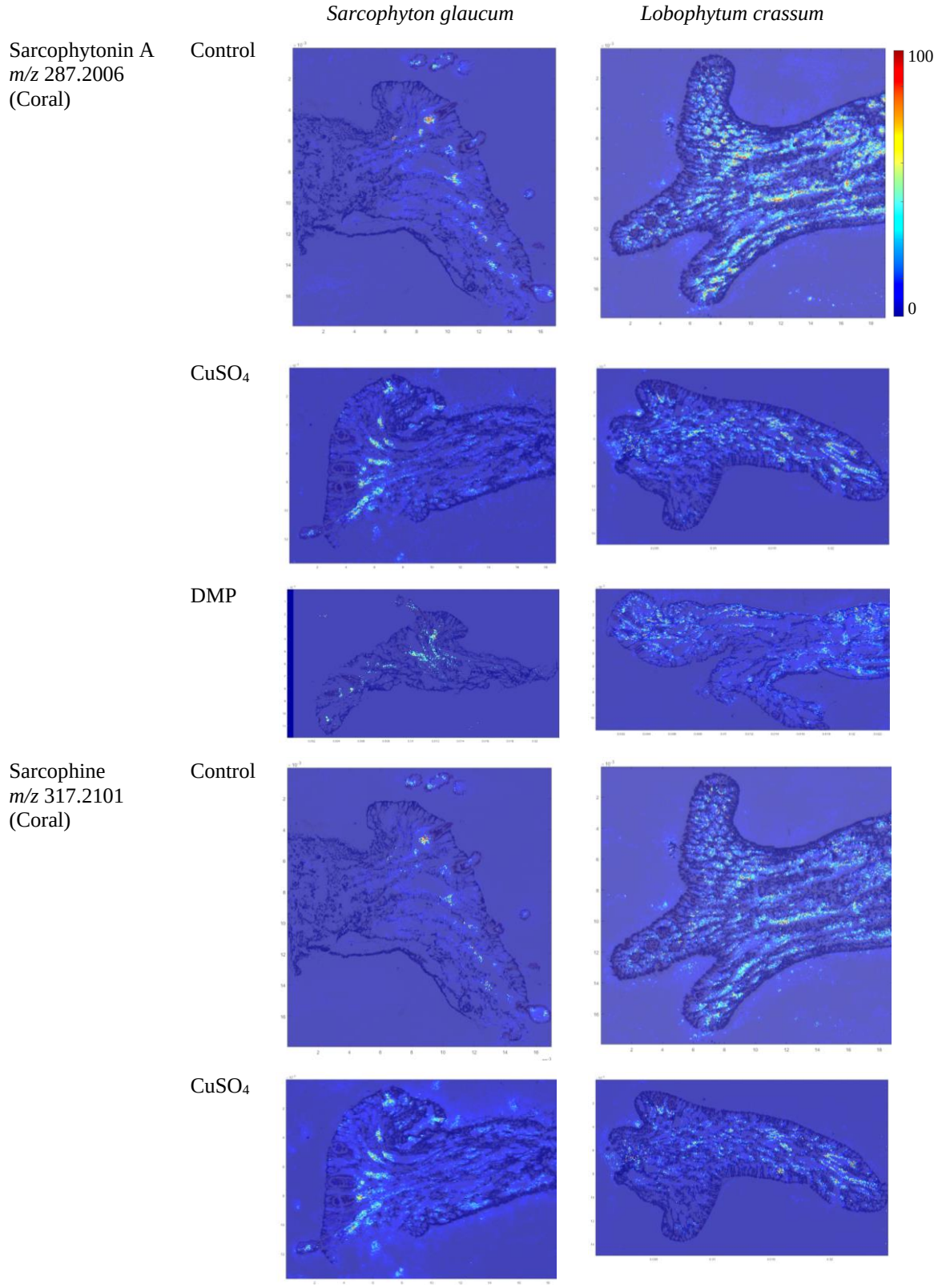

	DMP	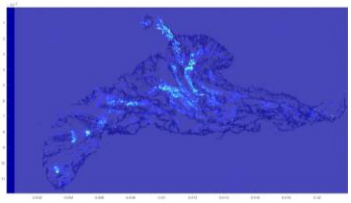	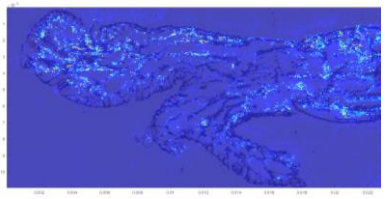
Crassumolide C *m/z* 345.2422 (Coral)	Control	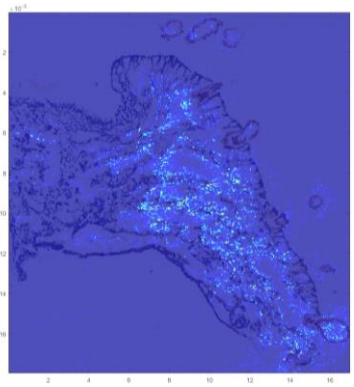	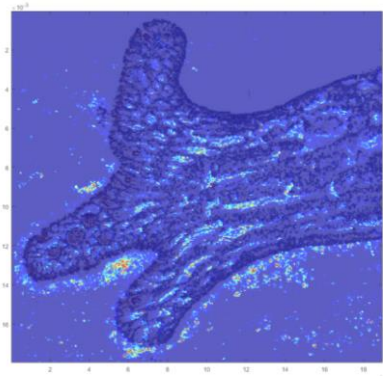
	$CuSO_4$	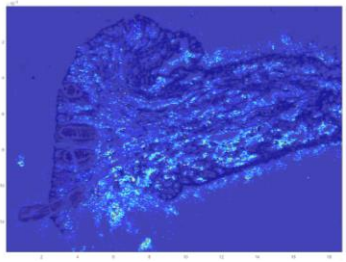	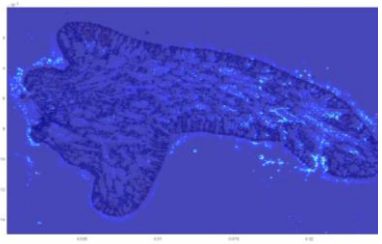
	DMP	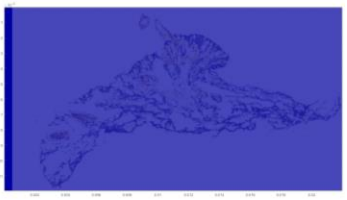	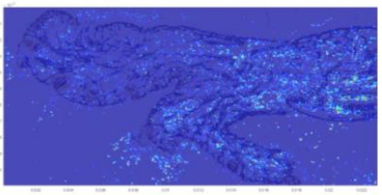
(4, 7, 10, 13)-4-Isopropenyl-7,11-dimethyl-14-oxabyclo[11.2.1]-hexadeca-1(16),7,10-triene-6,9,15-trione *m/z* 329.1750 (Coral)	Control	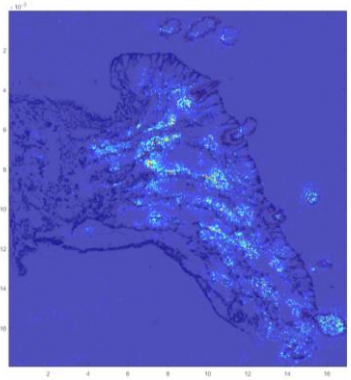	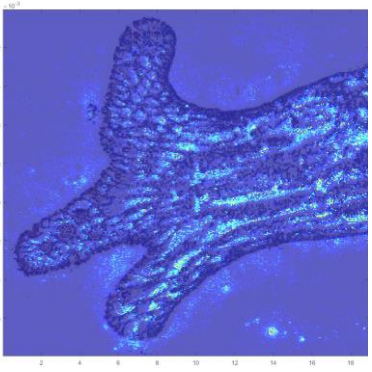
	$CuSO_4$	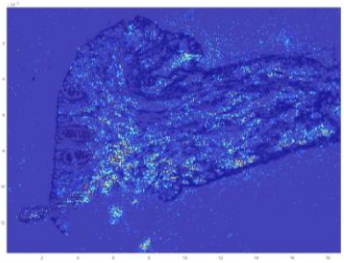	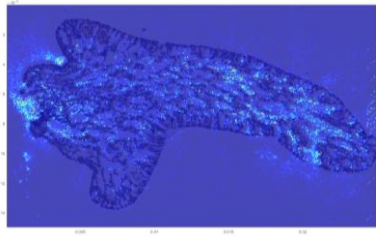

	DMP		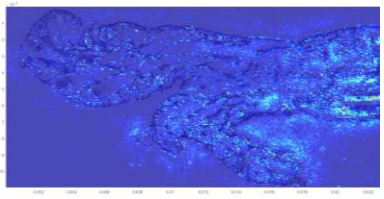
1-*O*-Arachidonoyl-sn-glycero-3-phosphoethanolamine *m/z* 502.2922 (Coral or zooxanthellae)	Control	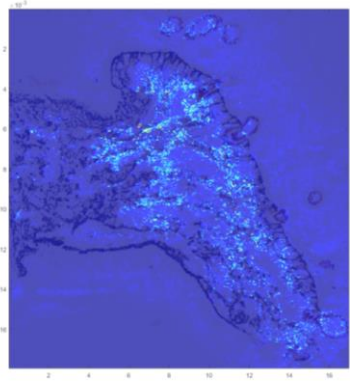	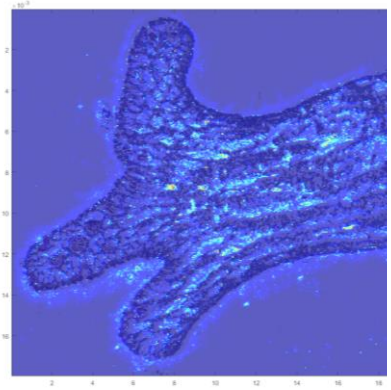
	$CuSO_4$	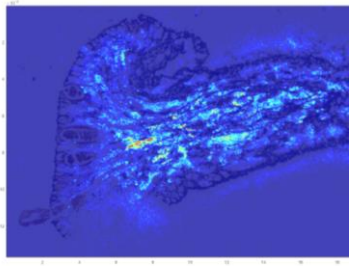	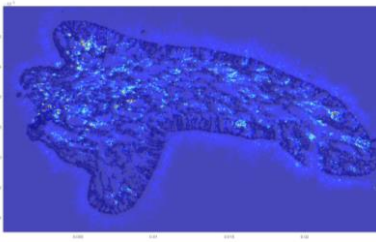
	DMP	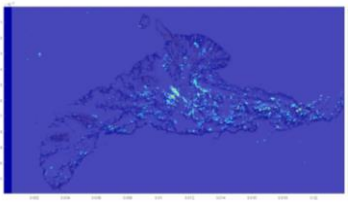	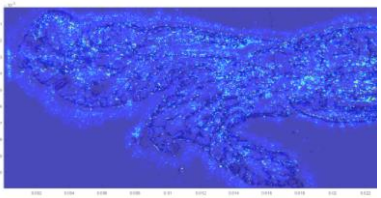
Cerebrosides 1-*O*-*β*-*DS*-Glucopyranosyl-(2, 3, 4, 8, 10)-2-[(2)hydroxydocosanoyl amini]-octadeca-4,8,10-triene-1,2-diol *m/z* 796.6213 (Coral)	Control	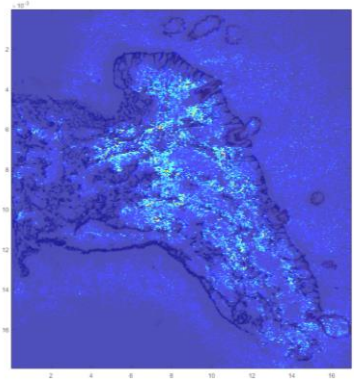	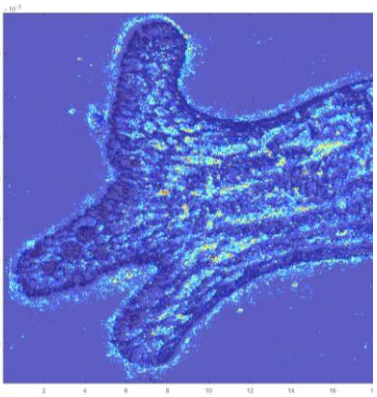
	$CuSO_4$	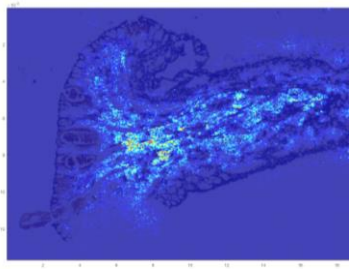	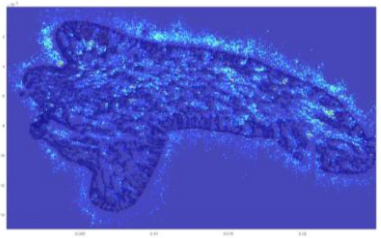

	DMP	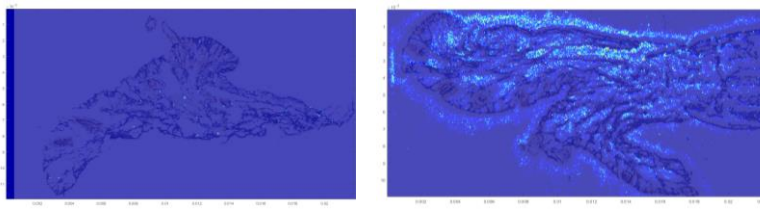
Nitrogenous lipid (5,7,9)-2,3-dihydroxy-*N*-((2,3,4,)-1,3,4-Trihydroxytetradec-6-en-2-yl)pentacosa-5,7,9-trienamide *m/z* 650.5358 (Coral)	Control	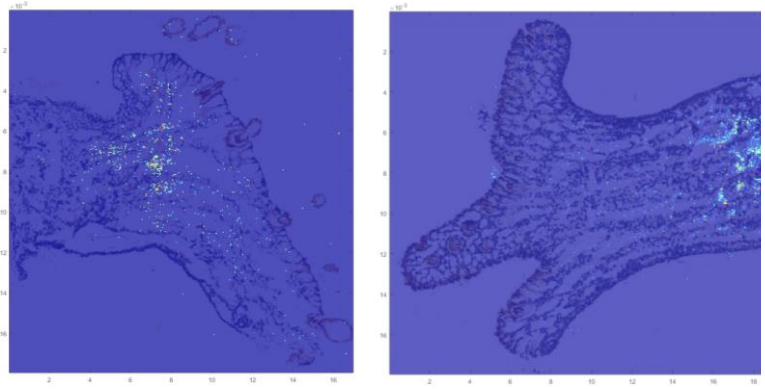
	$CuSO_4$	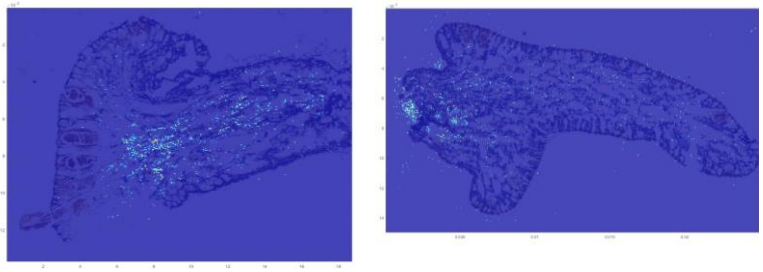
	DMP	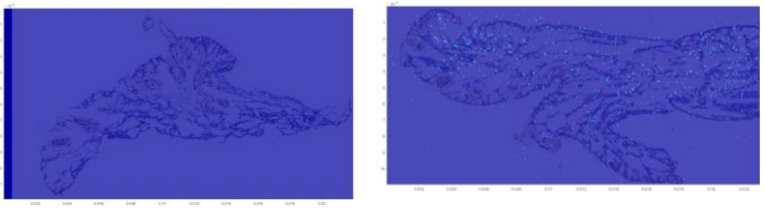
Phaeophytin A *m/z* 871.5711 (Zooxanthellae)	Control	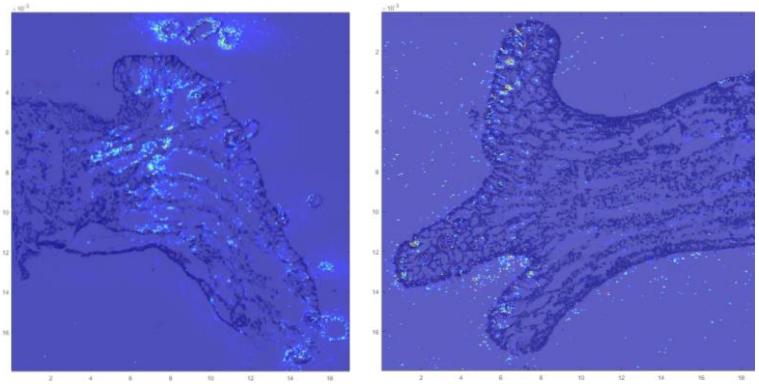
	$CuSO_4$	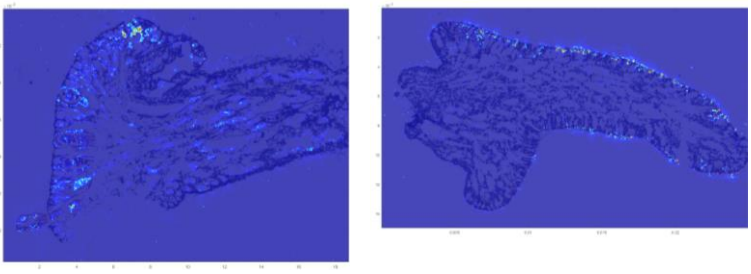

DMP

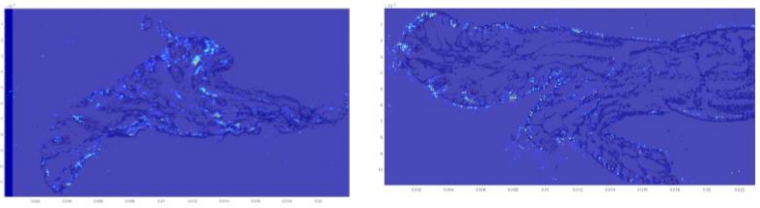

Diatoxanthin
m/z 567.4182
(Zooxanthellae)

Control

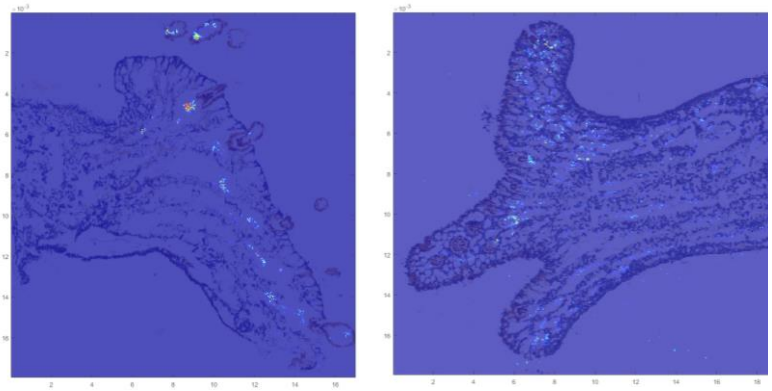

$CuSO_4$

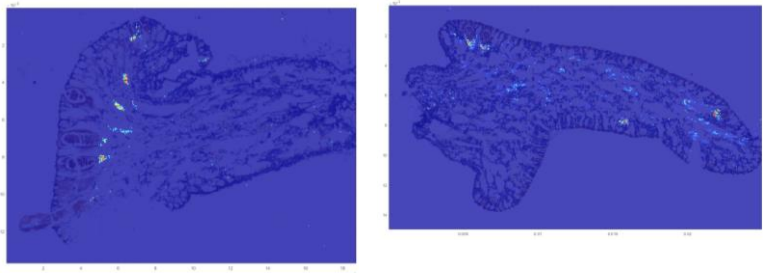

DMP

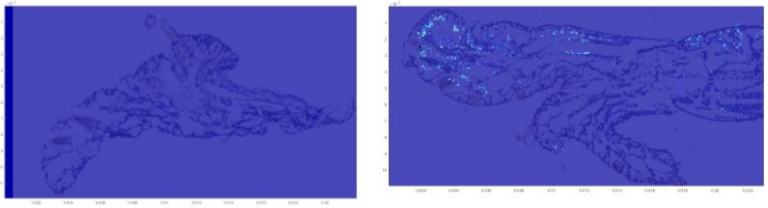

(3,4,3´)-4-
Hydroxyalloxant-
hin
m/z 581.3981
(Zooxanthellae)

Control

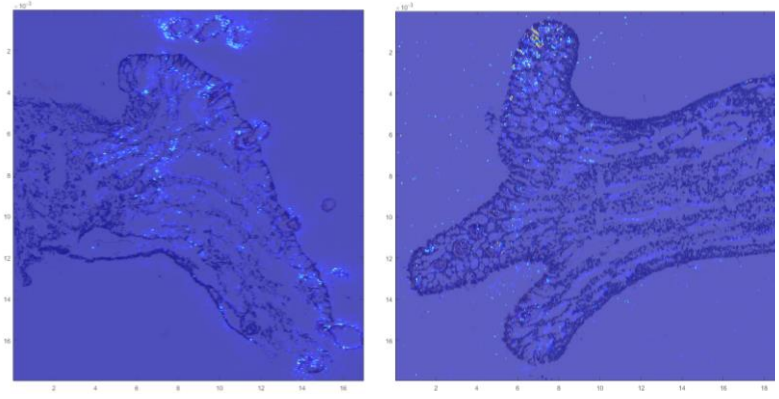

$CuSO_4$

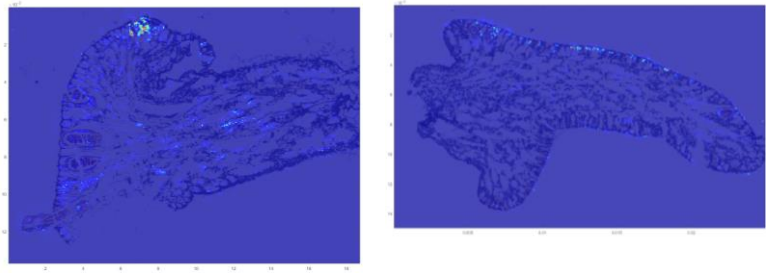

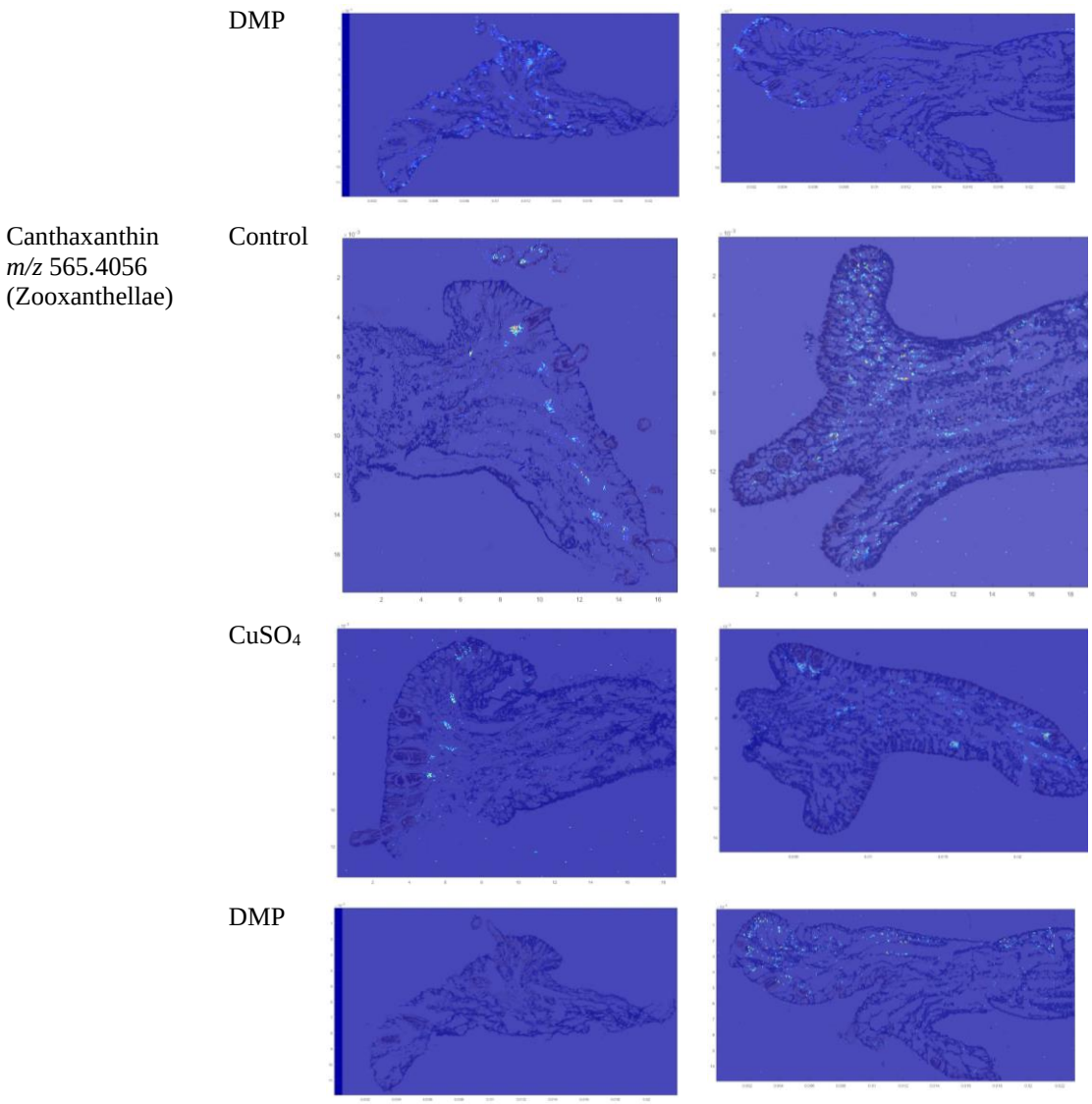

Figure A.8. AP-MALDI-MSI of soft coral *Sarcophyton glaucum* and *Lobophytum crassum* as well as the zooxanthellae after treated with various elicitors with the spatial distribution of zooxanthellae marker metabolites, and full imaging without microscopic image overlay

Appendix 5 Tentative assignments of metabolites in *S. glaucum*, *L. crassum*, *and X. umbellata* extracts based on ^{1}H and $^{1}H/^{13}C$-HSQC NMR spectra (at 600 MHz; solvent methanol-d4)

Table A.4. Tentative assignment of metabolites detected by ^{1}H-NMR (supported by 2D NMR data) in *Sarcophyton glaucum*, *Lobophytum crassum*, and *Xenia Umbellata* extracts (solvent: CD_3OD)

No.	Metabolite	Position	^{1}H, δ [ppm] multiplicity	^{13}C δ [ppm] HSQC	Species
1.	Gorgosterol 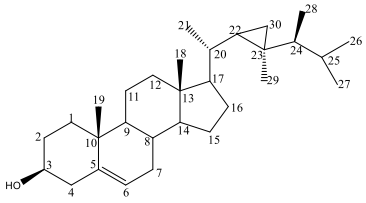	3	3.47 m	72.7	S, L, X
		6	5.37 m	129.3	
		21	1.03 s	21.7	
		22	0.26 m	30.8	
		26	0.98 s	22.7	
		27	0.87 s	20.9	
		29	0.90	14.5	
		30	0.48 dd	*n.d.*	
			-0.11 t		
2.	Sarcophine 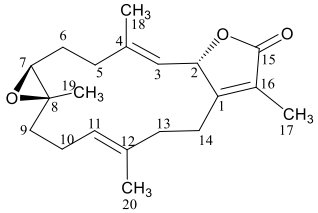	2	5.44	86.6	S
		3	5.35 dd	122.6	
		5	2.19 m	35.9	
		6	2.23 m	24.1	
		7	2.75	64.1	
		11	5.35	122.6	
		16	1.11 d	25.9	
		18	1.62 s	15.3	
		19	1.26 s	16.7	
		20	1.86 br s	18.1	
3.	Sarcophytoxide 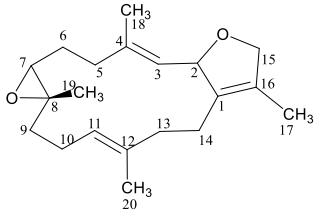	2	5.44	86.6	S
		3	5.25	126.3	
		5	2.19 m	35.9	
		6	2.23 m	26.1	
		7	2.75	64.1	
		16	4.46 m	79.1	
		18	1.62 s	15.3	
		19	1.26 s	16.7	
		20	1.86 br s	18.1	
4.	Sarcophytolol 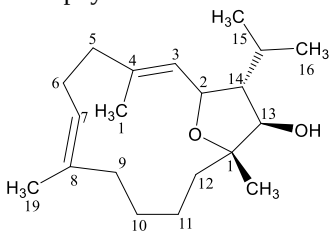	1	1.40 m	30.2	S
		2	4.50 dd	74.8	
		3	5.34[b] d	122.6	
		7	5.16 dd	124.8	
		11	1.78 m	28.7	
		14	3.89 d	70.4	
		15	1.18 m	30.0	
		17	0.77 d	20.2	
		19	1.60 s	16.2	
		20	0.90 s	14.5	
5.	Glaucumolide A/B 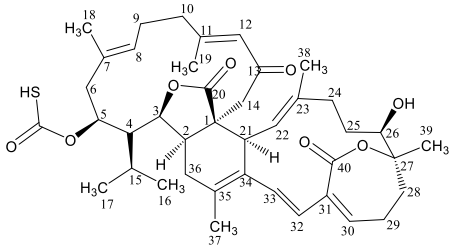	2	2.35 m	38.6	S
		6	2.22 m	43.0	
			2.14 m		
		8	5.24 dd	126.8	
		12	5.87 dd	122.4	
		15	2.23 m	24.1	
		17	1.11 d	26.1	
		19	2.15 s	30.7	
		22	5.16[c]	124.9	
		37	1.84 s	20.9	
6.	Sarglaucol	2	6.38 d	120.0	S
		3	6,14 d	117.6	
		5	2.23 m	24.2	

	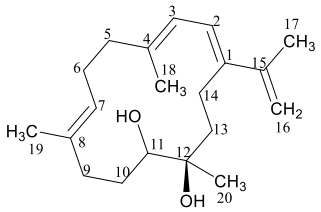		2.00 m		
		7	5.18 t	127.4	
		9	2.19 m	35.9	
		16	5.16[c] s	124.9	
		17	1.94 s	24.4	
		18	1.62 s	15.8	
		19	1.60[c] s	16.2	
7.	Sarcophytolide	2	2.35[cd] m	38.7	S
	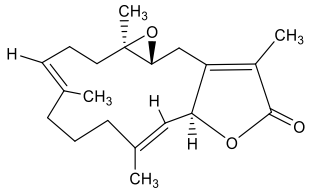	3	1.70 m	27.1	
			2.62 m		
		6	1.95 m	37.7	
		9	5.19[b]	127.4	
		13	5.45 d	126.7	
		14	5.97 d	122.5	
		15	2.32 s	35.2	
		16	1.04 d	21.6	
		17	1.55 s	22.2	
		20	1.75 s	17.8	
8.	Calamusin J/K	2	0.94 m	19.4	S
	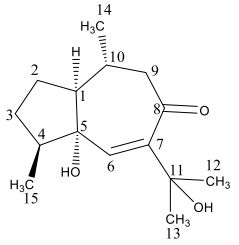	3	1.78 m	28.7	
		4	2.09[c] m	40.8	
		6	6.38 br d	120.1	
		9	2.72	49.2	
		10	2.62 m	27.1	
		13	1.42 s	30.2	
		14	1.02	19.8	
		15	0.89	14.5	
9.	Ent-Sarcophyolide E	2	5.57 d	85.3	S
	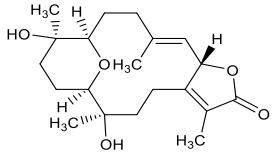	3	4.96	126.3	
		5	2.19[b]	35.9	
		10	1.39 m	28.8	
		11	3.21 d	75.8	
		13	1.63 m	27.1	
			1.35 m		
		17	1.68 s	10.2	
		18	1.84 s	18.1	
		19	1.02 s	19.9	
10.	Emblide	2	7.21 d	121.7	S
	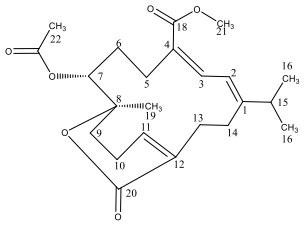	3	6.38 dd	120.3	
		5	2.08[b] m	28.3	
		9	2.29 m	39.5	
			1.94 m		
		17	1.13 s	27.2	
		19	1.42 s	19.5	
		21	3.82 s	34.1	
11.	Loliolide	2	1.79 dd	44.7	S
	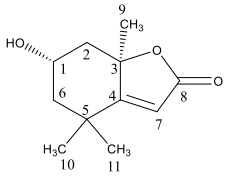	3	4.36 d	63.5	
		4	1.95[f] dd	37.7	
		7	5.76	110.5	
		9	1.29[a]	33.1	
		11	1.76 s	28.7	
12.	Sarcophytol A	2	4.95 m	n.d.	S
		3	2.19[b] m	35.9	
			2.37[cd] m		
		5	5.17[b] m	124.8	
		6	2.30 m	28.1	
		13	5.97 d	125.5	

	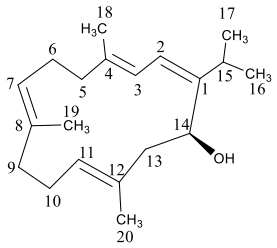	14	6.13 d	117.3	
		15	2.62 m	27.1	
		16	1.03 d	21.7	
		17	1.11[bd] d	25.9	
		18	1.60 s	15.6	
		20	1.71 s	15.2	
13.	Bisglaucumlide	2	3.90	49.3	S
	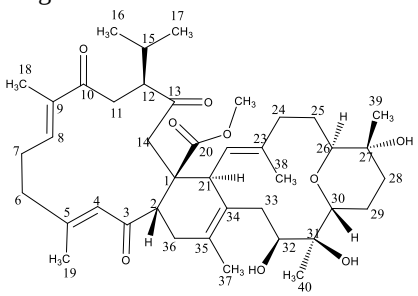	4	5.96[b] d	122.4	
		8	6.21	139.5	
		11	2.05	39.9	
		16	0.81 d	18.0	
		17	0.99 d	22.7	
		18	1.75 s	17.8	
		24	2.34	24.6	
		30	3.60 m	70.3	
		32	5.03 m	74.7	
		36	2.83 br d	26.6	
		38	1.86 s	18.1	
		40	1.16 s	17.2	
14.	Guaiacophine	1	2.35[b] m	38.6	S
	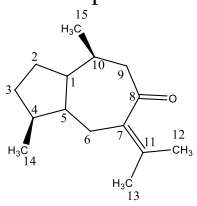	2	1.78	29.7	
		3	1.40 m	30.2	
		4	2.56 br d	27.5	
		6	6.09 s	116.0	
		12	1.86 s	18.1	
		14	1.19 s	20.2	
		15	0.97 s	16.0	
15.	Fatty acid	(CH2-)n	1.29	30.8	S, L, X
		CH3 terminal	0.90	14.5	
	Arachdonic acid (AHA), eicosapentaenoic acid (EPA), docosahexaenoid acid	CH-5/6-8/9-11/12-14/15-17/18	5.32-5.40 m		
16.	Locrassolide A	1	2.83 m	40.2	L
	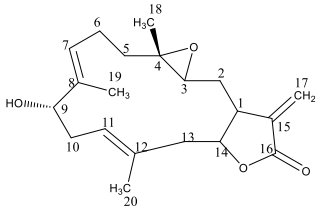	3	2.62 m	61.8	
		5	1.55 m 2.11 m	30.7	
		7	5.37	122.6	
		9	4.07	65.6	
		11	5.35 dd	122.7	
		14	4.46 ddd	79.1	
		17	6.38 d 5.57 d	120.1	
		18	1.32 s	17.7	
		19	1.66 s	10.1	
17.	Crassumolide B	1	3.08 t	48.9	L
	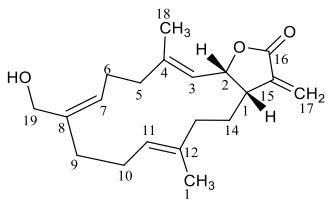	2	5.57 dd	85.3	
		3	5.06 d	125.9	
		5	2.32 m	35.1	
		7	4.96 br d	126.9	
		11	5.35 t	122.7	
		17	6.38 d 5.57 d	120.1	

		18	1.62 s	15.3	
		19	4.14 d	63.7	
		20	1.84	15.8	
18.	Crassumolide C 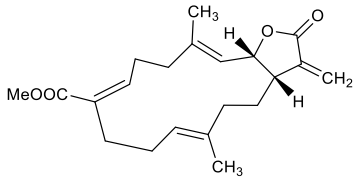	2	5.57 dd	85.3	L
		3	5.06 dd	125.9	
		5	2.32 m	35.1	
		7	4.96 br d	*n.d.*	
		11	5.35 t	122.7	
		17	6.38 d	120.1	
			5.57 d		
		18	1.62 s	15.3	
		20	1.84 s	15.8	
		OMe	3.62 s	59.5	
19.	Lobocrassin A 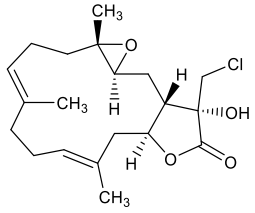	3	2.76 d	63.6	L
		5	1.95 m	37.7	
			2.35 m		
		6	2.29 m	24.5	
		7	5.16 t	125.1	
		10	1.61 m	26.2	
		11	5.18 t	127.4	
		14	4.47	79.1	
		19	1.62 s	15.3	
		20	1.84 s	15.8	
20.	Lobocrasol A 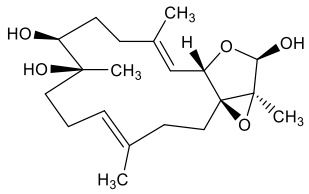	3	5.37 d	129.3	L
		5	2.21 m	35.1	
		6	1.63 m	29.7	
			1.71 m		
		7	3.47 m	72.7	
		9	1.71 m	37.7	
		11	5.35 dd	122.7	
		16	3.36	*n.d.*	
		17	1.52 s	14.9	
		18	1.62 s	15.3	
		19	1.28[d] s	17.1	
		20	1.84 s	15.8	
21.	Crassumol D 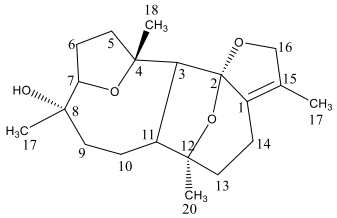	3	2.00 d	26.3	L
		5	2.35 m	37.8	
			1.92 m		
		7	4.07 t	65.5	
		10	1.70 m	27.1	
			1.35[a] m		
		13	1.55 m	30.7	
			1.29[a] m		
		16	4.46 dd	79.1	
		17	1.62 d	9.9	
		20	1.24 s	29.4	
22.	Crassumol E 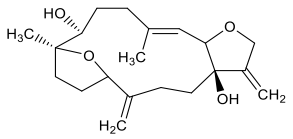	3	5.87 dd	122.4	L
		5	2.35 m	38.6	
		6	1.55 m	30.7	
		7	3.48 dd	72.6	
		9	2.10 m	40.0	
		13	2.63	27.1	
		16	4.48 m	79.2	
		17	5.16[h] dt	125.0	
		18	1.84 br s	15.8	
		19	1.24 s	18.5	
23.	Lobolide	1	2.84 m	26.7	L
		2	1.94 dt	24.5	
		3	2.92 dd	58.9	
		7	4.95 br t	126.8	

	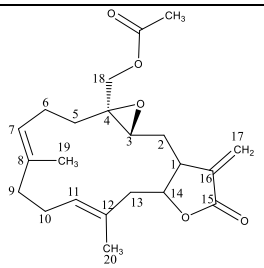	11	5.15 dd	125.1	
		14	4.14 m	63.8	
		17	5.97 d	n.d.	
		18	4.46[h] d	63.6	
		19	1.68	10.1	
		20	1.84	15.7	
		OAc	2.15	30.7	
24.	Crassumtocopherol C	3	1.71 m	27.1	L
	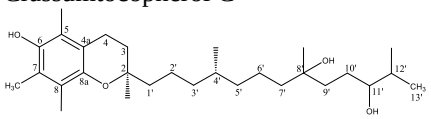	4	2.63 t	27.1	
		1'	1.55 m	30.7	
		4'	1.41 m	30.2	
		7'	1.55 m	30.7	
		10'	1.60 m	26.2	
		11'	3.46 m	72.7	
		13'	1.02 d	19.8	
		2-Me	1.24 s	29.3	
		7-Me	2.16 s	30.7	
		4'-Me	0.89 d	21.9	
		12'-Me	0.98 d	15.9	
25.	(2*S*, 2*S*, 4*R*)-2-[(*R*)-2`-hydroxytrolosanaylamino]-1,3,4-tridecanetriol	1	4.14 m	63.8	L
	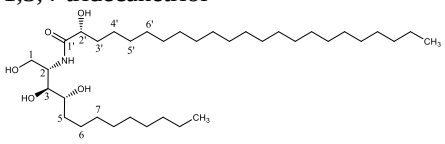	6	1.40[i] m	30.24	
		11	1.24[a] s	29.36	
		13	0.97[i] t	15.9	
		2´	5.27 m	71.8	
		4´	1.70	27.1	
		5´	1.60	26.2	
		21´	1.29[a] brs	33.1	
		NH	7.35		
		2OH	3.60 m		
26.	Locrassumin A	2	6.39 d	120.0	L
	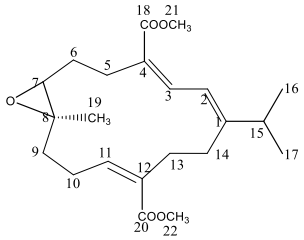	3	7.28 d	129.7	
		5	2.63 m	27.1	
		6	2.00 m	26.3	
			1.60 m		
		11	6.83 t	116.9	
		13	2.83 m	26.7	
			2.63 m		
		15	3.31 m	30.9	
		17	0.99 d	22.7	
		21	3.87 s	36.2	
		22	3.82 s	33.9	
27.	Lobophycrasin A	2	6.38 d	120.0	L
	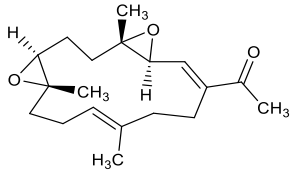	3	3.66 d	67.5	
		5	1.95 m	37.7	
		6	2.21[h] m	26.0	
		7	2.75 t	63.6	
		9	2.10 m	40.0	
		11	5.19 t	127.3	
		17	2.32 s	27.4	
		19	1.26[a] s	12.2	
		20	1.62 s	15.2	
28.	Umbellactal	3	9.19 s	*n.d.*	X
		4a	2.74 t	33.8	
		6	1.79 m	29.1	
		8	4.43 t	63.6	
		9	2.08 m	29.1	
			1.77 s		
		10	1.72 s	35.0	

	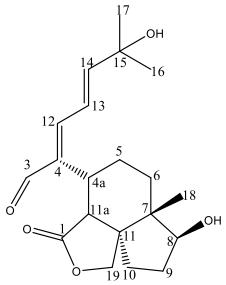	11a	2.78 d	52.9	
		13	6.51 dd	124.6	
		14	6.25 d	159.5	
		17	1.41 s	33.3	
		18	0.89 s	17.8	
29.	Xeniumbellal	1	3.03 m	58.8	X
	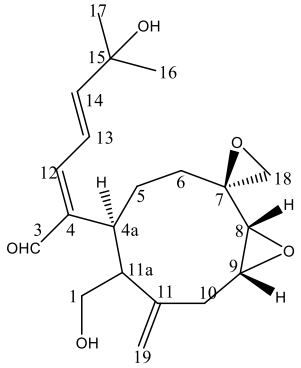	3	9.19 s	*n.d.*	
		4a	3.50 dd	33.2	
		5	2.08 m	29.2	
			1.13 m		
		6	2.83 m	26.4	
			2.23 m		
		8	3.02 d	58.6	
		9	3.25 t	57.4	
		11a	3.25 t	52.2	
		13	6.51 dd	124.3	
		14	6.25 d	159.5	
		16	1.42 s	33.4	
		18	3.17 s	53.7	
30.	Gorgst-3β-5α, 6β, 11α, 20(s)-pentol-3-monoacetate	3	5.19 ddd	73.2	X
	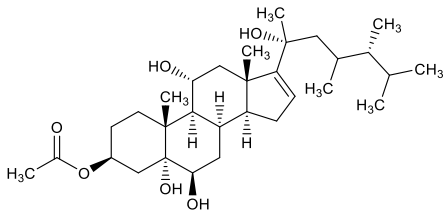	4	2.22 m	26.4	
		6	3.49 br t	72.6	
		11	3.72 ddd	63.9	
		16	5.24 dd	121.2	
		18	0.69 s	12.4	
		21	1.03 s	21.6	
		22	0.26 td	52.4	
		26	0.98 d	22.7	
		29	0.48 dd	22.8	
		30	0.89 s	14.5	
		2` CH_3	2.04 s	21.0	
31.	Xenibellol B	1	9.51 s	*n.d.*	X
	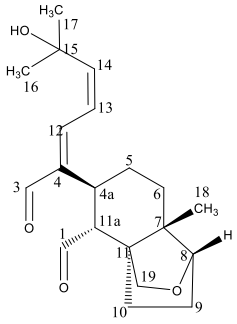	3	9.19 s	*n.d.*	
		4a	2.74 m	33.8	
		6	1.78 m	29.2	
		8	3.75 s	66.3	
		9	1.78 m	29.2	
			1.29*a* m		
		13	6.51 dd	123.3	
		14	6.25 dq	159.5	
		16	1.42*e* s	33.4	
		18	1.29*a* s	15.4	
		19	3.74 m	75.5	
32.	Umbellacin A	1	9.51 s	*n.d.*	X
	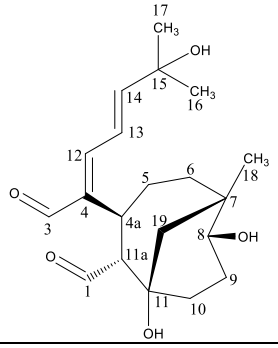	3	9.19 s	*n.d.*	
		4a	3.49 m	42.4	
		5	2.08 m	29.2	
			1.13 m		
		8	3.39	72.5	
		9	1.76 m	27.2	
			1.53 m		
		13	6.51 dd	124.3	
		14	6.25 d	159.5	
		16/17	1.42 s	33.4	
		18	1.03 s	21.6	
33.	Umbellacin C	3	4.42	62.6	X

	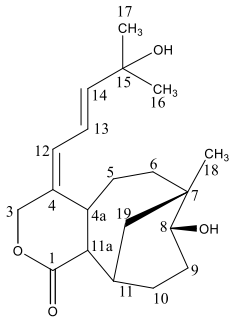	4a	3.50 t	42.4	
		5	2.06 m	29.2	
			1.79 m		
		6	1.53[k] m	27.3	
		8	3.39 t	72.7	
		10	5.87 br d	n.d.	
		11a	3.25 br d	53.6	
		12	5.99 d	n.d.	
		13	6.26 dd	n.d.	
		16/17	1.32[a] s	27.3	
		18	1.03	21.6	
34.	Xenibecin	1	4.48 d	104.8	X
	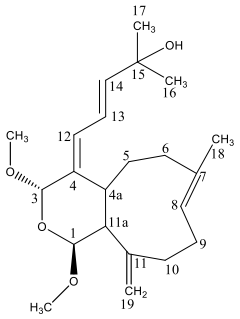	3	4.25 d	105.4	
		5	1.54[k] m	30.8	
			1.94 m		
		6	2.34[k] m	34.9	
			2.37[k] m		
		8	5.39[a] t	123.7	
		9	2.22[k] m	26.3	
			2.04[j] m		
		12	5.87 d	109.2	
		13	6.51 dd	227.7	
		17	1.42 s	33.4	
		18	1.76 s	18.7	
35.	Xenitacin	3	3.51[j] d	72.3	X
	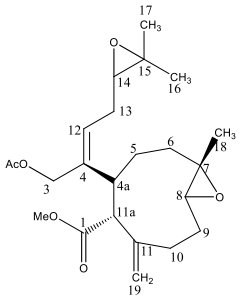	4	3.50[j] m	42.4	
		5	1.62[k] m	25.9	
		6	1.19 m	41.2	
		11a	3.49[j] m	72.7	
		12	5.56 d	122.5	
		14	2.76 dd	64.6	
		18	1.03 s	21.6	
		19	5.06 s	113.7	
		OMe-1	3.75 s	66.4	
		OAc	2.04 s	n.d.	
36.	Xenibellal	3	9.51 s	n.d.	X
	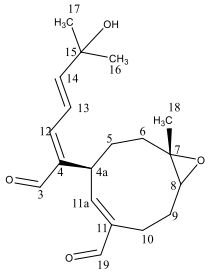	5	1.86 m	28.9	
		6	2.23[jk] m	26.4	
		8	3.03[j] dd	58.8	
		10	2.95 m	20.2	
		11a	6.52[l] d	143.7	
		12	6.70[j] m	155.6	
		16	1.42 s	33.3	
		18	0.97 s	16.0	
37.	9-Deoxyxeniloide-E	3	4.43 m	62.4	X
	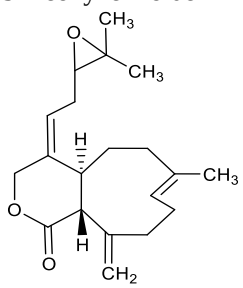	4a	2.88 m	30.4	
		5	1.69 m	26.0	
			1.75 m		
		6	2.22[jk]	43.0	
		8	5.39[a] dd	123.7	
		9	2.34[k] m	34.9	
		12	5.56 br t	128.0	
		14	2.82[j] br t	60.3	
		16	1.37[a] s	24.1	
		19	5.00 s	113.6	
38.	Xeniolide O	1	6.35 brs	92.5	X
		3	6.40 s	141.9	

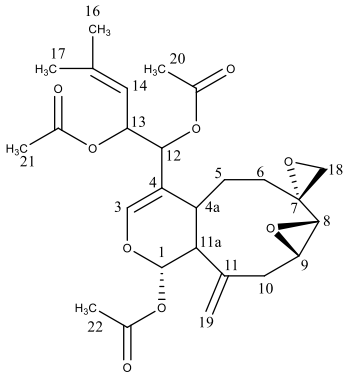	4a	2.88 m	30.5
	6	2.00 m	26.3
		2.22 m	
	8	3.33 d	57.7
	9	3.03 m	58.7
	11a	3.04 brs	39.4
	12	5.24 d	77.0
	13	5.74 dd	70.9
	14	5.04 d	121.1
	16	1.72 s	25.9
	18	2.77 d	51.9
	19	5.00 s	113.5
		5.06 s	
	20	1.94 s	171.5
	21	1.96 s	171.5
	22	2.07 s	171.1

[a] Corresponds to overlapping NMR signals in fatty acids signal
[b] Corresponds to overlapping NMR signals in 2
[c] Corresponds to overlapping NMR signals in 3
[d] Corresponds to overlapping NMR signals in 5
[e] Corresponds to overlapping NMR signals in 7
[f] Corresponds to overlapping NMR signals in 10
g Corresponds to overlapping NMR signals in 18
h Corresponds to overlapping NMR signals in 19
i Corresponds to overlapping NMR signals in 24
j Corresponds to overlapping NMR signals in 29
k Corresponds to overlapping NMR signals in 30
l Corresponds to overlapping NMR signals in 34

Appendix 6 The relative concentration of fatty acids in the extracts of *L. crassum* treated with different elicitors based on ^{1}H-NMR metabolite profiling

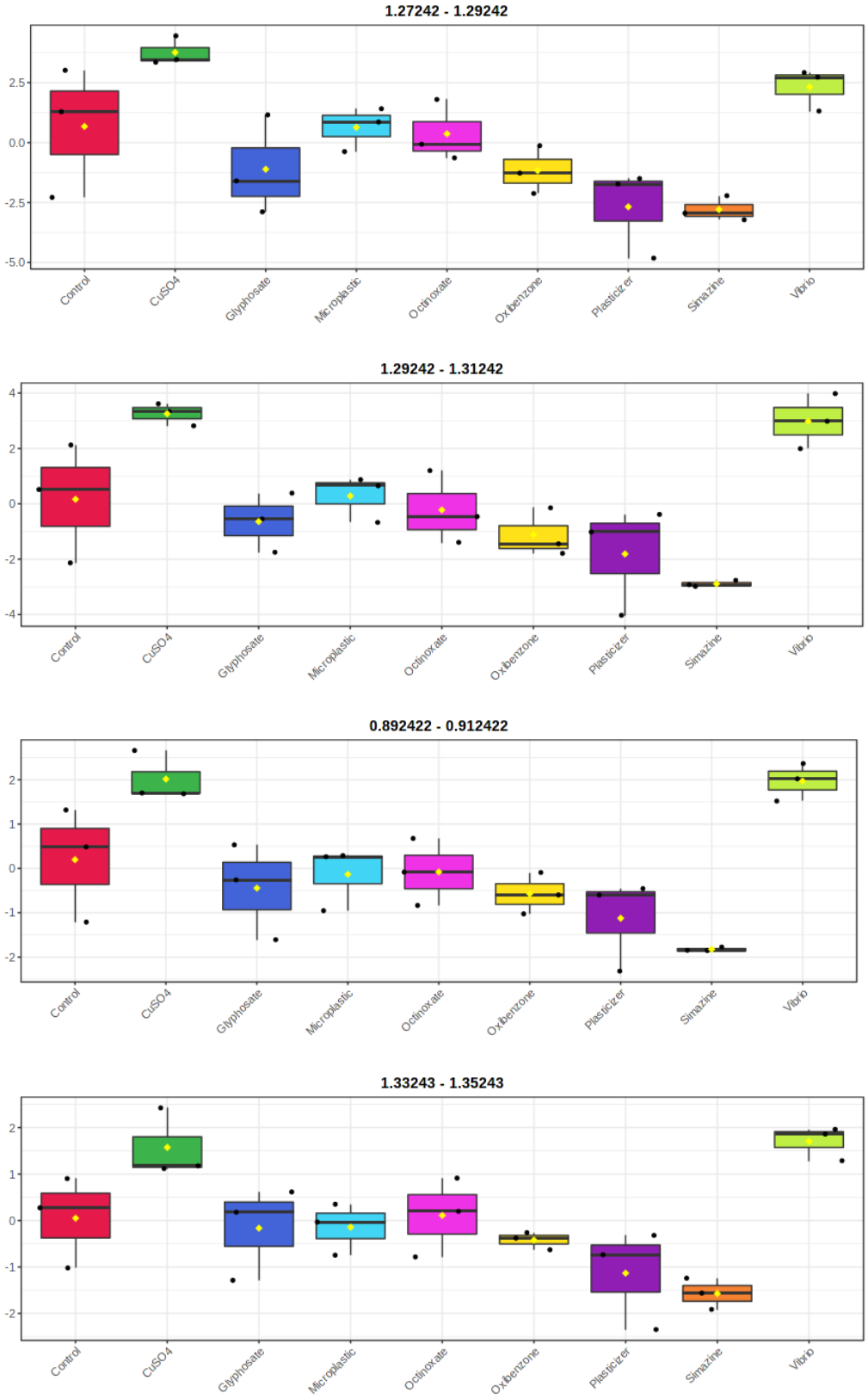

Figure A.9. Box plot relative concentration of fatty acids in the extracts of *L. crassum* treated with different elicitors based on ^{1}H-NMR metabolite profiling

Appendix 7 The relative concentration of xenibellal and umbellacin C in extracts of *X. umbellata* treated with DMP based on ^{1}H-NMR metabolite profiling

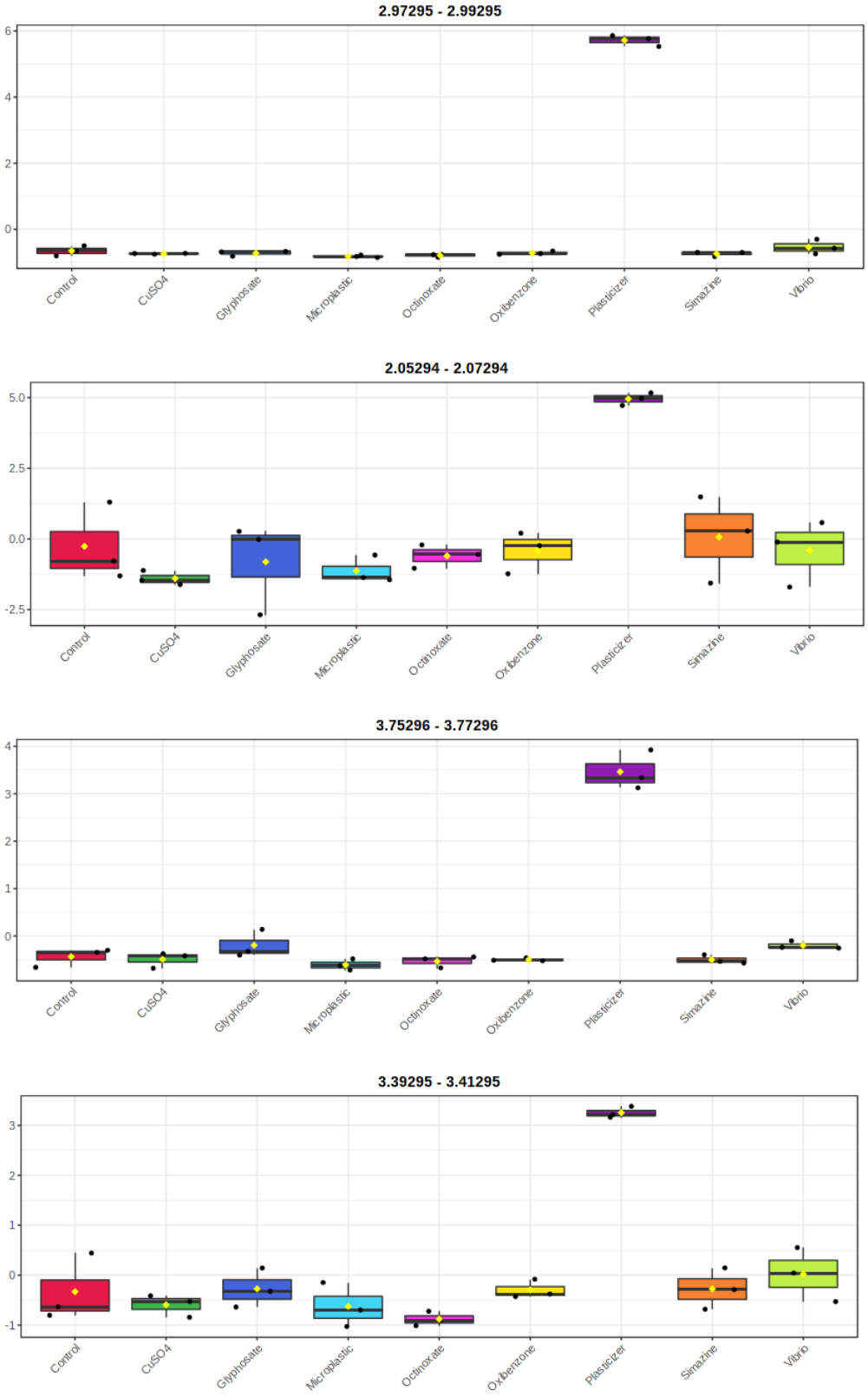

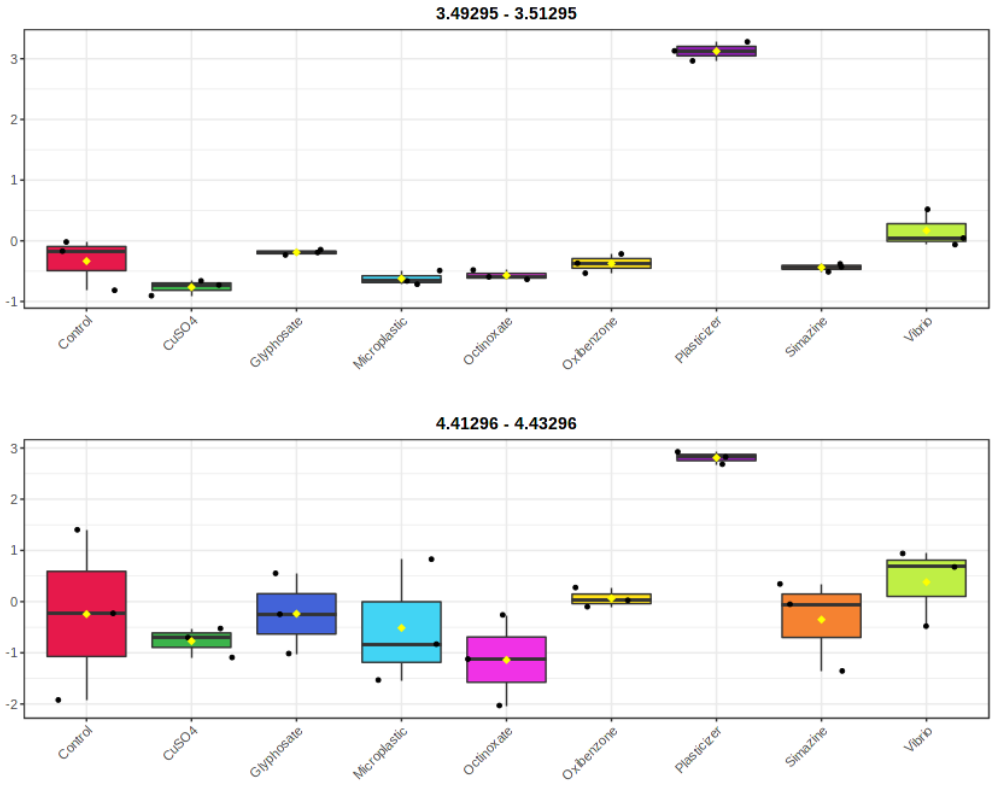

Figure A.10. Box plot relative concentration of xenibellal and umbellacin C in extracts of *X. umbellata* treated with DMP based on ^{1}H-NMR metabolite profiling

Appendix 8 The relative concentration of xenibecin in extracts of *X. umbellata* treated with $CuSO_4$ based on ^{1}H-NMR metabolite profiling

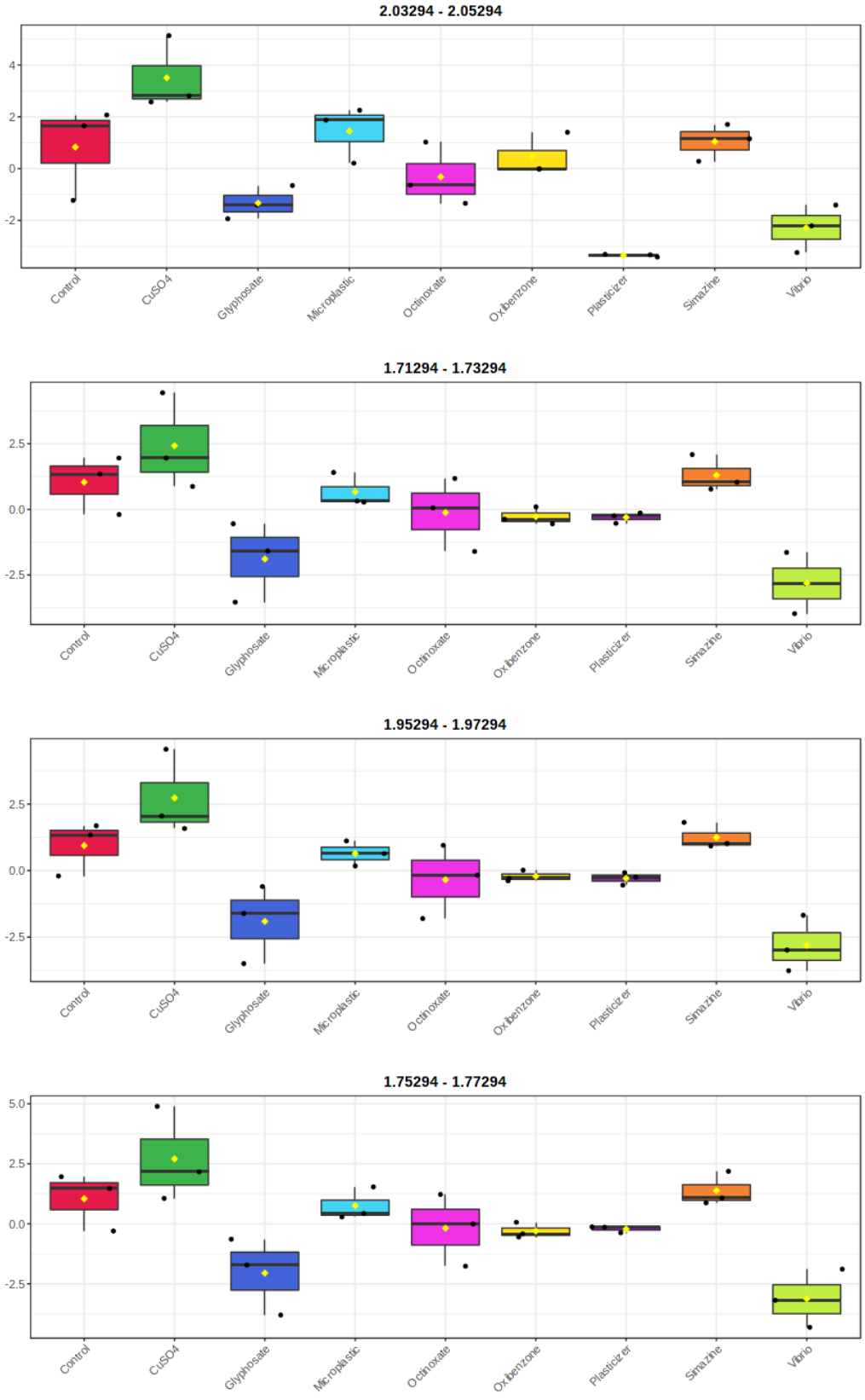

Figure A.11. Box plot relative concentration of xenibecin in extracts of *X. umbellata* treated with $CuSO_4$ based on ^{1}H-NMR metabolite profiling

Appendix 9 The LC-ESI-HRMS chromatogram of *S. glaucum* extracts (extracted with different solvents)

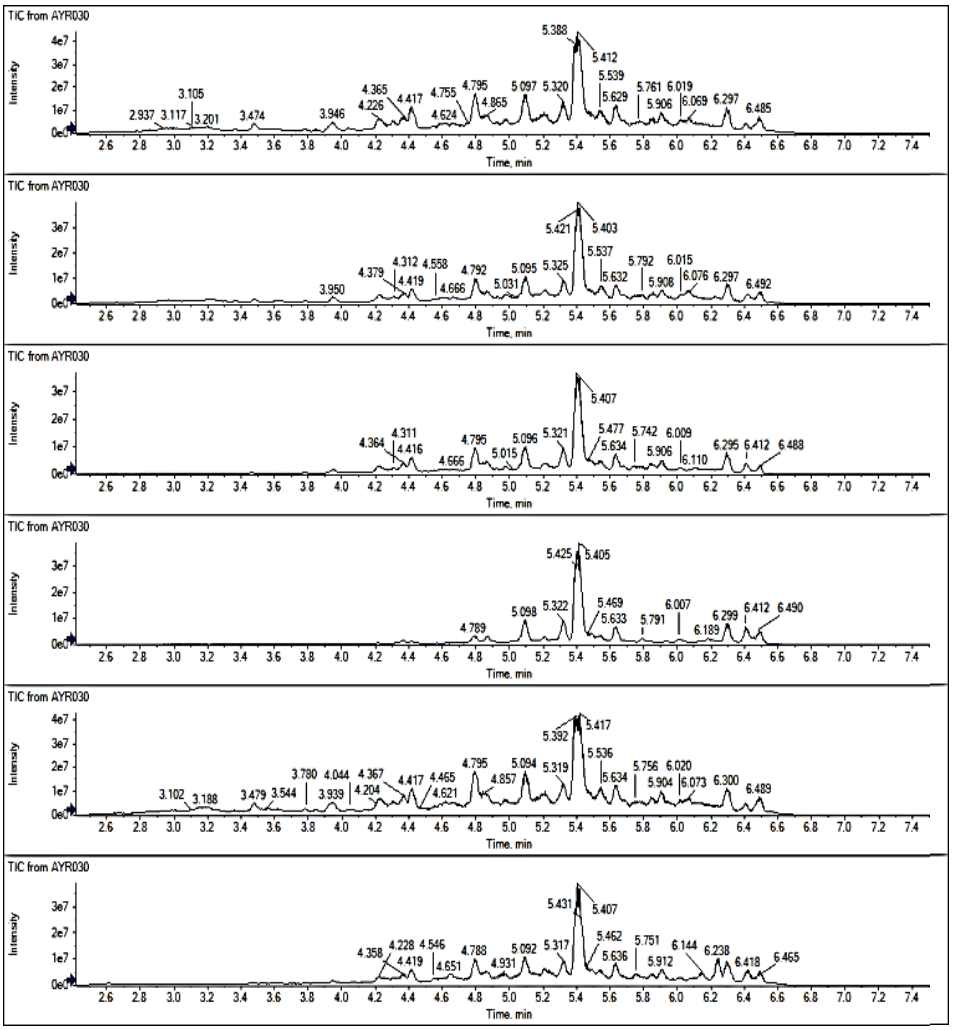

Figure A.12. The LC-ESI-HRMS chromatogram of *S. glaucum* extracts (extracted with different solvents) in order to select the best solvent for extraction

Appendix 10 The antibacterial activity of glyphosate and $CuSO_4$ against *Aliivibrio fischeri* and *Bacillus subtilis*

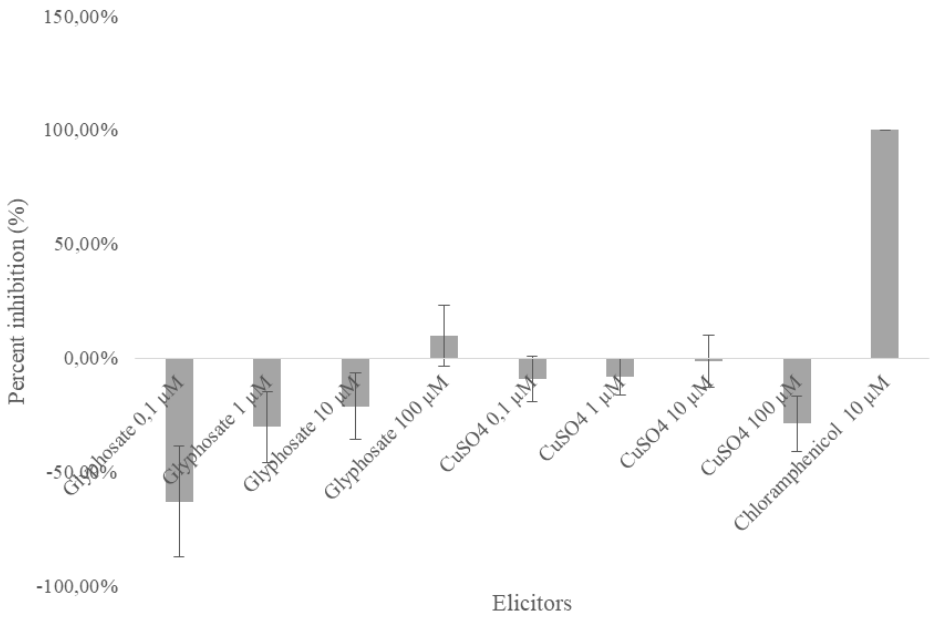

Figure A.13. Antibacterial activity of glyposate and $CuSO_4$ against *Aliivibrio fischeri*, positive control= chloramphenicol

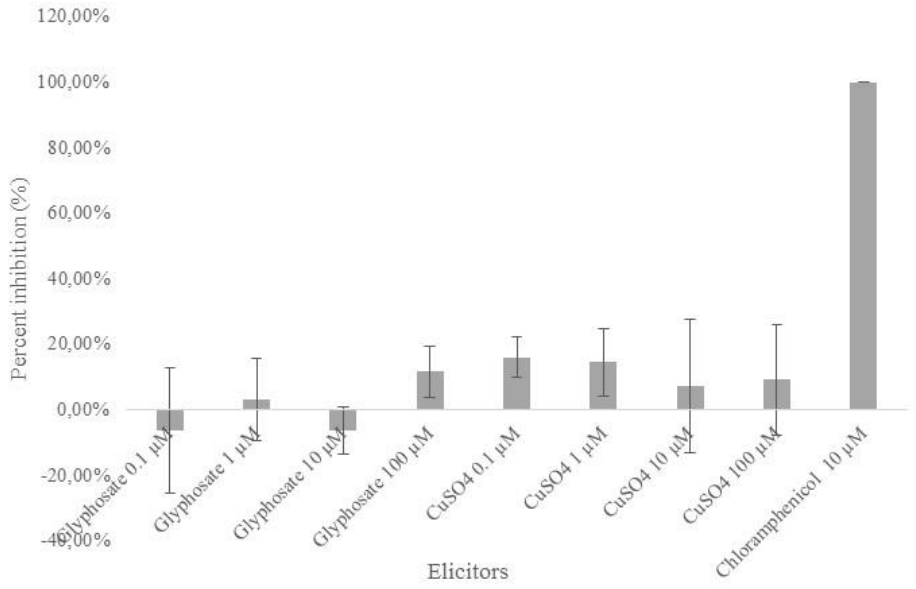

Figure A.14. Antibacterial activity of glyphosate and $CuSO_4$ against *Bacillus subtilis*, positive control= chloramphenicol

Appendix 11 Morphology of the soft corals after glyphosate exposure (in three biological replicates)

Table A.5. Morphology of the soft corals *Sarcophyton glaucum*, *Lobophytum crassum*, and *Xenia umbellata* after glyphosate exposure (in three biological replicates)

Soft coral sample / treatment		**Morphology**	
		Color of colony	**Tentacle/siphonozooid**
S. glaucum	Glyphosate 1000 mg/L 1	Dark brown-grey	The colony is dead
	Glyphosate 1000 mg/L 2	Dark brown-grey	The colony is dead
	Glyphosate 1000 mg/L 3	Dark brown-grey	The colony is dead
	Glyphosate 100 mg/L 1	Dark brown	Mostly retract
	Glyphosate 100 mg/L 2	Dark brown	Mostly retract
	Glyphosate 100 mg/L 3	Dark brown	Mostly retract
	Glyphosate 50 mg/L 1	Brown-greenish	Half retract
	Glyphosate 50 mg/L 2	Brown-greenish	Half retract
	Glyphosate 50 mg/L 3	Brown-greenish	Half retract
	Glyphosate 25 mg/L 1	Brownish	Extend
	Glyphosate 25 mg/L 2	Brownish	Extend
	Glyphosate 25 mg/L 3	Brownish	Extend
	Glyphosate 10 mg/L 1	Brown-greenish	Extend
	Glyphosate 10 mg/L 2	Brown-greenish	Extend
	Glyphosate 10 mg/L 3	Brown-greenish	Extend
	Glyphosate 5 mg/L 1	Brown	Extend
	Glyphosate 5 mg/L 2	Brown	Extend
	Glyphosate 5 mg/L 3	Brown	Extend
	Control 1	Brown	Extend
	Control 2	Brown	Extend
	Control 3	Brown	Extend
L. crassum	Glyphosate 50 mg/L 1	Brownish	Mostly retract
	Glyphosate 50 mg/L 2	Brownish	Mostly retract
	Glyphosate 50 mg/L 3	Brownish	Mostly retract
	Glyphosate 25 mg/L 1	Brownish	Half retract
	Glyphosate 25 mg/L 2	Brownish	Half retract
	Glyphosate 25 mg/L 3	Brownish	Half retract
	Glyphosate 10 mg/L 1	Brownish	Extend
	Glyphosate 10 mg/L 2	Brownish	Extend
	Glyphosate 10 mg/L 3	Brownish	Extend
	Glyphosate 5 mg/L 1	Brownish	Extend
	Glyphosate 5 mg/L 2	Brownish	Extend
	Glyphosate 5 mg/L 3	Brownish	Extend
	Control 1	Brown	Extend
	Control 2	Brown	Extend
	Control 3	Brown	Extend
X. umbellata	Glyphosate 50 mg/L 1	Brown-greynish	Half contract
	Glyphosate 50 mg/L 2	Brown-greynish	Half contract
	Glyphosate 50 mg/L 3	Brown-greynish	Half contract
	Glyphosate 25 mg/L 1	Light brown	Expand
	Glyphosate 25 mg/L 2	Light brown	Expand
	Glyphosate 25 mg/L 3	Light brown	Expand
	Glyphosate 10 mg/L 1	Light brown	Expand
	Glyphosate 10 mg/L 2	Light brown	Expand
	Glyphosate 10 mg/L 3	Light brown	Expand
	Glyphosate 5 mg/L 1	Brown	Expand
	Glyphosate 5 mg/L 2	Brown	Expand
	Glyphosate 5 mg/L 3	Brown	Expand
	Control 1	Brown	Expand
	Control 2	Brown	Expand
	Control 3	Brown	Expand

Appendix 12 The relative concentration of fatty acid in the extracts of *S. glaucum* treated with glyphosate based on ^{1}H-NMR metabolite profiling

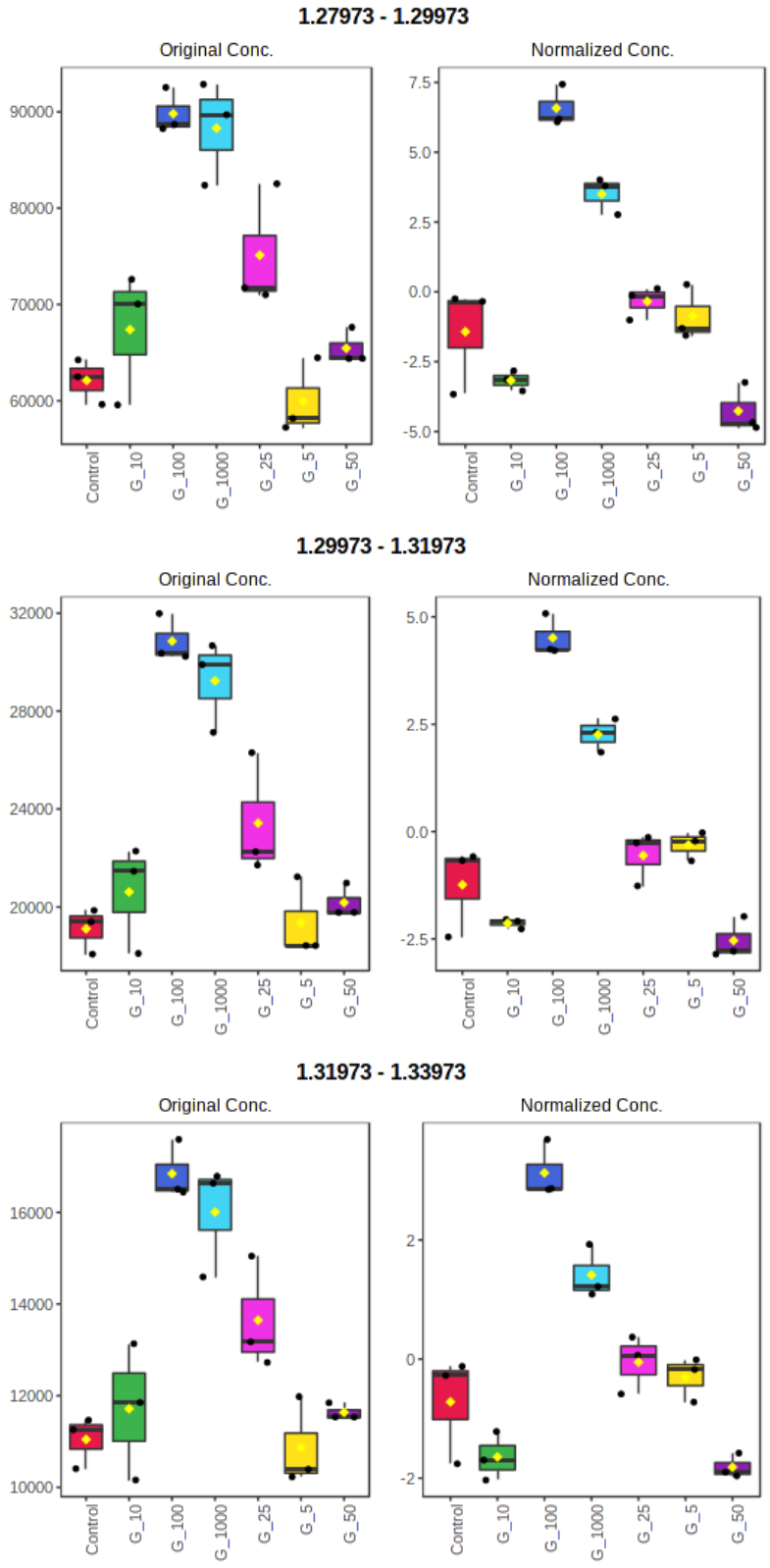

Figure A.15. Box plot relative concentration of fatty acid in the extracts of *S. glaucum* treated with glyphosate based on ^{1}H-NMR metabolite profiling

Appendix 13 The relative concentration of sarcophytolol and sarcophytoxide in the extracts of *S. glaucum* treated with glyphosate based on ^{1}H-NMR metabolite profiling

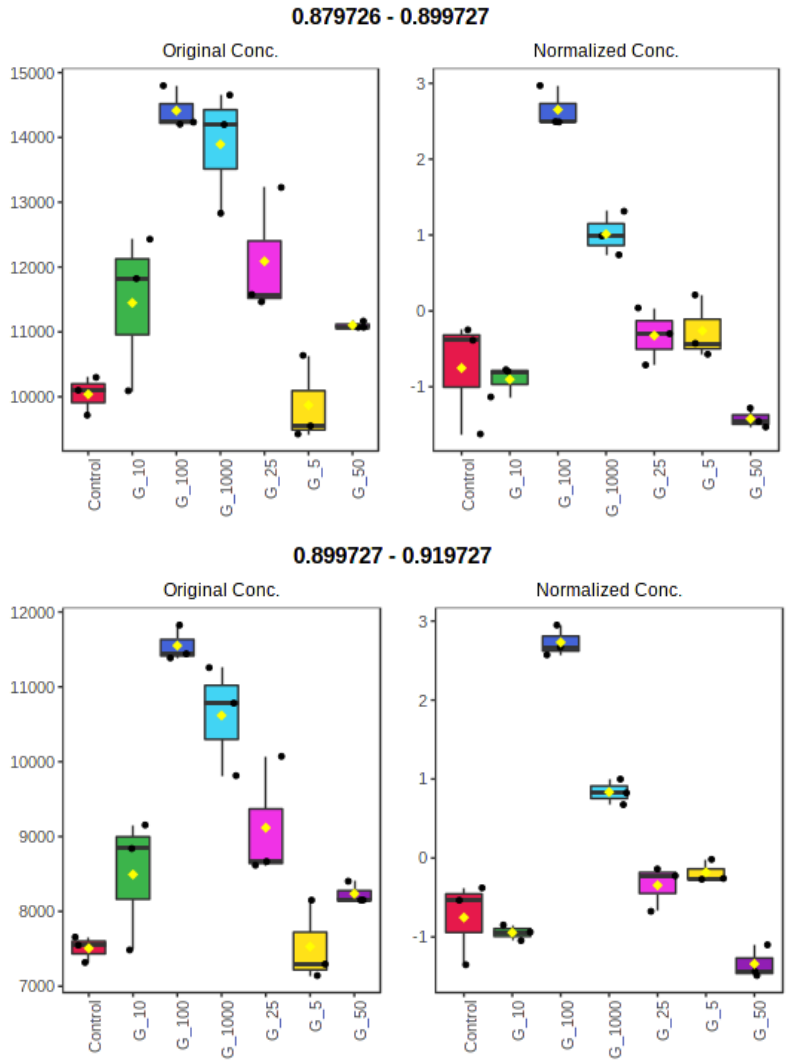

Figure A.16. Box plot relative concentration sarcophytolol and sarcophytoxide in the extracts of *S. glaucum* treated with glyphosate based on ^{1}H-NMR metabolite profiling

Appendix 14 AP-MALDI-MSI of soft coral *L. crassum* and *S. glaucum* marker metabolites after treated with glyphosate 50 mg/L

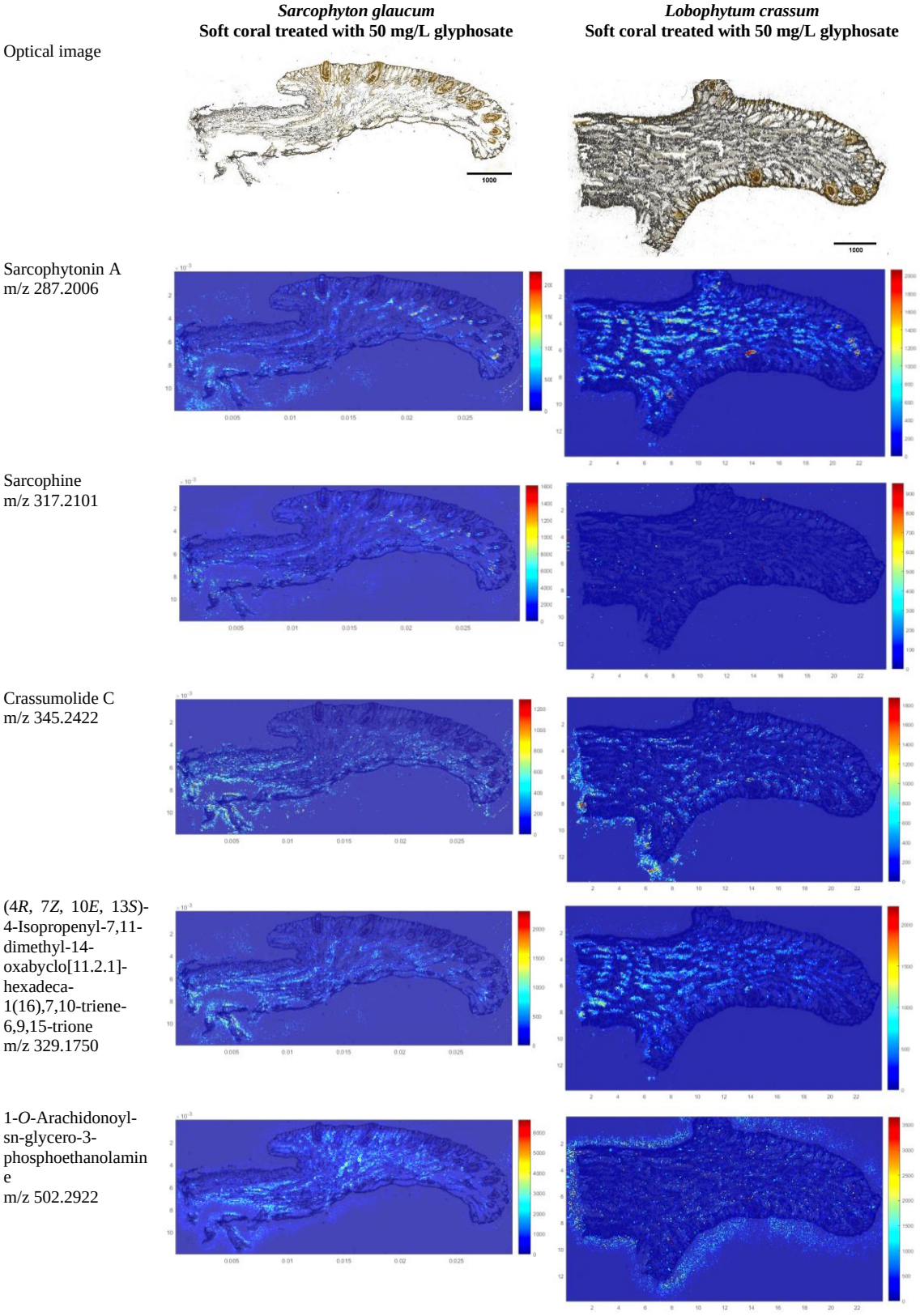

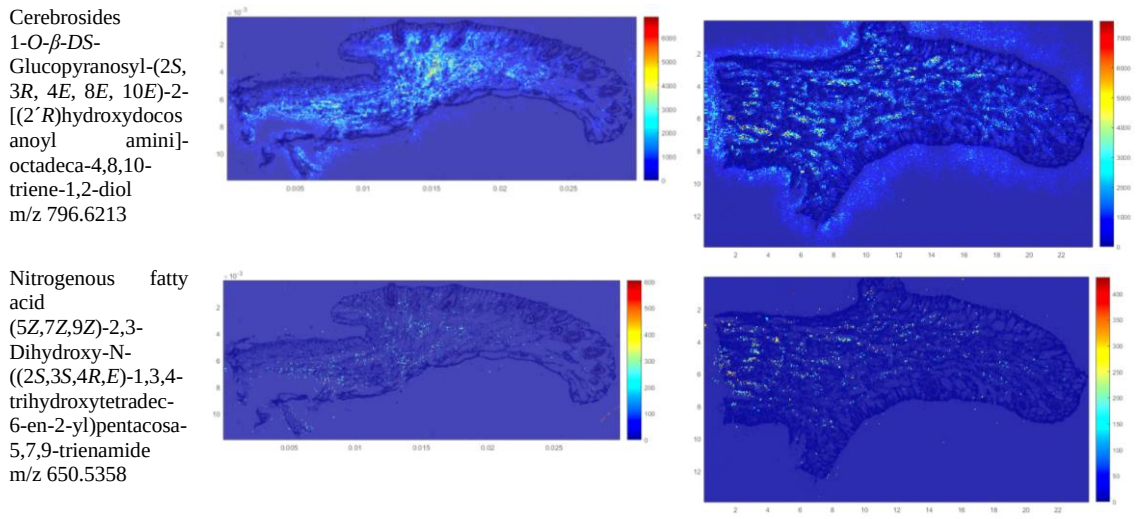

Figure A.17. AP-MALDI-MSI of soft coral *Sarcophyton glaucum* and *Lobophytum crassum* as well as the zooxanthellae after treated with glyphosate 50 mg/L with the spatial distribution of zooxanthellae marker metabolites, and full imaging without microscopic image overlay

Appendix 15 Two Ways ANOVA statistical analysis (significance difference) by using Dunnett's multiple comparisons test of the soft corals treated various elicitors (Chapter V)

Table A.6. Dunnett's multiple comparisons test of the pumping rate of *Xenia umbellata* before and after elicitation to various elicitors

Dunnett's multiple comparisons test	**Significant?**	**Summary**	**Adjusted P Value**
Before treatment			
Control vs. Glyphosate	No	ns	0,7214
Control vs. Simazine	No	ns	0,9979
Control vs. Oxybenzone	No	ns	0,9979
Control vs. Octinoxate	No	ns	0,9475
Control vs. $CuSO_4$	No	ns	>0.9999
Control vs. DMP	No	ns	0,9979
Control vs. Micro-plastic	No	ns	0,2125
Control vs. *Vibrio campbellii*	No	ns	0,429
After treatment			
Control vs. Glyphosate	No	ns	0,7214
Control vs. Simazine	Yes	****	<0.0001
Control vs. Oxybenzone	Yes	****	<0.0001
Control vs. Octinoxate	Yes	****	<0.0001
Control vs. $CuSO_4$	Yes	****	<0.0001
Control vs. DMP	Yes	****	<0.0001
Control vs. Micro-plastic	Yes	****	<0.0001
Control vs. *Vibrio campbellii*	Yes	****	<0.0001

Table A.7. Dunnett's multiple comparisons test weight of *Sarcophyton glaucum* before and after elicitation to various elicitors

Dunnett's multiple comparisons test	**Significant?**	**Summary**	**Adjusted P Value**
Before treatment			
Control vs. Glyphosate	No	ns	0,4666
Control vs. Simazine	No	ns	0,3269
Control vs. Oxybenzone	No	ns	0,5456
Control vs. Octinoxate	No	ns	0,9995
Control vs. $CuSO_4$	No	ns	0,9812
Control vs. DMP	No	ns	0,1392
Control vs. Micro-plastic	Yes	*	0,0219
Control vs. *Vibrio campbellii*	No	ns	0,0508
After treatment			
Control vs. Glyphosate	Yes	**	0,0048
Control vs. Simazine	Yes	****	<0.0001
Control vs. Oxybenzone	Yes	****	<0.0001
Control vs. Octinoxate	Yes	****	<0.0001
Control vs. $CuSO_4$	Yes	****	<0.0001
Control vs. DMP	Yes	****	<0.0001

Control vs. Micro-plastic	Yes	**	0,0013
Control vs. *Vibrio campbellii*	Yes	****	<0.0001

Table A.8. Dunnett's multiple comparisons test weight of *Lobophytum crassum* before and after elicitation to various elicitors

Dunnett's multiple comparisons test	**Significant?**	**Summary**	**Adjusted P Value**
Before treatment			
Control vs. Glyphosate	No	ns	0,9941
Control vs. Simazine	No	ns	0,3554
Control vs. Oxybenzone	No	ns	0,9994
Control vs. Octinoxate	No	ns	0,9941
Control vs. $CuSO_4$	No	ns	0,9998
Control vs. DMP	No	ns	0,9941
Control vs. Micro-plastic	No	ns	0,3554
Control vs. *Vibrio campbellii*	No	ns	0,4395
After treatment			
Control vs. Glyphosate	Yes	**	0,002
Control vs. Simazine	Yes	****	<0.0001
Control vs. Oxybenzone	Yes	****	<0.0001
Control vs. Octinoxate	Yes	****	<0.0001
Control vs. $CuSO_4$	Yes	****	<0.0001
Control vs. DMP	Yes	****	<0.0001
Control vs. Micro-plastic	Yes	**	0,0063
Control vs. *Vibrio campbellii*	Yes	****	<0.0001

Table A.9. Dunnett's multiple comparisons test weight of *Xenia umbellata* before and after elicitation to various elicitors

Dunnett's multiple comparisons test	**Significant?**	**Summary**	**Adjusted P Value**
Before treatment			
Control vs. Glyphosate	No	ns	0,9996
Control vs. Simazine	No	ns	0,9996
Control vs. Oxybenzone	No	ns	0,8266
Control vs. Octinoxate	No	ns	0,9522
Control vs. $CuSO_4$	No	ns	0,9943
Control vs. DMP	No	ns	0,8266
Control vs. Micro-plastic	No	ns	0,9996
Control vs. *Vibrio campbellii*	No	ns	0,9522
After treatment			
Control vs. Glyphosate	Yes	*	0,0142
Control vs. Simazine	Yes	****	<0.0001
Control vs. Oxybenzone	Yes	****	<0.0001
Control vs. Octinoxate	Yes	****	<0.0001
Control vs. $CuSO_4$	Yes	****	<0.0001

Control vs. DMP	Yes	****	<0.0001
Control vs. Micro-plastic	Yes	*	0,0142
Control vs. *Vibrio campbellii*	Yes	****	<0.0001

Table A.10. Dunnett's multiple comparisons test of photosisytem II efficiency of *Sarcophyton glaucum* before and after elicitation to various elicitors

Dunnett's multiple comparisons test	**Significant?**	**Summary**	**Adjusted P Value**
Before treatment			
Control vs. Glyphosate	No	ns	0,9996
Control vs. Simazine	No	ns	0,9716
Control vs. Oxybenzone	Yes	*	0,0205
Control vs. Octinoxate	No	ns	0,5733
Control vs. $CuSO_4$	No	ns	0,9996
Control vs. DMP	No	ns	0,9941
Control vs. Micro-plastic	No	ns	0,8049
Control vs. *Vibrio campbellii*	Yes	****	<0.0001
After treatment			
Control vs. Glyphosate	Yes	**	0,0048
Control vs. Simazine	Yes	****	<0.0001
Control vs. Oxybenzone	Yes	****	<0.0001
Control vs. Octinoxate	Yes	****	<0.0001
Control vs. $CuSO_4$	Yes	****	<0.0001
Control vs. DMP	Yes	****	<0.0001
Control vs. Micro-plastic	Yes	****	<0.0001
Control vs. *Vibrio campbellii*	Yes	****	<0.0001

Table A.11. Dunnett's multiple comparisons test of photosisytem II efficiency of *Lobophyum crassum* before and after elicitation to various elicitors

Dunnett's multiple comparisons test	**Significant?**	**Summary**	**Adjusted P Value**
Before treatment			
Control vs. Glyphosate	No	ns	0,5159
Control vs. Simazine	No	ns	0,9239
Control vs. Oxybenzone	No	ns	0,8511
Control vs. Octinoxate	No	ns	0,9971
Control vs. $CuSO_4$	No	ns	0,9996
Control vs. DMP	No	ns	0,9996
Control vs. Micro-plastic	No	ns	0,8716
Control vs. *Vibrio campbellii*	No	ns	0,908
After treatment			
Control vs. Glyphosate	Yes	****	<0.0001
Control vs. Simazine	Yes	****	<0.0001
Control vs. Oxybenzone	Yes	****	<0.0001
Control vs. Octinoxate	Yes	***	0,0003

Control vs. $CuSO_4$	Yes	****	<0.0001
Control vs. DMP	Yes	****	<0.0001
Control vs. Micro-plastic	Yes	***	0,0005
Control vs. *Vibrio campbellii*	Yes	*	0,041

Table A.12. Dunnett's multiple comparisons test of photosisytem II efficiency of *Xenia umbellata* before and after elicitation to various elicitors

Dunnett's multiple comparisons test	**Significant?**	**Summary**	**Adjusted P Value**
Before treatment			
Control vs. Glyphosate	No	ns	0,3472
Control vs. Simazine	No	ns	0,6948
Control vs. Oxybenzone	No	ns	0,9918
Control vs. Octinoxate	No	ns	>0.9999
Control vs. $CuSO_4$	No	ns	0,9817
Control vs. DMP	No	ns	0,5708
Control vs. Micro-plastic	No	ns	0,5103
Control vs. *Vibrio campbellii*	No	ns	0,9051
After treatment			
Control vs. Glyphosate	Yes	****	<0.0001
Control vs. Simazine	Yes	****	<0.0001
Control vs. Oxybenzone	Yes	****	<0.0001
Control vs. Octinoxate	Yes	***	0,0001
Control vs. $CuSO_4$	Yes	****	<0.0001
Control vs. DMP	Yes	****	<0.0001
Control vs. Micro-plastic	Yes	**	0,0046
Control vs. *Vibrio campbellii*	Yes	****	<0.0001

Table A.13. Dunnett's multiple comparisons test of the number of zooxanthellae associated *Sarcophyton glaucum* in the water column before and after elicitation to various elicitors

Dunnett's multiple comparisons test	**Significant?**	**Summary**	**Adjusted P Value**
Before treatment			
Control vs. Glyphosate	No	ns	0,9973
Control vs. Simazine	No	ns	0,9973
Control vs. Oxybenzone	No	ns	0,9489
Control vs. Octinoxate	No	ns	0,9077
Control vs. $CuSO_4$	No	ns	0,9973
Control vs. DMP	No	ns	0,9973
Control vs. Micro-plastic	Yes	**	0,0027
After treatment			
Control vs. Glyphosate	Yes	*	0,0213
Control vs. Simazine	Yes	****	<0.0001
Control vs. Oxybenzone	Yes	****	<0.0001
Control vs. Octinoxate	Yes	****	<0.0001

Control vs. $CuSO_4$	Yes	****	<0.0001
Control vs. DMP	Yes	****	<0.0001
Control vs. Micro-plastic	Yes	***	0,0002

Table A.14. Dunnett's multiple comparisons test of the number of zooxanthellae associated *Lobophytum crassum* in the water column before and after elicitation to various elicitors

Dunnett's multiple comparisons test	**Significant?**	**Summary**	**Adjusted P Value**
Before treatment			
Control vs. Glyphosate	No	ns	0,9996
Control vs. Simazine	No	ns	0,9996
Control vs. Oxybenzone	No	ns	>0.9999
Control vs. Octinoxate	No	ns	>0.9999
Control vs. $CuSO_4$	No	ns	>0.9999
Control vs. DMP	No	ns	>0.9999
Control vs. Micro-plastic	No	ns	0,6554
After treatment			
Control vs. Glyphosate	No	ns	0,3262
Control vs. Simazine	Yes	****	<0.0001
Control vs. Oxybenzone	Yes	****	<0.0001
Control vs. Octinoxate	Yes	**	0,0058
Control vs. $CuSO_4$	Yes	****	<0.0001
Control vs. DMP	Yes	****	<0.0001
Control vs. Micro-plastic	Yes	****	<0.0001

Table A.15. Dunnett's multiple comparisons test of the number of zooxanthellae associated *Xenia umbellata* in the water column before and after elicitation to various elicitors

Dunnett's multiple comparisons test	**Significant?**	**Summary**	**Adjusted P Value**
Before treatment			
Control vs. Glyphosate	No	ns	>0.9999
Control vs. Simazine	No	ns	>0.9999
Control vs. Oxybenzone	No	ns	0,9994
Control vs. Octinoxate	No	ns	0,9994
Control vs. $CuSO_4$	No	ns	>0.9999
Control vs. DMP	No	ns	0,9998
Control vs. Micro-plastic	Yes	***	0,0002
After treatment			
Control vs. Glyphosate	Yes	*	0,0213
Control vs. Simazine	Yes	****	<0.0001
Control vs. Oxybenzone	Yes	****	<0.0001
Control vs. Octinoxate	Yes	*	0,0213
Control vs. $CuSO_4$	Yes	****	<0.0001
Control vs. DMP	Yes	****	<0.0001
Control vs. Micro-plastic	Yes	****	<0.0001

Appendix 16 Two Ways ANOVA statistical analysis (significance difference) by using Dunnett's multiple comparisons test of the soft corals treated with various concentration of glyphosate (Chapter VII)

Table A.16. Dunnett's multiple comparisons test of the pumping rate of *Xenia umbellata* before and after glyphosate exposure

Dunnett's multiple comparisons test	Significant?	Summary	Adjusted P Value
Before treatment			
Control vs. Glyphosate 50 mg/L	No	ns	0,6247
Control vs. Glyphosate 25 mg/L	No	ns	0,6247
Control vs. Glyphosate 10 mg/L	No	ns	0,3863
Control vs. Glyphosate 5 mg/L	No	ns	0,6247
After treatment			
Control vs. Glyphosate 50 mg/L	Yes	****	<0.0001
Control vs. Glyphosate 25 mg/L	Yes	****	<0.0001
Control vs. Glyphosate 10 mg/L	No	ns	0,6247
Control vs. Glyphosate 5 mg/L	No	ns	0,9864

Table A.17. Dunnett's multiple comparisons test of the photosisytem II efficiency of *Sarcophyton glaucum* before and after glyphosate exposure

Dunnett's multiple comparisons test	Significant?	Summary	Adjusted P Value
Before treatment			
Control vs. Glyphosate 1000 mg/L	No	ns	0,9997
Control vs. Glyphosate 100 mg/L	No	ns	0,9997
Control vs. Glyphosate 50 mg/L	No	ns	0,9846
Control vs. Glyphosate 25 mg/L	No	ns	0,9586
Control vs. Glyphosate 10 mg/L	No	ns	0,9996
Control vs. Glyphosate 5 mg/L	No	ns	0,8677
After treatment			
Control vs. Glyphosate 1000 mg/L	Yes	****	<0.0001
Control vs. Glyphosate 100 mg/L	Yes	****	<0.0001
Control vs. Glyphosate 50 mg/L	Yes	****	<0.0001
Control vs. Glyphosate 25 mg/L	No	ns	0,3263
Control vs. Glyphosate 10 mg/L	No	ns	0,1451
Control vs. Glyphosate 5 mg/L	No	ns	0,3526

Table A.18. Dunnett's multiple comparisons test of the photosisytem II efficiency of *Lobophytum crassum* before and after glyphosate exposure

Dunnett's multiple comparisons test	Significant?	Summary	Adjusted P Value
Before treatment			
Control vs. Glyphosate 50 mg/L	No	ns	0,0914
Control vs. Glyphosate 25 mg/L	No	ns	0,1578
Control vs. Glyphosate 10 mg/L	No	ns	0,7396
Control vs. Glyphosate 5 mg/L	Yes	*	0,0368

After treatment			
Control vs. Glyphosate 50 mg/L	Yes	****	<0.0001
Control vs. Glyphosate 25 mg/L	Yes	****	<0.0001
Control vs. Glyphosate 10 mg/L	Yes	****	<0.0001
Control vs. Glyphosate 5 mg/L	No	ns	0,7684

Table A.19. Dunnett's multiple comparisons test of the photosisytem II efficiency of *Xenia umbellata* before and after glyphosate exposure

Dunnett's multiple comparisons test	**Significant?**	**Summary**	**Adjusted P Value**
Before treatment			
Control vs. Glyphosate 50 mg/L	No	ns	0,053
Control vs. Glyphosate 25 mg/L	Yes	*	0,047
Control vs. Glyphosate 10 mg/L	No	ns	0,2688
Control vs. Glyphosate 5 mg/L	Yes	**	0,0054
After treatment			
Control vs. Glyphosate 50 mg/L	Yes	****	<0.0001
Control vs. Glyphosate 25 mg/L	Yes	****	<0.0001
Control vs. Glyphosate 10 mg/L	Yes	****	<0.0001
Control vs. Glyphosate 5 mg/L	No	ns	0,8299

Table A.20. Dunnett's multiple comparisons test of the number of zooxanthellae associated *Sarcophyton glaucum* in the water column before and after glyphosate exposure

Dunnett's multiple comparisons test	**Significant?**	**Summary**	**Adjusted P Value**
Before treatment			
Control 1 vs. Glyphosate 1000 mg/L	No	ns	>0.9999
Control 1 vs. Glyphosate 100 mg/L	No	ns	>0.9999
Control 1 vs. Glyphosate 50 mg/L	No	ns	0,9847
Control 1 vs. Glyphosate 25 mg/L	No	ns	0,9996
Control 1 vs. Glyphosate 10 mg/L	No	ns	0,9996
Control 1 vs. Glyphosate 5 mg/L	No	ns	0,9847
After treatment			
Control 1 vs. Glyphosate 1000 mg/L	Yes	****	<0.0001
Control 1 vs. Glyphosate 100 mg/L	Yes	****	<0.0001
Control 1 vs. Glyphosate 50 mg/L	Yes	****	<0.0001
Control 1 vs. Glyphosate 25 mg/L	Yes	****	<0.0001
Control 1 vs. Glyphosate 10 mg/L	Yes	****	<0.0001
Control 1 vs. Glyphosate 5 mg/L	Yes	****	<0.0001

Table A.21. Dunnett's multiple comparisons test of the number of zooxanthellae associated *Lobophytum crassum* in the water column before and after glyphosate exposure

Dunnett's multiple comparisons test	**Significant?**	**Summary**	**Adjusted P Value**
Before			
Control vs. Glyphosate 50 mg/L	No	ns	0,9733
Control vs. Glyphosate 25 mg/L	No	ns	0,9733

Control vs. Glyphosate 10 mg/L	No	ns	0,9733
Control vs. Glyphosate 5 mg/L	No	ns	>0.9999
After			
Control vs. Glyphosate 50 mg/L	Yes	****	<0.0001
Control vs. Glyphosate 25 mg/L	Yes	****	<0.0001
Control vs. Glyphosate 10 mg/L	Yes	****	<0.0001
Control vs. Glyphosate 5 mg/L	Yes	**	0,0056

Table A.22. Dunnett's multiple comparisons test of the number of zooxanthellae associated *Xenia umbellata* in the water column before and after glyphosate exposure

Dunnett's multiple comparisons test	**Significant?**	**Summary**	**Adjusted P Value**
Before			
Control vs. Glyphosate 50 mg/L	No	ns	0,9999
Control vs. Glyphosate 25 mg/L	No	ns	0,9323
Control vs. Glyphosate 10 mg/L	No	ns	0,9999
Control vs. Glyphosate 5 mg/L	No	ns	0,8331
After			
Control vs. Glyphosate 50 mg/L	Yes	****	<0.0001
Control vs. Glyphosate 25 mg/L	Yes	****	<0.0001
Control vs. Glyphosate 10 mg/L	Yes	***	0,0003
Control vs. Glyphosate 5 mg/L	Yes	**	0,0014

Appendix 17 Identification of major compound in *Sarcophyton glaucum*, *Lobophytum crassum* and *Xenia umbellata* by NMR

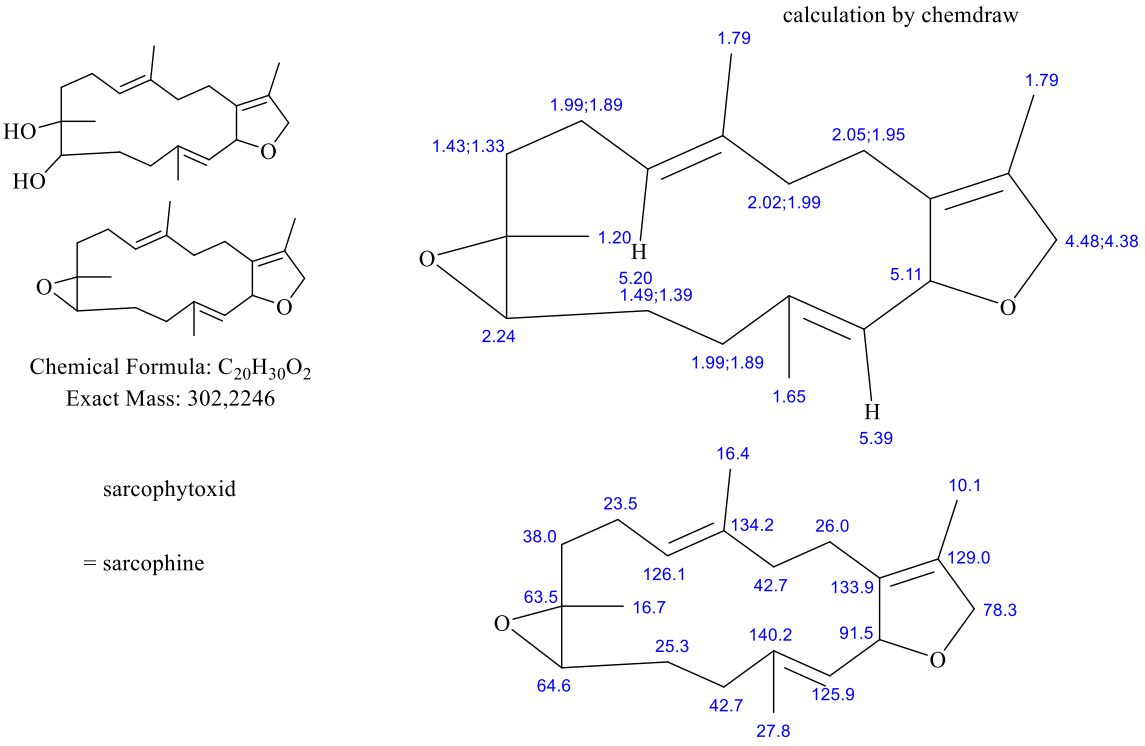

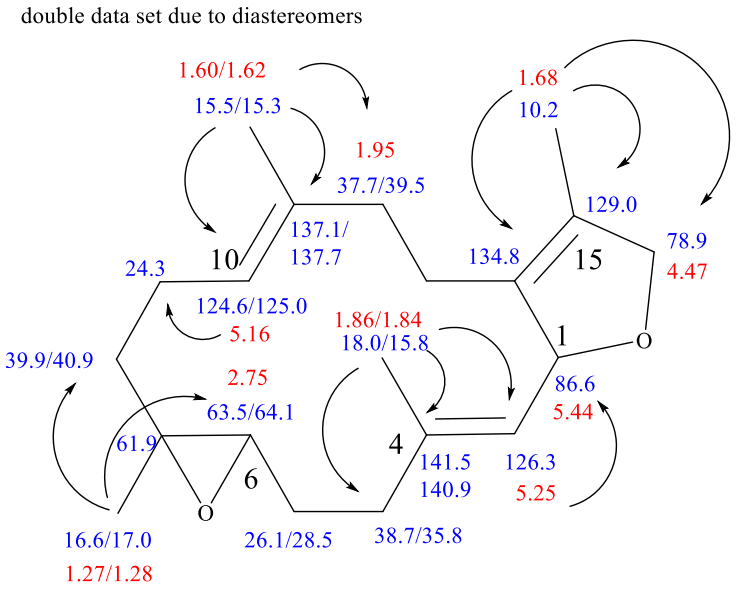

Figure A.18. Major compounds in the extract of *Sarcophyton glaucum*

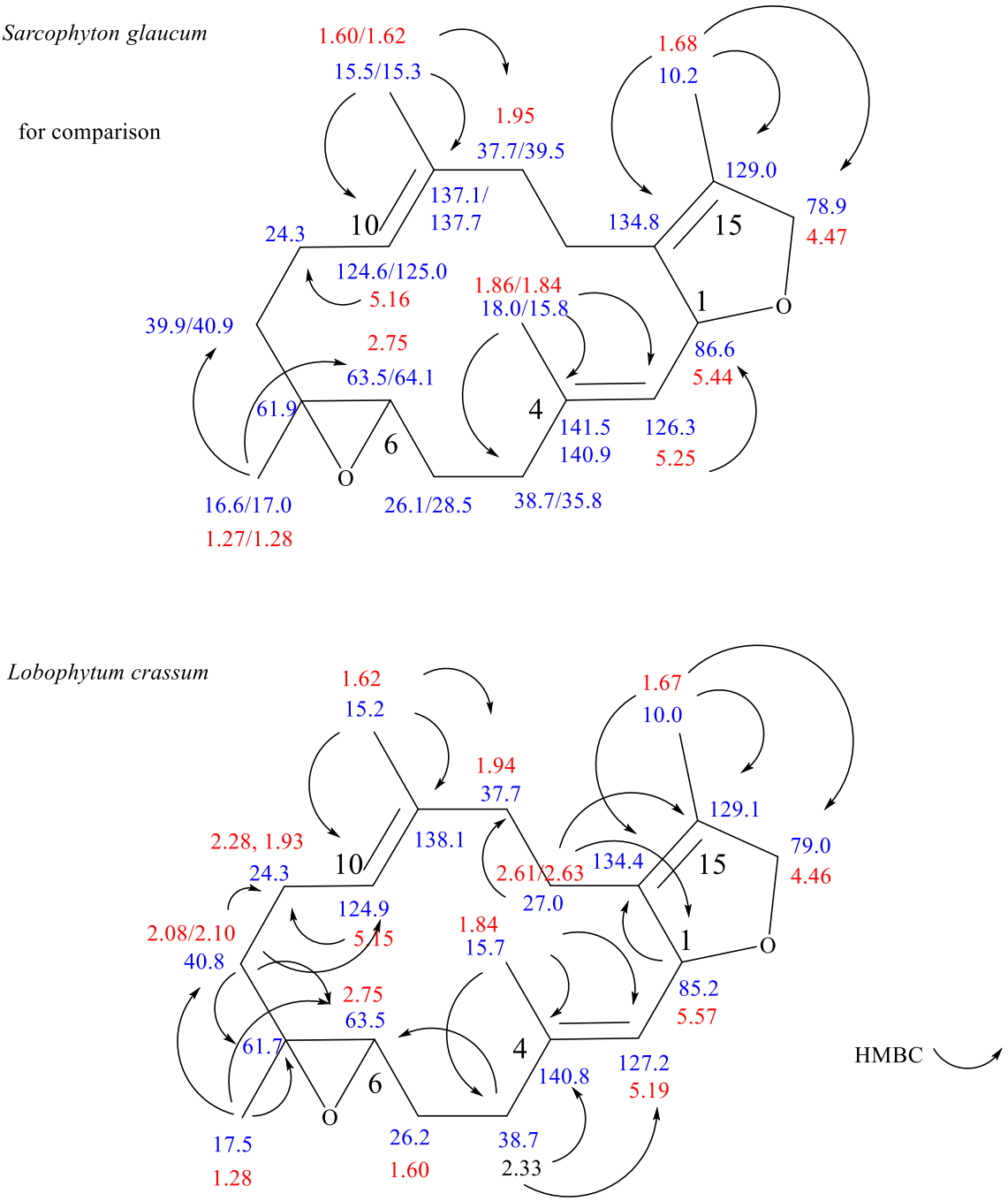

Figure A.19. Major compounds in the extract of *Lobophytum crassum*

Xeniolide O

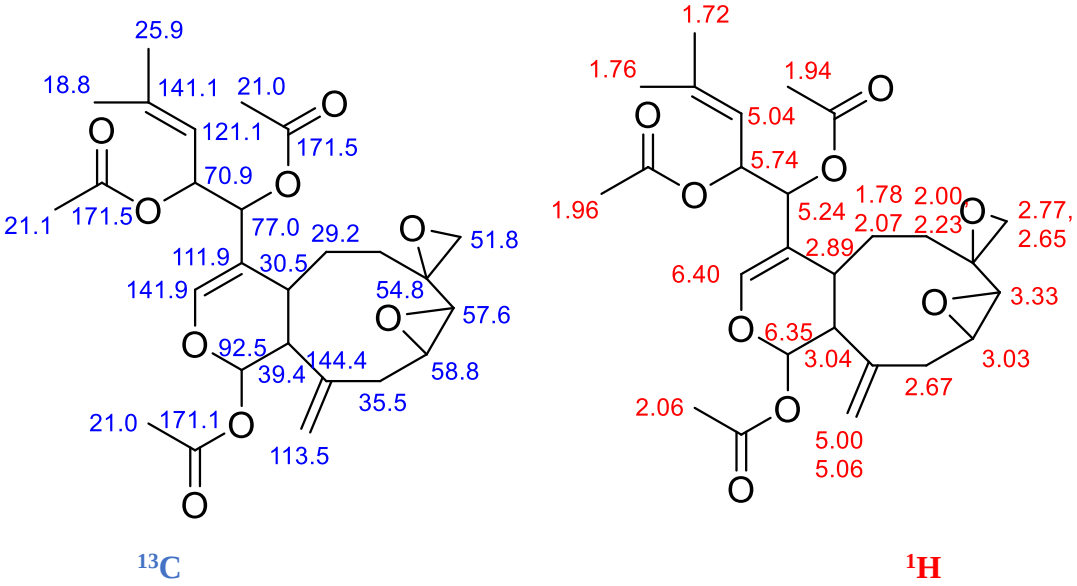

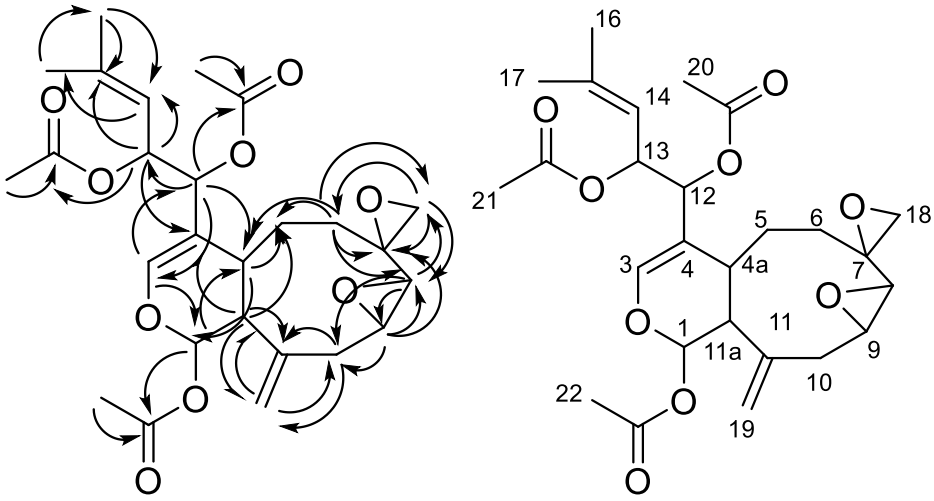

HMBC

Figure A.20. Major compounds in the extract of *Xenia umbellata*

Curriculum vitae

M.Sc. Ayu Christien Rahaweman

Education

2017-2023	PhD in Chemistry Bioorganic, Leibniz Institute of Plant Biochemistry *Supported by the DAAD research grant for the Biodivesity and Health programm*
2014-2016	Master`s Degree in Aquatic Product Technology, IPB University, Indonesia
2008-2013	Bachelor`s Degree (with Honors) in Biology Education, Pattimura University, Indonesia
2013	The certification (training) for Professional Teacher, Faculty of Education and Teacher Training, Pattimura Univesity, Indonesia

Fellowship/Awards/Honors

2017-2021	Doctoral Scholarship by German academic Exchange Service (DAAD)
2016	Most Outstanding Postgraduate Student; summa cum laude graduate in IPB University
2013	Master scholarship by Indonesian Ministry of Education
2011	Most Outstanding Undergraduate Student; summa cum laude in Pattimura university
2011	Runner-up of Biology Olympiad n in Mathematics and Science National Competition

Work/Research Experience

2022-present	Postdoctoral Researcher at Anhalt University of Applied Science, Germany
2021-2022	Research associate in Bioorganic Chemistry Department, Leibniz Institute of Plant Biochemistry, Germany
2017-2022	Research (Natural Product Group), Department of bioorganic Chemistry, Leibniz institute of Plant Biochemistry, Germany

Publications/Poster

2023 Indonesian marine and its medicinal contribution. Nugraha, AS., Firli, LN., Rani, MD., Hidayatiningsih, A., Lestari, ND., Wongso, H., Tarman, K., Rahaweman, AC., et. al. *Natural Products and Bioprospecting*, 13(38).

2020 Metabolite Profiling and Bioactivity of Microalgae *Phaeodactylum tricornutum*. Rahaweman, AC., Porzel, A., Griehl, C., Wessjohann, LA. 15th Plant Student Science Conference (PSSC)

2019 Metabolite Profiling of the Microalgae *Phaeodactylum tricornutum*. Rahaweman, AC., Porzel, A., Griehl, C., Wessjohann, LA. 4th International Conference on Natural Product Untilization (ICNPU)

2016 Cytotoxic activity of Endophytic Fungal Extract against Vero cell Line. Rahaweman, AC., Tarman, K., Pamungkas J. 8th International Seminar of Indonesian Society for Microbiology (ISISM)

Declaration (Eidesstattliche Erklärung)

Ich erkläre an Eides statt, dass ich die vorliegende Arbeit selbstständig und nur unter Verwendung der angegebenen Hilfsmittel und Quellen angefertigt habe.
Alle Stellen, die wörtlich oder sinngemäß aus Veröffentlichungen entnommen sind, habe ich als solche kenntlich gemacht. Des Weiteren versichere ich, dass ich diese Arbeit an keiner anderen Institution eingereicht habe.
Mir ist bekannt, dass bei Angabe falscher Aussagen die Prüfung als nicht bestanden gilt. Mit meiner Unterschrift versichere ich die Richtigkeit dieser Angaben und erkenne die rechtlichen Grundlagen an.

Datum (Ayu Christien Rahaweman)